

Max-Planck-Institut für Biochemie
Martinsried

Lead Structures for Inhibition of Drugable Proteases

Cyclic statine-peptides for BACE-1 and selective bivalent constructs for MMP-9

Alessandra Barazza

Vollständiger Abdruck der von der Fakultät für Chemie der Technischen Universität München zur Erlangung des akademischen Grades eines

Doktors der Naturwissenschaften

genehmigten Dissertation.

Vorsitzender: Univ.-Prof. Dr. St. J. Glaser
Prüfer der Dissertation: 1. apl. Prof. Dr. L. Moroder
2. Univ.-Prof. Dr. H. Kessler

Die Dissertation wurde am 23.03.2006 bei der Technischen Universität München eingereicht und durch die Fakultät für Chemie am 18.05.2006 angenommen.

A Gary
e ai miei genitori

This work was performed from March 2003 to March 2006 at the Max-Planck-Institut für Biochemie (Martinsried) in the Arbeitsgruppe Bioorganische Chemie, under the supervision of Prof. Luis Moroder.

I am especially thankful to Prof. Moroder for giving me the opportunity to work in his lab and for the constant trust and support he gave me in the development of these projects. He has always been available for discussions and he has given me significant guidance during scientific as well as personal and professional conversations.

I would like to thank the people that were involved in my projects, measuring the biological activities for BACE-1 (Dr. Marion Götz and Dr. Michael Willem) and MMP-9 (Prof. W. Bode, Dr. Klaus Maskos and Anna Tochowicz). Many thanks also to Dr. Frank Siedler for the mass spectrometric analysis of compounds 1, 2, 3 and 4 and to Dr. Sergio Cadamuro for the structure of the "mythical" AL125.

Many thanks to Jürgen, for helping me in the synthesis of my compounds for MMP-9 and for being a living library, available to discuss all the chemical problems I had to face; to Lissy, for all the Mass Spectrometric analysis (and especially for performing so many "miracles" for me!!) and for being so patient while I was exercising my Deutsch. Thanks also to "mamma" Silva, for the super lunches she prepared and for being always so cheerful.

Thank you to Prof. Dr. Christian Renner for helping me with the modelling of my molecules on BACE-1 and for the suggestions during the progression of my projects; to Dr. Stella Fiori for revealing to me all the secrets of Insight II; to Prof. Dr. Norbert Schaschke, for the discussions and suggestions on my syntheses.

During this time, I had the good fortune of enjoying the company of the best lab-mates one could desire and I would like to thank them for having been good colleagues from the very first moment and great friends soon afterwards: Alina Ariosa Alvarez, who I have to thank for introducing me to salsa dancing with the Cuban community and for her always cheerful/Caribbean attitude; and Mariolina Götz, for all the wonderful Tuesday night dinners, the Weihnachten Plätzchen mess and all the crazy/serious/funny experiences we had together. I really hope that, no matter where we are, we will always be able to overcome distances and that our telephone numbers will never disappear from our phones.

Special thanks to my two "guardian angels" in the lab: Sergio Cadamuro for all the coffees, the operas and the good time we have spent together having a looot (Jamaican) of fun (plus the help with daddy's heart); and to Cyril-lo Boulegue (sillyyy) for the help with my syntheses, for being a constant reference, with all the literature/jobs/fun emails he sent me, for the many "Mahlzeit!" and for participating, with his supervice girlfriend Daniela, in a very important moment in my life.

A deep thanks to all the people that I had the chance to work with in the lab, in the present and the past, for a long or a short time, and I hope that they will forgive me if I'll mention them briefly, even though the experience with them was certainly intense: Ullly (my official English-German reference), Larsoliiiiino (also for my new orange friend Moyshe), Jose' (the

great Tiramisu´ maker), Tabby (for her wonderful dinners), Markolino Müller (for apartment searches, German traditions explanations and... das ist keine Mütze!!!), Markus Schütt (for his great accent), Marta (who joined the Mediterranean lab for a while), Vidya (my most recent lab mate), as well as Carlo, Shou-Liang, Alex, Frank, Barbara, Markus Kaiser, Alex Hermann, Leslie and Dirk.

Thank you also to the very nice people from the Core Facility who recently joined our group and that supported a very pleasant atmosphere in the lab: Dr. Stephan Uebel (also for the important suggestions on my inhibitor immobilization), Dr. Sabine Suppmann, Kornelia and Manuela, Ralph, Snezan, Andrea and Wolfgang.

Many thanks to "my two men" in Munich: Stef Pegoraro, for all the experiences we have enjoyed together, the serious scientific/cultural/political discussions as well as for the funny ones, and for all the good wine I could drink, while eating his great cooking productions; and Massimo -Stelín- Tesoro, who could make me laugh whatever mood I was in and with whom I enjoyed so many -late- salsa nights. With them, I would like to thank the "Italian enlarged community" (Camí, Barbarella, Franci, Bernadetta, Sylvie) for all the 12.30 Mensa/Fresh Maker lunches, schlitten fahren trips and all the great moments we had together.

A special thanks to Sabine Karl, who has made my experience in Munich much richer and enjoyable: I am going to miss our Italienisch-Deutsch chiacchierate, our risotti and our beautiful days Bergsteigen. I feel super (!!!) lucky to have met her (die Cenerentola!), she motivated me during my difficulties learning German and I really hope we will find a way to keep spending time together even when we will be out of sight.

I want also to thank those friends that have tried to keep the binding tight, with calls or coming to visit me many times here, making me feel that, after all, distance is not such a big problem: Devís, Sabrina, Federico, Ornella, Diego, Oliver, Giorgio, among others.

Voglio ringraziare in modo speciale tutta la mia famiglia: mamma e papa´, Francesca, Roberta e Stefano, Martino e Paola, per avermi sempre appoggiato nelle mie decisioni, anche se difficili, e per aver sempre cercato di diminuire le distanze con la costanza di telefonate settimanali o visite, facendomi così´ pesare meno la mancanza di una famiglia vicina. E un grazie per la pazienza che portano alle piccoline, Elisabetta, Paola e Margherita, che spero non si stancheranno mai di chiedere "ma quando torni?".

Finally, a deep thank you to Gary: this work and this entire adventure would not have been started and accomplished without his constant encouragement: thank you for always supporting and re-motivating me in my searches and discoveries, as well as for being a source of inspiration for new ones; thank you for pushing me gently with good advice to try and be always better; thank you for not stopping me from making this experience and waiting for me for so long.

Part of the results obtained in the three years of PhD work in the group of Prof. Moroder were published. The relative publications are listed below.

Manuscripts in Preparation

Barazza A.; Götz M.; Willem M.; Renner C.; Moroder L. (2006) Macrocyclic inhibitors of β -secretase.

Barazza A.; Tochowicz A.; Maskos K.; Bode W.; Moroder L. (2006) Structure-based design of bivalent inhibitors for MMP-9.

Publications in Books and Proceedings

Barazza A.; Götz, M.; Renner C.; Willem M.; Moroder L. (2005) Cyclic phenylstatine-based tetrapeptides as inhibitors of β -secretase. In *Understanding Biology Using Peptides* (Blundelle S. ed.) Springer, *in press*.

Lectures and Poster Presentations at National and International Symposia

Barazza A.; Götz, M.; Renner C.; Willem M.; Moroder L. (2005) Cyclic phenylstatine-based tetrapeptides as inhibitors of β -secretase. *Biopolymers (Peptide Science)* 80, 554 (P), 19th APS, San Diego.

Barazza A.; Götz, M.; Willem M.; Moroder L. (2005) Structure-based design and synthesis of conformationally restricted cyclic BACE inhibitors. 22nd Winter School "Proteinases and their Inhibitors – Recent Developments", Tiers; L-Abstract.

Barazza A.; Willem M.; Moroder L. (2004) Synthesis of peptoidic statin-based inhibitors of BACE. 21st Winter School "Proteinases and their Inhibitors – Recent Developments", Tiers; L-Abstract.

Table of Contents	I
Abbreviations	III
1. Introduction	1
1.1 Proteases and their Classification	1
1.2 Aspartic Proteases	3
1.2.1 Mechanism of Peptide Hydrolysis by Aspartic Proteases	4
1.2.2 Inhibitors of Aspartic Proteases	6
1.2.2.1 <i>Transition-State Analogues as Inhibitors of Aspartic Proteases</i>	9
1.2.3 Alzheimer's Disease and BACE	11
1.2.3.1 <i>The Amyloid β-Peptide</i>	13
1.2.3.2 <i>BACE (β-Secretase)</i>	16
1.2.3.3 <i>Crystal Structure of BACE-1</i>	18
1.2.3.4 <i>Inhibitors of BACE-1: State of the Art</i>	23
1.3 Matrix Metalloproteinases and their Role in Various Diseases	26
1.3.1 The Metzincin Superfamily	28
1.3.2 Structural Properties and Functions of MMPs	28
1.3.3 Regulation of MMP Activity	34
1.3.4 Structure of MMPs	37
1.3.4.1 <i>The MMP Catalytic Domain</i>	37
1.3.4.2 <i>The MMP Pro-Domain and Hemopexin-like Domain</i>	39
1.3.5 The Reaction Mechanism	40
1.3.6 Matrix Metalloproteinase Inhibitors	43
2. Aim of the Present Work	45
3. Results and Discussion	47
3.1 Structure-based Design of BACE-1 Inhibitors	47
3.1.1 Peptoid and Retroinverted Peptide Approach	47
3.1.1.1 <i>Peptoidic and Retroinverted BACE-1 Inhibitors</i>	50
3.1.1.2 <i>Synthesis of the Peptoidic Compounds</i>	54
3.1.1.3 <i>Bioactivities</i>	57
3.1.1.4 <i>Mass Spectrometry of Peptoids: General Considerations</i>	60
3.1.1.5 <i>Mass-Spectrometric Characterization of Peptoids</i>	63
3.1.1.6 <i>Tandem MS-MS Experiments for Compound 3</i>	70

3.1.2	Macrocyclic BACE Inhibitors	74
3.1.2.1	<i>Determination of the Minimum Size of Inhibitory Statine-Peptides</i>	75
3.1.2.2	<i>Modelling of Macrocyclic Statine-Peptides</i>	79
3.1.2.3	<i>Synthesis of Macrocyclic Statine-Peptides</i>	83
3.1.2.4	<i>Inhibitory Potencies of the Macrocyclic Statine-Peptides</i>	89
3.1.2.5	<i>Molecular Modeling of Compounds 23 and 39</i>	93
3.1.3	Amino-Benzoic Acid Approach	95
3.1.4	Synthesis of Di-Substituted Statines	98
3.1.4.1	<i>Lithium Enolates</i>	100
3.1.4.2	<i>Boron Enolates</i>	104
3.1.4.3	<i>Epoxide Opening with a Grignard Reagent</i>	109
3.2	MMP-9: a Target for Drug Development	111
3.2.1	Synthesis of the Bivalent Inhibitors	115
3.2.2	Inhibitory Potencies	124
4.	Perspectives	127
5.	Zusammenfassung	129
6.	Experimental Part	133
6.1	Materials and Methods	133
6.2	Synthesis	138
6.2.1	Peptoids, Peptide-Peptoid Hybrids and Retroinverted Peptides Approach	138
6.2.1.1	<i>Peptides Synthesis</i>	138
6.2.1.2	<i>Peptide and Peptide-Peptoid Hybrids Synthesis</i>	140
6.2.2	Macrocycles Approach	141
6.2.2.1	<i>Synthesis of Peptides 8-19</i>	141
6.2.2.2	<i>Macrocycles</i>	143
6.2.3	Amino-Benzoic Acid Containing Molecules	162
6.2.4	Di-Substituted Statines	163
6.2.4.1	<i>Lithium Enolates</i>	163
6.2.4.2	<i>Boron Enolates</i>	166
6.2.4.3	<i>Epoxide Opening with Grignard Reagent</i>	168
6.2.5	Synthesis of Bivalent Inhibitors for MMP-9	170
6.2.5.1	<i>Route A</i>	170
6.2.5.2	<i>Route B: PEG₄</i>	176
6.2.5.3	<i>Route B: PEG₆</i>	182
6.2.5.4	<i>Route B: PEG₈</i>	186
7.	References	191

Abbreviations

AA	amino acid residue
A β	β -amyloid peptide
Ac	acetyl (CH ₃ C=O)
AD	Alzheimer's disease
AIDS	acquired immunodeficiency syndrome
Ala (A)	alanine
APP	amyloid precursor protein
Arg (R)	arginine
Asn (N)	asparagine
Asp (D)	aspartic acid
BACE	β -APP-cleaving enzyme, β -secretase
Boc	<i>tert</i> -butoxycarbonyl
Bzl	benzoyl
Bu	butyl
<i>c</i> Hex	cyclohexyl
Cys (C)	cysteine
DANLME	diazoacetylnorleucine methyl ester
DCC	1,3-dicyclohexylcarbodiimide
DCM	dichloromethane
DCU	1,3-dicyclohexylurea
DIC	diisopropylcarbodiimide
DIEA	diisopropylethylamine
DMAP	4-dimethylaminopyridine
DMF	<i>N,N</i> -dimethylformamide
DMSO	dimethylsulfoxide
DPPI	dipeptidyl peptidase I
DTT	dithiothreitol
<i>E</i>	entgegen (opposite, trans)

Abbreviations

E-64	<i>L-trans</i> -epoxysuccinyl-leucylamido(4-guanidino)butane
ECM	extracellular matrix
EDC	1-(3-dimethylaminopropyl)-3-ethylcarbodiimide hydrochloride
EDTA	ethylenediaminetetraacetic acid
EPNP	1,2-epoxy-3-(4-nitrophenoxy)propane
ESI-MS	electrospray ionization mass spectrometry
Et	ethyl
Et ₃ N	triethylamine
Et ₂ O	diethyl ether
EtOAc	ethyl acetate
FAD	familial Alzheimer's disease
Fmoc	9-Fluorenylmethoxycarbonyl
Gln (Q)	glutamine
Glu (E)	glutamic acid
Gly (G)	glycine
HATU	<i>O</i> -(7-azabenzotriazol-1-yl)- <i>N, N, N', N'</i> -tetramethyl-uronium hexafluorophosphate
HBTU	2-(1H-benzotriazol-1-yl)-1,1,3,3-tetramethyl-uronium hexafluorophosphate
His (H)	histidine
HIV	human immunodeficiency virus
¹ H-NMR	proton nuclear magnetic resonance
HOBt	1-hydroxybenzotriazole
HOAt	1-hydroxy-7-azabenzotriazole
HPLC	high performance liquid chromatography
<i>i</i> Bu	<i>iso</i> -butyl
Ile (I)	isoleucine
K _i	inhibition constant
LDA	lithium diisopropylamide
Leu (L)	leucine
Lys (K)	lysine
M	molarity (moles/liter)

MBHA	4-methylbenzhydramine
MCPBA	<i>m</i> -chloroperoxybenzoic acid
Me	methyl
MeOH	methanol
Mes	mesityl (2,4,6-trimethylphenyl)
Met (M)	methionine
MHz	megahertz
min	minutes
mM	millimolar
MMP	matrix metalloproteinase
ml	milliliter
MS	mass spectrometry
MS/MS	tandem mass spectrometry
MT-MMP	membrane-type matrix metalloproteinase
MW	molecular weight
NMM	<i>N</i> -methylmorpholine
NMR	nuclear magnetic resonance
OBzl	benzyloxy
P	peptide
Pd	palladium
PEG	polyethylene glycol
Ph	phenyl
Phe (F)	phenylalanine
Pro (P)	proline
Py	Pyridine
PyBOP	1-benzotriazolylloxy-tris-pyrrolidinophosphonium hexafluorophosphate
RECK	reversion-inducing cysteine-rich protein with Kazal motifs
R _f	retention factor
RT	room temperature
S	subsite
Sar	sarcosine, <i>N</i> -methylglycine
Ser (S)	serine

Abbreviations

Suc	succinyl
Sta	statine
t	time
TACE	TNF (tumor necrosis factor)- α -converting enzyme, α -secretase
TBTU	2-(1H-benzotriazole-1-yl)-1,1,3,3-tetramethyluronium tetrafluoroborate
TEA	triethylamine
Tf	triflate (CF ₃ SO ₂)
TFA	trifluoroacetic acid
THF	tetrahydrofuran
Thr (T)	threonine
TIMP	tissue inhibitor of metalloproteinases
TIS	triisopropylsilane
TLC	thin layer chromatography
TNBS	trinitrobenzene sulfonic acid
Trp (W)	tryptophan
TSA	transition state analogue
Tyr (Y)	tyrosine
Trityl	triphenylmethyl
Val (V)	valine
Z	zusammen (together, cis)

1. Introduction

1.1 Proteases and their Classification

Proteases (also called peptidases or proteinases) are proteolytic enzymes that catalyze the hydrolysis of peptide bonds by the nucleophilic attack of a water molecule on the carbonyl carbon of the scissile bond. These proteins represent one of the largest and most diverse families of known enzymes in all kingdoms of life and are involved in every aspect of organism functions. Their importance is well documented by the fact that about 2% of all genes encode proteases in humans resulting in over 550 active or putative proteases in the human genome. These enzymes play crucial roles in many physiological and pathophysiological processes such as protein catabolism, blood coagulation, cell growth and migration, tissue turnover, differentiation, inflammation, tumour growth and metastasis, activation of zymogens, release of (neuro) hormones, neurotransmitters and other bioactive peptides from precursor forms as well as transport of secretory proteins across membranes. In physiological conditions these enzymes are under strict control of endogenous inhibitors, they are in form of zymogens and their conversion into active forms is regulated by enzyme cascades with highly specialized gating mechanisms. If out of control pathophysiological processes are initiated that are destructive to cells and organisms making these enzymes promising drugable targets with selective synthetic bioavailable inhibitors with therapeutic indications e.g. for viral and parasitic infections, cancer, stroke, Alzheimer's disease, neuronal cell death and arthritis.¹

Proteases are designated either as endopeptidases, when they catalyze the cleavage of a bond within a polypeptide chain or protein, or as exopeptidases,

when cleavage takes place at the N- or C-terminal or at the next-to-it peptide bond, leading to a release of single amino acids or dipeptides. The mechanisms of cleavage and the active-site residues involved vary among the different protease subtypes. This provides the basis for their classification into aspartic-, serine-, cysteine- and metallo-proteases depending upon the residues responsible for peptide hydrolysis, i.e. Asp, Ser, Cys or a coordinated metal ion. There are a few miscellaneous protease that do not precisely fit into the standard classification as e.g. the ATP-dependent proteases.² Due to the growing number of proteases discovered, a more in depth classification has become necessary^{3,4} which organizes the various proteases into evolutionary families and clans, leading to a comprehensive and continuously expanding catalogue of proteases: the MEROPS database [<http://merops.sanger.ac.uk>].^{5,6}

Proteases bind the substrate along the active site cleft with the single residues (P) of the peptide chain occupying the enzyme subsites (S) on both sides of the scissile bond which, according to Berger and Schechter,⁷ are numbered in both direction as shown in Figure 1.1. Optimal complementarity between the S subsites and the amino acid side-chains dictates the enzyme specificity for the substrate.

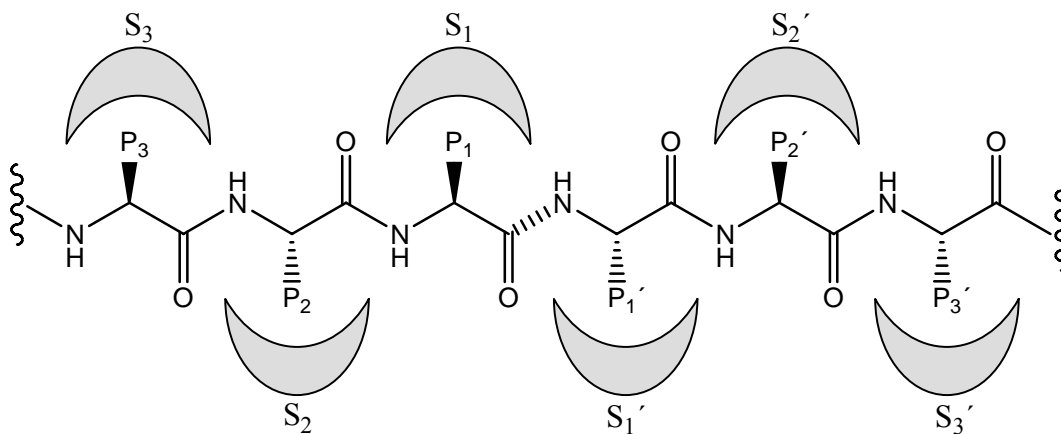


Figure 1.1. Nomenclature for protease subsite specificity. The scissile peptide bond is dashed.

1.2 Aspartic Proteases

Among the various types of proteases the aspartic proteases represent one of the most important family since they are associated with several pathophysiological conditions such as hypertension (renin), gastric ulcers (pepsin), neoplastic disease (cathepsins D and E) and AIDS (HIV protease).

The MEROPS database lists a number of families of the aspartic proteases where the catalytic Asp residues occur within the sequence motif Asp-Xaa-Gly with Xaa = Ser or Thr. Although the presence of this motif in a protein does not correspond in all cases to the active site of an aspartic protease, it is typical for the pepsin family. Pepsin is undoubtedly the most thoroughly studied aspartic protease; it is responsible for the digestions of food in the stomach in higher animals. The aspartic peptidases belonging to the pepsin-like family share the same catalytic apparatus and usually function only under acidic conditions. This limits their action to some specific loci in living organisms, making them less abundant than other proteases such as the serine-proteases. Typical pH optima for aspartic proteases are in the range 3.5-5.5. This value lies between the pK values of the two catalytic carboxyl groups, but of course other factors are involved too. Furthermore, most pepsins are irreversibly denatured at neutral pH and above. For example, the gastric aspartic proteinases of higher animals are secreted from the gastric cells as zymogens, i.e. as inactive precursors that are converted to the active enzymes by proteolytic cleavage at the N-terminus; this limited proteolysis is mediated by the zymogens themselves at acid pH. Pepsin A is irreversibly inactivated at neutral pH and above, which is probably the physiological mechanism by which its activity is kept localized to the stomach. Pepsinogen, on the other hand, is stable to neutral pH.

Aspartic proteases have been isolated from a wide range of organisms, varying from vertebrates to plants, fungi, parasites, retroviruses, and more recently bacteria.⁸ Of the five currently known human aspartic proteases, three (pepsin, gastricsin and renin) are secretory, one, cathepsin D, is found

ubiquitously in the lysosomes of most cells⁹ while the fifth, cathepsin E, is neither secretory nor lysosomal, but located within the endoplasmic reticulum/trans-Golgi network/endosomal compartments of cells.¹⁰ Cathepsin E differs from the other aspartic proteases not only because of its location in defined compartments of the cells, but also because of its unique molecular architecture.¹¹

X-ray structures of aspartic proteases of the pepsin family revealed a bilobed architecture with the active-site cleft located between the two lobes, and with each lobe contributing one aspartate residue to the catalytic diad of aspartates. These two aspartyl residues are in close geometric proximity in the active site, one being ionized and the second one non-ionized in the optimum pH range of 2 to 3.¹² The two lobes are homologous in the sequence and spatial array strongly supporting their evolution by gene duplication.¹³ Moreover, since each of the two lobes itself represents a duplicated structure, these proteases consist of four copies of one ancestral subunit. In this context it is worthy to note that retropepsins are monomeric and that these proteases carrying only one catalytic aspartate have to dimerize to form an active enzyme.¹⁴

1.2.1 Mechanism of Peptide Hydrolysis by Aspartic Proteases

Aspartic proteases hydrolyze the amide bond through a concerted action of one aspartic acid and one aspartate residue with formation of a noncovalent neutral tetrahedral intermediate via a “push-pull” mechanism.¹⁵⁻¹⁸ This mechanism of hydrolysis of all aspartic proteases is based on a proton transfer to the substrate and a low-barrier hydrogen bond that holds the two aspartic carboxyls in a coplanar conformation.¹⁷ A water molecule is hydrogen bonded to the two Asp residues and acts as the nucleophile that attacks the carbonyl carbon of a peptide bond arranged in the active site. More precisely, the Asp²²⁸ acts as a general base to remove one proton from the water molecule while Asp³² donates a proton to the carbonyl oxygen atom of the scissile peptide bond (Fig. 1.2). In the

tetrahedral intermediate, Asp²²⁸ is hydrogen bonded to the attacking oxygen atom, while the hydrogen remaining on that oxygen is hydrogen bonded to the inner oxygen of Asp³². Transfer of the hydrogen from Asp²²⁸ to the nitrogen of the scissile peptide bond is accomplished by inversion of configuration around the nitrogen atom. Following this step, the C-N bond breaks forming the two products. The carboxyl product remains hydrogen-bonded to Asp³², and Asp²²⁸ is in the negatively charged form, ready for the next round of catalysis. In this mechanism, the free enzyme E binds to the substrate to form a loose complex (ES) (Fig. 1.2).

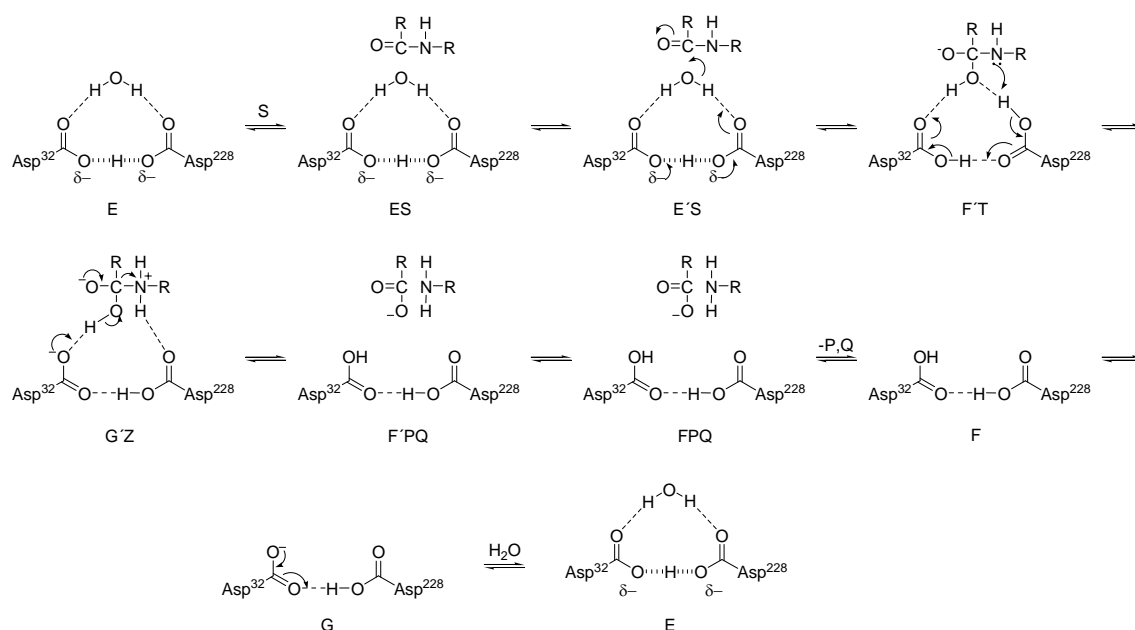


Figure 1.2. Catalytic mechanism proposed by Northrop.¹⁷ In this mechanism, species E is the free enzyme poised for catalysis. Step 1 is the binding of substrate to form a loose complex (ES). Step 2 is the closing of the flap down upon the substrate to squeeze all components into the correct geometry and distances for the catalytic process to begin (E'S). Step 3 includes the removal of a proton from the bound water molecule to stimulate attack on the carbonyl carbon (F'T). Step 4 involves a proton transfer to the nitrogen of the peptide bond (G'Z). Step 5 is the bond cleavage event (F'PQ). Step 6 is the opening of the flap to free the products (FPQ) and step 7 is release of the products (F). Step 8 includes a loss of one proton (G) and step 9 involves binding of a new water molecule and re-formation of the low-barrier hydrogen bond (E).

A flap, present in all pepsin-like enzymes, closes the catalytic cleft and forces the components into the correct geometry and distances to initiate the catalytic process. A proton is transferred from the water molecule bound to the two aspartic acids responsible for catalysis, thereby stimulating the attack on the carbonyl carbon. A proton is then transferred to the nitrogen of the peptide bond, followed by the final bond cleavage event. The flap re-opens to free the products, loosing one proton and binding to a new water molecule to re-form the low-barrier hydrogen bond.

1.2.2 Inhibitors of Aspartic Proteases

Most structural information for the design of inhibitors of this therapeutically interesting enzyme family has been derived from pepsin and the tight-binding reversible inhibitor pepstatin (Fig. 1.3).¹⁹ Conversely, covalently reacting inhibitors of pepsin such as diazoacetylnorleucine methyl ester (DANLME), 1,2-epoxy-3-(4-nitrophenoxy) propane (EPNP), and *p*-bromophenacyl bromide, have only been used as diagnostic reagents for aspartic endopeptidases. Each of these latter inhibitors reacts specifically with the side-chain carboxyl of a distinct aspartic acid residue to inactivate the enzyme.

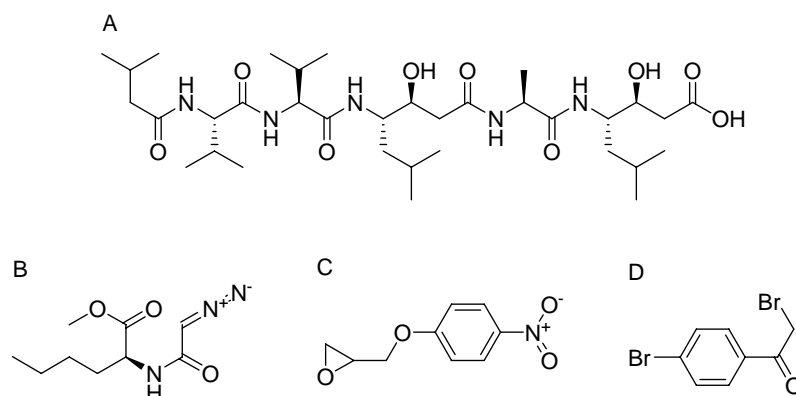


Figure 1.3. Inhibitors of aspartic peptidases: (A) pepsin, (B) diazoacetylnorleucine methyl ester, (C) 1,2-epoxy-3-(4-nitrophenoxy) propane, and (D) *p*-bromophenacyl bromide.

Aspartic proteases generally bind 6 to 10 amino acid residues of the peptide substrate in their active-site clefts,²⁰ and one or more flaps that close down on top of the substrate add even more interactions sites to the complex increasing in this way the substrate/inhibitor selectivity. Pepstatin was the first potent and specific inhibitor of aspartic proteases that was discovered.²¹⁻²³ It inhibits pepsin ($K_i = 4.5 \text{ pM}^{24,25}$), cathepsin D ($K_i = 0.1 \text{ nM}^{26}$), and other aspartic proteases,²⁷ but to a lesser extent renin ($K_i = 0.1\text{-}1 \text{ }\mu\text{M}^{28}$). Since its discovery many synthetic analogues have been synthesized to evaluate the effect of the peptide chain length and to disclose the mechanism of inhibition of this natural peptidic compound. The minimal sequence required for inhibition of pepsin corresponds to a peptide extending from P_3 to P_3' (Iva-Val-Sta-Ala-Iaa,²⁹⁻³¹ with Iaa = isoamylamide), whereby the statine moiety is considered as a dipeptide replacement thus occupying both P_1 and P_1' (*vide infra*). These early structure-activity studies indicated the central statine residue and specifically its 3*S*-hydroxyl group as the crucial structural element for potent inhibition of aspartic proteases. Acetylation²⁴ or inversion of the configuration from 3*S* to 3*R*³² reduces substantially the binding to the enzyme. The importance of the 3*S*-hydroxyl group in statine-containing peptides has been rationalized in terms of transition-state analogue mechanism of inhibition³³⁻³⁵ where the 3*S*-hydroxyl group mimics one of the hydroxyl groups in the tetrahedral intermediate formed during hydrolysis (Fig. 1.4).

The transition-state analogue inhibitor hypothesis³⁶⁻³⁸ foresees a tight binding of inhibitors by the enzyme because of their geometry that closely mimics the transition state or the tetrahedral intermediate for the enzyme-catalyzed reaction (Fig. 1.4). Since peptide bond hydrolysis by the proteases proceeds via the tetrahedral transition-state intermediate, a stable tetrahedral species placed in a substrate sequence at the point of cleavage should act as inhibitor, and the more an enzyme resistant compound "looks" to the enzyme like a substrate in the middle of its conversion to its products, the greater should be its

affinity for the enzyme. This concept has been successfully used in the design and synthesis of potential inhibitors of pepsin-like aspartic proteases.

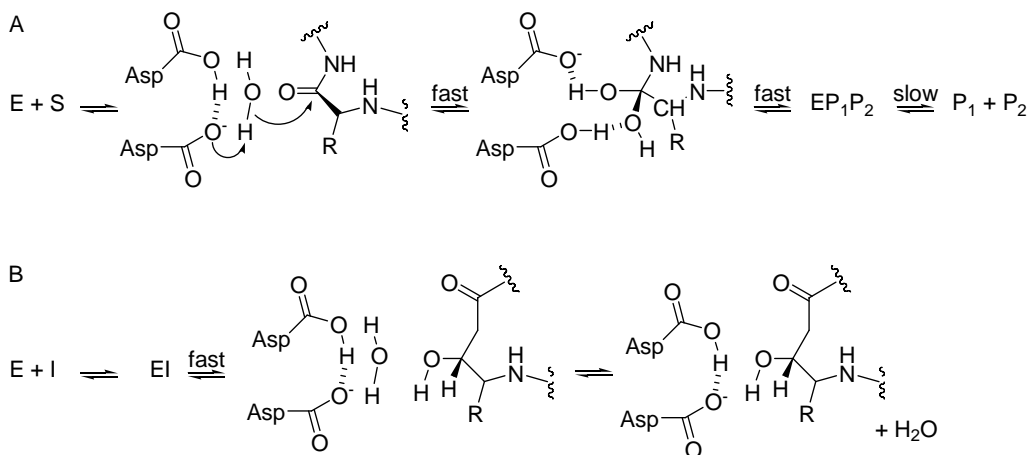


Figure 1.4. Schematic representation of the relationships between proposed catalytic and inhibitory mechanisms. (A) General acid-base catalyzed mechanism for substrate hydrolysis by an aspartate protease. The water molecule is hydrogen bonded to both aspartic acid residues and other sites in the active site. The oxyanion derived from the amide carbonyl may be stabilized by hydrogen bonds to other acceptors. (B) Postulated collected-substrate mechanism for inhibition of aspartic proteases by transition-state analogue (statine-derived) inhibitors. The *S*-hydroxyl group of the inhibitor displaces the enzyme-bound water molecule shown in Fig. 1.2.

The relationships between the main-chain statine atoms and the main-chain atoms in a dipeptide substrate or tetrahedral intermediate sequence have intrigued medicinal chemists since the structure of pepstatin was first discovered. In fact, because of its C-1 and C-2 atoms, statine is either two atoms too long to be isosteric with a normal amino acid or one atom too short to be isosteric with a dipeptide. On the basis of an extensive comparison of pepsin substrate sequences to pepstatin Powers *et al.*³⁹ sustained that statine might better mimic a dipeptide. Using the X-ray data provided by Bott *et al.*,⁴⁰ Boger proposed a precise model in which statine represents an analogue of the enzyme-bound dipeptide in its tetrahedral intermediate form.⁴¹ To prove this hypothesis several analogues of

renin substrate (6-13) were synthesized and indeed the most potent inhibitors of renin were obtained with statine replacing the cleavage dipeptide Leu-Leu in pig renin and Leu-Val in human renin consistent with the predictions derived from the molecular modelling studies.³²

1.2.2.1 Transition-State Analogues as Inhibitors of Aspartic Proteases

A large number of native and enzyme-inhibitor crystal structures are presently available¹⁸ for medicinally relevant enzymes such as renin, plasmepsin, HIV protease, β -secretase, and cathepsin D, as well as for other aspartic proteases (penicillopepsin, endothiapepsin, chymosin, pepsin, and *Rhizopus chinensis* pepsin). Both peptide-derived and non-peptide inhibitors have been developed and the relationships between the different peptidomimetics can be analyzed in terms of enzyme-inhibitor crystal structure complexes. A key structural element in most of the inhibitors is the hydroxyl or hydroxyl-like moiety that binds to the two catalytically active aspartic acids instead of the Asp-bound water molecule. As transition-state analogue (TSA) the amino acid statine (Figure 1.5, **2**) from the natural product pepstatin²¹⁻²³ was often used³³⁻³⁵ for the design of selective inhibitors of aspartic proteases including the therapeutically most promising enzymes renin, HIV protease and β -secretase.⁴²

In addition to statine, numerous structural motifs have been developed such as those reported in Figure 1.5. Among these special attention has been paid to the hydroxyethylene (**4**)^{43,44} and the hydroxyethylamine moieties (**5**),^{45,46} the latter for the development of HIV protease inhibitors.⁴⁷ Replacement of the dipeptidyl cleavage site of a native substrate with a TSA effectively generates an inhibitor specific for the peptidase that recognizes the TSA side chains plus amino acid side chains both up- and downstream from the cleavage site. Since the active-site cleft of aspartic proteases is generally capable of accommodating up to nine amino acid residues of the substrate (or the inhibitor), the inhibitor's

selectivity can be significantly improved by exploiting the complementary interaction between all these enzyme binding sites (S_6-S_3') and the inhibitor residues P_6-P_3' . Very unfortunately such large peptide sequences generally are not clinically useful due to limited oral bioavailability and their fast enzymatic degradation as well assessed in the case of renin TSA-based inhibitors developed for treatment of hypertension.⁴⁸

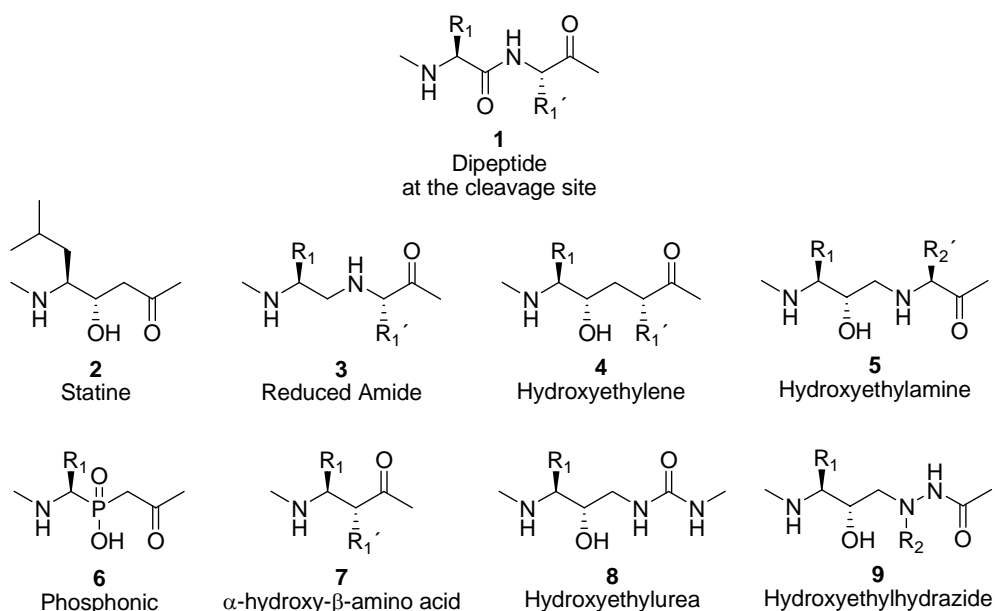


Figure 1.5. Structures of some transition-state analogues (TSA) units effective for aspartic peptidases inhibition.

The development of HIV protease inhibitors was found to be substantially easier than for renin, since HIV protease recognizes a significantly smaller minimum substrate sequence. Correspondingly, smaller size molecules were obtained that act as highly selective HIV protease inhibitors.⁴⁷ Among these, several compounds (Figure 1.6) are presently in clinical use because of their sufficient oral bioavailability.

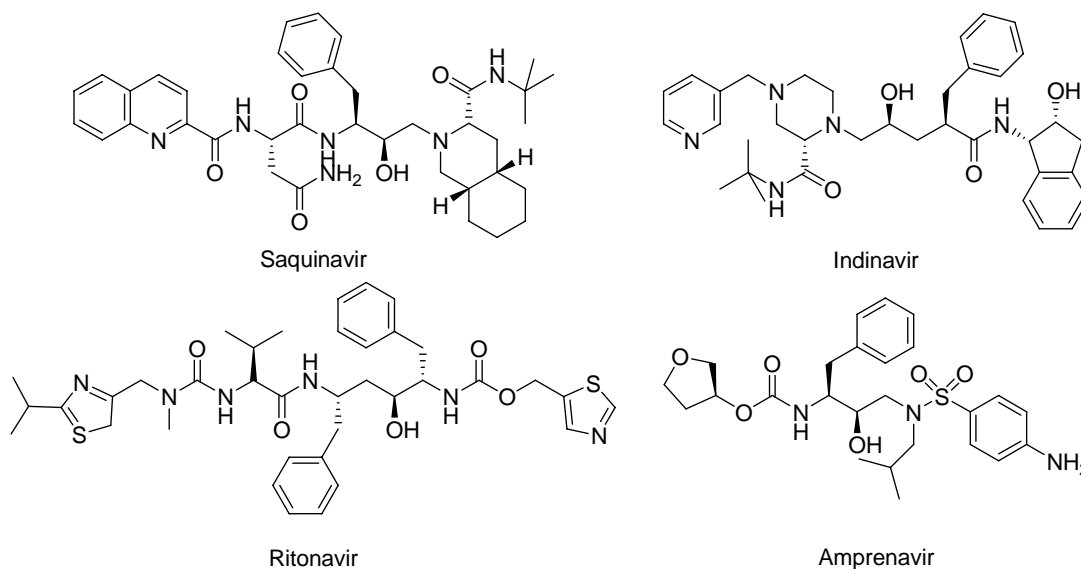


Figure 1.6. Examples of peptide-derived TSA inhibitors of HIV protease used in AIDS therapies.

1.2.3 Alzheimer's Disease and BACE

Dementia is the loss of mental functions that is severe enough to interfere with a person's daily functioning, such as thinking, memory, and reasoning.⁴⁹ Dementia is not a disease itself, but rather a group of symptoms that are caused by various diseases or conditions. Among these the major causes of dementia are associated with diseases that cause degeneration or loss of nerve cells in the brain such as Alzheimer's, Parkinson's, Huntington's or Lewy body disease and Pick's disease, previously diagnosed as variants of Alzheimer's disease. Alzheimer's disease (AD) is the leading cause of dementia in the elderly, accounting for 45 to 67% of all cases.⁵⁰⁻⁵² The degeneration of neurons in regions of the brain important for cognition results in progressive dementia that slowly deprives AD patients of their memories, personalities and eventually their lives. No therapies currently exist that treat the underlying cause of AD, and if none are found, the incidence of AD patients will rise dramatically as the population ages.⁵³

The name of the disease is eponymic for Alois Alzheimer, a German psychiatrist and neuropathologist, who at a meeting of the South-West German

Society of Alienists in November 1906 described "eine eigenartige Erkrankung der Hirnrinde" (a peculiar disease of the cerebral cortex) by presenting the clinical and neuropathological features of a woman aged 51 years who had died in the Munich mental asylum. The woman had experienced the first symptoms 5 years previously. She became successively unable to care for herself at home and rejected all attempts to help her. Upon hospitalisation her symptoms included disorientation, impaired memory, as well as difficulties reading and writing. The symptoms increased gradually to hallucinations and a corresponding loss of higher mental functions.⁵⁴

The pathological-anatomical investigation of the brain showed the cerebral cortex to be thinner than normal (Fig. 1.7 A). Alzheimer noted two further abnormalities in the brain (Fig 1.7 B). The one being senile plaques, a structure previously described in the brain of elderly people and now known to be due to the deposition of the 4 kDa β -amyloid peptide ($A\beta$). The other abnormality was neurofibrillar tangles evident in histological material from her cerebral cortex, a fibre structure derived from the accumulation of τ -protein.⁵⁵ The neurofibrillary tangles had not been previously described, and it was mainly this abnormality that defined the new disease.

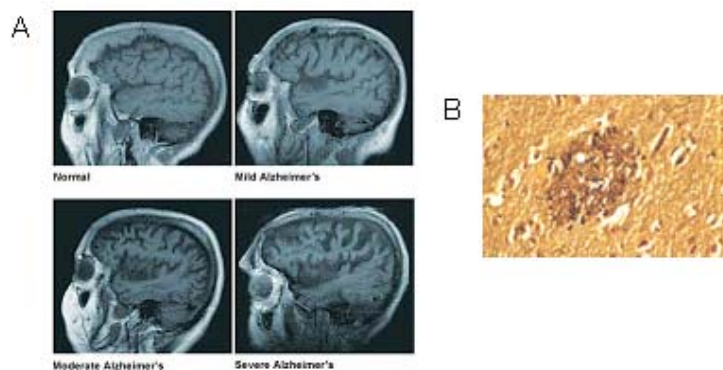


Figure 1.7. (A) Four magnetic resonance images showing four different people (with differently sized and shaped brains). The widening grooves and fissures of the cerebral cortex indicate progressively severe brain atrophy and loss of brain mass. (B) The $A\beta$ peptide aggregates and precipitates in amyloid plaques. This event initiates the amyloid cascade resulting in additional intracellular aggregations of the tau protein, which then form tangles (the black structures surrounding the amyloid plaque).

Subsequent to the description of this first patient, millions have been identified worldwide. With aging as the major risk factor for AD, a further sharp increase in the number of patients in the near future is expected, if no therapeutic treatment against this disease is discovered. Fortunately, major progress has been made in the last years, which has led to the first trials with drugs designed to lower the impact of the major compound responsible for the disease, the neurotoxic amyloid β -peptide.⁵⁶ $A\beta$ is a highly hydrophobic peptide, which aggregates to form oligomers. A further aggregation of these oligomers produces fibers, which eventually precipitate and accumulate in amyloid plaques.

1.2.3.1 The Amyloid β -Peptide

First studies in the early 1990s showed unexpectedly that $A\beta$ is a physiologically normal metabolite generated in healthy persons,⁵⁵ present in small quantities as soluble monomers that circulate in cerebrospinal fluid and blood. In AD patients, however, the level is significantly increased and accumulation as insoluble, fibrillar plaques starts. The $A\beta$ peptide consists of 40 to 42 amino acid residues and it originates from the proteolytic cleavage of the amyloid precursor protein (APP).⁵⁷ Processing of APP *in vivo* occurs by the two major pathways shown in Fig. 1.8. Cleavage of APP at the N-terminus of the $A\beta$ region by β -secretase and at the C-terminus by γ -secretases represents the amyloidogenic pathway for processing of APP. The β -secretase cleaves APP between residues Met⁶⁷¹ and Asp⁶⁷² yielding β -APPs and C99 fragments.⁵⁸ The β -secretase involved in this process has been identified as an aspartic protease⁵⁷ (BACE-1, acronym of β -site APP cleaving enzyme, also called memapsin 2 or Asp-2). The newly generated membrane-bound APP C-terminal fragment (C99) is the immediate precursor for the intramembraneous γ -secretase cleavage at residue 711 (between Val and Ile) or 713 (between Ala and Thr), resulting in the intracellular release of the peptide P6 and extracellular $A\beta$.⁵⁹

APP can also be processed in a non amyloidogenic pathway by α -secretase (TACE), which cleaves within the A β domain between Lys⁶⁸⁷ and Leu⁶⁸⁸ and produces a large soluble α -APP domain and the C-terminal fragment C83.^{60,61} The latter can then be cleaved by γ -secretase to release P3 and P6 fragments.^{62,63} This pathway does not yield A β peptide. Consequently directing APP towards the α -secretase pathway may have a beneficial effect in lowering A β peptide levels.

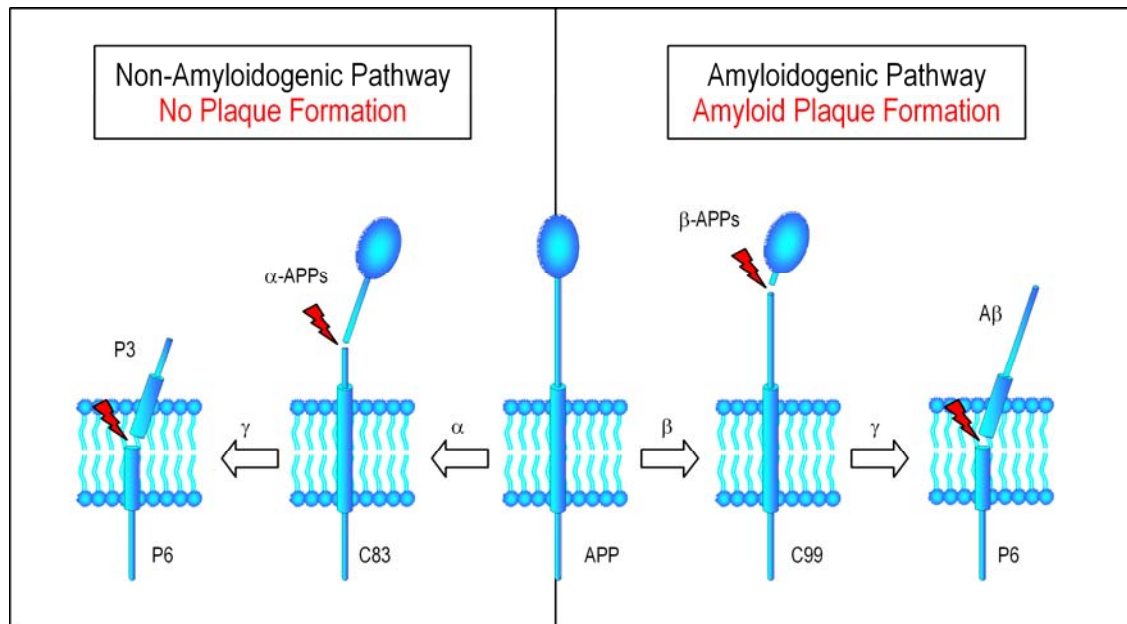


Figure 1.8. Alternative cleavage events of secretase-mediated cleavage of APP. While β - and γ -secretases mediate the amyloidogenic pathway, α -secretase prevents A β generation by cleaving APP in the middle of the A β domain.

The A β is a neurotoxic, highly aggregation prone peptide and represents the principal component of the neuritic plaque found in the brain of AD patients. The amyloid hypothesis suggests that the neuronal dysfunction and clinical manifestation of AD are a consequence of the long-term deposition and accumulation of the 40-42 membered A β peptides and that this process leads to the onset and progression of AD.

1.2.3.2 BACE (β -Secretase)

BACE has been isolated in 1999⁶⁵⁻⁶⁸ as a membrane-bound aspartic protease with all the known functional properties and characteristics of β -secretases, namely the ability to cleave APP at the so-called β -processing site. It is a 501 amino acid sequence protein most closely related to the pepsin aspartic protease family (Fig. 1.10).

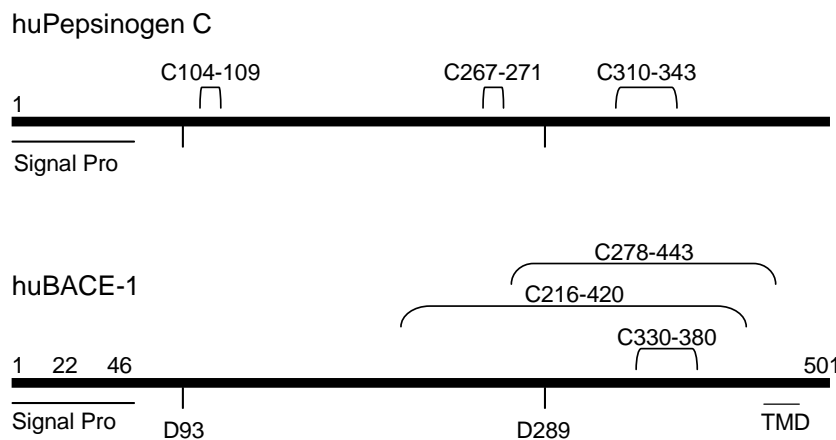


Figure 1.10. Schematic view of the structure of BACE-1. Full length BACE-1 is a type I membrane-bound aspartic protease with a signal sequence (1-22), an intermolecularly cleaved prosequence (22-46) and a transmembrane domain (TMD) at the C-terminal end. The catalytically active aspartic acids are in positions 93 and 289. The major difference between the BACE family and other aspartic proteases is the disulfide network in the catalytic domain. The only conserved disulfide bridge is C330-380. The schematic view of human pepsinogen C is given for comparison.

Two aspartic protease active-site motifs with the sequences **DTGS** (residues 93-96) and **DSGT** (289-292) are present; mutation of either aspartic acid residue abolishes the catalytic activity of the enzyme.⁶⁵ A unique feature of BACE-1, which distinguishes it from the other human aspartic proteases, is the presence of a C-terminal extension that includes a transmembrane domain (residues 455-480) and a signal peptide; it also contains four predicted glycosylation sites. A distinguishing feature of the protein is the pro-domain

(residues 22-46), which is shorter than that of other human aspartic proteases. Six cysteine residues are present in the catalytic domain to form three intramolecular disulfide bonds. The number of disulfide bridges is identical to other aspartic proteases such as pepsin. While the disulfide bridge between Cys³³⁰-Cys³⁸⁰ is conserved, the positions of two disulfides Cys²⁷⁸-Cys⁴⁴³ and Cys²¹⁶-Cys⁴²⁰ are quite different when compared to pepsin, without causing structural changes of the shape of the catalytic domain.^{69,70}

The expression pattern of BACE-1 is highest in pancreas and brain, and significantly lower in most other tissues. The enzyme is present in neurons but almost not detectable in glial cells of the brain. The high expression level in pancreas can be attributed to a catalytically inactive splice variant of BACE-1 lacking part of exon 3.⁷¹ Three additional neuronal splice variants of BACE-1 with very low catalytic activity have been characterized.⁷² The physiological functions of these isoforms are still unknown.

The identification of BACE-1 as a protease with a well-defined β -secretase activity was unequivocally shown with the generation of BACE knockout (BACE -/-) mice, shown to be devoid of the ability to generate A β , in cases in which APP was endogenous⁷³ or when crossed to transgenic mice expressing APP as a FAD mutant.⁷⁴ Remarkably, the BACE -/- animals were found to be normal in gross anatomy, tissue histology and clinical chemistry, undistinguished from the BACE +/- animals except for their inability to generate A β . On the other hand, overexpression of BACE-1 in cells leads to an increase in β -secretase activity;⁶⁵⁻⁶⁷ and consequently the content of C99 and APP is enhanced several-fold compared to untransfected cells. The encouraging results from the knockout mice suggest that a potential mechanism-based toxicity might not be an issue for specific BACE-1 inhibitors, in contrast to the current controversy about γ -secretase inhibitors and their potential interaction with Notch signaling.^{75,76}

BACE-2, also called Asp-1, memapsin-1 or DRAP (Down's region aspartic proteinase), is a second member of the BACE subfamily of membrane-anchored aspartic proteases with a high degree of similarity to BACE-1. BACE-2 exhibits an α -secretase-like activity, which cleaves APP in the middle of the A β domain between amino acids 19 and 20, in this way not contributing to the amyloidogenic processing of APP. The Flemish (but not the Dutch) FAD mutation of APP (A21G of A β) is adjacent to the α -cleavage site and causes an increase in A β production mediated by BACE-2, but not BACE-1, in transfected cells.⁷⁷ This observation, together with a markedly different expression level compared to BACE-1, argues against a major role for BACE-2 in the generation of A β . If this is the case, the optimal inhibitor would block selectively BACE-1 without interacting with BACE-2.

Little is known about the physiological substrates of BACE-1, but the evidence that APP is not the optimal cleavage site for BACE-1, suggests that it is also not the main substrate. In fact, one of the FAD-associated mutations in APP (the Swedish mutation) strongly enhances BACE-1 cleavage of APP simply by creating an "optimized" cleavage site.⁶⁴

1.2.3.3 Crystal Structure of BACE-1

Because of all these findings including the absence of deleterious phenotypes, great attention was focused on BACE-1 as therapeutic target for Alzheimer's disease. The resolution crystal structures of the fully active recombinant BACE-1 (memapsin 2) containing 21 residues of the putative pro-region, but lacking the transmembrane and intracellular domains, were solved in complex with the two inhibitors OM99-2⁶⁹ and OM00-3⁷⁸ (Fig. 1.11).

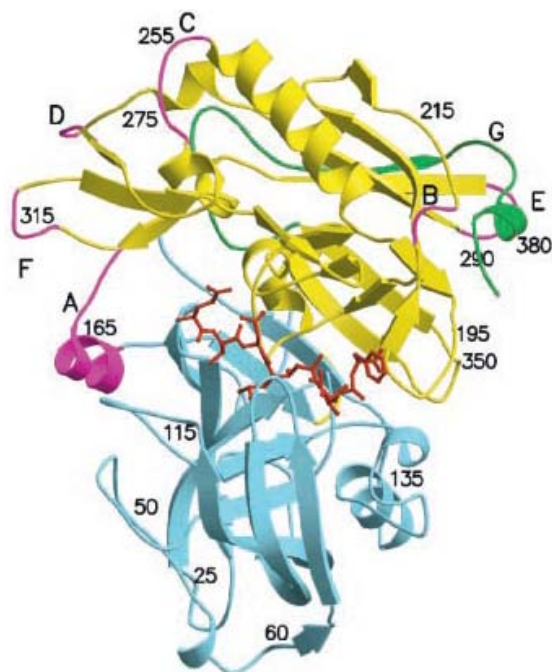


Figure 1.11. The crystal structure of BACE-1 (memapsin 2) complexed with the inhibitor OM99-2. View of the polypeptide backbone of the enzyme shown as a ribbon diagram. The N- and C-lobe are blue and yellow, respectively, except for the magenta insertion loops, designated A to G in the C-lobe and the green COOH-terminal extension. The inhibitor bound between the lobes is shown in red.

The bilobal structure and other main structural features of the aspartic proteases of the pepsin family were confirmed. The eight residues of the inhibitor OM00-3 (Fig. 1.12) are accommodated within the substrate-binding cleft, which is located between the N- and C- terminal lobes. The active-site Asp³² and Asp²²⁸ and the surrounding hydrogen-bonding network are located in the centre of the cleft. The inhibitor is placed in the active site with the TSA hydroxyethylene coordinated by four hydrogen bonds to the two catalytic Asp residues as schematically represented in Fig. 1.12. Further 10 hydrogen bonds are detectable between the inhibitor, the binding pockets and the flap region.

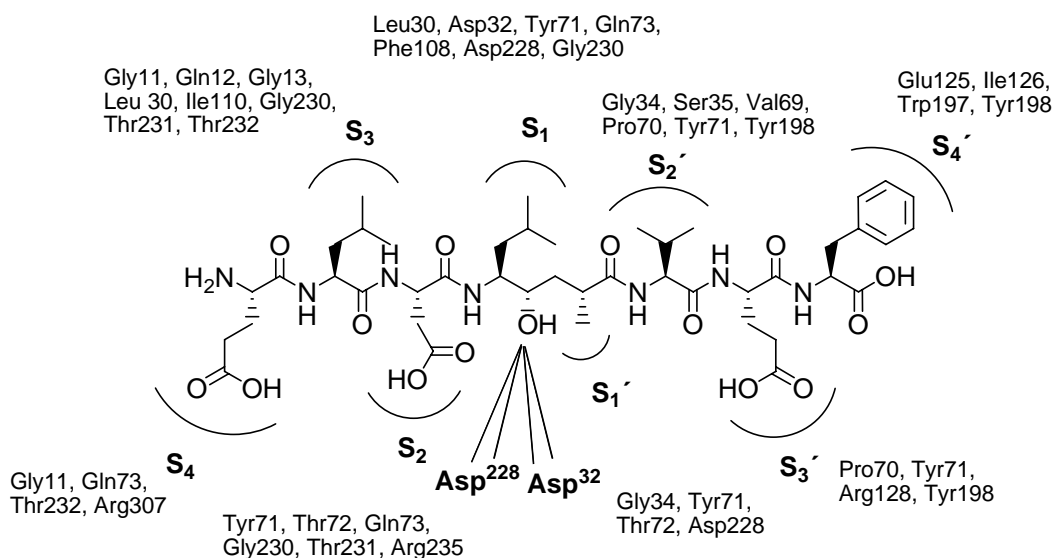


Figure 1.12. Structural representation of OM00-3 in the catalytic cleft of BACE-1; the enzyme's residues are in contact with the inhibitor (distance $< 4 \text{ \AA}$) at the subsites S₄ to S₄'.

The active site of BACE-1 is more open than that of pepsin and in addition the protease residues interacting with the inhibitor side chains are quite different compared to other aspartic proteases.

The hairpin loop known as the “flap”, partially covers the cleft and is one of the characteristics of pepsin-like proteases (Fig. 1.13). In eukaryotic aspartic proteases the flap opens during the catalytic cycle to allow the entrance of the substrate into the catalytic cleft; it then tightly covers the substrate/inhibitor removing effective contact between the solvent and residues P₁ and P₁' (the flap residue Tyr⁷¹ contributes to the binding of the side chains of the P₁ and P₂' residues) and releases the hydrolytic products.⁷⁹ Interestingly enough, conformational flexibility must be present in several side chains of both the inhibitor/substrate and enzyme, for the inhibitor to enter the cleft. This is particularly true for the side chains of P₁ Leu from the inhibitor and residues Thr⁷², Arg²³⁵, Ser³²⁸ and Thr³²⁹ around the cleft. Together, these residues create the narrowest point, a bottleneck, of the opening. The fact that these side chains

need to be rotated to avoid steric clashes when the inhibitor is entering the cleft, illustrates that the opening of the cleft is barely adequate for such a process. This observation is consistent with the hypothesis that the specificity for substrates of BACE-1 is governed by this narrow opening. In other words, even though the structural basis for the flap opening is still obscure, it is supposed to strongly contribute to hydrolytic specificity. Recently, the structure of unbound human BACE-1 protease domain has revealed a new position of the flap region, which appears to be locked in an “open” form.⁸⁰ The flap shows a large, 4.5 Å movement at the tip, which represents the main structural difference between the bound and unbound forms. This information offers new perspectives in the inhibitor design.

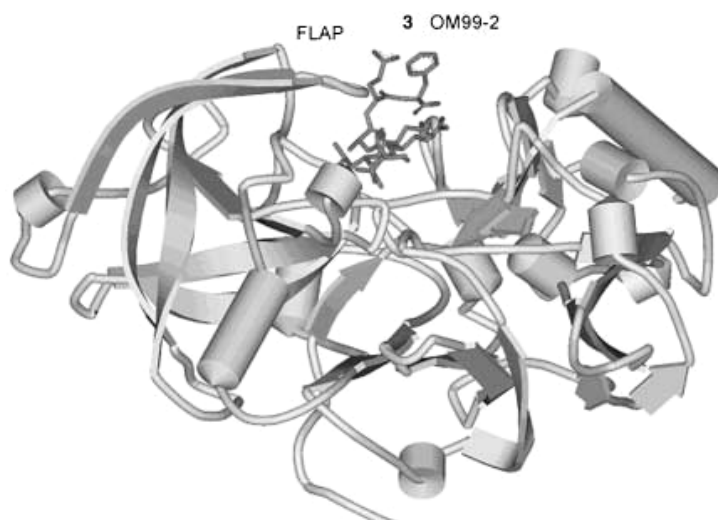


Figure 1.13. The side view of the crystal structure of BACE-1 complexed with OM99-2 illustrates the position of the flap region over the catalytic cleft.

Even though the overall structure of the β -secretase is very similar to pepsin, there are small differences in the positions of several surface loops that may impact substrate and inhibitor specificity. The most significant structural difference consists of six insertions and a C-terminal extension. The insertions together significantly enlarge the structure as compared to pepsin.⁶⁹ In addition,

the C-terminal portion, not completely resolved in the crystallographic analysis, is longer than those observed previously for aspartic proteases and conformationally quite different; it provides anchoring of the enzyme to the membrane. This transmembrane domain is responsible for localizing the enzyme in late Golgi compartments where it has access to the APP.⁸¹ In addition, as mentioned before, the disulfide pairings of the protein are atypical for pepsin family members. Disulfides are found at positions Cys²¹⁶-Cys⁴²⁰, Cys²⁷⁸-Cys⁴⁴³, and Cys³³⁰-Cys³⁸⁰ (Fig. 1.10). Disulfide bridges in the pepsin-like enzymes tend to connect residues that are near neighbours in the sequence; in this respect, the β -secretase is unusual in that it connects amino acids separated by 50 to 204 amino acids.

Inhibitors OM99-2 (H-Glu-Val-Asn-Leu*Ala-Ala-Glu-Phe-OH, with Leu*Ala representing the hydroxyethylene TSA) and OM00-3 (H-Glu-Leu-Asp-Leu*Ala-Val-Glu-Phe-OH) bind to the enzyme in essentially identical mode, as shown in Fig. 1.14.

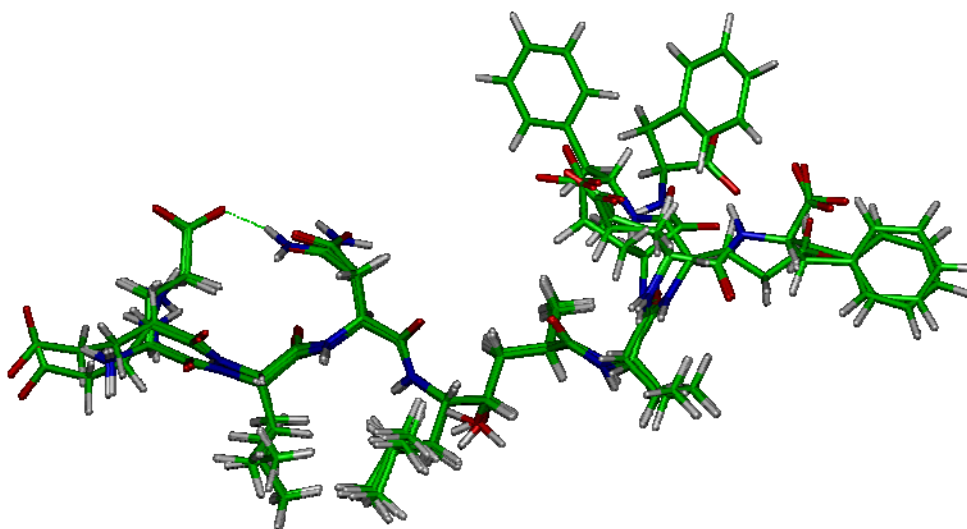


Figure 1.14. Superimposition of the X-ray structures of the BACE-1 inhibitors OM99-2 and OM00-3.

In the case of the BACE-1/OM99-2 complex, residues P₄-P₂' assume an essentially extended conformation with the active site aspartates positioned near

the TSA isostere at positions P₁ and P₁'. The backbone of the inhibitor deviates at Ala (P₂') from the extended conformation to produce a kink. The protease subsites S₄, S₃' and S₄' are hydrophilic and readily water accessible; this may explain the occurrence of two conformationally distinct binding modes of OM99-2 at residues P₃' and P₄'. Furthermore, with less defined electron density, the side chains of Glu and Phe appear to be located on the molecular surface and to interact weakly with the protease. These observations led to the hypothesis that the S₃' and S₄' subsites in BACE-1 were not well formed and perhaps contribute little to interactions with substrates and inhibitors. Thus, at P₂' the inhibitor points toward the protein surface as induced by a hydrogen bond of the hydroxyl group of Tyr¹⁹⁸ with the carbonyl oxygen of Ala (P₂'). An intramolecular hydrogen bond of OM99-2 between the side chains of Glu (P₄) and Asn (P₂) stabilizes the complex preventing interaction of the Glu side chain (P₄) with the protease and may also explain why the shorter analogue OM99-1, which lacks the P₄ residue is 10-fold less active.⁸²

In the OM00-3 structure the P₂ residue is Asp, which makes an interaction with Glu in P₄ unfavourable. Correspondingly, the newly observed S₄ pocket contributes more strongly to the inhibitor binding. In contrast to the OM00-2/BACE-1 complex, the conformation of residues P₃' and P₄' is well defined by electron densities and the extended conformation of the inhibitor is stabilized by a hydrogen bond from the P₃' backbone carbonyl to Arg¹²⁸.

1.2.3.4 Inhibitors of BACE-1: State of the Art

The broad-spectrum aspartic protease inhibitor pepstatin (Table 1.1, compound **1**) as well as the renin inhibitor remikiren and the human immunodeficiency virus-protease inhibitor saquinavir (Fig. 1.6) were unable to inhibit both BACE-1 and BACE-2.^{66,83} Using the amino acid sequence around the cleavage site of APP as P₁₀-P₄' peptide and (S)-statine (Sta) as P₁ residue the resulting

KTEEISEVNStaDAEF compound was found to weakly inhibit BACE-1 with an $IC_{50} \sim 40$ mM.⁶⁶ Replacement of the P_1' residue Asp by Val led to compound **2** with a significantly improved inhibitory activity of 30 nM (Table 1.1) which then allowed the affinity purification of the enzyme. Again the *S* configuration of the hydroxyethyl moiety in P_1 was found to be essential and displacement of the catalytic water by the 3-(*S*)-hydroxy group account for the slower association of the inhibitor compared with the substrate,⁸⁴ as proposed for other aspartic proteases.⁸⁵ As alternative to (*S*)-statine as TSA, the isosteric hydroxyethyl Leu*Ala dipeptide mimic was developed as a P_1 - P_1' mimetic for the design of BACE-1 inhibitors. Using the APP sequence and replacing the P_1' residue Asp by Ala, peptides **3** (OM99-2) and **4** were synthesized which behaved as tight-binding inhibitors with K_i values of 9.6 nM and 68 nM, respectively.⁸² Finally, applying synthetic libraries to identify the optimal amino acid composition of octameric inhibitors compound **5** (OM00-3, ELDL*AVEF) was obtained with a $K_i = 0.3$ nM,⁸⁶ while changes in P_1 and P_1' positions with the F*A or F*G dipeptide isosters led to lower potencies (see compound **6** of Table 1.1).⁸⁷ Even using the hydroxyethylene Ile*Val dipeptide isostere inhibitors more potent than related compounds with a statine-Val moiety were obtained,⁸⁸ confirming a general enhancement in potency for the hydroxyethylene derivatives over the statine analogues. Attempts to reduce the peptidic character in order to improve oral absorption and blood-brain barrier penetration led to compounds **7** and **8**.^{89,90} Non-peptidic inhibitors, known so far, are the tetraline **8**⁹¹ and latifolin⁹² (Fig. 1.15, **9** and **10**), for which the binding mode is not known.

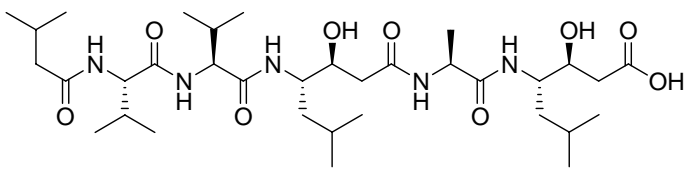
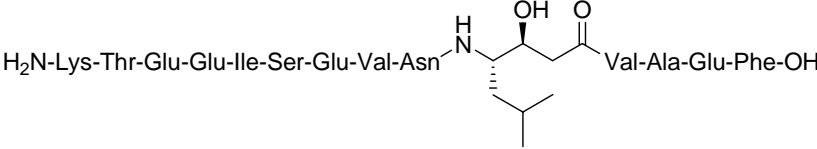
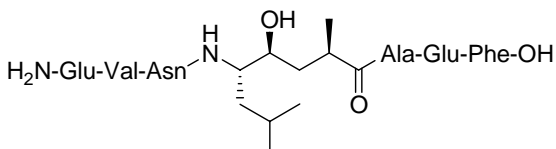
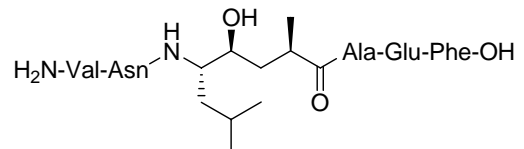
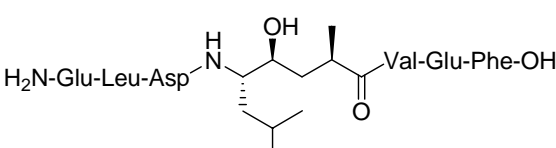
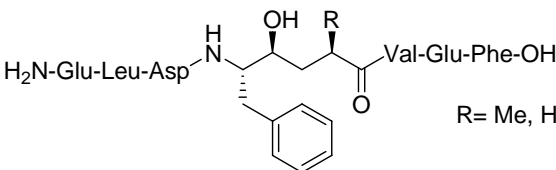
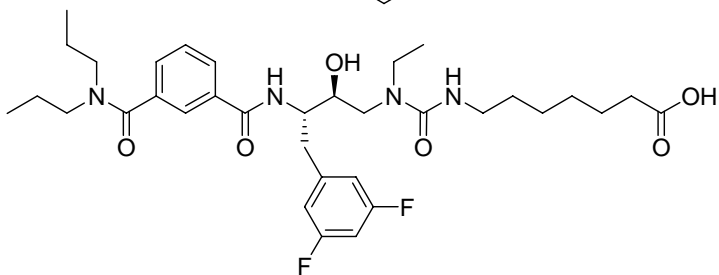
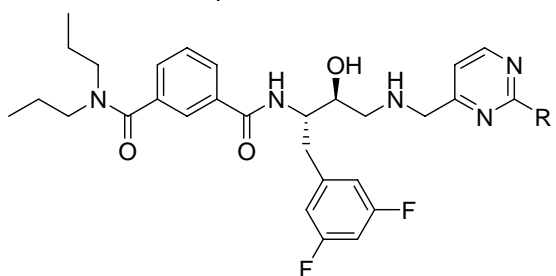
		K_i
1	 <p>pepstatin</p>	inactive
2	 <p>H₂N-Lys-Thr-Glu-Glu-Ile-Ser-Glu-Val-Asn-CH(CH₂-CH(CH₃)₂)-CH(OH)-C(=O)-Val-Ala-Glu-Phe-OH</p>	30nM
3	 <p>H₂N-Glu-Val-Asn-CH(CH₂-CH(CH₃)₂)-CH(OH)-C(=O)-Ala-Glu-Phe-OH</p> <p>OM99-2</p>	9.6nM
4	 <p>H₂N-Val-Asn-CH(CH₂-CH(CH₃)₂)-CH(OH)-C(=O)-Ala-Glu-Phe-OH</p>	68nM
5	 <p>H₂N-Glu-Leu-Asp-CH(CH₂-CH(CH₃)₂)-CH(OH)-C(=O)-Val-Glu-Phe-OH</p> <p>OM00-3</p>	0.3nM
6	 <p>H₂N-Glu-Leu-Asp-CH(CH₂-CH(CH₃)₂)-CH(OH)-C(=O)-Val-Glu-Phe-OH</p> <p>R= Me, H</p>	7nM
7		<50μM
8		<50μM

Table 1.1. Peptidic BACE inhibitors

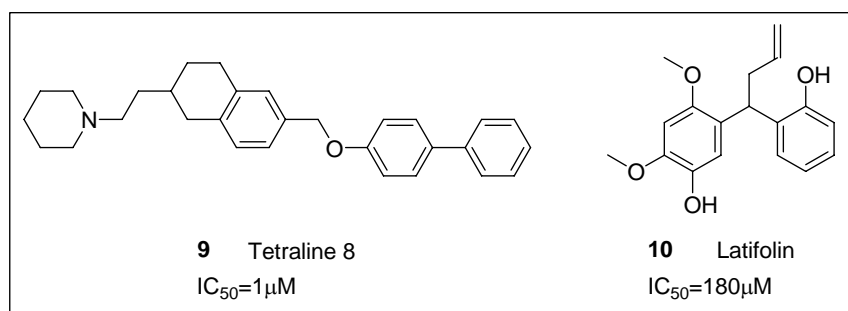


Figure 1.15. Non peptidic inhibitors of BACE.-1.

1.3 Matrix Metalloproteinases and their Role in Various Diseases

Matrix metalloproteinases (MMPs) are proteolytic enzymes that are involved in the remodelling of the extracellular matrix (ECM) in a variety of physiological and pathological processes. The ability to degrade extracellular proteins is essential for any individual cell to interact properly with its surroundings and for multicellular organisms to develop and function normally.

This was obviously known, but it was unquestionably proved only when it was shown for the first time that diffusible enzymes produced by fragments of involuting tadpole tail could degrade gels made of native fibrillar collagen.⁹³ Since then, a family of related enzymes has been identified in species from hydra to humans and collectively called matrix metalloproteinases because of their dependence on metal ions for catalytic activity, their potent ability to degrade structural proteins of the extracellular matrix, and specific evolutionary sequence considerations that distinguish them from other closely related metalloproteinases.⁹⁴

In addition to their ECM substrates, MMPs also cleave cell surface molecules and other pericellular nonmatrix proteins, thereby regulating cell behaviour in several ways.⁹⁵ Normal physiological processes such as foetal development, inflammatory cell migration, wound healing and angiogenesis depend on the controlled and concerted activity of these extracellular enzymes

and their natural endogenous inhibitors, tissue inhibitors of metalloproteinases (TIMPs). Under certain conditions, MMP expression or activation can become deregulated, resulting in pathological states such as cancer invasion and metastasis, arthritis, inflammatory and autoimmune diseases, tissue ulceration, atherosclerosis, aneurysm and heart failure.⁹⁶⁻¹⁰¹

For example, MMPs are invariably upregulated in rheumatoid arthritis and malignant cancer, with more severe increases often indicating a worse prognosis. Moreover, a major characteristic of these diseases is the capacity of cells to cross tissue boundaries and, in the case of cancer, spread to distant sites in the body. Thus, ECM-degrading enzymes must be present to break down the structural barriers to invasion. Extensive experimental work supports this supposition, but the mechanisms may be more complex than originally thought. Furthermore, in vivo genetic approaches that test the consequences of selective gains or losses of MMP function have led to the surprising finding that MMPs promote the initial stages of cancer development itself but may decrease the severity of the ultimate malignancy.^{102,103} In arthritis, the loss of certain MMPs surprisingly intensifies rather than alleviates the disease.¹⁰⁴ Considerable evidence implicates MMPs as important players in several biologic processes, yet the actual mechanisms underlying their influence are mostly unsolved. It is hoped that understanding these processes will result in a more rational approach toward reducing or entirely alleviating the ill effects of MMPs in diseases while maintaining their necessary and beneficial functions.

Because MMPs can catalyze the degradation of all the protein constituents of the ECM, it is important that their activities are kept under tight control to prevent tissue destruction. The activity of MMPs is regulated mainly in three ways: gene transcription, proenzyme activation and by the action of inhibitors. Harper *et al.* were the first able to demonstrate that MMPs are synthesized as inactive zymogens that require activation.¹⁰⁵ Later on, Bauer *et al.* showed the existence of the first of at least four endogenous metalloproteinase inhibitors, now

called tissue inhibitors of metalloproteinases, or TIMPs.¹⁰⁶ Since then, other levels of MMP regulation have been elucidated (*vide infra*), although, because of their complexity, other systems of control are still left to be fully understood. In particular, in addition to being differentially regulated at the level of transcription, MMPs can be controlled at the protein level by their endogenous activators and inhibitors and by factors that influence their secretion, their cell surface localization, and their own degradation and clearance. Moreover, higher organisms express multiple MMPs, each with its own profile of expression, localization, activation, inhibition, and clearance, as well as its own, sometimes broad, range of preferred substrates. Thus multiple modifiers, each with its own regulatory inputs, control different MMP functions *in vivo*.

1.3.1 The Metzincin Superfamily

The metalloproteases are classified into five superfamilies based on sequence considerations. Of these, the metzincin superfamily is distinguished by a highly conserved motif containing three histidines that bind zinc at the catalytic site and a conserved methionine turn that sits beneath the active site zinc.⁹⁴ In the characteristic zinc-binding motif HEBXHXBGBXHZ the His, Glu and Gly residues are invariant, B is a bulky hydrophobic residue, X is a variable residue, and Z is a family-specific amino acid. The metzincins are further subdivided into four multigene families, the serralysins, astacins, ADAMs/adamalsins, and MMPs, based primarily on the identity of the Z residue: Pro for serralysins, Glu for astacins, Asp for ADAMs/adamalsins and Ser for all but a few MMPs.⁹⁴

1.3.2 Structural Properties and Functions of MMPs

At present, 25 vertebrate MMPs and 22 human homologues have been identified,^{107,108} in addition to several nonvertebrate MMPs and MMPs from plant sources. Each of the vertebrate MMPs has distinct but often overlapping substrate

specificities, and together they can cleave numerous extracellular proteins, including virtually all ECM components. In addition to their conserved zinc-binding motif (usually **HEF/LGHS/ALGLXHS**, where bold-noted amino acids are always present) and “Met turn” (usually **ALMYP**), the MMPs share a common multidomain structure and a significant sequence homology, giving them a fairly conserved overall structure.⁹⁴

Individual MMPs are referred to by their common names or according to a sequential numeric nomenclature reserved for the vertebrate MMPs (Table 1.2). In addition, they are often grouped according to their modular domain organization structure (Fig. 1.16); it is also customary to divide them into four main classes on the basis of their preferred known substrates: collagenases, gelatinases, stromelysins and membrane-type (MT) MMPs. It has to be kept in mind that with the discovery that some MMPs have overlapping substrate specificities, the boundary between the previously used enzyme classes became blurred. Nevertheless, the trivial names are often useful, particularly if they reflect a function or a distinct structural feature or location, and they have therefore been retained (and are indicated in Table 1.2).

Most members of the MMP family are organized into three basic, distinctive, and well-conserved domains based on structural considerations: an amino-terminal propeptide, a catalytic domain, and a hemopexin-like domain at the C-terminus. The propeptide consists of approximately 80-90 amino acids containing a cysteine residue, which interacts with the catalytic zinc atom via its side chain thiol group. A highly conserved sequence (PRCGXPD) is present in the propeptide. Removal of the propeptide by proteolysis results in zymogen activation, as all members of the MMP family are produced in a latent form.¹⁰⁷

Members	MMP-n	Domain organization	Main substrates
Collagenases			
Interstitial Collagenases	MMP-1	b	ProMMP-2, proMMP-9, helical collagens
Neutrophil Collagenases	MMP-8	b	Helical collagens
Collagenase-3	MMP-13	b	Helical collagens
Collagenase-4 (<i>Xenopus</i>)	MMP-18	b	Helical collagens
Gelatinases			
Gelatinase A (72 kDa)	MMP-2	c	ProMMP-9, gelatin, elastin
Gelatinase B (92 kDa)	MMP-9	c	Gelatin, elastin
Stromelysins			
Stromelysin-1	MMP-3	b	ProMMP-1, proMMP-7, proMMP-8, proMMP-9, proMMP-13, aggrecan, matrix components
Stromelysin-2	MMP-10	b	Aggrecan, fibronectin
Stromelysin-3	MMP-11	d	Serpin, weak activity for matrix components
Membrane-type MMPs			
MT1-MMP	MMP-14	e	ProMMP-2, proMMP-13, helical collagen
MT2-MMP	MMP-15	e	Gelatin, fibronectin, ProMMP-2
MT3-MMP	MMP-16	e	ProMMP-2, proMMP-13
MT4-MMP	MMP-17	f	Gelatin, fibronectin
MT5-MMP	MMP-24	e	Gelatin, fibronectin, ProMMP-2, proMMP-13
MT6-MMP	MMP-25	f	Collagen IV, gelatin, fibronectin, ProMMP-2
Others			
Matrilysin	MMP-7	a	ProMMP-2, aggrecan, matrix components
Matrilysin	MMP-12	b	Elastin
Matrilysin	MMP-19	b	Collagen IV, gelatin, fibronectin
Enamelysin	MMP-20	b	Enamel matrix
XMMP (<i>Xenopus</i>)	MMP-21	g	α_1 -antitrypsin
CMMP (chicken)	MMP-22	b	Not known
CMMP (chicken)	MMP-23	h	Gelatin
Endometase, Matrilysin-2	MMP-26	a	Collagen IV, gelatin, fibronectin
Endometase, Matrilysin-2	MMP-27	b	Not known
Epilysin	MMP-28	d	Casein

Table 1.2. Members of the vertebrate MMP family.

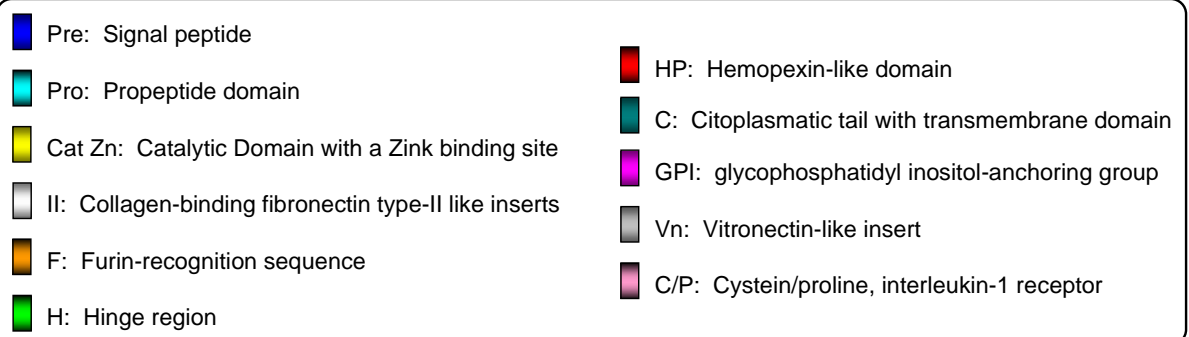
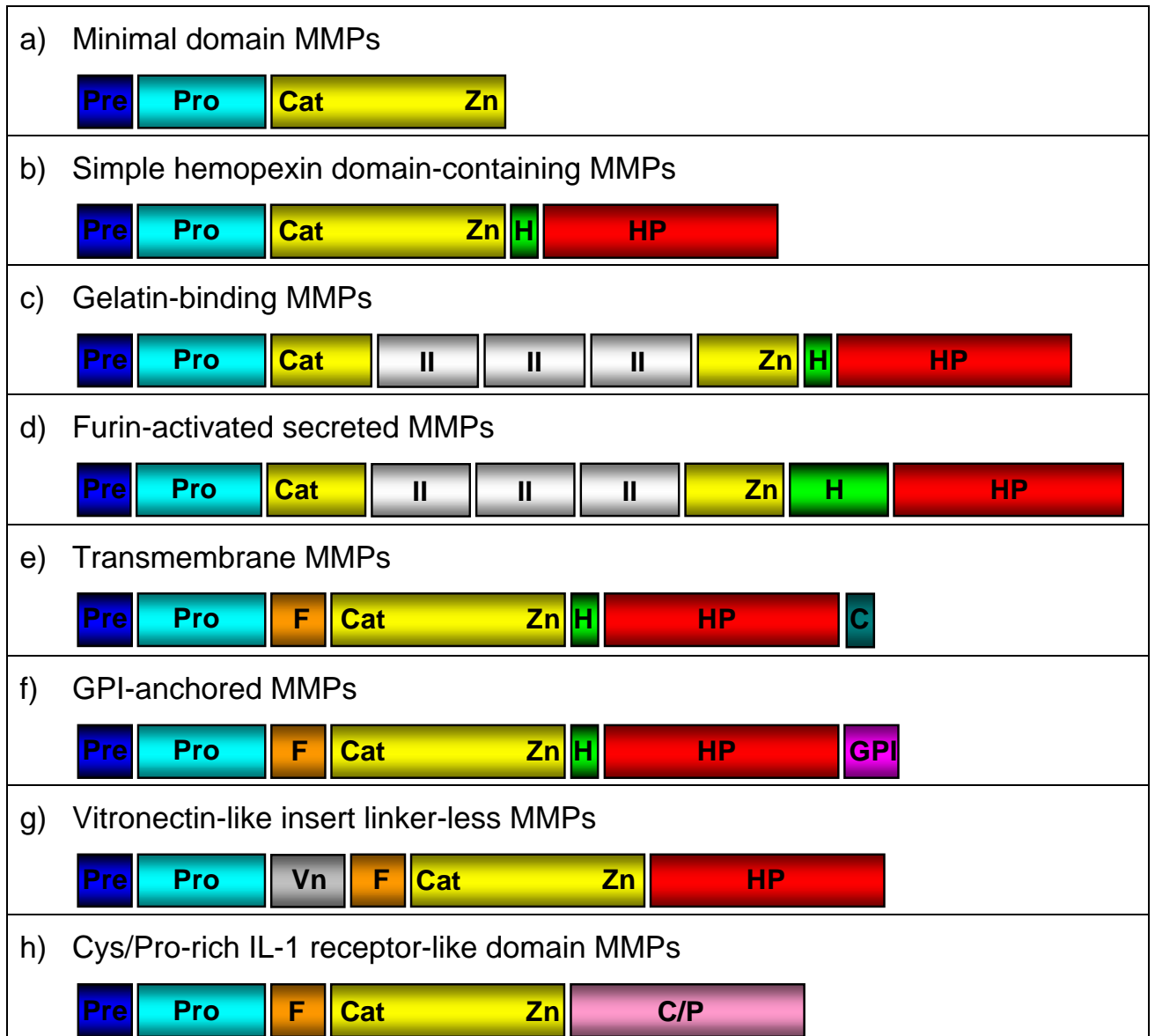


Figure 1.16. Schematic representation of the domain structures of the MMPs.

The about 170-residues catalytic domain contains the conserved zinc-binding region, two zinc ions and at least one calcium ion coordinated to various residues. One of the two zinc ions is present in the active site and is involved in the catalytic processes of the MMPs. The second zinc ion (also known as structural zinc) and the calcium ion are present in the catalytic domain approximately 12 Å away from the catalytic zinc. The catalytic zinc ion is essential for the proteolytic activity of MMPs; the three histidine residues that coordinate with the catalytic zinc are conserved among all the MMPs. Little is known about the roles of the second zinc ion and the calcium ion within the catalytic domain, but the MMPs are shown to possess high affinities for structural zinc and calcium ions.^{109,110} The catalytic domain dictates cleavage site specificity through its active site cleft, through specificity sub-site pockets that bind amino acid residues immediately adjacent to the scissile peptide bond, and through secondary substrate-binding exosites located outside the active site itself.

In both gelatinases MMP-2 and -9, the catalytic domains have an additional 175-amino acid residues insert comprising three head-to-tail cysteine-rich repeats conferring gelatin and collagen binding. These inserts resemble the collagen-binding type II repeats of fibronectin and are required to bind and cleave collagen and elastin.^{111,112} This domain, known as the gelatin binding domain or fibronectin type-II like domain, is unique to the gelatinases, and so these enzymes are regarded as a separate subgroup among members of the MMP family. In addition, MMP-9 has a unique type V collagen-like insert of unknown importance at the end of its hinge region.

All MMPs, with the exception of MMP-7 (matrilysin), MMP-26 (endometase/matrilysin-2), and MMP-23, have an about 195-residues C-terminal hemopexin-like domain that is connected to the catalytic domain by a hinge or linker region. MMP-7 and MMP-26 merely lack these extra domains, whereas MMP-23 has unique cysteine-rich, proline-rich, and IL-1 type II receptor-like domains instead of a hemopexin domain.^{113,114} When present, the hemopexin

domain influences TIMP binding, the binding of certain substrates, membrane activation, and some proteolytic activities. For example, chimeric enzyme studies indicate that both ends of MMP-1 (collagenase-1) are required for it to cleave native fibrillar collagens.^{115,116} This collagenolytic activity requires the initial binding and orientation of the collagen fibril (which is normally resistant to proteolysis), local unwinding of its triple-helical structure, and a characteristic cleavage at $\frac{3}{4}$ length of each α -chain individually, because the catalytic cleft is too narrow to accommodate the entire triple helix. Apparently, the hemopexin domain participates in all but the last of these steps. Interestingly enough, removal of this haemopexin-like domain in the collagenases eliminates their characteristic capability to cleave triple-helical collagen, but does not significantly affect hydrolytic activity toward gelatin, casein or synthetic substrates.¹¹⁷

The hinge region, in turn, connecting the catalytic domain and the hemopexin-like domain, varies in length (from 10 to 70 residues) and composition among the various MMPs and also affects substrate specificity.¹¹⁸

Finally, the membrane-type (MT) MMPs possess an additional 75- to 100-residue extension, which presumably forms a single-pass transmembrane domain and a short cytoplasmic C-terminal tail (MMPs 14, 15, 16, and 24) or a C-terminal hydrophobic region that acts as a glycosylphosphatidylinositol (GPI) membrane anchoring signal (MMP-17 and MMP-25).¹¹⁹⁻¹²¹ These domains play an essential role in the localization of several important proteolytic events to specific regions of the cell surface.

The hemopexin-like domain of MMPs is highly conserved and shows sequence similarity to the plasma protein hemopexin. The hemopexin-like domain has been shown to play a functional role in substrate binding and/or in interactions with the tissue inhibitors of metalloproteinases (TIMPs), a family of specific MMP protein inhibitors.¹²² In addition to these basic domains, the family

of MMPs evolved into different subgroups by incorporating and/or deleting structural and functional domains.

1.3.3 Regulation of MMP Activity

Once activated, MMPs are subject to inhibition by endogenous proteinase inhibitors such as α 2-macroglobulin and more importantly the family of tissue inhibitors of metalloproteinases, TIMPs 1-4.¹²³⁻¹²⁶ These negative regulatory controls are clearly important for a family of enzymes with such destructive potential. Finely regulated MMP activity is associated with processes of ovulation,¹²⁷ trophoblast invasion,¹²⁸ skeletal¹²⁹ and appendageal development,¹³⁰ and mammary gland involution.¹³¹ However, it appears that these controls do not always operate as they should, and there is now a substantial body of observational and experimental data which indicates that inappropriate expression of MMP activity constitutes part of the pathogenic mechanism in several diseases. These include the destruction of cartilage and bone in rheumatoid and osteoarthritis,^{97,132} tissue breakdown and remodeling during invasive tumour growth and tumour angiogenesis,¹³³ degradation of myelin-basic protein in neuroinflammatory diseases,^{134,135} opening of the blood-brain barrier following brain injury,¹³⁶ increased matrix turnover in restenotic lesions,¹³⁷ loss of aortic wall strength in aneurysms,¹³⁸ tissue degradation in gastric ulceration,¹³⁹ and breakdown of connective tissue in periodontal disease.¹⁴⁰ As the role of MMPs in disease has become better understood, interest in the control of their activity has increased. This has led to considerable effort, largely on the part of the pharmaceutical industry, in the development of MMP inhibitors.

In keeping with their potential for tissue destruction, MMPs are rigorously regulated at multiple levels, including transcription, activation of the zymogen forms, extracellular inhibitors, location inside or outside the cell and internalization by endocytosis. The first level of regulation is given by the pro-

domain, that keeps the enzyme latent using the thiol group of a highly conserved, unpaired cysteine at its carboxyl terminus. This conserved cysteine acts as a fourth inactivating ligand for the catalytic zinc atom in the active site, resulting in the exclusion of water and rendering the enzyme inactive (Fig. 1.17). For the enzyme to be activated, this cysteine-zinc pairing needs to be disrupted by a conformational change or by proteolysis (such as by the protease plasmin or by other MMPs). Once the thiol group is replaced by water, the enzyme is able to hydrolyze the propeptide to complete the activation process and can then cleave the peptide bonds of its substrates. This system of regulation is referred to as the “cysteine-switch” mechanism.¹⁴¹ Most MMPs are not activated until they are outside the cell, but the MT-MMPs and MMP-11, MMP-23 and MMP-28 are activated by a proprotein convertase (such as furin) within the secretory pathway.^{119,142-144}

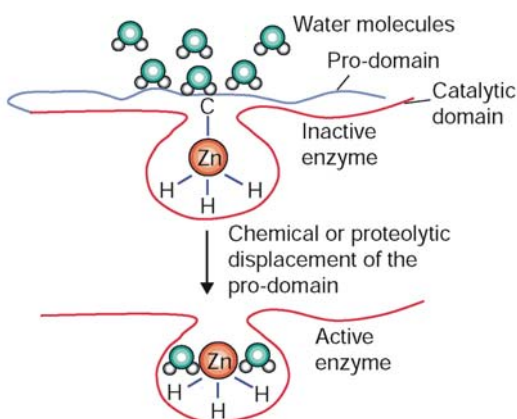


Figure 1.17. The “cysteine-switch” mechanism¹⁴¹ regulating the MMP zymogen. The thiol group of a conserved cysteine (C) at the carboxyl terminus of the pro-domain acts as a fourth inactivating ligand for the catalytic zinc atom in the active site; this results in the exclusion of water and keeps the enzyme latent. Displacement of the pro-domain by conformational change or proteolysis disrupts this cysteine-zinc pairing and the thiol group is replaced by water. The enzyme can then cleave the peptide bonds of its substrates.

Once activated, there are multiple mechanisms that can inactivate the MMPs.¹⁴⁵ Four classes of metalloproteinase inhibitors are found in extracellular spaces and body fluids that have broad inhibitory activity against many MMPs. One class is the tissue inhibitors of metalloproteinases (TIMPs), presently including four proteins (TIMP-1, TIMP-2, TIMP-3, and TIMP-4), which are disulfide-bonded proteins of 20-30 kDa that directly interact with the MMP active site through a small number of their amino acids.

Other molecules have been proven to function as endogenous inhibitors for MMPs. For example, an unrelated small inhibitor derived by proteolysis of the procollagen C-proteinase enhancer has structural similarity to TIMPs and may inhibit MMPs through a similar mechanism.¹⁴⁶

Recently, a membrane-anchored molecule, reversion-inducing cysteine-rich protein with Kazal motifs (RECK), has been discovered that appears to regulate MMP-2, MMP-9 and MMP-14 post-transcriptionally by affecting secretion and activation as well as by inhibition of the active site¹⁴⁷ (Fig. 1.18).

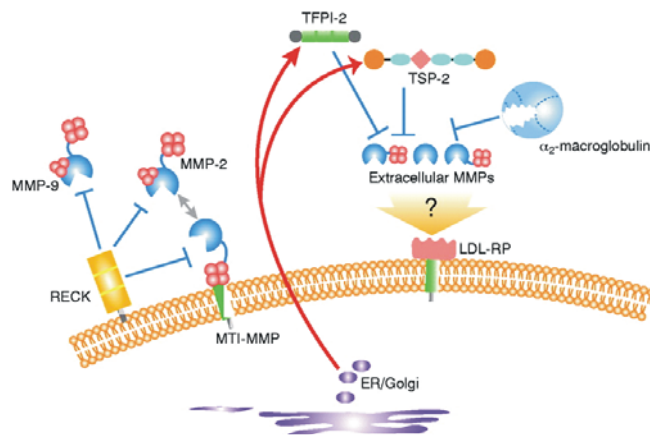


Figure 1.18. Inhibitors of matrix metalloproteinase. RECK (reversion inducing cysteine rich protein with Kazal motifs) is a GPI-anchored glycoprotein that binds and inhibits a number of MMPs. The pan proteinase inhibitor α_2 -macroglobulin, although very large, has some access to the pericellular space in vascularised tissues and may be involved in MMP endocytosis through the low density lipoprotein receptor-related protein (LDL-RP). The roles of the LDL-RP in MMP-2 removal via a thrombospondin-2 (TSP-2) complex and in direct MMP-9 removal have been described. The tissue factor pathway inhibitor (TFPI-2) has also been described as an MMP binding agent.

In the circulation, the protease inhibitor α 2-macroglobulin inactivates active MMPs by a “bait and trap” mechanism:^{145,148} when protease-sensitive sites within the inhibitor are cleaved, it closes around the proteinase and isolates it from potential substrates.

1.3.4 Structure of MMPs

The first X-ray crystal structures of the catalytic domains of human fibroblast collagenase/MMP-1¹⁴⁹⁻¹⁵¹ and human neutrophil collagenase/MMP-8,^{109,152} and a nuclear magnetic resonance (NMR) structure of the catalytic domain of stromelysin-1/MMP-3¹⁵³ became available only in early 1994. They were later complemented by additional catalytic domain structures of MMP-1,^{154,155} matrilysin/MMP-7,¹⁵⁶ MMP-3,^{122,157-160} MMP-8^{161,162} and MT1-MMP.¹⁶³ In 1995, the first X-ray structure of an MMP pro-form, the C-terminally truncated pro-stromelysin-1, was published,^{157,160} and the first and only structure of a mature full-length MMP, namely of porcine fibroblast collagenase/MMP-1,¹⁶⁴ was described. At that time, structures of the isolated haemopexin-like domains from human gelatinase A/MMP-2^{165,166} and from collagenase-3/MMP-13^{167,168} were also reported.

1.3.4.1 The MMP Catalytic Domain

The catalytic domains of the MMPs exhibit the shape of an oblate ellipsoid. In the “standard“ orientation, which is in most MMP papers the preferred orientation for the display of MMPs, a small active-site cleft is carved into the flat ellipsoid surface and extends horizontally across the domain to bind peptide substrates from left to right (Fig. 1.19).

This cleft harbouring the “catalytic zinc” separates the smaller “lower subdomain” from the larger “upper subdomain”. This upper subdomain formed by the first three quarters of the polypeptide chain (up to Gly225) consists of a

five-stranded β -pleated sheet, flanked by three surface loops on its convex side and by two long regular α -helices on its concave side embracing a large hydrophobic core. In the active-site, helix hB (Fig. 1.19) provides the first (218) and the second His (222) that bind the catalytic zinc; between them, the “catalytic Glu²¹⁹”, all of them representing the N-terminal part of the so called “zinc-binding consensus sequence” HEXXHXXGXXH characteristic of the metzincin superfamily.^{94,169}

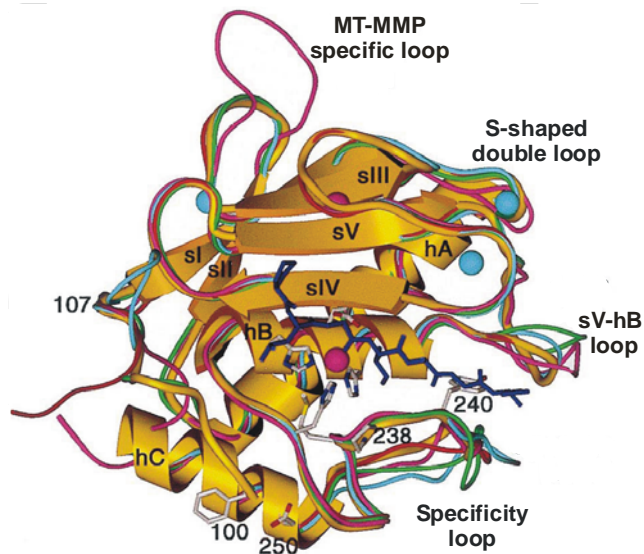


Figure 1.19. Ribbon structure of the MMP catalytic domain shown in standard orientation. The catalytic domain of MMP-8¹⁵² shown together with the modelled heptapeptide substrate¹⁶¹ (dark blue) is superimposed with the catalytic domains of MMP-3¹²² (blue), MMP-1¹⁴⁹ (red), MMP-14¹⁶³ (pink) and MMP-7¹⁵⁶ (green). The catalytic and the structural zinc (center and top) and the three calcium ions (flanking) are displayed as pink and blue spheres, respectively, and the three His residues liganding the catalytic zinc, the catalytic Glu in between, the characteristic Met, the Pro and the Tyr of the S₁' wall-forming segment, the N-terminal Phe and the first Asp of the Asp pair forming the surface-located salt bridge are shown with all nonhydrogen atoms. The chain segment forming the extra domain of both gelatinases will be inserted in the sV-hB loop (center, right) and presumably extends to the right side.

Besides the catalytic zinc, all MMP catalytic domains possess another zinc ion, the structural zinc, and two (MMP-8, MT1-MMP) or three bound calcium ions (MMP-1, MMP-3, MMP-7). In the vast majority of MMPs, the structural zinc is coordinated by three His residues and by one carboxylate oxygen of an

Asp residue. This zinc is completely buried in the protein matrix; the impossibility of exchanging it in the MMP-8 crystals¹⁰⁹ suggested its extremely tight binding.

The overall structures of all MMP catalytic domains known so far are very similar, with the collagenase structures resembling one another most, and MMP-7 and the MT1-MMP structures deviating most.

1.3.4.2 The MMP Pro-Domain and Hemopexin-like Domain

The pro-peptide has an egglike shape, attached with its rounded-off side to the active site of the catalytic domain (Fig. 1.20). It essentially consists of three mutually perpendicular α -helices and a segment connecting it with the catalytic domain.

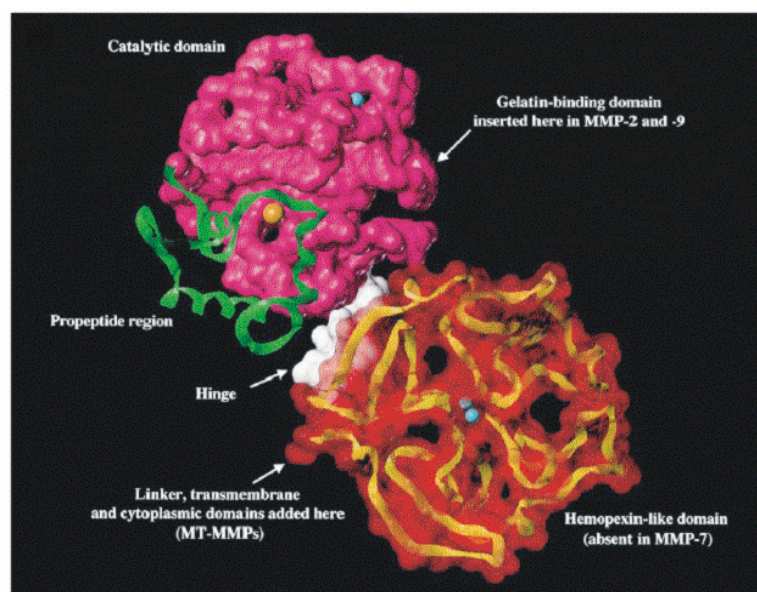


Figure 1.20. Modelled structure of the full length proMMP. The images for the propeptide region and the catalytic and homopexin-like domains shown here are from different crystallographic sources. The propeptide region and the catalytic domain are taken from the X-ray structure for MMP-3¹⁵⁷ and the remaining portions of the structure are taken from the X-ray structure of the full-length MMP-1.¹⁶⁴ Catalytic zinc is shown as an orange sphere; calcium ions in the catalytic domain and the hemopexin-like domain are shown in cyan. The propeptide region is shown by the green ribbon, catalytic domain as a surface in pink, hinge region as a surface in white, and the hemopexin-like domain is represented by the ribbon drawing in yellow.

Along with the conserved -VAAHEXGHXXGXXH- sequence of the catalytic domain,^{169,170} a second conserved sequence - P⁹⁰RCGXP⁹⁶ - is found in the propeptide amino-terminal domain. The thiol group of the cysteine residue within the propeptide coordinates the catalytic zinc atom and thereby confers latency, as seen before. This interaction must be broken by proteolytic cleavage or conformational modification, of the amino-terminal domain, before the metalloproteinase can degrade matrix proteins. The weakening and finally destruction of the Cys-catalytic zinc interaction, eventually leads to a liberation and flexibilization of the activation cleavage peptide bond (as originally predicted by the “cysteine switch hypothesis”¹⁴¹). In this movement, the Pro¹⁰⁷ residue acts as a flexible joint, with its main chain angles changing from an α -helix-like (in the proform) to a polyproline-II-like conformation (in the mature form). It might be worth noticing that from this Pro residue onwards the polypeptide chain of the pro-MMP is in register with that of the mature, activated MMPs.

Except for MMP-7, all vertebrate and human MMPs are expressed with a C-terminal haemopexin-like domain. The haemopexin-like domains of the classical MMPs have the shape of an oblate ellipsoidal disc and exhibit very similar structures.¹⁶⁴⁻¹⁶⁷

1.3.5 The Reaction Mechanism

The reaction mechanism for proteolysis by MMPs¹⁷¹ has been rationalized on the basis of structural information (Fig. 1.21).¹⁵⁴ It is proposed that the scissile amide carbonyl coordinates to the active-site zinc(II) ion. This carbonyl is attacked by a water molecule that is both hydrogen bonded to a conserved glutamic acid (Glu¹⁹⁸ in MMP-8) and coordinated to the zinc(II) ion. The water donates a proton to the Glu residue which transfers it to the nitrogen of the scissile amide with resultant peptide bond cleavage. During this process the positively charged zinc(II) ion helps to stabilize the negative charge at the carbon

of the scissile amide and a conserved alanine (Ala¹⁶¹ in MMP-8) residue helps to stabilize the positive charge at the nitrogen of the scissile amide.¹⁵⁴

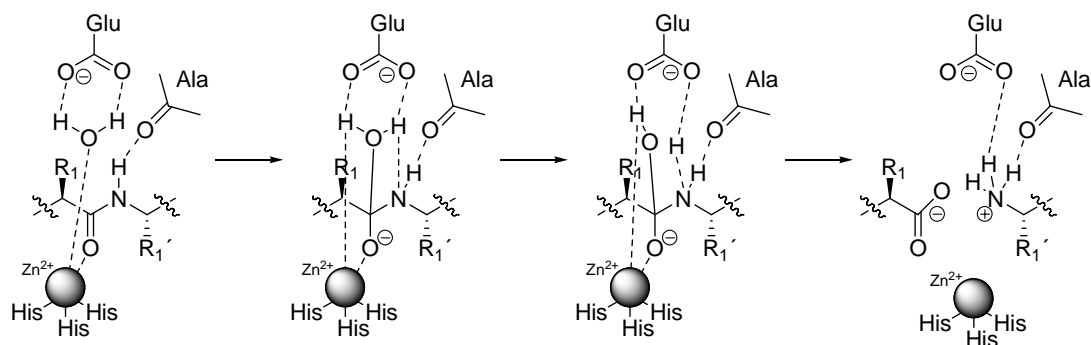


Figure 1.21. Reaction mechanism for proteolysis by MMPs described by Lovejoy *et al.*¹⁵⁴

Comparison of the structures of the various MMP inhibitor complexes reveals valuable information on the differences in the active sites of the MMPs studied and on the binding modes of inhibitors.¹⁷² A schematic representation of a hexapeptide substrate bound into an MMP active site is given in Figure 1.22.

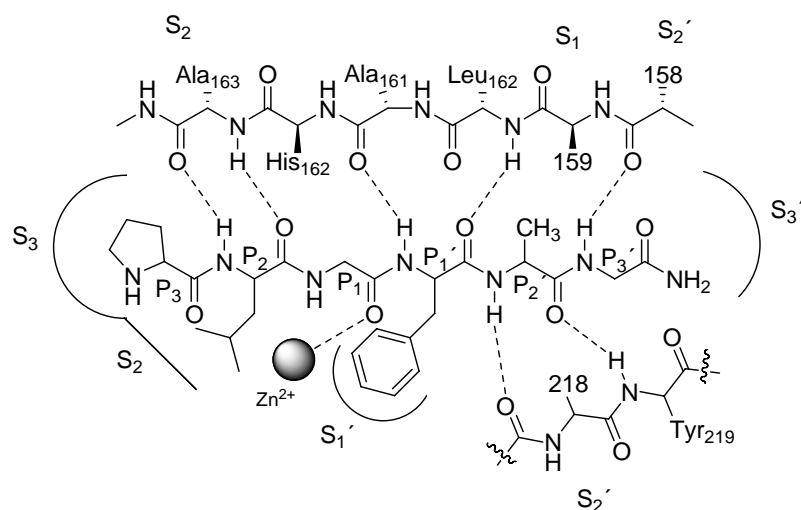


Figure 1.22. Schematic representation of MMP active-site with the substrate Pro-Leu-Gly-Phe-Ala-Gly-NH₂.¹⁶¹ Numbering follows that for MMP-8.

The S₃-S₁ subsites form a shallow region bordered on one side by the β-strand IV and which features a hydrophobic proline binding cleft at S₃. Proline is a preferred P₃ group in MMP substrates as shown for inhibitor Pro-Leu-Gly-NHOH ligated to the catalytic domain of MMP-8.^{109,161}

Differences between the various MMPs in the S₃-S₁ region are relatively subtle. However, substantial differences in enzyme selectivity have been reported for thiadiazolyl MMP inhibitors, which have been observed from structural studies to bind to the unprimed enzyme subsites.^{173,174} A significant interaction between the MMPs and their substrates or inhibitors occurs between the S₁' subsite and the P₁' residue. There are variations between the MMPs in the amino acid residues that form the S₁' pocket and for this reason the S₁' pocket is referred to as the “selectivity pocket”. It is supposed that inhibitors can be obtained which exhibit degrees of enzyme selectivity for the known MMPs, and there has been considerable debate concerning the possible therapeutic advantages of selective inhibition. From X-ray crystallographic analysis and homology modeling the MMPs may be classified as falling into two broad structural classes dependent on the depth of the S₁' pocket. This “selectivity pocket” is relatively deep for the majority of the enzymes (e.g., MMP-2, MMP-9, MMP-3, MMP-8, MMP-13, etc.), but for certain enzymes (e.g., MMP-1, MMP-7, and MMP-11) it is partially or completely occluded due to an increase in the size of the side chain of the amino acid at position 193 from leucine to arginine (MMP-1), tyrosine (MMP-7), glutamine (MMP-11), or one of the amino acid residues that form the pocket.

The S₂' subsite is a solvent-exposed cleft with a general preference for hydrophobic P₂' residues in both substrates and inhibitors. The S₃' subsite is a relatively ill-defined solvent exposed region. While there are some variations in residues for this subsite for the various MMPs, the introduction of different P₃' substituents in general tends to have only a modest effect on inhibitor selectivity.

1.3.6 Matrix Metalloproteinase Inhibitors

The hallmark of diseases involving MMPs appears to be a stoichiometric imbalance between active enzymes and TIMPs, leading to excessive tissue disruption, and often degradations. It is this imbalance that a pharmacological approach, based on specific enzyme inhibitors, promises to readdress.

Both small molecules (synthetic and natural products) and macromolecular endogenous inhibitors such as TIMP-1 and TIMP-2 have been considered as potential therapies for diseases in which excess MMP activity has been implicated. Various research groups have attempted large-scale production of TIMPs with the aim of reaching therapeutic trials. However, technical difficulties with the production and use of these proteins have so far prevented their development.

Big efforts have been put in the development of small molecule inhibitors, which have produced a large quantity of compounds,¹⁷⁵ some of which have been tested in clinical trials.

There are mainly three requirements for a molecule to be an effective inhibitor of the MMP class of enzymes. The first important requirement is relative to the center of inhibitory activity: various functional groups capable of chelating the active-site zinc(II) ion have been exploited (such as carboxylic acid, hydroxamic acid, and sulfhydryl, etc.). This group is normally referred to as zinc binding group or ZBG. Further features for an active inhibitor are at least one functional group which provides a hydrogen bond interaction with the enzyme backbone, and one or more side chains which undergo effective van der Waals interactions with the enzyme subsites. It is now clear that these requirements can be satisfied by a variety of different structural classes of MMP inhibitors which have been discovered by a number of methods including structure-based design and combinatorial chemistry.¹⁷⁶

The discovery of MMP inhibitors accelerated these methods and followed a substrate-based approach to inhibitor design which had been pioneered by early workers in the field.¹⁷⁷ The earliest MMP inhibitors were designed from a knowledge of the amino acid sequence of human triple helical collagen at the site of cleavage by MMP-1 and subsequently using information derived from substrate specificity studies. In the substrate-based design, a ZBG is attached to peptide derivatives which mimic part of the cleaved sequence.

The worldwide effort on MMP research has led to the discovery of a remarkably diverse group of compounds which are effective inhibitors of these enzymes. Despite this structural diversity, it has not yet been possible to identify specific inhibitors for each of the MMP enzymes. Only an exiguous number of compounds have been identified which exhibit a preference for the inhibition of MMPs with a deep S₁' pocket over those with a short S₁' pocket.

Thus, MMP inhibitors may be an important new class of therapeutic agents for the treatment of diseases characterized by excessive extracellular matrix degradation and/or remodeling, such as cancer and chronic inflammatory diseases such as rheumatoid arthritis, atherosclerosis, and MS. In addition, they may also be useful in more acute inflammatory settings such as stroke and meningitis.

2. **Aim of the Present Work**

As discussed in the introductory chapter, the aspartic-protease BACE-1 and the metallo-protease MMP-9 have been recognized as most promising drug targets for serious diseases. For both proteases potent inhibitors have been produced in the academic and industrial research which however did not fulfil the requirements for an application to in vivo biological and clinical studies. Aim of the present work was to attempt a structure based-design of new lead structures that would allow their conversion into highly selective and potent inhibitors well suited for biological studies.

The identification of BACE-1 as the major responsible enzyme for the development of AD plaques has attracted great attention over the last years. The common efforts of various laboratories led to the discovery of peptidic inhibitors that exploit the transition-state inhibition concept and the large substrate binding cleft of this aspartic protease to achieve potency and selectivity. Together with various advantages such as the lack of accumulation in organs, low toxicity, and low immunogenicity, peptidic inhibitors exhibit undesired properties, when compared to small molecules: protease sensitivity, limited oral availability, fast clearance rates, unfavourable intracellular targeting, and inability to cross the blood-brain barrier. Therefore conversion of such peptidic inhibitors into peptidomimetic structures is essential for studying the pathophysiological role of BACE-1. This can be accomplished either by chemical modification of the amide bonds of the peptide molecule itself, or by modification of the peptide backbone structure. For this purpose in first instance the aim was to analyze peptoidic and retro-inverted peptidic structures for their usefulness in the design of BACE-1 inhibitors. Alternatively, conformational constraints should be exploited to lock-

in β -type extended structures as it was known from the X-ray structures of BACE-1/inhibitor complexes that this aspartic protease binds larger substrate-based peptidic inhibitors in extended conformation. The use of cyclic scaffolds was expected to freeze inhibitory peptides into β -strand conformations and thus to preorganize them for binding to the protease. An increase of binding affinities by entropic contributions and enhanced enzyme resistance and thus reduced biological clearance rates should be the beneficial effects of such peptide cyclizations. In this context, exchange of the transition state-analogue statine by a double-substituted analogue containing at the C-2 carbon an additional substituent mimicking the P_1' residue was suggested by modelling experiments.

In the case of MMPs numerous inhibitors have been reported to exhibit high and even subnanomolar binding affinities, but generally with limited specificity among these metallo-proteases. Because of the broad-spectrum activities of most of the known MMP inhibitors, an association of single MMPs to well defined (patho)physiological events has been very difficult. Aim of the study was to address this essential problem by designing inhibitors that allow to discriminate the biological functions of gelatinases (MMP-2 and MMP-9) and other members of the MMPs family, in particular collagenases. A possible approach to the design of highly specific inhibitors was expected from the principle of multivalency that exploits the additivity of the free energy of binding of two spacer-linked heads to two sites of the enzyme, i.e. the active site and an exosite. Since the gelatinases contain, in addition to the catalytic domain, the fibronectin domain which binds and orients gelatine for its degradation, attempts should be made to construct bivalent inhibitors that address simultaneously the catalytic active site with a metallo-coordinating head group and the fibronectin domain with a specifically designed peptide moiety. Highly selective inhibition of MMP-9 was expected from this novel concept.

3. Results and Discussion

3.1. Structure-based Design of BACE-1 Inhibitors

The known BACE-1 inhibitors discussed in the introductory chapter are of peptidic nature and peptides are usually characterized by high clearance rates because rapidly degraded in vivo by proteases. By oral application, peptides are known to be digested by the enzymes from the gastric and intestinal juices rich in proteases such as trypsin or chymotrypsin. Furthermore, the brush border membrane (the highly specialized mucosa of the small intestine that is responsible for the absorption of many nutrients) and the cytosol of the absorptive cells are full of proteases that will degrade such peptides making even cellular experiments rather difficult. To develop peptides enzymatically more resistant inhibitors peptidomimetic structures are required.¹⁷⁸ The main approach in first instance is generally on replacement of the protease sensitive amide moiety.

Although backbone modifications in peptides can affect the conformational properties, biopotency and enzymatic stability of the resulting analogues, this approach has attracted considerable attention. It consists of incorporation of non-proteinogenic or unnatural amino acids, modification of peptide bonds and/or the replacement of L- by D-amino acid residues.

3.1.1 Peptoid and Retroinverted Peptide Approach

Among the various methods of isosteric peptide bond modifications, the peptoid strategy has attracted considerable interest. Peptoids consist of N-substituted glycines where the side chains of the α -carbon atoms of the peptide chain are shifted by one position along the backbone to the nitrogen atom.¹⁷⁹ The

resulting compound is a polymer of N-substituted glycines which, aligned with the peptide with the side chains in register, presents the carbonyl groups shifted to the right by one position. In order to maintain the relative orientation of the carbonyl groups and the side chains, the order of the amino acids has to be reversed in the peptoid sequence (Fig. 3.1).

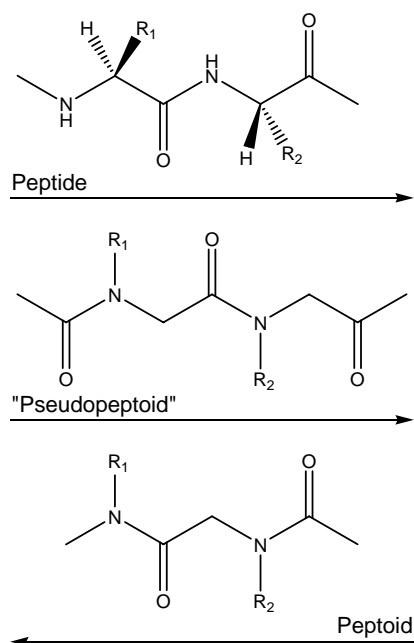


Figure 3.1. Comparison of a peptide, pseudo-peptoid and peptoid chains.

A comparison of peptides and peptoids backbones shows that peptoids are achiral and that, being the nitrogen trisubstituted, hydrogen bonds are possible only between the carbonyls and hydrogen donors from other side chains. This has important consequences for the secondary structure of a peptoid. Furthermore, peptoids are more hydrophobic than the corresponding peptides, which makes them suitable candidates in the search for peptidomimetics that target intracellular receptors. In summary this type of structures offers various advantages^{180,181}:

- 1) Like other N-alkylated peptides,^a peptoids are metabolically stable and resistant to the most common proteases¹⁸² and thus even in blood plasma.¹⁸³
- 2) The chemical synthesis is simple and a great variety of functional groups can be incorporated.^{181,184}
- 3) The higher flexibility of the backbone (if compared with the corresponding peptide) and the lack of chirality allow probing of a large conformational space.
- 4) Biologically active small peptoids (di-, tri-, and tetrapeptoids) comply with the Lipinski/Veber rules^{185,186} (depends on the structure of the side-chains and end-capping groups) and thus are excellent candidates for orally available drugs. However, a comparative study¹⁸³ of the oral availability in rat of a labelled tetrapeptide and an end-capped tripeptoid, having the same side chains, revealed that the peptide has a much better oral bioavailability than the peptoid. Nevertheless some peptoids and peptoid-peptide hybrids are in clinical trials.

Another widely used peptidomimetic approach is based on retro-inverso analogues of natural peptides. This modification, which affects the backbone of peptides but not the orientation of side chains, has been introduced in many biologically active peptide analogues. Retro-inverso peptides (also called all-D retro-peptides or retro-enantio-peptides), are composed of D-amino acid residues assembled in the reverse order of the parent L-sequence (Fig. 3.2). By this way the orientation of the side chains is very similar to that of the parent peptide, while the direction of the peptide bonds is reversed, i.e. [$\Psi(\text{NH-CO})$ instead of the parent $\Psi(\text{CO-NH})$ peptide bond]; in other words the carbonyl groups and the nitrogen atoms are switched. Consequently, the retro-inverso modification of

^a The nomenclature of the peptoids monomers that have the same side chain as a corresponding amino acid, consists of an N prefix followed by the three letter code of the amino acid in small letters or an n prefix followed by the one letter code of the amino acid in capital letters.

peptides preserves the overall topology of the parent L-peptide. At the same time the reversed amide bonds enhance stability toward hydrolysis and enzymatic degradation.¹⁸⁷⁻¹⁸⁹

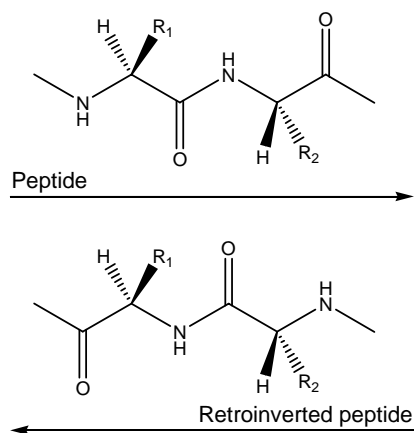


Figure 3.2. Comparison of a peptide and a retroinverted peptide.

3.1.1.1 Peptoidic BACE-1 Inhibitors

In addition to the two peptidic inhibitors OM99-2 and OM00-3 containing the hydroxyethyl Leu*Ala dipeptide mimic as TSA which were used for X-ray analysis of BACE-1, also the statine-based inhibitor KTEEISEVNStaVAEF covering a substrate sequence from P₁₀ to P₄' was found to exhibit an IC₅₀ value of ~30 nM.⁶⁶ The sequence was derived from the Swedish mutant variant (SEVNLDAEFR) of APP and the Asp residue in P₁' position was replaced by a Val residue which led to increased potency.⁶⁶ Comparison of this inhibitor with OM99-2 and OM00-3 suggested that part of the N-terminus was not necessary for recognition by the enzyme. Therefore the peptide sequence was shortened by us at the N-terminus to position P₄ leading to an eight-mer peptide. The resulting compound (EVNStaVAEF, **1**) showed good inhibition with a K_i value of 33 nM. This peptidic statine inhibitor was then used as lead for all subsequent optimizations by the peptoid approach.

Since no crystal structures of BACE-1 in complex with a statine-containing inhibitor have been solved so far, docking experiments with compound **1** on the available crystal structures of the enzyme were performed. These fully confirmed that extension of the peptide sequence at the N-terminus would not improve interaction with the protein. Moreover, the docking studies clearly revealed that by placing the statine unit with its side chain in the subsite S_1 and the hydroxyl group in interaction with the residues aspartic acids 32 and 228, the two lateral chains of the amino acids in P_1' and P_2' (Val and Ala, respectively) were shifted to the right in an intermediate position between $S_1'-S_2'$ and $S_2'-S_3'$ pockets respectively (Fig. 3.3 B). This observation resulted particularly evident when the Val side chain was P_1' , because of its sterical hindrance. Nevertheless, the flexibility of the inhibitor and the relatively large catalytic cleft of the enzyme, especially of the S_2' pocket, could allow the rearrangement of the lateral chains in the enzyme's pockets.

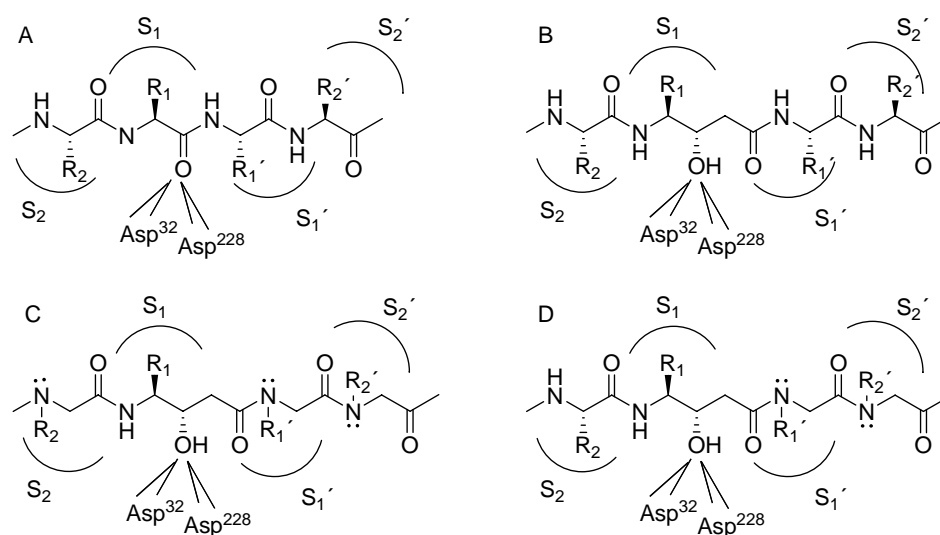


Figure 3.3. Schematic representation of the binding pocket of BACE-1 with A) a hypothetical substrate; B) a designed inhibitor containing statine; C) the peptoid analogous; D) the analogous hybrid, characterized by a peptide-like sequence at the N-terminus and a peptoid-like sequence at the C-terminus.

Shifting the lateral chains from the α -carbon to the nitrogen atom in each amino acid along the chain, allowed the repositioning of the residues of the lead compound **1** closer to the center of the corresponding subsites (Fig. 3.3 C). This introduced a better recognition on the C-terminal side, but pushed the residues in the N-terminal side further to the left, away from the centers of the subsites. In order to reposition the side chains in register with the corresponding peptide at the N-terminus, hybrids peptide-peptoids were designed, in which the C-terminus was tailored in a peptoid-like manner, while the N-terminus carried the normal peptide-like sequence (Fig. 3.3 D)

In order to verify the feasibility of a peptoid and peptoid-peptide hybrid approach as suggested by the docking experiments, a series of inhibitors of BACE-1 was synthesized. In these peptoid and peptoid-peptide hybrids some or all amino acid residues were substituted by N-substituted glycine residues. In the design of such inhibitors, the side chain of statine and its hydroxyl group has to be maintained in the same relative position. Since this was not feasible with inverted sequences the side chains of the amino acid residues were simply shifted in the backbone from the α -carbon to the amide nitrogen. In Fig. 3.4 the peptoid structures are compared with the parent peptidic inhibitor **1**. In the peptoid **2** all the side chains except for the hydroxy group and the lateral chain of statine as P₁ residue are shifted by one position to the left, both at the C- and N-terminus. Since in the highly potent inhibitor OM00-3⁷⁸ the lateral chains of Glu and Phe on the C-terminus are further shifted to the left by one position, it was expected that the enzyme could tolerate the variation. Repositioning of the side chains in register with the corresponding peptide at the N-terminus was achieved with peptide-peptoid hybrids, in which the C-terminus was tailored in a peptoid-like manner while the N-terminus was kept in its peptidic structure.

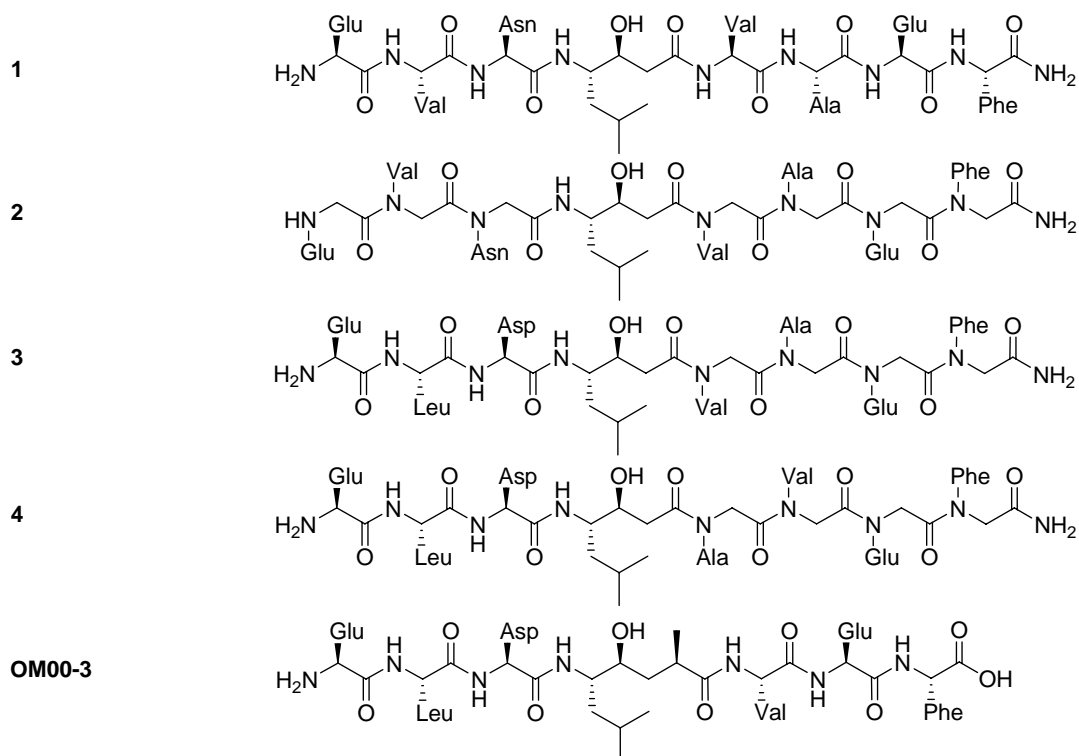


Figure 3.4. Schematic comparison between peptides and peptoids showing the similarity of spacing of the side chains, and the lack of stereochemistry of the peptoid monomers (OM00-3⁷⁸ is reported).

As an alternative approach, retroinverted peptides were envisaged which represent mirror images of the parent compound, characterized by the reverse orientation in the sequence and D-amino acids. In order to explore the conformational characteristics of these molecules, three retroinverted all-D mimetic compounds were synthesized, based on the sequence of peptide **1**, OM00-3 and the Swedish mutation peptide. The structures are reported in Fig. 3.5.

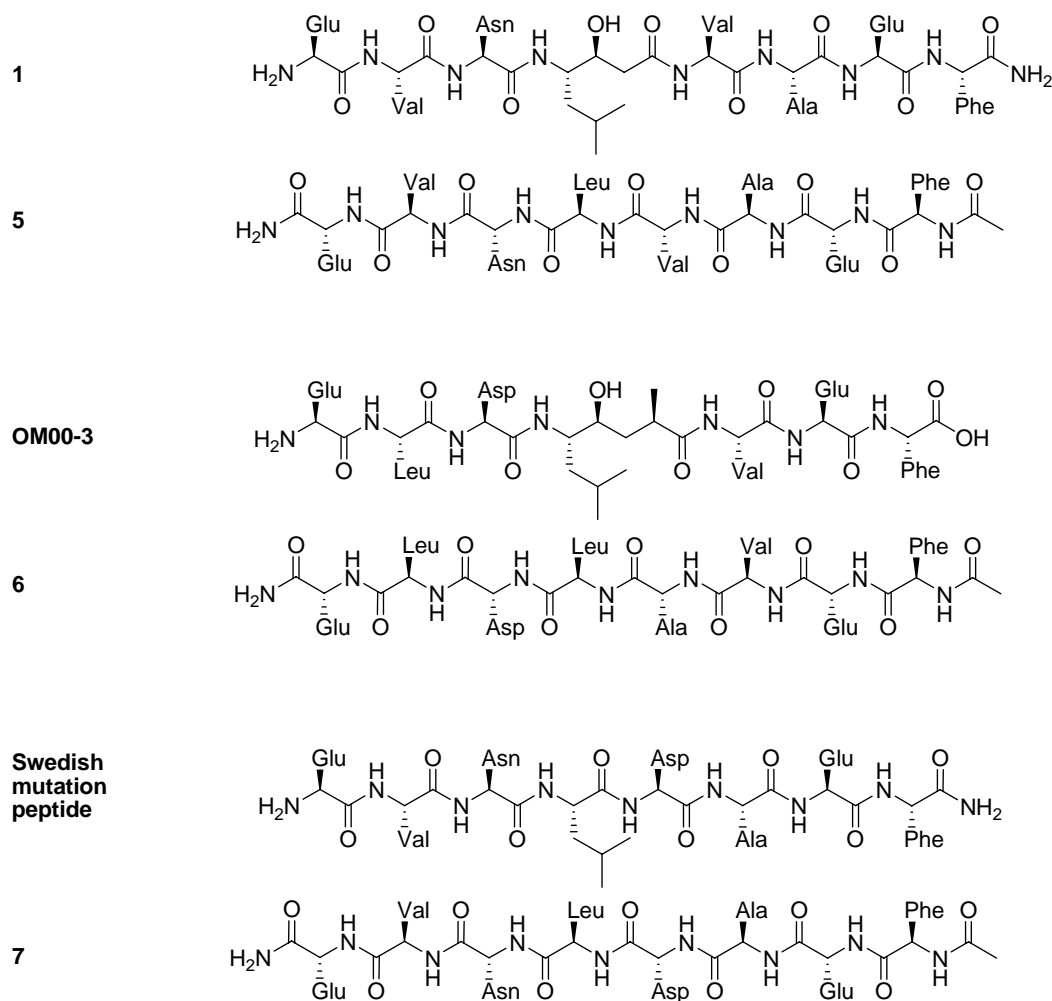
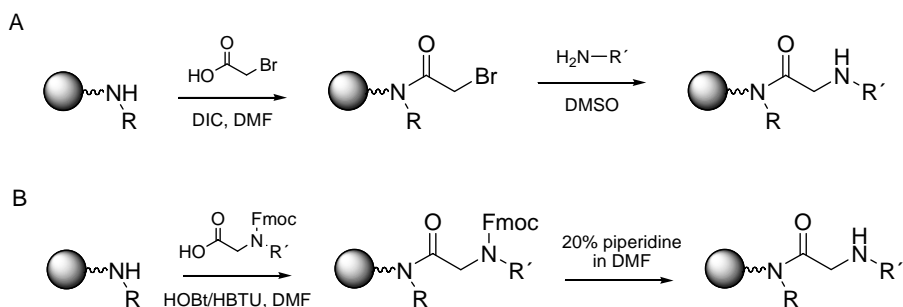


Figure 3.5. Schematic comparison between peptides and retroinverted peptides showing the similarity of spacing of the side chains (compounds Swedish mutation and OM00-3⁷⁸ are reported).

3.1.1.2 Synthesis of the Peptoidic Compounds

Two methods for the synthesis of peptoids by organic solid phase chemistry have been described in the literature: the *submonomer* and the *monomer method*. The general strategy for the two methods is reported in Scheme 3.1. Both approaches were employed for the synthesis of the peptoid and peptoid-peptide hybrids, according to commercially available intermediates.



Scheme 3.1. Two methods for the synthesis of peptoids on solid phase. (A) Submonomer approach: the first step is the acylation of the resin-bound amine with bromoacetic acid activated in situ with *N,N'*-diisopropylcarbodiimide (DIC); the second is the nucleophilic displacement of the bromide with a primary amine. (B) Monomer approach: Fmoc-protected *N*-substituted glycines are presynthesized and coupled on the resin.

In the *submonomer method* proposed by Zuckermann and associates,¹⁹⁰ the oligomer is prepared on the resin by repeated coupling cycles of haloacetic acid (backbone formation) followed by a substitution reaction with an appropriate amine that incorporates the side chain functionality (side-chain introduction). Each cycle of monomer addition consists therefore of an acylation step with haloacetic acid and a nucleophilic displacement step with a primary amine. The method is unique in that each monomer is assembled on the solid support from two simple submonomers, without the need of main chain protecting groups.

Diverse reasons make this method very advantageous: i) the haloacetyl monomer is common to all backbone elongation cycles; ii) the monomers do not have to be synthesized separately; iii) in principle, any arbitrary amine can be employed in the synthesis of peptoids. While this approach may be the method of choice when small quantities of relatively small peptoids are needed, it suffers from the disadvantage that large excesses of reagents (especially the amines) have to be employed and that completion of the acylation and substitution reactions cannot be determined; this is essential for preparation of larger peptoids of reasonable purity. In the present case this strategy proved to be the most effective.

The amines that have been used in the substitution reactions are commercially available. In the case of the nonfunctional Nphe, Nval and Nleu side chains, their incorporation into the backbone was straightforward. For Nasn, no protection was used and the side-chain was introduced as glycine amide. Finally, a *tert*-butyl based protection, i. e. H- β -Ala-O*t*Bu-HCl, was used for the incorporation of the Nglu side chain.

In the *monomer approach*, 9-fluorenylmethoxycarbonyl (Fmoc)-protected N-substituted glycines are directly coupled using the conventional peptide chemistry on solid support. In the present work, a single N-substituted glycine derivative for the solid-phase synthesis of the peptoid and peptoid-peptide hybrids was utilized, i. e. Fmoc-Sar-OH as N-substituted glycine analogue of Ala.

The peptoid **2** and hybrids **3** and **4** were synthesized manually on Rink amide MBHA resin containing an acid-labile linker attached via a norleucine to the MBHA resin. *N,N'*-diisopropylcarbodiimide¹⁹¹ was used for coupling of bromoacetic acid according to the known protocol by Zuckermann.¹⁹⁰ The syntheses were straightforward, except for two insertions that were particularly difficult to achieve; these correspond to the coupling with Sta and the subsequent Nasn residue. Truncated sequences related to these two residues were found in the final product despite repeated couplings and extended reaction times. In order to bypass this problem as well as the difficult acylation of the sterically hindered Nval, the initially employed HOAt/HATU method¹⁹²⁻¹⁹⁴ was replaced with PyBOP^{195,196} coupling. Other coupling reagents such as *N,N'*-diisopropylcarbodiimide or HOBt/HBTU^{197,198} allowed only partial acylation reactions, resulting in a mixture of the product and truncated sequences.

Acylation with bromoacetic acid was monitored with the TNBS¹⁹⁹ or Keiser tests²⁰⁰ for primary amines and the chloranil test²⁰¹ for secondary amines. With the exclusion of the difficult couplings mentioned where multiple acylations with longer times were applied, couplings on average were carried out for 30 min and were then repeated.

For the displacement step with the primary amines, direct assays for monitoring are not available; as a consequence, large excesses of amines were used, and the reactions were carried out for 1 hour and in the case of isopropyl amine (Nval), it was repeated a second time. Analytical cleavage tests on small amounts of resin confirmed that this procedure was sufficient for the quantitative reactions.

After completing the synthetic steps, cleavage from the resin and simultaneous removal of the protecting groups was accomplished with TFA with TIS and water as scavengers. Mass spectrometric analysis of the final mixtures obtained for analogue **2** clearly revealed contaminations by deletion sequences corresponding mainly to products missing Sta or Nasn, with other unidentified structures and the desired product accounting for only 20% of the total yield. The optimization efforts by longer coupling times and the use of more efficient coupling reagents, such as PyBOP, resulted in a significant improvement of the quality of crude products and acceptable yields. In the case of peptide-peptoid hybrids, the major component in the crude compound was identified as the final correct product with a relatively small impurity corresponding to a deleted Sta residue.

Since the bromoacetic acid was activated with DIC, acylation of the unprotected hydroxyl group of Sta was expected to occur at least to some extents. However, no significant level of alkylation of the Sta was observed.

3.1.1.3 Bioactivities

The absence of amides in peptoids, which can act as hydrogen-bond donors, was expected to decrease the solubility in polar and increase it in more apolar solvents. The presence of tertiary amide bonds leads to *cis/trans* rotamers around each tertiary amide bond in a peptoid. Despite this potential *cis/trans*

3. Results and Discussion

isomerism, the peptoid compounds were found to elute as single, well-defined peaks in HPLC (Fig. 3.6) in contrast to some proline-rich peptides.²⁰²

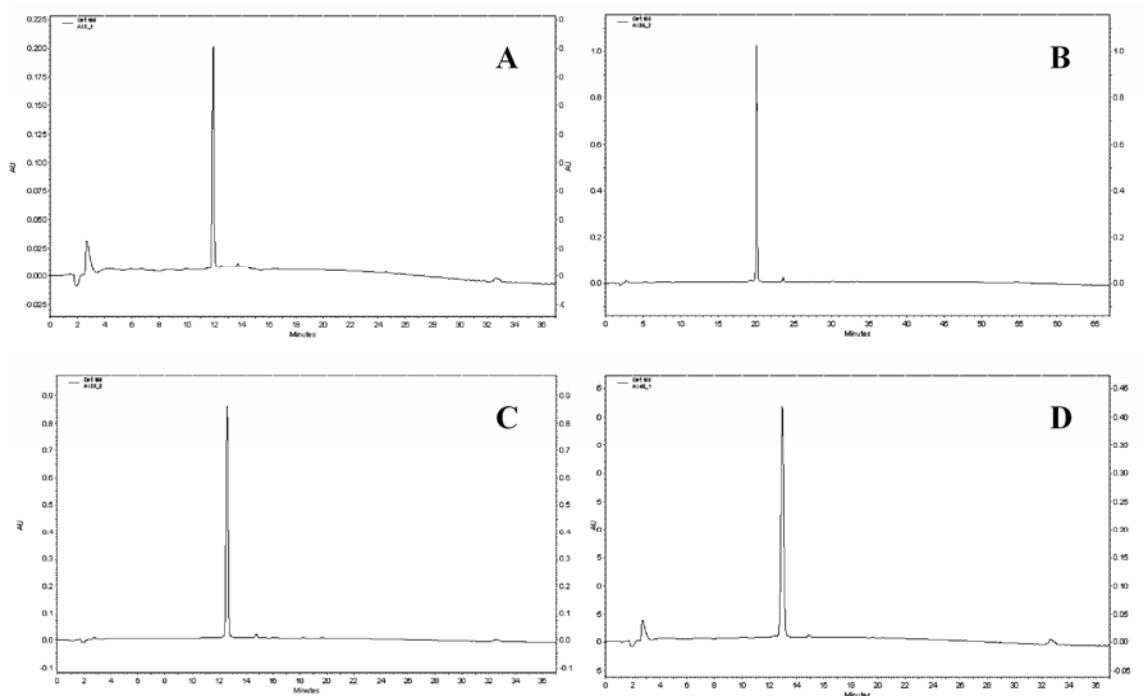


Figure 3.6. Chromatograms of compounds (A) **1**, (B) **2**, (C) **3**, (D) **4**.

The absence of hydrogen-bonding potential was also expected to affect the binding affinities to BACE-1. Indeed, peptoid **2** with all side chains shifted to the backbone nitrogen atom, did not show any inhibitory activity up to a concentration of 1 mM. This result raised the question to what extent peptide **1** can be transformed into a peptoid while retaining its affinity for BACE, that is, which side chains are allowed to be shifted on the backbone and which are not. Although from the known X-ray structures a weaker interaction of BACE-1 with the C-terminal portion of peptidic inhibitors could be assumed, the peptoid-peptide hybrids containing a C-terminal peptoid and N-terminal peptide sequence (**3** and **4**) were unable to inhibit the protease. Apparently, the shift of one or both the two side chains at the C- and at the N-terminus results in a complete loss of binding capacity.

The schematic comparison of peptides, peptoids and peptide-peptoid hybrids provided in Fig. 3.4 shows the similarities in the spacing of the side chains and the carbonyl groups, and the differences in the chirality of the two monomers. Although these peptoids and hybrids are simply isomers of the parent inhibitory peptides, there are important differences in hydrogen bonding, stereochemical and conformational characteristics between the oligomers. In more detail, the relative distances between side chains with respect to their position on the backbone, the altered hydrogen bond characteristics of the backbone, the lack of stereochemical preorganization of the lateral chains, and the increased flexibility of the backbone of peptoids-like compounds with respect to the parent peptide has significant consequences when peptides are transformed into peptoid mimics. Indeed, the absence of substituted backbone carbons and of amide hydrogens removes not only the intermolecular CO--HN hydrogen bonds between the inhibitor and the enzyme, but also changes the intramolecular interactions that induce secondary structure in the peptidomimetics themselves. These features may serve to further increase the conformational space that the peptoid can explore. This also suggests that there will be an increased flexibility of the backbone and a greater diversity of conformational states for a peptoid than for a peptide, being the former deprived of some degrees of liberty by the possible intramolecular hydrogen bonding. This conformational freedom increases in significant manner the entropic penalty raising serious question marks on the use of the peptoid strategy for ligand design.

More difficult is the interpretation of the absence of inhibitory activities for the retroinverted peptides. The not perfect overlapping of the active inhibitor **1** with the retroinverted **5**, due to the presence of the statine residue (Fig. 3.5), could well account for the decreased potency of **5** compared to the parent peptide. But the lack of activity of the two compounds **6** and **7** clearly confirms that the opposite orientation of the backbone disrupts critical hydrogen bonds involved in the stability of the inhibitor/enzyme complex.

3.1.1.4 Mass Spectrometry of Peptoids: General Considerations

A full structural characterization of peptoids and peptoid-peptide hybrids by NMR was reported to be severely complicated by the presence of multiple *cis/trans* rotamers.²⁰³ This flexibility results from rotation about the tertiary amide bond, which is favoured compared to the isomerization of a secondary amide bond in peptides. Conversely, a positive ion mass spectrometry analysis should not distinguish between a peptide and its corresponding peptoid analogue since the compounds are isobaric; therefore the spectra should exhibit great similarities. Nonetheless it was shown that mass spectrometry can play a key role in the unambiguous characterization of peptoids.^{204,205}

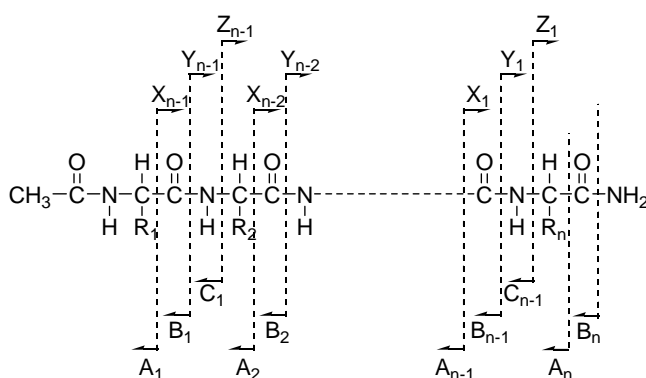


Figure 3.7. Nomenclature of peptide backbone sequence ions.

The types of fragment ions observed in a tandem MS/MS spectrum of a peptide depend on many factors including primary sequence, the amount of internal energy, how the energy was introduced, charge state, etc. The accepted nomenclature for fragment ions was first proposed by Roepstorff and Fohlman,²⁰⁶ and subsequently modified by Johnson *et al.*²⁰⁷ (Fig. 3.7). Fragments will only be detected if they carry at least one charge. If this charge is retained on the N terminal fragment, the ion is classified as either A, B or C. If the charge is

retained on the C terminal, the ion type is either X, Y or Z. A subscript indicates the number of residues in the fragment.

In addition to the proton(s) carrying the charge, C ions and Y ions abstract an additional proton from the precursor peptide. For example, the structures of the six singly charged sequence ions for a tripeptide is reported in Fig. 3.8.

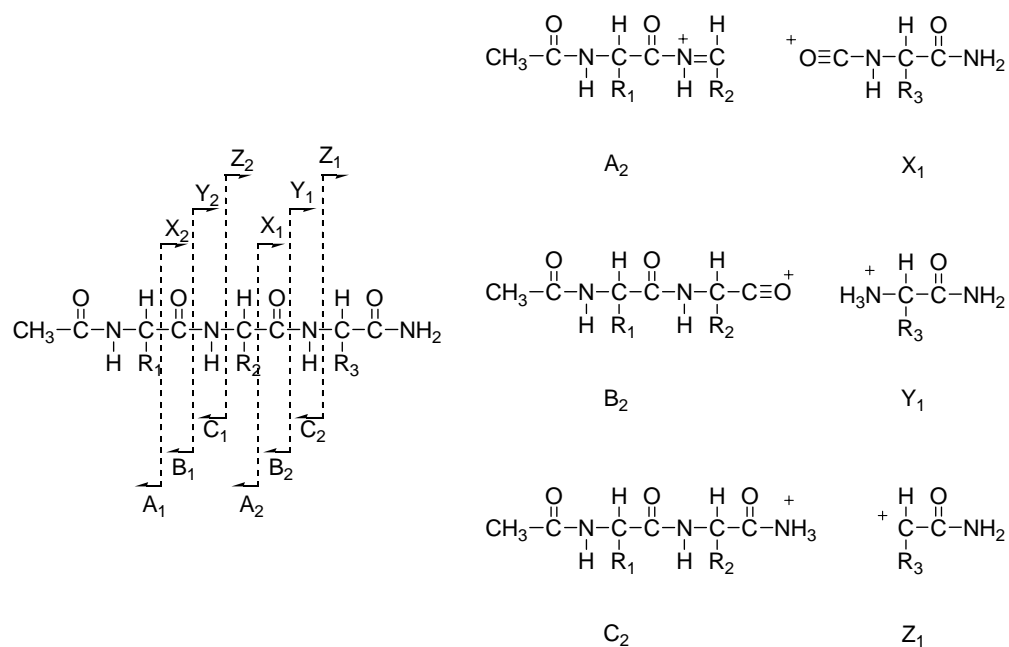


Figure 3.8. The six singly charged sequence ions for a tripeptide

Double backbone cleavage gives rise to internal fragments (Fig. 3.9). Usually, these are formed by a combination of B-type and Y-type cleavage to produce an amino-acylium ion. Sometimes, internal cleavage ions can be formed by a combination of Y-type and A-type cleavages, to give an amino-immonium ion. Internal fragments are labelled with their one-letter amino acid code. An internal fragment with just a single side chain formed by a combination of Y-type and A-type cleavage is called an immonium ion. These ions are labelled with the one-letter code for the corresponding amino acid.

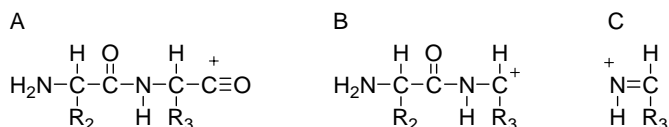


Figure 3.9. Internal cleavage ions: (A) amino-acylium ion, (B) amino-immonium ion, (C) immonium ion.

The proposed nomenclature for assigning sequence ions in peptoids²⁰⁴ is very similar to that generally used for peptides and is represented in Fig. 3.10.

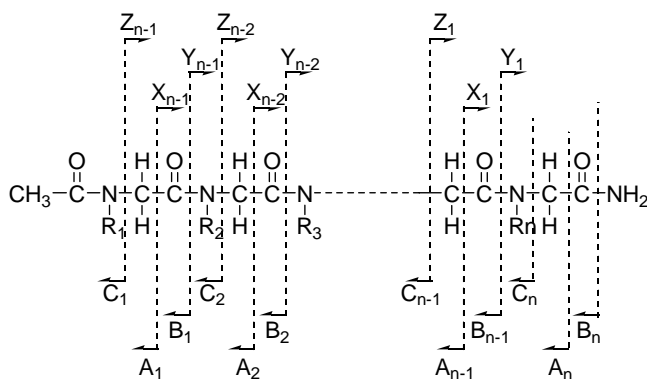


Figure 3.10. Nomenclature of peptoid backbone sequence ions.

The convention is applied in such a way that cleavage of the peptoid backbone still results in couples of complementary sequence ions, A and X, B and Y, C and Z. Corresponding completely to the nomenclature of peptides, the N-terminal acyl ions in peptoids are B-type ions, while the A-type ion is a CO group smaller. Similarly the Y-type ions of peptides and peptoids have a terminal $-\text{NH}_3$ and $-\text{NH}_2\text{R}$ group, respectively. In peptoids, A-, B-, X- and Y-sequence ions have the same mass and elemental composition as those in the corresponding peptide, and therefore computer programs which correlate mass spectral data to peptide structures can also be used for these compounds. The C- and Z-type ions of peptoids, however, are not isobaric and differ by a $\text{CH}_2\text{-CO-NH}$ group (57 amu less or more, respectively) from the corresponding ions in a peptide (compare

Figs. 3.7 and 3.10). The order of mass increase for N-terminal sequence ions A_n^- , B_n^- and C_n^- in peptides has changed into C_n^- , A_n^- and B_n^- in peptoids. In order to indicate peptoid amino acid residues, the prefix N in the three-letter code or n in the one-letter code is used.

3.1.1.5 Mass-Spectrometric Characterization of Peptoids

In order to obtain experimental evidence for the occurrence of compound-specific sequence ions we have studied the spectra of the four molecules whose structure and fragment-ion assignments are given in Fig. 3.11. The mass spectra obtained for these compounds are given in Figs. 3.12.

Some general observations can be made for the spectra of all the four compounds. The peaks observed in the spectra show identity with the desired products in all four cases. For the two peptide/peptoid hybrids it was possible to identify the complete Y'' -ion series, as well as part of the B-ion series. The analogue series for the peptide and peptoid compounds were not complete: this low sequence coverage is most likely due to the fragmentation of the singly charged precursor. Furthermore, only one peak of the A-ion series was identified in the spectrum of peptide **1**. In general, each peak in the B- and Y-series was accompanied by peaks at -17, -18 and -35 with respect to its value, corresponding to the loss of H_2O and NH_3 : intense losses of water and ammonia are a common event in peptides and analogues containing Glu and Asn residues.

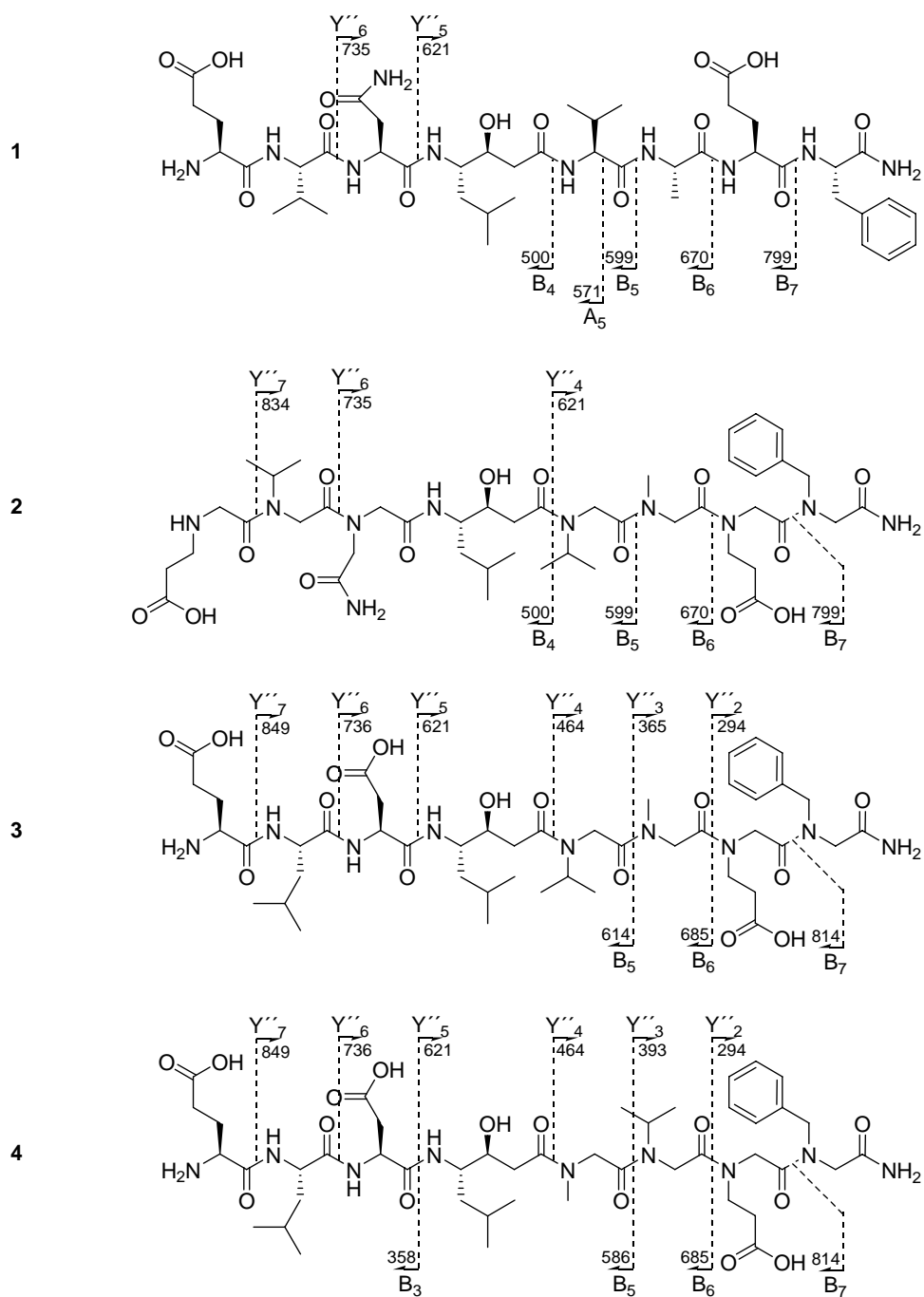
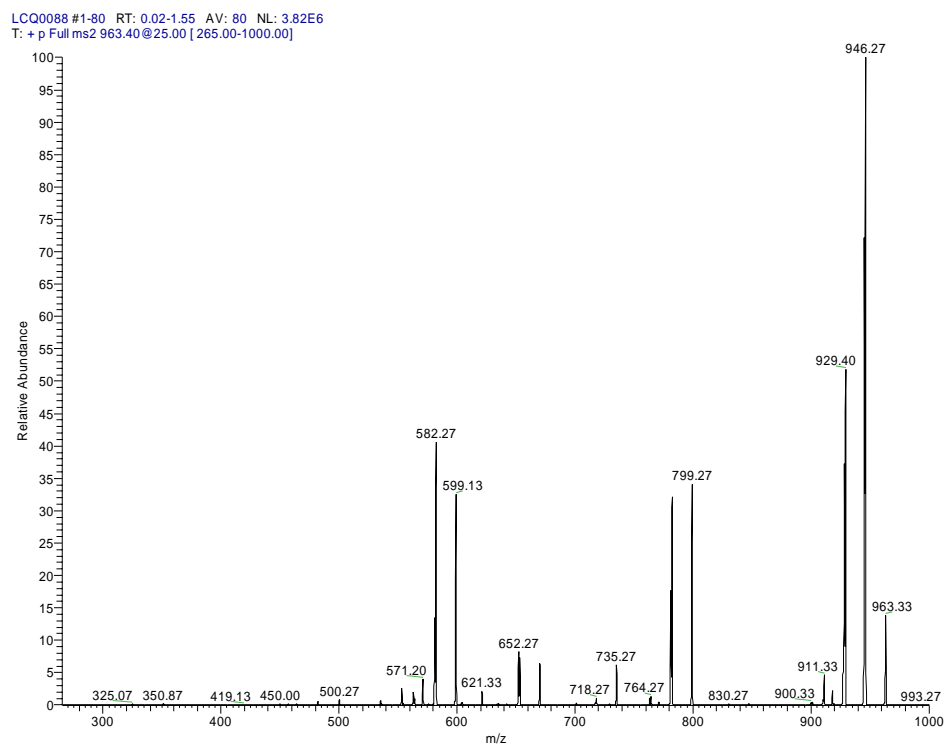
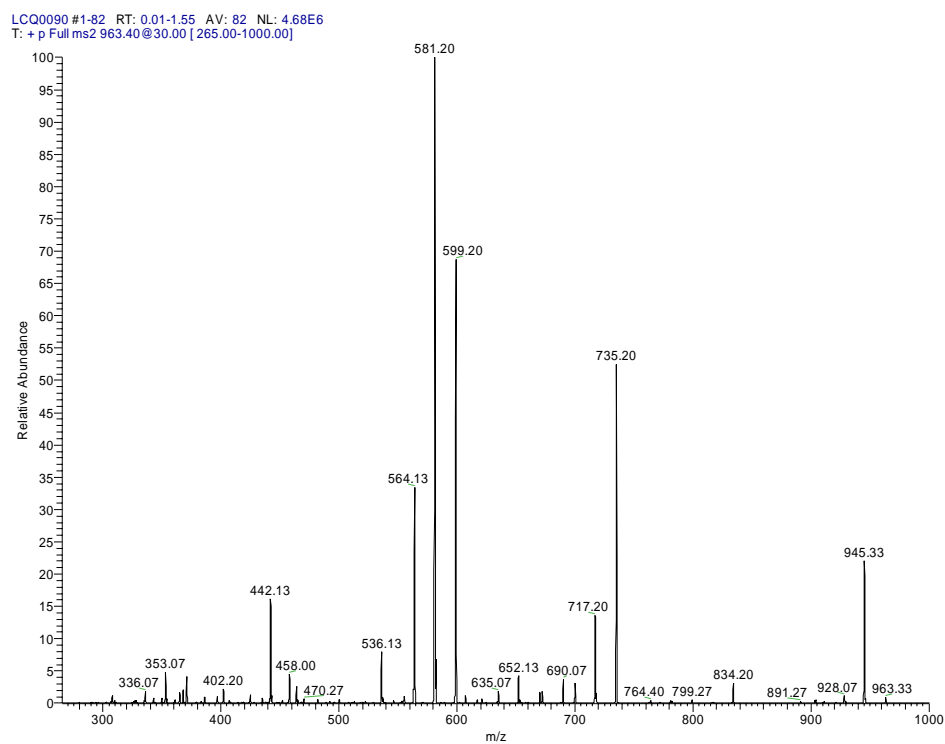


Figure 3.11. Structures and sequence ions of compounds 1, 2, 3, 4.



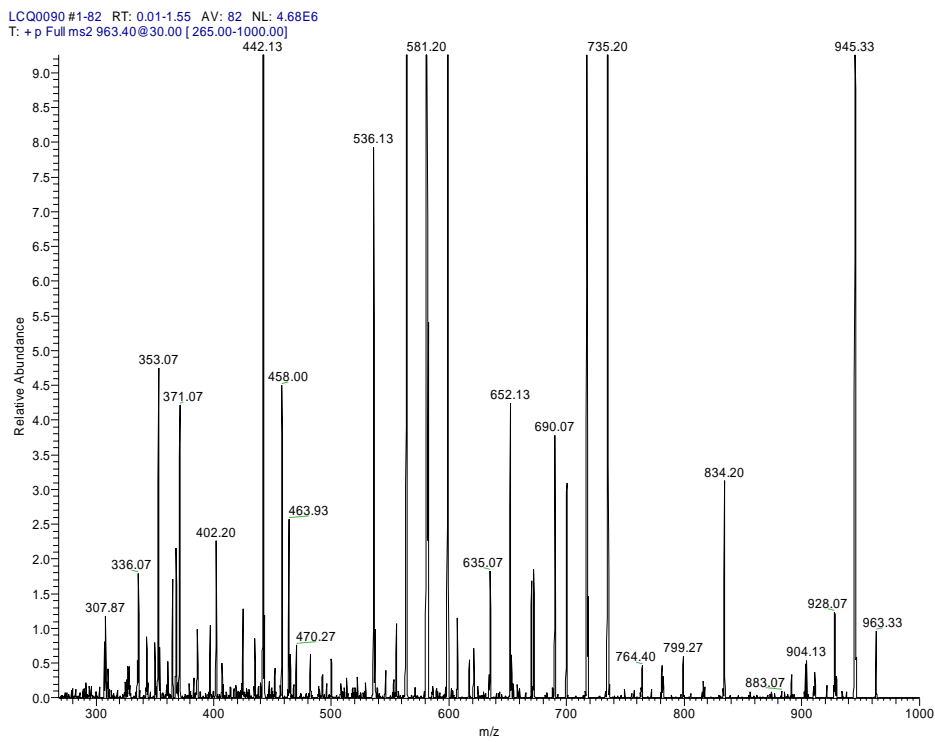
Compound 1



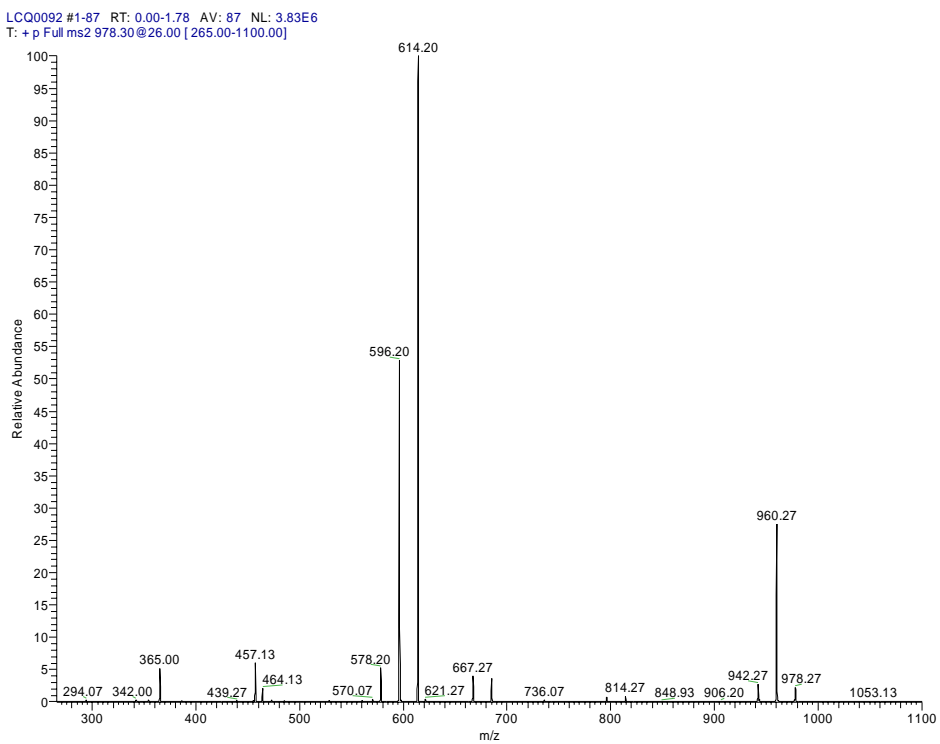
Compound 2

Figure 3.12. (Continue)

3. Results and Discussion



Compound 2, zoom view



Compound 3

Figure 3.12. (Continue)

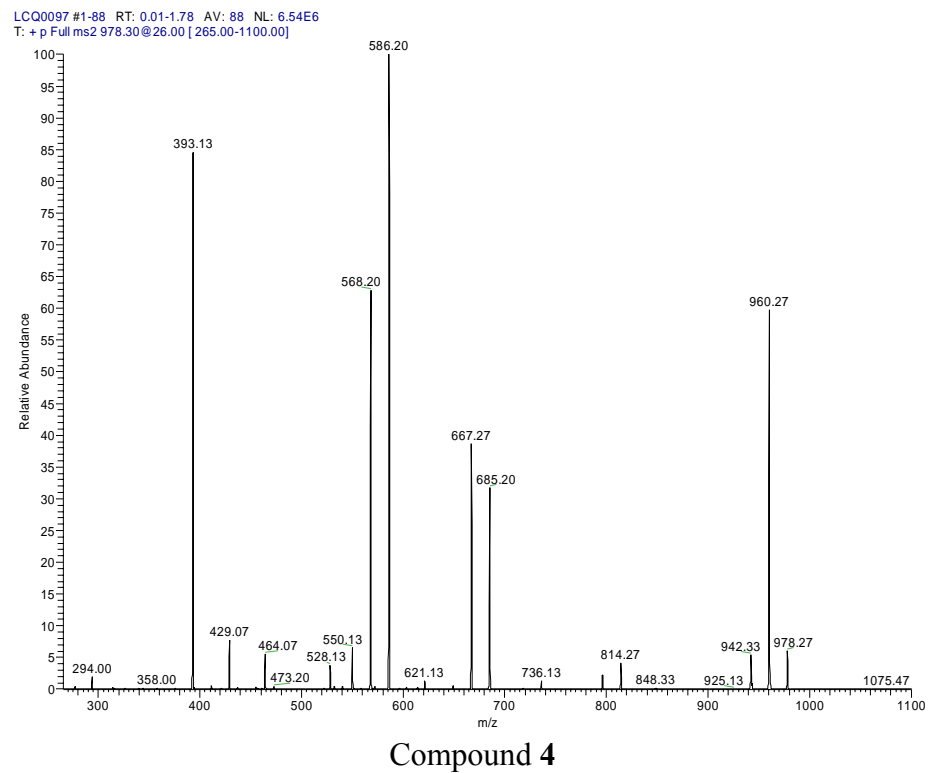
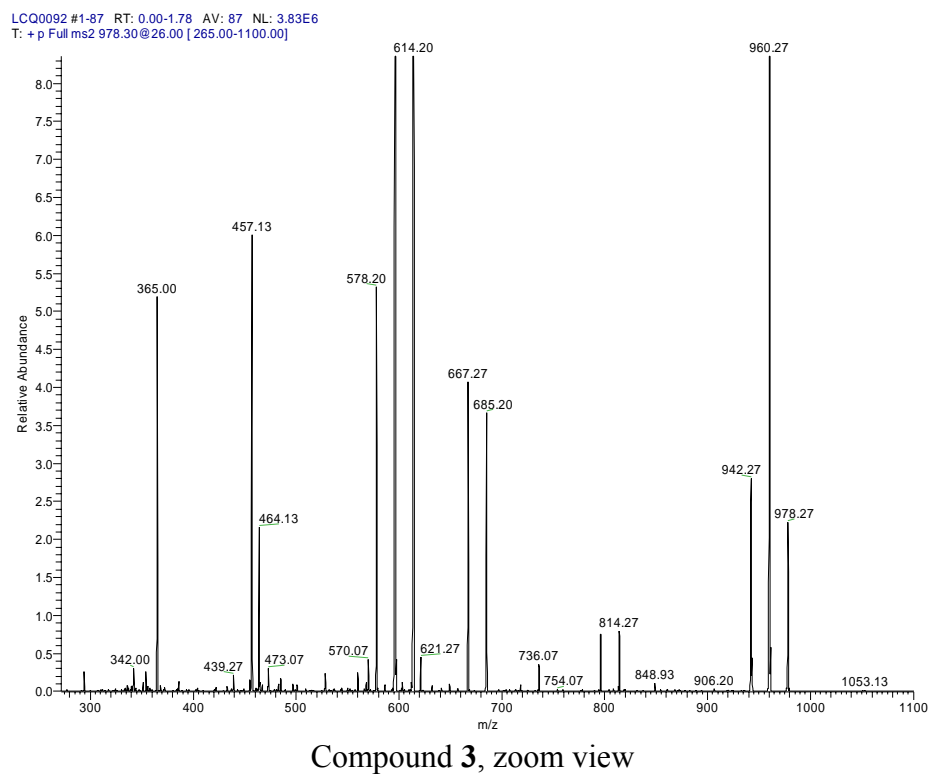


Figure 3.12. Mass spectra of compounds 1, 2, 3 and 4.

The spectra of peptide **1** and peptoid **2** (Fig. 3.12 A and 3.12 B) show the same order of amino acid residues by the occurrence of sequence ions at the identical masses, although their intensity distribution differs from that in the peptide. The relative intensity of the m/z 735 and 599 peaks for **2** (Fig. 3.12 B), corresponding to the B_5 - and Y_6'' -ions (in a cluster with the peaks associated with the loss of water and ammonia) has increased considerably in the peptoid spectrum, indicating a preferential charge retention on the Nasn nitrogen atom and C=O of the Val.

Bearing in mind that the spectra of the hybrids differ entirely from the former spectra because of their different sequences, so that the analogous ions are found at different masses, it was still possible to verify that the B_5 -ion is the most abundant product ion to the highest degree in the spectrum of compound **3** (Fig. 3.12 D and E) and, to a lesser extent, also of **4** (Fig. 3.12 F).

Another important difference, visible both by comparing the peptide and the peptoid and peptidic and peptoidic parts in the hybrids, is the relative abundance of the peptoidic Y'' ions corresponding to peptoidic parts respect to peptidic ones. This phenomenon of increased Y'' -ion abundances has been observed previously to even greater extents in the analysis of the CID spectrum of the pentapeptide Leu-enkephalin²⁰⁴ or in other peptoids-peptides comparisons.²⁰⁵ In particular, while in peptide **1** the only two Y'' -type ions of relative intensity are the heavy Y''_5 and Y''_6 (at m/z 621 and 735 respectively), in the hybrid structures the Y'' -type ions corresponding to the highest m/z are considerably less intense than the peaks at lower m/z (especially Y''_3 and Y''_4), which correspond to the peptoidic immonium ions. Interestingly, in the peptoid compound **2** not only the identified ions are the largest in the series (Y''_7 , Y''_6 and Y''_4), but the only missing in the series is the one corresponding to the monosubstituted Sta immonium ions, confirming the lower stability of those ions. The increased intensity of Y'' -type ions in the case of peptoids compared with corresponding peptides could be caused by the enhanced proton affinity of the N-atom of the

amide bond when it is substituted by the amino acid side-chain. It acts this way as a more basic secondary amine group than the primary amine group in common peptides. With the exception of the spectrum of the peptic compound **1**, all the other spectra present peaks identified as internal fragments, derived by a combined type-B and type-Y (amino-acylium ion) or type-Y and type-A fragmentation (amino-immonium ion). These fragmentations are reported in Table 3.1, with the proposed structures.

Compound 2			
m/z	m/z calc	Structure	(type ion)
690.07	690.81	nN-Sta-nV-nA-nE-nF	(amino-immonium)
458.00	457.27	Sta-nV-nA-nE-nF	(amino-acylium)
442.12	442.27 442.30	nN-Sta-nV-nA nV-nN-Sta-nV	or (amino-acylium) (amino-immonium)
371.07	371.23 371.23	nN-Sta-nV nV-nN-Sta	or (amino-acylium) (amino-acylium)
353.07	353.22 353.22	nN-Sta-nV – H ₂ O nV-nN-Sta – H ₂ O	or (amino-acylium – H ₂ O) (amino-acylium – H ₂ O)

Compound 3			
m/z	m/z calc	Structure	(type ion)
457.13	457.27 457.30	Sta-nV-nA-nE L-D-Sta-nV	or (amino-acylium) (amino-immonium)

Compound 4			
m/z	m/z calc	Structure	(type ion)
528.13	527.36	L-D-Sta-nA-nV	(amino-immonium)
429.07	429.27 429.27	L-D-Sta-nA Sta-nA-nV-nE	or (amino-immonium) (amino-immonium)

Table 3.1. Masses of fragmentation peaks for peptoid **2** and hybrids **3** and **4**.

3.1.1.6 Tandem MS-MS Experiments for Compound 3

Given the double structure possibility for some of the fragmentation peaks identified, a detailed investigation of the peak of relative high intensity present at m/z 457 in the spectrum of **3** was performed.

In order to obtain structural information, additional MS^n experiments were conducted. In a typical tandem MS/MS experiment, a selected ion is isolated and fragmented. The daughter ions which are generated depend unequivocally on the structure of the parent ion. This process can be repeated by isolating and fragmenting a daughter ion in an MS^2 experiment and the process repeated n times. Even though the instruments are theoretically capable of MS^n with n up to 10, the value of n is typically limited to 3 or 4, because of the diminishing ion abundance as n increases.

Therefore, by running an MS^3 experiment on the daughter ion at m/z 457, we were able to exclude one of the two possible fragments reported in Table 3.1. The first possible internal fragment Sta-nV-nA-nE, which is characterized by a calculated m/z of 457.27, would result, in a higher order parent ion scan, in ions at m/z 328 (-E, that is - m/z 129) and/or 300 (-Sta, - m/z 157). Fig. 3.13 A, B and C show the three tandem mass spectra of the ion m/z 457, its daughter at m/z 229 and its daughter at 201 respectively. As evident in the figures, neither of the fragments was detected.

The second possible internal fragment corresponds to the amino-immonium ion L-D-Sta-nV. A proposed fragmentation pathway (after analysis with the computer program MassFrontier 4.0) for this ion is reported in Fig. 3.14, which explains all the major peaks present in the MS^n spectra (Figs. 3.13). We concluded then that the L-D-Sta-nV structure of the amino-immonium ion correspond in fact to the right hypothesis.

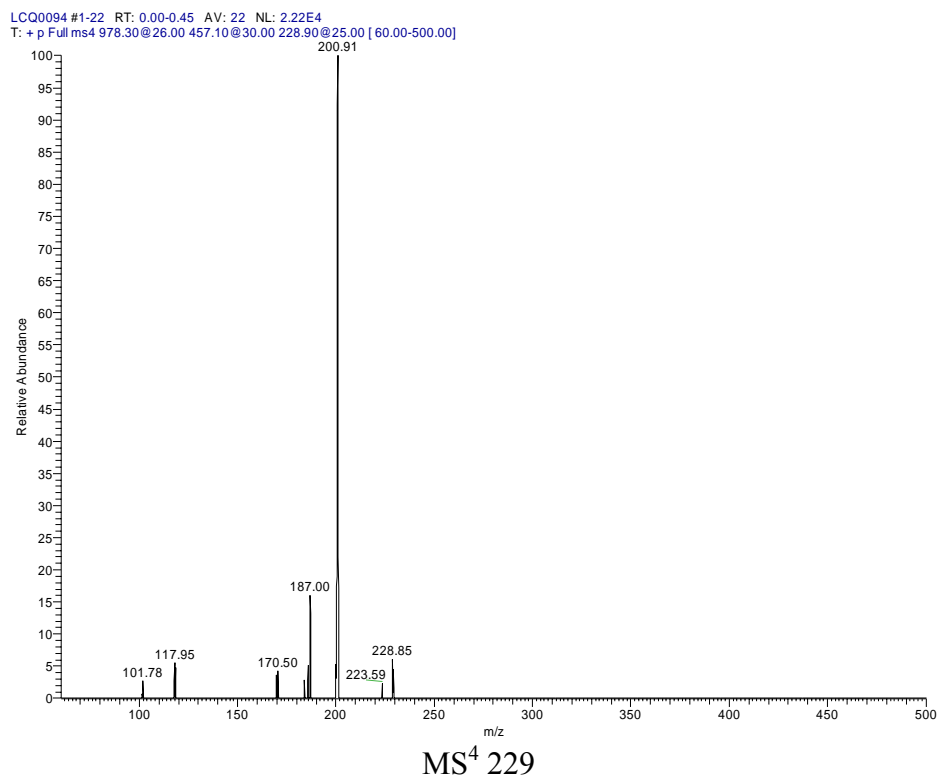
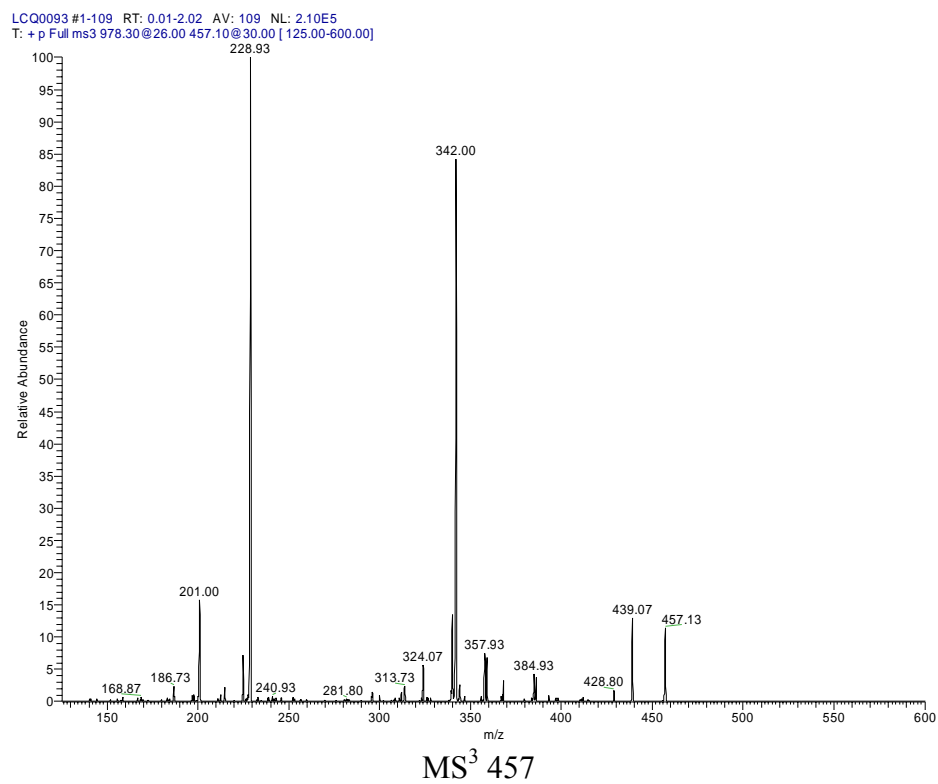


Figure 3.13. (Continue)

3. Results and Discussion

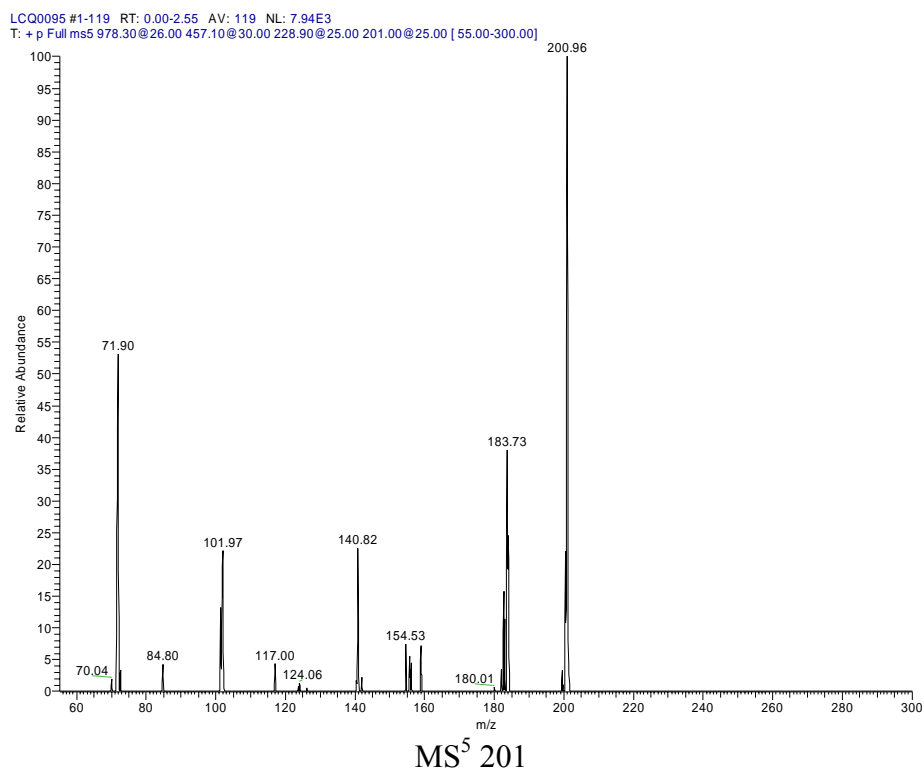


Figure 3.13. Tandem mass spectra (MS/MS) of the ion m/z 457 (A), its daughter at m/z 229 (B) and its daughter at 201(C).

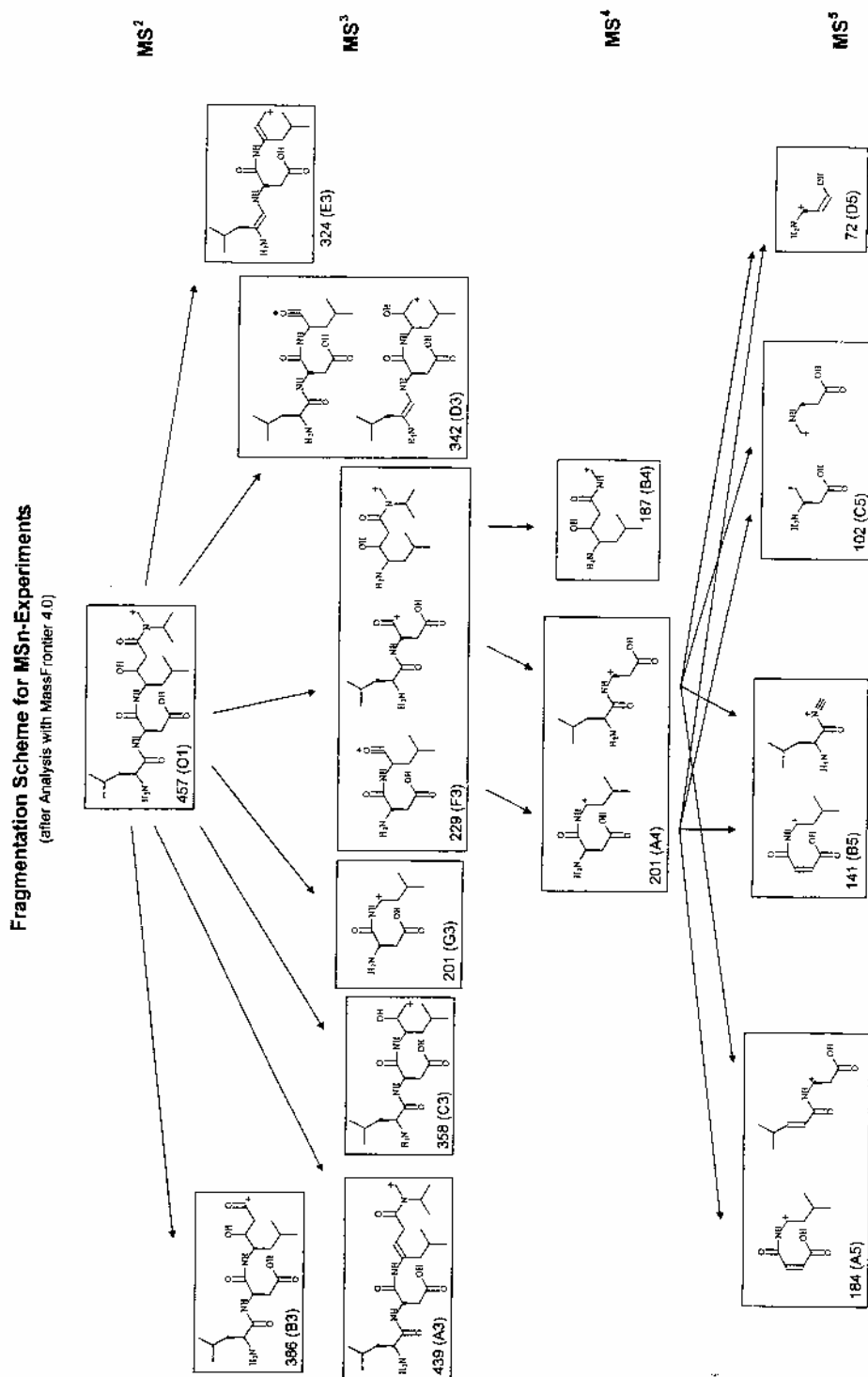


Figure 3.14. Proposed fragmentation pathway for the amino-immonium ion L-D-Sta-nV derived from the mass fragmentation of compound 3. The proposed fragmentation is derived by analysis with the program MassFrontier 4.0.

3.1.2 Macrocyclic BACE Inhibitors

Macrocyclic inhibitors are a novel category of synthetic BACE inhibitors which preserve a fixed β -strand peptide conformation. We want to test the proposition that cyclization might force inhibitors into a protease-binding conformation, namely the β -strand. The induction of the extended conformation in the macrocycles, if optimally realized by cyclization, is known to increase binding affinities to the active site cleft because the peptide backbone would be conformationally preorganized, significantly reducing the entropic penalty in the binding process and thus inducing enhanced binding affinities. For these reasons, each macrocycle designed in our current work was conceived to serve as a structural mimic of a tri-, tetra- or pentapeptide in a constrained β strand.

Pseudopeptides OM00-3 and OM99-2, known to be BACE inhibitors and for which crystal structures are known,^{69,78} were used as template structures to study the plausibility of a cyclic inhibitor series. The superimposition of the four inhibitors derived from the two crystal structures of BACE showed a strong overlapping of the backbone in the extended conformation of the latter between residues P_3 - P_2' . As already discussed in chapter 1.2.3.3, the extended conformation is interrupted at residue P_2' to produce a kink, which leads to a less rigid preference for both the N- and the C-terminal side of the molecules (Fig. 3.15). These observations suggested the possible truncation of the octapeptide inhibitors to a shorter length comprising only residues P_3 - P_2' and the subsequent cyclization of this shortened peptide via a side chain-to-side chain or side chain-to-peptide backbone ring closure.

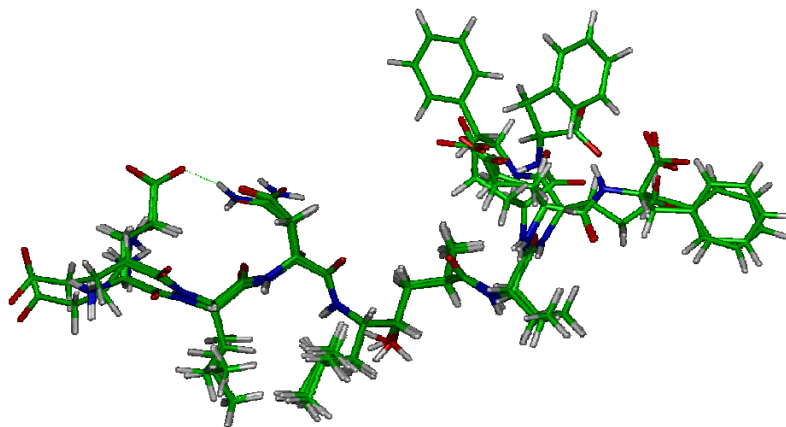


Figure 3.15. Superimposition of the X-ray structures of the BACE-1 inhibitors OM99-2 and OM00-3. An almost perfect superposition of both the peptide backbone and side chains are observed in the sequence portion P₃ to P₂'. Interestingly, the side chain of the Asn residue (P₂ in OM99-2) is displayed in hydrogen bonding distance to the carboxylate of Glu (P₄).

The investigation was then divided in various parts. The first part focused on the definition of the minimum sequence still retaining activity. A further effort was put in selecting the best N-terminal portion; we then performed the evaluation of the best ring pattern; and finally, different diamine linkers were inserted, with the aim of identifying the optimal length and rigidity necessary to obtain the entropic advantages potentially offered by macrocyclic BACE inhibitors.

3.1.2.1 Determination of the Minimum Size of Inhibitory Statine-Peptides

To achieve the entropic advantages potentially offered by macrocyclic BACE inhibitors in first instance a screening of the minimal sequence retaining binding affinity of the linear octapeptides BACE inhibitors OM00-3 and OM99-2 was performed, replacing in those peptides the isosteric hydroxyethyl Leu*Ala peptidomimetic with either statine, with its leucine-mimetic side chain, or (phenyl)statine, with the sterically bulkier aromatic group as P₁ residues. As

extensively discussed in the *Introduction* to the present work (chapter 1.2.2), statines are one backbone atom shorter with respect to a dipeptide or two atoms longer with respect to a single amino acid, and this characteristic rises the question to what extent a statine can mimic a dipeptide substrate. The thorough study done by Powers *et al.*³⁹ suggested that statine might better mimic a dipeptide. The *in silico* docking experiments that we performed to clarify the concern shows as well that in the presence of statine the Val residue occupies a position which is intermediate between S_1' and S_2' . The first preliminary docking experiments performed on the proposed macrocycles suggested also that cyclization would push Val further down in the catalytic clef, undoubtedly confining its lateral chain in the S_2' pocket. For these reasons, statine is considered here as a dipeptide replacement and thus occupies both P_1 and P_1' .

Peptide ladders were thus designed by the removal of aminoacids from the fully active octapeptides (Table 3.2). The analysis performed on the crystallized structure suggested that initially the octapeptide could be shortened to the (Phe)Sta-tetrapeptide **8** spanning P_3 - P_2' . The compounds were all synthesized as *N*-acetyl amide derivatives and the N-terminus was acetylated, strategy that allows the prolonging of the amide module repetitions in two more units with respect to the unfunctionalized backbone.

Despite the significant size reduction, compound **8** still showed inhibitory potency in the low micromolar range ($K_i = 5.4 \pm 1.0 \mu\text{M}$). The further shortening at the C-terminus of the molecule (as in compound **9**) corresponded to the total loss of activity, demonstrating that the interaction between Val and the enzyme is a prerequisite for binding. On the N-terminal side, the removal of Ile (compound **10**) depleted also the pseudopeptide of any inhibitory activity. These results taken together indicate that the sequence P_3 - P_2' can not be further shortened without loss of activity.

The active compound **8** was extended at the C-terminus by an aspartyl residue (compound **11**), which was conceived as a possible anchoring motif for

the subsequent macrocycles design. The introduction of the new P₃' residue had mild influence on the activity ($K_i = 5.4 \pm 1.1 \mu\text{M}$), which also suggests that, since Asp P₃' is not fundamental for enzyme recognition, its lateral chain could be effectively utilized for the construction of macrocycles in which the side chain of this Asp is covalently linked to a second Asp in position P₃ through a linear aliphatic or aromatic linker. Truncation of this compound at the N-terminus resulted again disruptive for the activity (compound **12**).

Finally, the comparison between compounds **11** and **13**, demonstrates that replacement of (Phe)Sta with the parent Sta, introduced only a slight decrease in activity, under the conditions of the study.

Name	Formula	K _i (μM)
8	Ac-Ile-Asp-(Phe)Sta-Val-NH ₂	5.4±1.0
9	Ac-Ile-Asp-(Phe)Sta-NH ₂	>1000
10	Ac-Asp-(Phe)Sta-Val-NH ₂	>1000
11	Ac-Ile-Asp-(Phe)Sta-Val-Asp-NH ₂	5.4±1.1
12	Ac-Asp-(Phe)Sta-Val-Asp-NH ₂	>1000
13	Ac-Ile-Asp-Sta-Val-Asp-NH ₂	8.4±2.6

Table 3.2. Peptide ladders for determination of the minimum size required for inhibitory activity, expressed as K_i (μM).

Having developed an understanding of the minimal sequence preference for the enzyme, we next evaluated the possible accepted modifications on the N-terminal side of the inhibitor. For this purpose, a variety of branched chains or aromatic groups that mimic the P₃ isoleucine lateral moiety was introduced, targeting the important hydrophobic pocket that accommodates residue P₃ on the enzyme (Table 3.3).

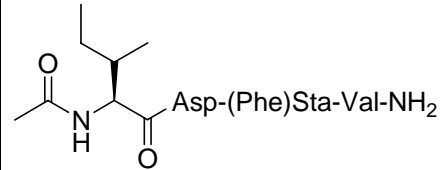
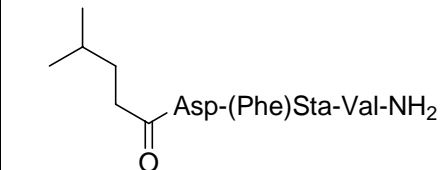
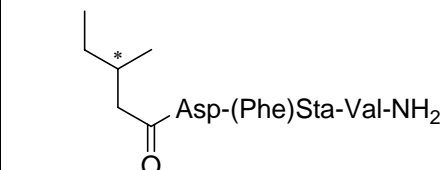
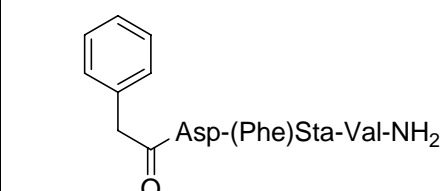
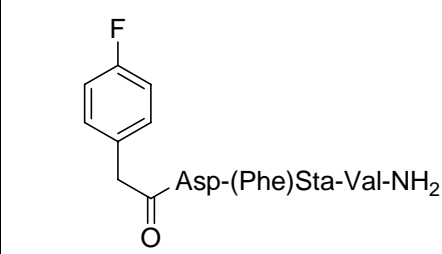
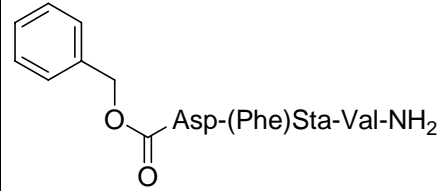
Name	Formula	K _i (μM)
8	 Asp-(Phe)Sta-Val-NH ₂	5.4±1.0
14	 Asp-(Phe)Sta-Val-NH ₂	>1000
15	 Asp-(Phe)Sta-Val-NH ₂	>1000
16	 Asp-(Phe)Sta-Val-NH ₂	>1000
17	 Asp-(Phe)Sta-Val-NH ₂	>1000
18	 Asp-(Phe)Sta-Val-NH ₂	>1000

Table 3.3. Hydrophobic lateral chains mimicking the Ile moiety, which were introduced to replace the amino acid in position P₃.

Very surprisingly, all replacements resulted in complete loss of inhibitory activity toward BACE, relative to the activity of the base compound **8**. The reasons for such a trend possibly reside in either the lack of the N-terminal amide

group, which might be involved in a stabilizing H-bond net, and/or in the high regiospecificity of the interactions between the acetyl-Ile moiety and the enzyme, where the stereochemical orientation of the side chain is playing a crucial role, as shown in particular by the comparison between **8** and **15**.

3.1.2.2 Modelling of Macrocyclic Statine-Peptides

A further development in our study was the screening and identification of the cyclic pattern that would be subsequently used for the optimization.

For this purpose the statine-peptides **8** and **11** were docked to the X-ray structure of BACE and possible ring closure patterns were analyzed, in which the main site of interaction with the enzyme would be maintained unaltered and the backbone of the statine-peptides forced in an extended conformation. Among the larger variety of possible cyclic structural motifs three approaches were considered in first instance as promising. These patterns are shown in Fig. 3.16.

The first series of compounds are derived from the crosslinking of the side chain carboxy groups of the two aspartyl residues in position P₂ and P₃' with diamine linkers of different length and structural character (*side-chain-to-side-chain* cyclization) (Fig. 3.16, type A).

As observed with the activity tests for the linear compound **8**, aspartic acid P₃' was not necessary for recognition by the enzyme. This indicated the possibility of reducing the length of the sequence to the P₂' Val and closing the ring between Asp P₂ and the main backbone chain in a *side-chain-to-head* cyclization with a diamine spacer (Fig. 3.16, type B).

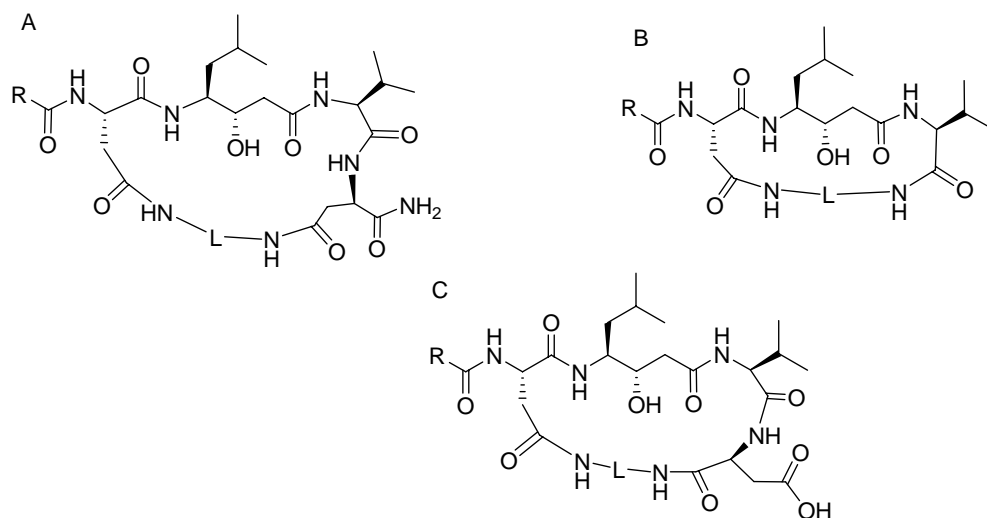


Figure 3.16. Cyclic peptide motifs designed for the development of potential BACE inhibitors: A) cyclization is performed between the side chain β -carboxy groups of the two aspartyl residues of compound **8**; B) cyclization occurs between the β -carboxy group of the Asp residue in P_2 position and the C-terminal α -carboxy group of the Val residue via diamine spacers; and C) cyclization is performed between the side chain β -carboxy group of Asp in P_2 and the α -carboxy group of the C-terminal Asp via diamine spacers to allow installment of a potential salt bridge between the C-terminal Asp residue and Arg¹²⁸ of the enzyme.

Additionally, a close inspection of the inhibitor **11**/enzyme interaction revealed that the residue Arg¹²⁸ is in relative close proximity to the lateral chain of Asp P_3' in the linear compound. It was therefore argued that a free Asp P_3' could be utilized in this case to form a salt bridge with the Arg guanido group, and to address this possibility, we synthesized a compound in which the cycle is created between the Asp P_2 and the backbone (*side-chain-to-head*), carrying a non protected Asp P_3' (Fig 3.16, type C).

The next step was the definition of the ring size and rigidity. Computer modeling based on the crystal structure of the enzyme-peptide inhibitor complexes suggested that the enzyme could effectively accommodate cyclized tri-, tetra- and pentapeptide analogues of structure types A, B or C using different diamines as spacers. The diamines were chosen based on length and rigidity, and the first proposed were 1,3-propanediamine, 1,4-butanediamine, 1,5-

pentanediamine and the more or less rigid 1,4-phenylenediamine or 1,3-phenylenedimethanamine.

Inhibitors following this design would have the advantage of being conformationally restrained and preorganized for binding to the protease with reduced entropic cost, favoring the acquisition of a β -extended conformation, as confirmed by molecular dynamics experiments. In addition to this entropic advantage, cyclic inhibitors are also known to be more resistant to proteolytic degradation than linear peptidomimetic inhibitors.

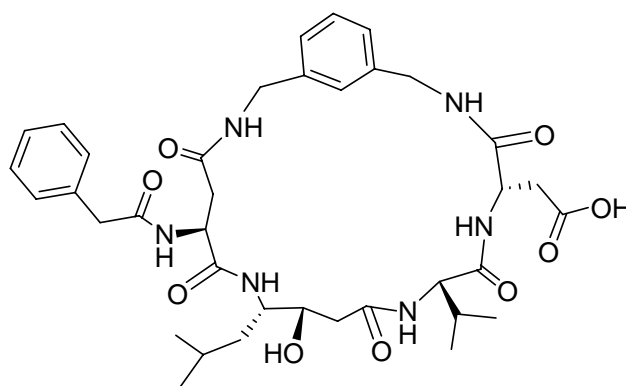
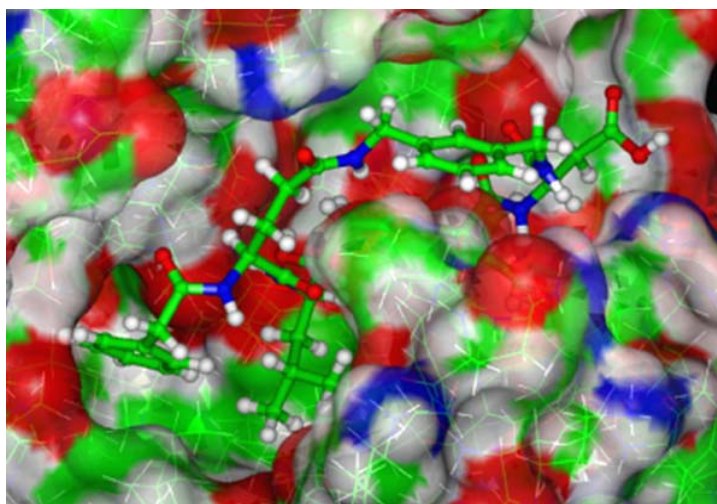


Figure 3.17. *Top:* side view of the catalytic cleft accommodating a macrocyclic compound of the type C with 1,3-phenylenedimethanamine as linker; *bottom:* the chemical structure of the 22-membered macrocycle.

Fig. 3.17 shows an example of the modeling experiments: it shows the modeling of one of the type C cycles, which reveals how the lateral chain of Sta and the aromatic ring of the N-terminal benzyloxycarbonyl group are well accommodated in two deep hydrophobic pockets corresponding to the enzyme subsites S_1 and S_3 respectively. It also shows the position of the OH group of statine, responsible for the inhibitory interaction with Asp³² and Asp²²⁸, directed toward the hydrophilic cavity created by the two residues. Furthermore, it demonstrates that the side chain carboxy group of Asp is indeed positioned in close proximity to the guanido group of Arg¹²⁸ confirming the working hypothesis for this type of macrocycles.

In Fig. 3.18 the same cycle is slightly flipped to display the position of the linker externally on top of the closed flap. No steric clashes resulted between the enzyme and any part of the cycle.

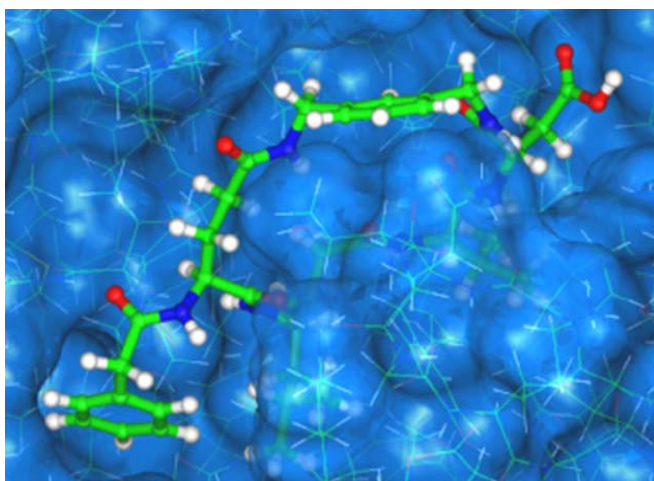


Figure 3.18. Side view of the catalytic cleft of BACE with the *in silico*-bound structure of a type C macrocyclic compound. The relative position of the protein flap domain and the spacer of the inhibitor, i.e. the 1,3-phenylenedimethanamide, is well evidenced.

To further confirm the correctness of this working hypothesis, molecular dynamics were performed on various designed macrocycles and the results, which will be described in more detail in chapter 3.1.2.5, fully confirmed a strongly restricted conformational space with the peptide backbone locked in

extended conformations. In conclusion the results of both molecular modelling and molecular dynamics confirmed the proposed supposition that this type of macrocyclic statine-peptides could become a novel category of BACE inhibitors in which the preorganized β -type conformation of the backbone is stabilized by the more or less rigid ring structures.

3.1.2.3 Synthesis of Macrocyclic Statine-Peptides

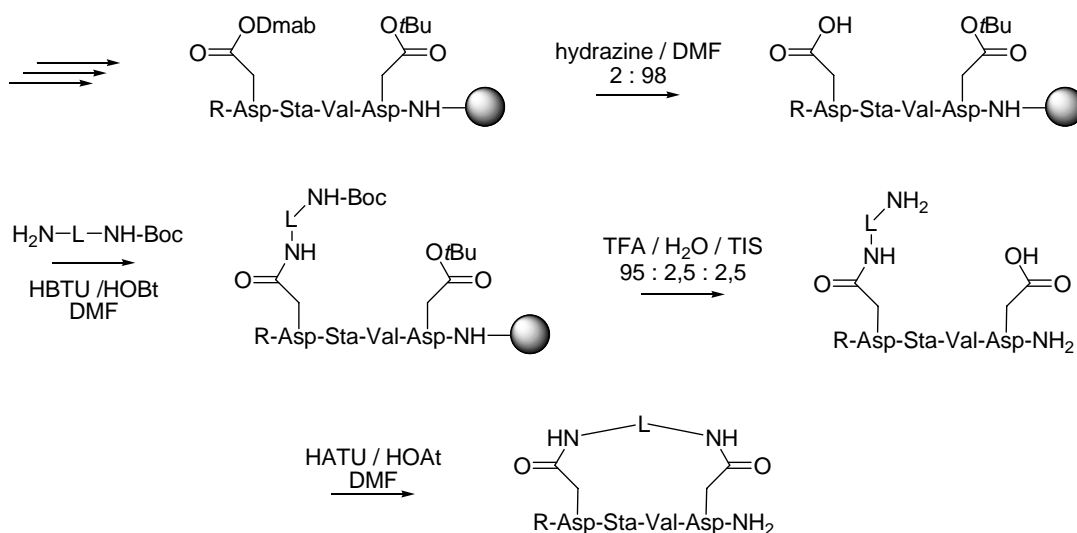
For the synthesis of the linear precursors we have selected the Fmoc/*t*Bu strategy²⁰⁸ with acid labile resin linkers depending upon the the target C-terminal functionality (amide or free carboxy group). The statine derivative used for the synthesis of the linear precursor was Fmoc protected at the *N*-terminus and not protected at the hydroxyl group, since *O*-acylation was found to occur at negligible extents even using HOAT/HATU. For the subsequent steps on resin and cyclization in solution at high dilution, optimal synthetic routes had to be elaborated for each type of macrocycle.

Synthesis of type A macrocycles

The most suitable way of synthesis of the cycle type (A) was delineated after a series of preliminary trial synthesis, reported in Scheme 3.2, 3.3 and 3.4.

The first synthetic route was based on the synthesis of peptides protected on the lateral chain of either one of the two Asp residue with orthogonally protecting groups that can be removed and further reacted with the monoprotected diamine linker (Scheme 3.2). The two more suitable orthogonal protecting groups resulted Dmab²⁰⁹ and All²¹⁰, which we then used in our synthesis. Dmab $\{\beta$ -4-[N-{1-(4,4-dimethyl-2,6-dioxocyclohexylidene)-3-methylbutyl} amino] benzyl ester} is a quasi-orthogonally protecting group that can be removed selectively in the presence of *t*Bu- groups by treatment with 2% hydrazine in DMF. In our case, a non quantitative cleavage of the Dmab group

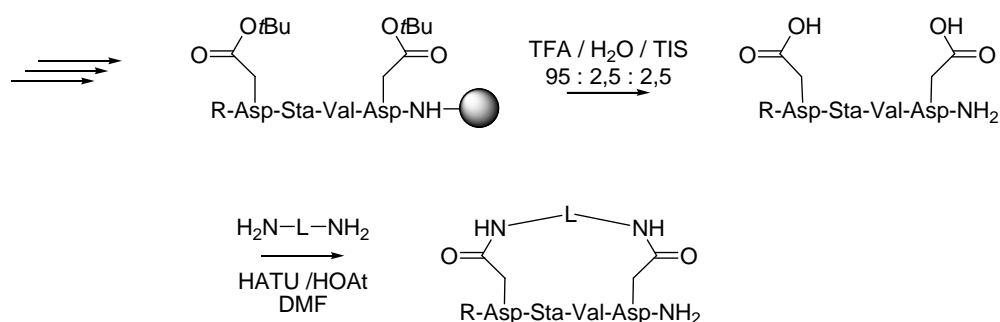
was observed in experiments performed on aliquots of the resin-linked fully protected peptide. The same poor deprotection capability was found using aspartic acid β -allyl ester [Asp(OAll)], which can be selectively cleaved in the presence of Fmoc- and *t*Bu-based protecting groups by treatment with $\text{Pd}(\text{Ph}_3\text{P})_4/\text{PhSiH}_3$ in DMF.²¹¹ Only after repetitive deprotection cycles and extended reaction times in both cases, the reaction proceeded to extents that allowed the subsequent step to be performed. However, the following coupling with the monoprotected diamine linker 1,3-phenylenedimethanamine, monoprotected as Boc derivative, with HOBt/HBTU resulted in extremely low yields. From these experiments we argued that the lateral chain of Asp was probably not completely exposed to solvent due to a seemingly difficult sequence, forcing us to a new strategy of synthesis.



Scheme 3.2. This synthetic route foresees the synthesis of a suitably protected statine-tetrapeptide with the two Asp residues protected in selective manner at the carboxy side-chain groups to allow for regioselective deprotection of one carboxy group for subsequent attachment of the diamine spacer and after full deprotection and cleavage from the resin, to perform the final cyclization in solution. The route failed in the coupling step of the mono-protected diamine on resin.

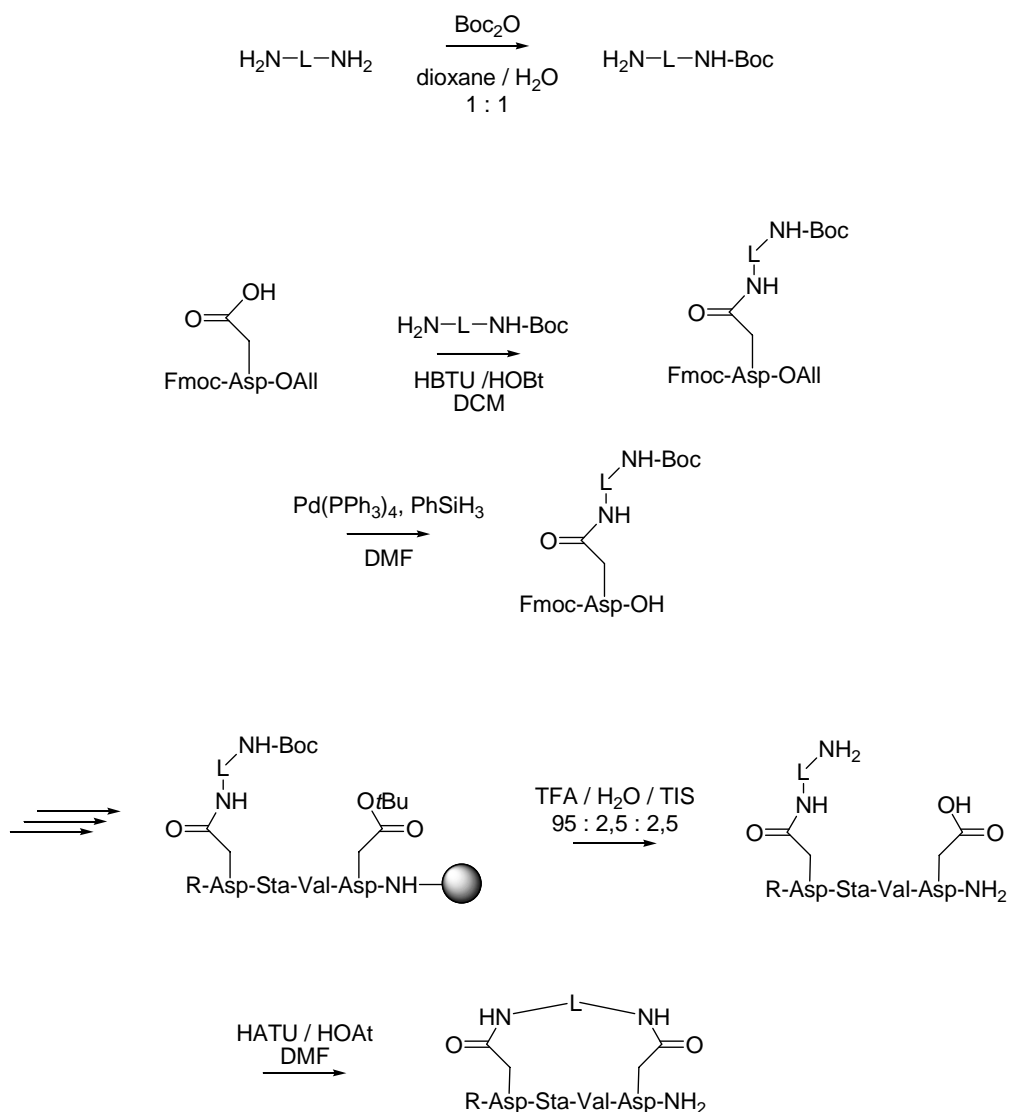
A second strategy was the synthesis of the peptide amide on the resin using Fmoc chemistry on the main chain and the classical *tert*-butyl esters protection

for both the Asp residues. After acidolytic cleavage from the resin and complete deprotection, it was reacted with the free diamine linker (Scheme 3.3), applying the principle of high dilutions (10^{-4} M). Under these conditions, a reaction between three molecules should represent an extremely rare event, in both the possibilities of a coupling between one molecule of peptide and two diamines or the cross coupling between one diamine and two peptides. Once a diamine reacts with one free Asp, the vicinity of the second Asp to the second amine group should drive to the formation of the cycle. This second way resulted more effective, some level of cyclization was detected but the final reaction mixture proved to be rather complex for isolation of the desired product in satisfactory yields, and for these reasons a more adequate approach was attempted.



Scheme 3.3. Synthesis of the linear precursor followed by simultaneous resin-cleavage and deprotection of both side-chain carboxy functions for subsequent one-pot cyclization in solution via the unprotected diamine spacer.

The third and most efficient way for the synthesis of the cycles is outlined in Scheme 3.4 and required the preliminary synthesis of the Asp building block, protected at the *N*-terminus with either Fmoc- or Z- (according to the target macrocycle) and the incorporation of the Boc- monoprotected diamine linker in solution. Such functionalized Asp is then incorporated in the chain during the elongation steps of the linear peptide on solid support. After the cleavage from the resin of the linear compound with concomitant removal of the Boc protecting group, a cyclization reaction is performed under high dilution conditions, which favour the intra- over the intermolecular reaction.



Scheme 3.4. The aspartyl residue is converted into the β -amide with the mono-protected diamine spacer and then directly used in the synthesis of the linear precursor. Deprotection and resin-cleavage afford the intermediate for the final cyclization with reagents such as HOAT/HATU.

Several important considerations were necessary for the cyclization step. In the synthesis of cyclic peptides, it is conventional wisdom that the ease of the reaction depends largely on the size of the ring to be closed, and that no difficulties arise for the cyclization of peptides containing seven or more amino acid residues. Although ring closure with hexa- and pentapeptides is more difficult, the ease of cyclization is often enhanced by the presence of turn structure-inducing amino acids such as glycine, proline, or a D-amino acid.²¹²⁻²¹⁴

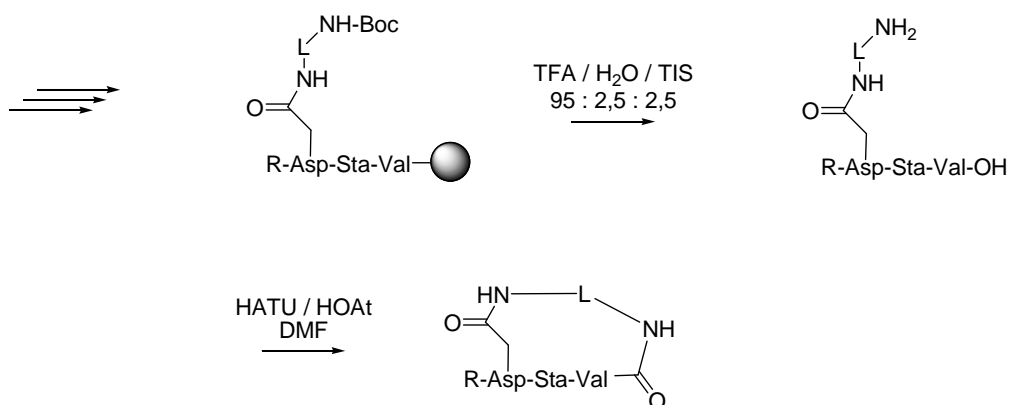
For linear peptides that do not contain amino acid residues that stabilize turn structures, the cyclization reaction is generally a disfavoured or slow process, and side reactions such as cyclodimerization, may prevail even operating at high dilutions (10^{-3} - 10^{-4} M). For such slow cyclizations the increased lifetime of the intermediate activated linear peptide provides an opportunity for increased epimerization at the C-terminal residue via the 5(4H)-oxazolone mechanism.²¹⁵ This aspect was a particular concern for type B and C macrocycles of the present study. The extent of epimerization may be diminished by application of the azide method.²¹⁶ However, this method and its modifications are extremely slow, usually requiring many hours or even several days for completion.^{216,217} In comparison with those methods, strong acylating procedures such TBTU/HOBt²¹⁸ and PyBOP^{195,196} provide fast cyclization²¹⁹ but may also lead to C-terminal epimerization levels that are comparable to those observed with DCC/HOBt.²²⁰

Taking into account these considerations, for a trial synthesis of cycle A (for which no epimerization at the C-terminus is possible) in first instance we used the coupling reagents PyBOP/HOBt, since PyBOP is reported to be particularly suited for sterically demanding or hindered coupling reactions. Even though the reaction proceeded with relatively good yields, it was accompanied by the formation of a subproduct characterized by an intense peak of m/z 258.2 $[M+1]^+$ and 515.6 $[2M+1]^+$ and identified as tripyrrolidinophosphonium oxide (MW_{calc} : 257.3), which was difficult to separate from the desired product via preparative HPLC.

For these practical reasons the second coupling reagent HATU/HOAt method was tested, which is known to give improved results with regard to both speed and maintenance of chiral integrity at the C-terminus;¹⁹⁴ moreover, the reaction results in water soluble subproducts, readily removed by regular washing steps. Accordingly, this reagent was applied for the production of the type A macrocycle, but also of the type B and C macrocycles

Synthesis of type B macrocycles

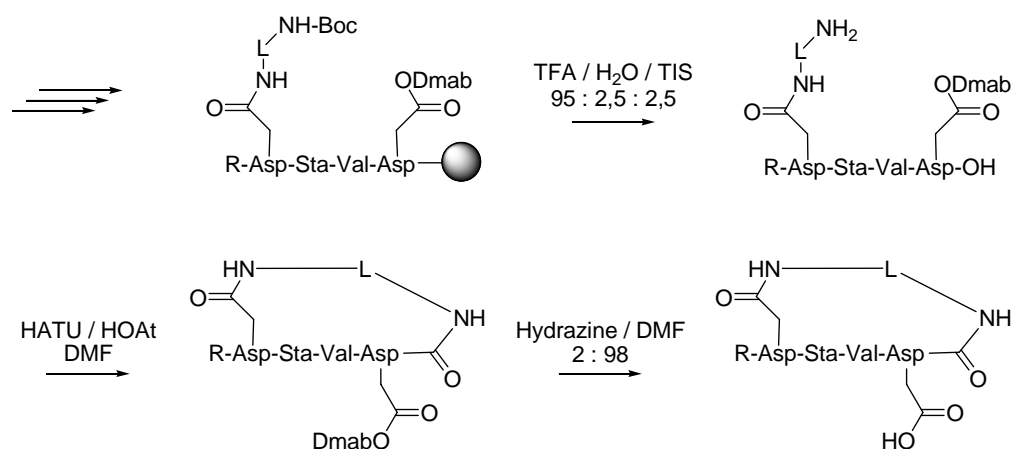
For the synthesis of the second class of cycles (Fig. 3.16, type B) again the Asp building block already derivatized with the protected diamine linker was introduced during the synthesis of the peptide acid on 2-chlorotrityl chloride resin (Scheme 3.5). After cleavage from the resin and the simultaneous deprotection step by acidolysis, cyclization is performed under conditions of high dilution by HATU/HOAt, yielding the desired product.



Scheme 3.5. Synthetic route for the synthesis of type B macrocycles. The Asp residue is derivatized with the monoprotected diamine and then introduced in the peptide using regular Fmoc/*t*Bu solid phase synthesis of the linear precursor on 2-chlorotrityl chloride resin. After acydolytic resin cleavage and deprotection, cyclization is performed in solution at high dilution (R- = Z-; L = spacer)

Synthesis of type C macrocycles

For the synthesis of type C macrocycles (Scheme 3.6), a protection of the β -carboxy group of the C-terminal aspartyl residue in P₃' orthogonal to Fmoc protection scheme was required. This protection has to be maintained during cyclization of the peptide between the C-terminal carboxy group and the amino group of the already incorporated diamine spacer. The Dmab ester protection was selected for this purpose. Following cyclization in high diluted conditions, deprotection with 2% hydrazine in DMF afforded the desired cyclic product in good yields (Scheme 3.6).



Scheme 3.6. Synthetic route for the type C macrocycles. The C-terminal Asp residue is orthogonally protected with Dmab, while the N-terminal Asp residue, derivatized with the monoprotected diamine, is incorporated in the linear precursor during the regular Fmoc/*t*Bu solid phase synthesis on 2-chlorotrityl chloride resin. Cyclization is performed after cleavage from the resin, followed by the final deprotection of Dmab (R- = Z-; L = spacer).

3.1.2.4 Inhibitory Potencies of the Macrocyclic Statine-Peptides

In a first generation of macrocycles A, B and C, statine was incorporated as transition state analogue and the isoleucine as P₃ residue was substituted by the more flexible and aromatic benzyloxycarbonyl (Z) group. The three different cyclic compounds were synthesized using two different aromatic spacers for cyclization, 1,3-phenylenedimethanamine and the more rigid 1,4-phenylenediamine. The inhibitory activities of a first series of the macrocycles type A, B and C are compared in Table 3.4, 3.5 and 3.6 with the linear precursors.

3. Results and Discussion

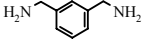
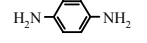
Spacer	R-Asp-X-Val-Asp-NH ₂ L	K _i [μM]	R-Asp-X-Val-Asp-NH ₂ └─┬─┘	K _i [μM]
H	19	>1000		
	20	>1000	21	>1000
	22	>1000	23	44 ± 18

Table 3.4. Inhibitory potencies of type A macrocycles and their linear precursors with X = Sta.

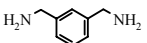
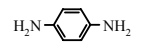
Spacer	R-Asp-X-Val-OH L	K _i [μM]	R-Asp-X-Val └─┬─┘	K _i [μM]
H	24	>1000		
	25	>1000	26	>1000
	27	>1000	28	>1000

Table 3.5. Inhibitory potencies of type B macrocycles and their linear precursors with X = Sta.

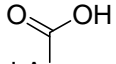
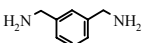
Spacer	R-Asp-X-Val-Asp-OH L	K _i [μM]	 R-Asp-X-Val-Asp └─┬─┘	K _i [μM]
H	29	>1000		
	30	>1000	31	>1000

Table 3.6. Inhibitory potencies of type C macrocycles and their linear precursors with X = Sta.

For the type A cycles (Table 3.4), all the linear compounds tested **19**, **20**, **22** resulted not active: this was not surprising if we keep into account the result of the linear compounds tested previously, in which the *N*-terminal Ile was replaced by a non chiral, flexible acyl moiety (see chapter 3.1.2.1). Also the attempt of *side-chain-to-side-chain* ring closure with a flexible diamine like 1,3-phenylenedimethanamine resulted in no improvement to the activity of those compounds. More interestingly, a more rigid diamine linker, such as 1,4-phenylenediamine, introduced to conformationally restrict the peptide, increased the inhibitory activity to the low micromolar range, demonstrating the potentials of a macrocyclic ring closure and confirming the working hypothesis.

Analogously, it was not surprising that the linear compounds **24**, **25**, **27**, **29** and **30** were not active. More surprising, given the promising results of the molecular modelling experiments, was that none of the cycles type B (Table 3.5) nor C (Table 3.6) resulted active.

Based on these results and taking into account the observation that the *N*-terminal hydrophobic pocket was essential for positive inhibitor/enzyme interaction, as well as the higher affinity showed by the enzyme for (Phe)Sta with respect to Sta, a new series of macrocycles type A was generated. The preferred Ile was introduced in position P₃ to replace the Z group at the N-terminus, while (Phe)Sta replaced Sta in the central inhibitory core. Cyclization reactions were performed with aromatic (1,3-phenylenedimethanamine and 1,4-phenylenediamine) and aliphatic (1,3-diaminopropane, 1,4-diaminobutane, 1,5-diaminopentane) linkers and a new series of compounds was studied. Inhibitory activities are reported in Table 3.7.

3. Results and Discussion

Spacer	R-Asp-X-Val-Asp-NH ₂ 	K _i [μM]	R-Asp-X-Val-Asp-NH ₂ 	K _i [μM]
H	11	5.4 ± 1.1		-
	32	135 ± 12	33	10.5 ± 1.5
	34	71 ± 8	35	12.5 ± 1.7
	36	16 ± 1.4	37	10.2 ± 1.6
	38	5.9 ± 0.6	39	2.8 ± 0.6
	40	7.5 ± 0.8	41	not soluble

Table 3.7. Inhibitory potencies of type A macrocycles and their linear precursors with R = Ac-Ile and X = (Phe)Sta.

The linear compounds carrying an aliphatic diamine linker on the Asp lateral chain (**32**, **34** and **36**) resulted all considerably less active with respect to the unmodified linear compound (**11**); nevertheless, cyclization resulted in macrocyclic peptides with a 13-, 5.6- and 1.5-fold increase in inhibition respectively (peptides **33**, **35** and **37**), despite their flexibility.

The insertion of aromatic linkers in the linear compound (compounds **38** and **40**), appeared to be less disturbing to the overall inhibitor recognition by the enzyme, if compared with the aliphatic spacers, showing activities that were comparable with the one of the linear, non modified compound (**11**). The closure of the macrocyclic ring via the aromatic relatively flexible diamine 1,3-phenylenedimethanamine to partially constrain peptide **11** resulted in a 2-fold enhanced binding affinity (peptide **39**). Unfortunately, the cyclic peptide **41**, incorporating the 1,4-phenylenediamine rigid linker to freeze the structure in an extended conformation, was insoluble in the assay buffer. Nevertheless, these findings confirm the validity of the concept and suggest that an improvement in solubility of compound **41** could lead to submicromolar inhibitors.

3.1.2.5 Molecular Modeling of Compounds **23** and **39**

In order to investigate the validity of the approach and the effects of cyclization on the conformational space of the macrocycles, compound **23** and **39** were additionally studied with molecular dynamics experiments. Fig. 3.19 presents the superimposition of the 10 lowest-energy structures of compound **23**.

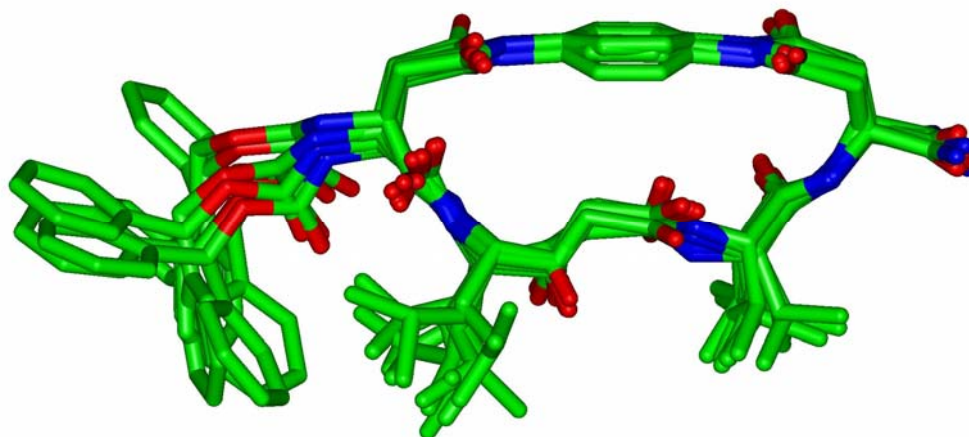


Figure 3.19. Ensemble of the 10 lowest energy structures of the macrocycle **23** as resulting from molecular dynamics.

The superimposition validates our reasoning that cyclization consents the building of a rigid structure in which the backbone of the peptide is constrained in a fully extended conformation. Only the benzyloxycarbonyl moiety appears to be occupying a relaxed conformational space. Superimposition of this structure with the inhibitor OM00-3 in the enzyme-bound state (Fig. 3.20) shows the reasonable backbone overlapping with the backbone of the molecule obtained from the crystal structure analysis; additionally the lateral chains responsible for recognition of the enzyme [namely (Phe)Sta or Sta in position P_1 , Z in P_3 , Val in P_2'] are positioned in the same range; most importantly the statine hydroxyl group responsible for inhibition is directed toward the enzyme in a manner similar to the reference inhibitor OM00-3. A similar good overlapping was also found for the more flexible macrocycle **39** (also represented in Fig. 3.20).

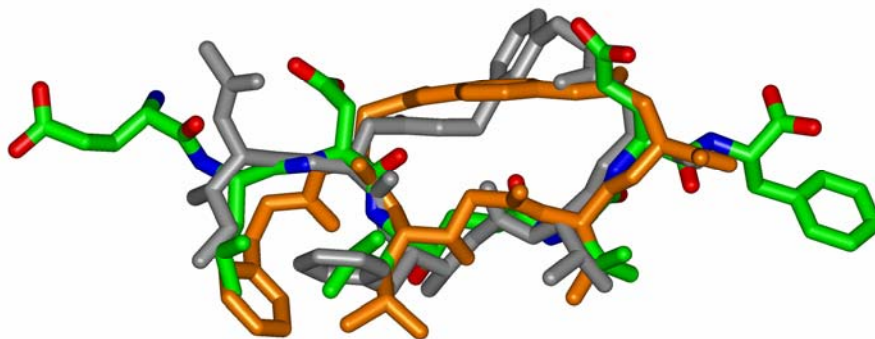


Figure 3.20. Superimposition of inhibitors OM00-3 (atom colour), compound **39** (grey) and compound **23** (orange).

Docking experiments were also performed for a better understanding of the interaction between the macrocycles and the enzyme. The structures of the inhibitors **23** and **39** resulting from the molecular dynamics were docked on the enzyme pocket (Fig. 3.21). It was possible to exclude clashes with the enzyme, also in the more rigid and possibly less accommodating structure of compound **23**. Pockets S_1 , S_3 and S_2' in the enzyme appear to well accommodate the hydrophobic lateral chains of the inhibitors and the linker appears to be positioned into the bulk water, not interfering with the flap domain that closes the proteolytic cavity.

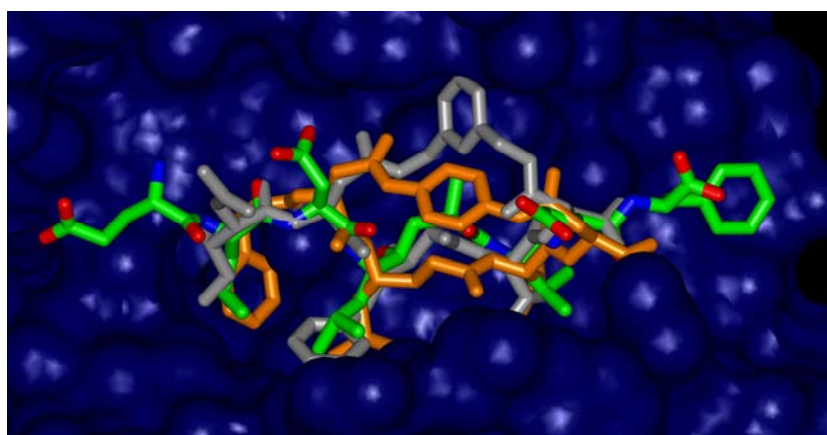
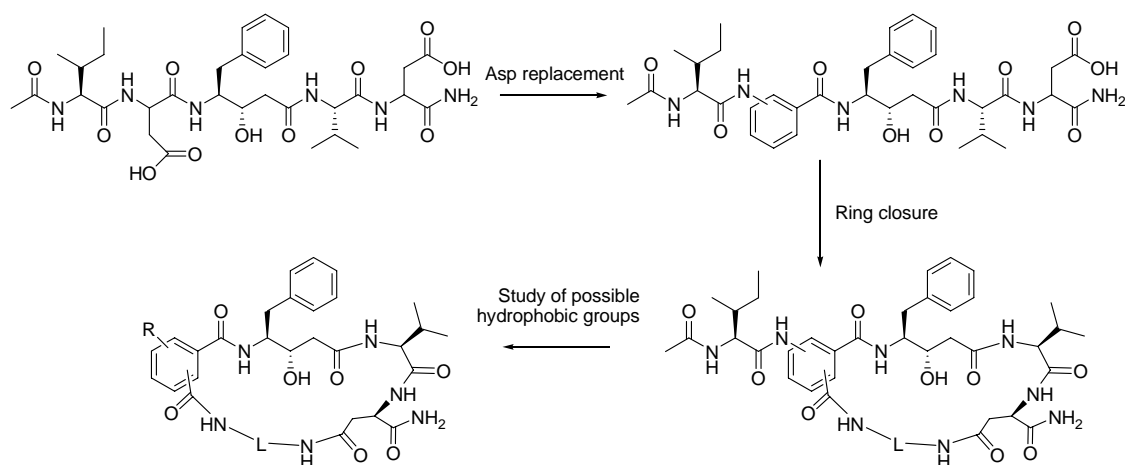


Figure 3.21. View of the binding pocket with the superimposed inhibitors OM00-3 (atom colour), compound **39** (grey) and compound **23** (orange)

3.1.3 Amino-Benzoic Acid Approach

In efforts to fight the human immunodeficiency virus (HIV-1), the cause of acquired immunodeficiency syndrome (AIDS), potent inhibitors of HIV-1 protease were identified with desirable antiviral activity and pharmacologic properties. Among those, Braztel and co-workers discovered isophthalamide through application of known asparagine replacements to the P₂-P₃ region of the molecule.²²¹ The isophthalamide was confirmed to be an optimal N-terminus for BACE-1 inhibitors as well.²²² The observation that replacement of the aspartic acid in position P₂ for a covalently bound (like in the cyclic BACE-1 inhibitors) or H-bonded (like in inhibitor OM99-2) aspartic acid suggests that both polar and lipophilic side chains in this region are well-tolerated by the enzyme. Furthermore, the aspartic acid was used in our design as an anchoring group for the construction of rigid rings.

With these observations in mind and in order to bias the molecule into a low energy conformation suitable for binding, we decided to use different amino-benzoic acid scaffolds to rigidify the backbone of the peptide in the otherwise flexible P₂ position. A second step would be to exploit the insertion of a carboxylic acid moiety in the aromatic ring that will serve to link it via a spacer to the Asp-P₃'. A further step could be the insertion of a hydrophobic chain oriented appropriately to bind to the S₃ pocket (Scheme 3.7).



Scheme 3.7. A new concept for the design of cyclic inhibitors of BACE-1: investigation of the insertion of an amino-benzoic acid in position P₂; assessment of the possibility of ring closure based on the amino-benzoic acid with a spacer L; minimization of the structure and addressing of special pockets.

The aim of the first series of molecules synthesized was to define the best amino-benzoic acid for our purposes. Four molecules were synthesized and tested for biological activities, the results are reported in Table 3.8.

From the modeling performed in advance, the less probable molecule to bind BACE-1 was compound **44**, a fact which was indeed confirmed by the activities: the reason has to be searched mainly in the long stretch that the aromatic ring produces, which forces the Ile further down in the catalytic cleft, away from the important hydrophobic pocket that should otherwise accommodate it. Modeling experiments supported that an *ortho* linkage (**42**) would serve to orient favourably the Ile CO to gain a hydrogen bond with the enzyme. However, the lack of activity clearly contrasts this modelling based expectation. The *meta* orientation of the ring **43** proved to be the most appropriate, both in terms of orientation of the amide ring and distance between the two amide bonds, and was then chosen for further studies.

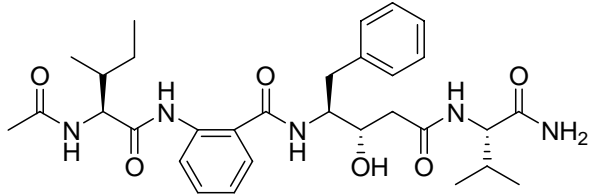
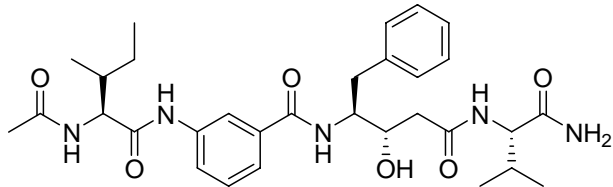
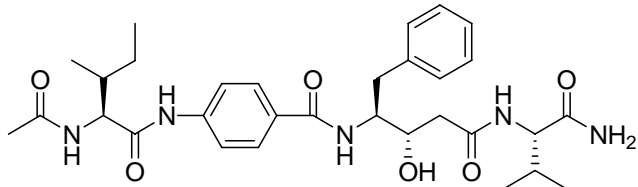
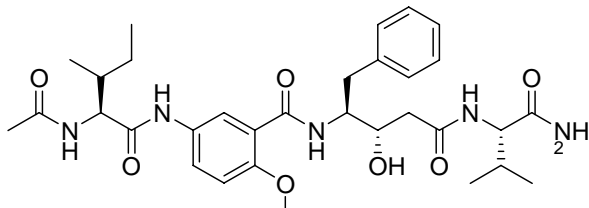
Compound	Peptide Structures	K_i (μM)
42		>1000
43		47±6.0
44		>1000
45		6.5±0.7

Table 3.8. Inhibitory activity data for the 4 compounds synthesized, carrying an amino-benzoic acid replacing the aspartic acid in position P₂.

A very interesting development was given by the methoxy substituent in *para* position of compound **45**. From the modelling it was not possible to identify favourable interactions that could explain the 7-fold increase in activity with respect to compound **43**; a plausible explanation is that the oxygen forms an H-bond with the amine group of statine, with an additional stabilizing effect of the structure. As a consequence, this substituent can be used either as the base for the closure of the macrocycle (Scheme 3.7) or as a general structural motif.

This first study, nevertheless, introduces interesting new structural aspects for further elaboration.

3.1.4 Synthesis of Di-Substituted Statines

When compared to a dipeptide (Fig. 3.22), statine is one backbone atom shorter than a dipeptide and it lacks a R_2 side chain; thus, as discussed previously, statines as TSA can not be considered as an ideal dipeptide isostere.

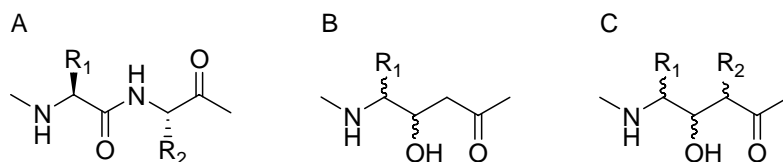


Figure 3.22. Structural differences between transition-state isostere dipeptide mimetics: (A) native peptide, (B) statine, (C) di-substituted statine.

Therefore, functionalization of the statine in position C_2 , could possibly improve the activity of aspartic protease inhibitors. Di-substituted statines are components of bleomycin^{223,224} and dolastatins,^{225,226} and a number of synthesis specific for these natural products have been developed. The (2,3)-*syn*-2-alkyl stereoisomers have been obtained also via a number of chiral auxiliary mediated reactions,^{227,228} while the 2,3-*anti* stereoisomer has been less explored.²²⁹

The aim of our project, the introduction of a side chain on the C_2 could open a completely new field in the search for small molecule inhibitors of BACE-1 particularly by improving the interactions between the cyclic inhibitors and the enzyme.

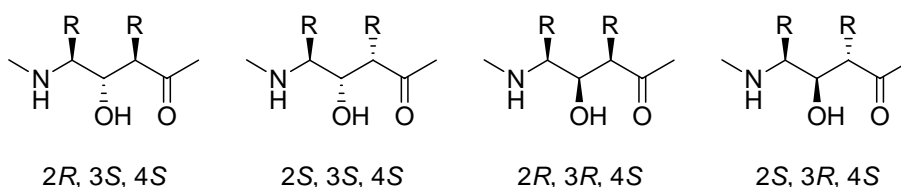


Figure 3.23. Structures of the 4 possible diastereoisomers of a di-substituted statine carrying a fixed $4S$ substituted carbon.

For this purpose molecular dynamics experiments were performed to identify the absolute configuration at the asymmetric centres C_3 , bearing the hydroxyl group, and C_2 , carrying the additional side chain; the stereochemistry for C_4 was maintained fixed as derived from L-amino acids (Fig. 3.23).

The known 1.9 Å⁶⁹ and 2.1 Å⁷⁸ crystal structures of BACE-1 bound to octapeptide mimetics were used as the starting point. An octameric inhibitor was constructed, of general formula Glu-Leu-Asp-*XSta*-Val-Glu-Phe, with *XSta* representing the di-substituted statine in 4 diastereoisomeric states that differ in the configuration at C_2 and C_3 , with either one of the two configurations *R* and *S*, while C_4 was maintained with an *S* configuration (corresponding to the natural L-configuration).

A conformational analysis of these initial structures was performed using the program Insight II. This program generates the most energetically stable conformations of a target molecule; by docking the resulting structures on the enzyme, we were able to evaluate the compounds with the highest affinity for the enzyme.

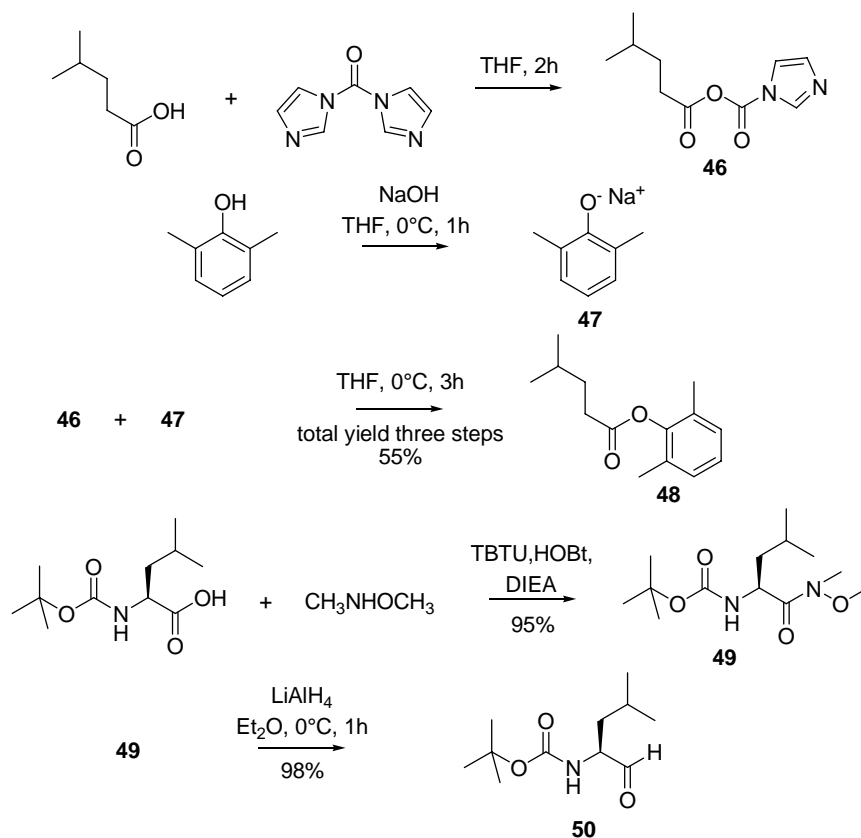
The resulting best structure was the one having carbons 2 and 3 respectively in *R* and *S* conformation. It was also noticed that even though a change in the absolute configuration at carbon 2 was still tolerated, the analogous modification at C_3 would create destabilizing clashes with the enzyme, besides moving the hydroxyl group away from the correct orientation toward the catalytic clef: the resulting *2R*, *3R* and *2S*, *3R* structures were thus the least tolerated of the series. The *2R*, *3S* conformer was therefore used to analyze different lateral chains on C_2 and C_4 . From all these iterations, a careful examination of each target in the active site of the enzyme allowed us to obtain a rough scale of possible alternatives to the amino acids already tested. The results are reported in Table 3.9.

P ₄	P ₃	P ₂	P ₁	P ₁ '	P ₂ '	P ₃ '	P ₄ '
Glu	Ile	Asp	Leu	Leu	Val	Glu	Tyr
	Phe		Phe	Phe		Gln	
			Met	Met		Met	
				Val		Lys	

Table 3.9. Analysis of the best accommodated amino acid chains in the pseudo octapeptide Glu-Leu-Asp-*XSta*-Val-Glu-Phe, where *XSta* is a di-substituted statine carrying the P₁ and P₁' lateral chains on the C₄ and C₂ of statine, respectively.

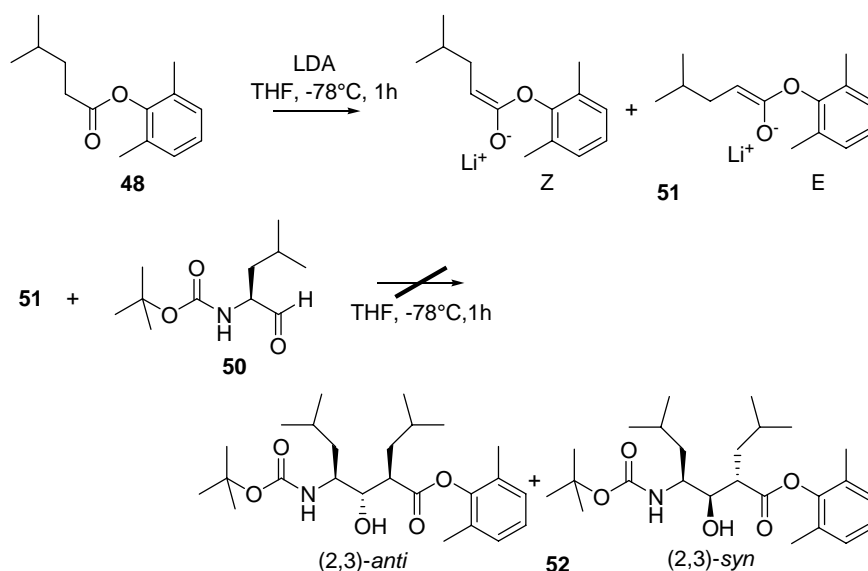
3.1.4.1 Lithium Enolates

A first approach to the synthesis of di-substituted statines started from a published procedure.²³⁰ According to this method, the (2,3)-*anti* stereoisomers are synthesized (Schemes 3.8 and 3.9) as separable diastereomers by employing an aldol methodology.



Scheme 3.8. General preparation of 2,6-dimethylphenyl isocaproate (48) and Boc-leucinal (50), starting materials for the subsequent aldol reaction.

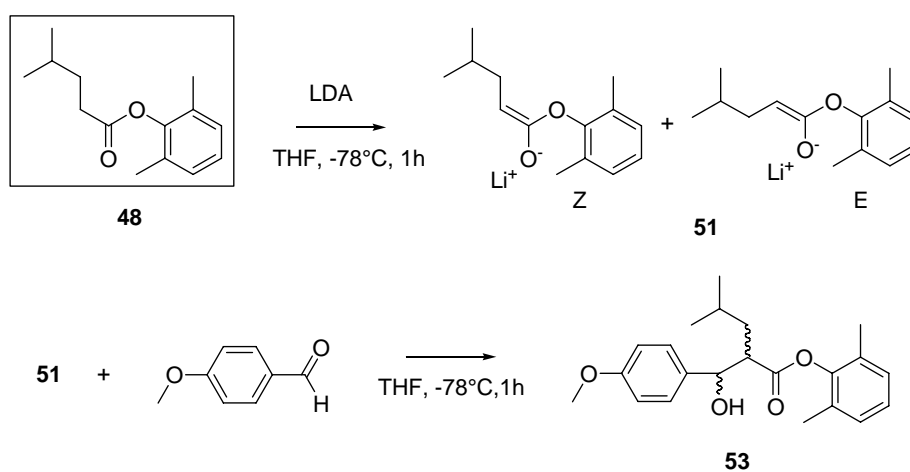
In order to achieve the synthesis of the two 2,3-*anti*-products **52**, the synthesis required the preparation of two adducts, 2,6-dimethylphenyl isocaproate **48** and Boc-leucinol **50**. Compound **48** was obtained in three steps: (1) 4-methylvaleric acid was added dropwise to a stirred solution of carbonyldiimidazole in THF and stirred for 2 h; (2) a solution of 2,4-dimethylphenol in THF was added to a suspension of NaH in THF at 0 °C and stirred for 60 min (during this time, the solution became homogeneous with a light purple color); (3) the acyl imidazole solution was added dropwise to the sodium phenolate solution at 0 °C, and was stirred for 3 h, to obtain the final desired 2,6-dimethylphenyl isocaproate **48** (total yield for all three steps was 55%). The aldehyde was obtained using the known Weinreb method:²³¹ the N-protected amino acid is converted to the N-methoxy-N-methyl amide (Weinreb amide) through a coupling with *N,O*-dimethylhydroxylamine and the Weinreb amide is then reduced to its aldehyde with LiAlH₄. The following deprotonation of 2,6-dimethylphenyl isocaproate **48** with LDA yielded the lithium *E*- and *Z*-enolates, which, as reported in the Ref²³⁰, should have reacted with Boc-leucinol to yield the pair of 2,3-*anti* and 2,3-*syn* products **52** via the Zimmerman-Traxler transition state.²³²



Scheme 3.9. Supposed preparation of the two possible 2,3-*anti* and -*syn* compounds **52** using 2,6-dimethylphenyl isocaproate (**48**) and Boc-leucinol (**50**) as starting materials.

The reaction was attempted several times, by vary temperature (-20 °C, 0 °C, RT), solvents (THF, Et₂O), lithium base (lithium diisopropylamide, butyl lithium), quantities of reactants and duration of the reaction, but neither of the products **52** was ever found in the final mixture in any of the experiments.

In order to exclude manual defects in carrying out the synthesis and to have a better understanding of the reaction system, the same procedure was performed using a less sterically hindered, commercially available aldehyde (anisaldehyde) and ester (ethyl acetate), as reported in Scheme 3.10 and 3.11.



Scheme 3.10. Aldol addition trial: 2,6-dimethylphenyl isocaproate (**48**) and the commercially available anisaldehyde were reacted in order to verify that the experimental procedure was correct.

The reaction was carried using the conditions reported in the original paper. Compound **53** was obtained in good yields (from HPLC) as the major peak of the reaction. Its identity was confirmed by mass spectrometry (Fig. 3.24) on the crude mixture from the reaction: compound **53** (MW: 356.47) gave a mass spectrum of 339.2 [M-H₂O+H]⁺ and 217.2 [M-(2,6-dimethylphenol)+H]⁺.

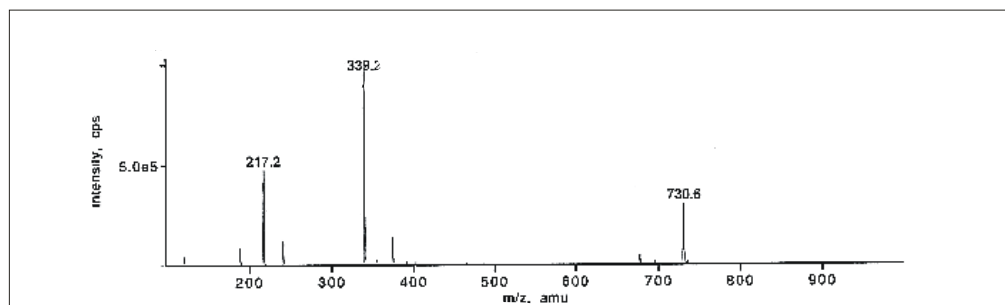
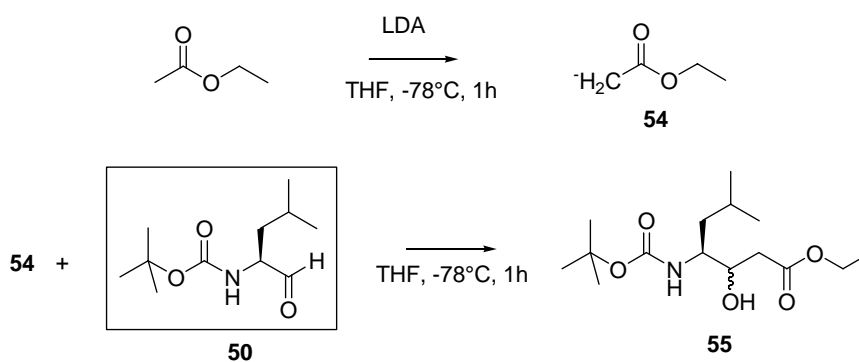


Figure 3.24. Mass spectrum of the crude mixture resulting from the reaction reported in Scheme 3.10.

The same critical test was performed on the synthesized Boc-leucinal (**50**) and ethyl acetate, which was previously treated with LDA (Scheme 3.11).



Scheme 3.11. Aldol addition trial: Boc-leucinal (**50**) and ethyl acetate were reacted in order to verify that the experimental procedure was correct.

Also in this case the reaction gave the desired product compound **55** (MW: 303.40), which showed a mass spectrum of 304.2 $[\text{M}+\text{H}]^+$, and the two characteristic peaks corresponding to the fragmentation of Boc at 248.2 and 204.2 (Fig. 3.25).

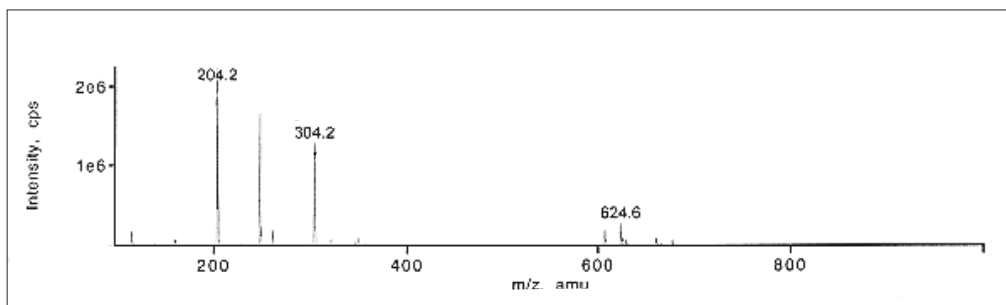


Figure 3.25. Mass spectrum of the crude mixture resulting from the reaction reported in Scheme 3.11.

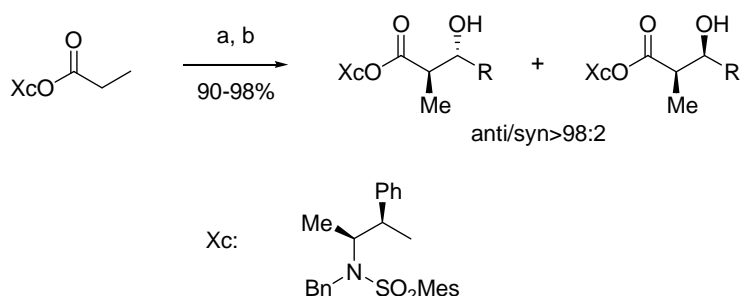
We interpreted these results from the trial reactions as proof that both the aldehyde and the ester were treated correctly during the procedure and that no technical problem was responsible for the absence of the desired product **52** in the reaction of interest. A possible, plausible explanation for this result is that the difference in sterical hindrance of compounds **50** and **51** with respect to the aldehyde and ester used in the trial reactions plays a major role in the reactivity of the two compounds.

3.1.4.2 Boron Enolates

A long standing problem associated with the aldol addition reaction in general and the chiral auxiliary mediated methodologies in particular, are the production of *anti*-aldol products. Most of the auxiliaries developed to date preferentially give *syn*-aldol products. The main problem arises from the fact that *E*-configured enolates, needed in the closed transition state to give the *anti* products, are not favored. Thus, one important direction of organic chemistry in the future is the development of practical and inexpensive reagents which induce preferential formation of *E*-enolates.

One potential class of such reagents has been presented by Abiko and Masamune starting from the commercially available (-)-norephedrine (Scheme 3.12).^{233,234} According to their work, under optimized conditions, the boron *E*-

enolate is obtained exclusively; it is reported then to react with a broad range of aldehyde substrates, including aliphatic, aromatic, α,β -unsaturated, and functionalized aldehydes, to afford aldols in up to 99:1 *anti:syn* selectivity ratio.



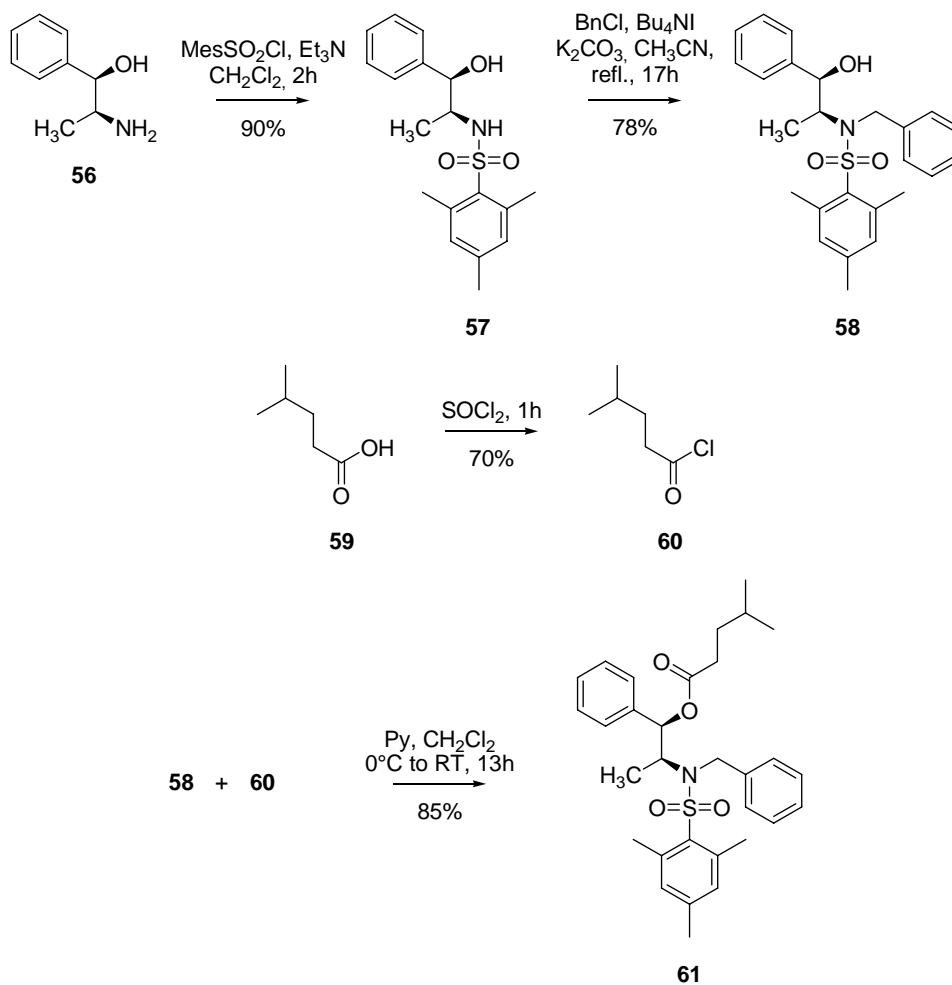
Scheme 3.12. *Anti*-selective boron-mediated asymmetric aldol reaction of carboxylic esters. a) $(c\text{Hex})_2\text{BOTf}$, Et_3N ; b) RCHO .

According to Abiko and Masamune's work, essential for the predominant formation of the *anti*-aldols is the reaction of an ester consisting of a sterically bulky alcohol with dicyclohexylboron triflate and then triethylamine. The use of other boron auxiliary groups (dibutylboron triflate, dicyclopentylboron triflate) or other amines (diisopropylethylamine) was also investigated, but it was shown that it would affect negatively the reactivity and/or the selectivity of the reaction.

The method presented the highest stereochemical selectivity among the ones found in literature, and for this reason, even though the reaction consisted of numerous steps and the use and preparation of non-commercially available boron auxiliaries required special care during operation, it was decided to use this method to attempt our synthesis.

The ester reported in Scheme 3.13, modified for our purposes as in compound **61**, was prepared from commercially available (-)-norephedrine (**56**) in four steps²³⁵ (Scheme 3.13): (1) selective sulfonylation of the amino group with mesitylenesulfonyl chloride and triethylamine to give compound **57**;²³⁶ (2) selective N-alkylation with benzyl bromide in the presence of base (K_2CO_3 in CH_3CN) afforded **58**; (3) synthesis of the 4-methylpentanoyl chloride **60** from 4-

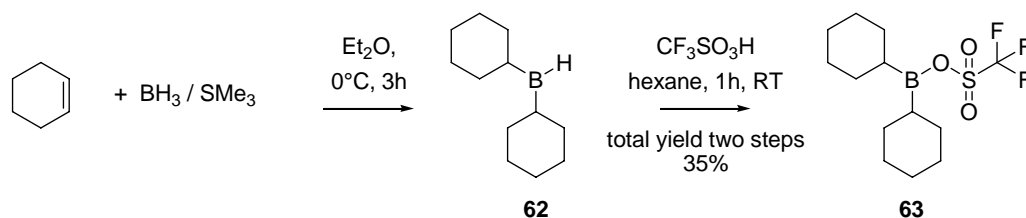
methylpentanoyl acid **59**; (4) the final acylation with 4-methylpentanoyl chloride and pyridine afforded compound **61**.



Scheme 3.13. Synthesis of the norephedrine-derived propionate ester designed for *E*-enolate and *anti*-aldols generation.

The reactions proceeded without difficulties in very good yields, as shown in the scheme.

The next step was the more difficult synthesis of the boron auxiliary^{237,238} (Scheme 3.14).

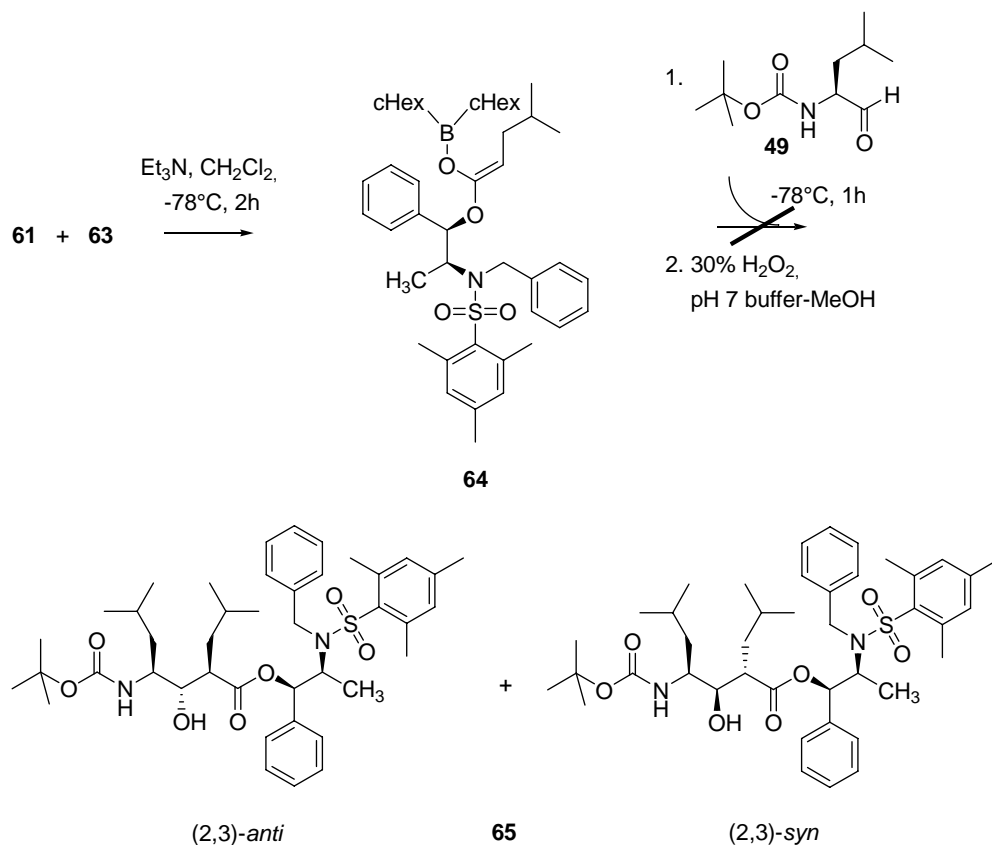


Scheme 3.14. Synthesis of dicyclohexylboron trifluoromethanesulfonate.

Given the presence of highly reactive boron compounds, the reactions had to be carried out in very dry conditions in argon atmosphere. All the solvents had to be dried and the glassware oven-dried overnight; argon had to be flushed before any addition of the reagents and the use of rubber septa was essential. The difficulty of the reaction required the setting up of all the material and the glassware in a very careful way, and it was necessary to repeat it several times before the yield given in the scheme (total for the two steps) could be obtained.

The cyclohexene was placed in an oven-dried, nitrogen flushed flask, capped with a rubber septum. Dry diethyl ether was added at 0°C and the borane-dimethyl sulfide complex was added dropwise, and then the whole reaction mixture was stirred for 3 h at 0°C . A solid formed, the supernatant organic solution was removed, and the residual solid was dried under vacuum to give dicyclohexylborane (**62**), which was used for the preparation of the triflate without purification. The solid was suspended in dry *n*-hexane and trifluoromethanesulfonic acid was added dropwise stirring. The solid gradually disappeared. The reaction was left for 1 h without stirring. A semi-solid phase appeared and the top layer was transferred into a dry flask with a syringe. Crystalline *c*-Hex₂BOTf (**63**) is obtained by placing the flask in a -20°C freezer for 36 hours, it was dried and redissolved in *n*-hexane to give the stock solution used for the next reaction (Scheme 3.15).

The aldehyde necessary for the following reaction was synthesized using the Weinreb amide procedure, as previously reported in Scheme 3.8.



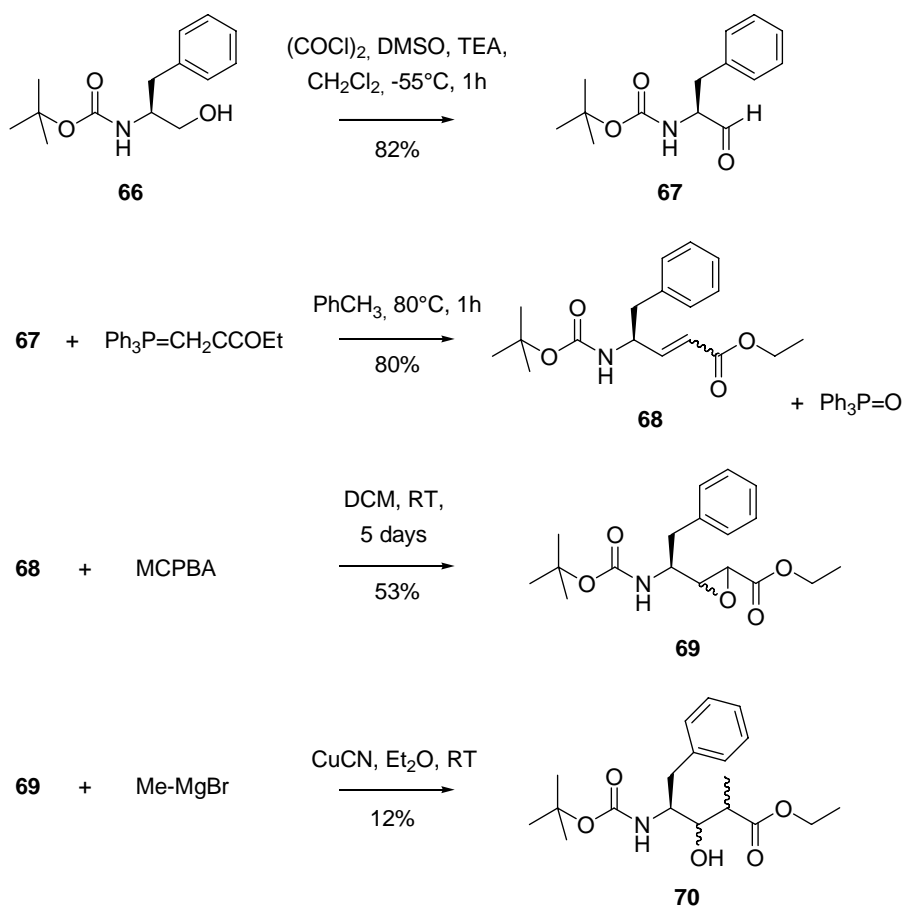
Scheme 3.15. Scheme of the *anti*-selective boron-mediated asymmetric aldol reaction of carboxylic esters.

According to the method, compound **61** should react with the dicyclohexylboron trifluoromethanesulfonate **63** and then triethylamine to form predominantly the *E*-enolate intermediate. The next reaction with a designated aldehyde should then afford essentially the *anti*-products **65**.

The reaction was attempted several times, with variations involving especially times and temperatures, but the products were never found in the final mixture. At the light of the previous reaction (chapter 3.1.4.1), this result was not surprising and our conclusion is that the sterical hindrance of the molecules indeed plays a major role in their scarce reactivity in this system.

3.1.4.3 Epoxide Opening with a Grignard Reagent

In this last attempt, we tried the development of a convenient procedure for the synthesis of di-substituted statine analogues from a modification of the synthesis of 2-heterosubstituted statine derivatives presented by Gstach and coworkers.²³⁹ The synthesis involves the conversion of a protected L-phenylalaninol to a γ -amino α,β -unsaturated ester, its highly diastereoselective epoxidation, followed by regioselective ring opening of the 2,3-epoxy esters with a Grignard reagent, resulting in 2-substituted statine derivatives. According to this work, the synthetic route was characterized by an extremely high stereochemical control, allowing the preparation of molecules with the desired stereochemical orientation. The synthesis, modified for our purposes, followed the routes described in Scheme 3.16.



Scheme 3.16. Epoxide opening with a Grignard reagent for the synthesis of di-substituted statines.

According to this scheme, protected (*S*)-phenylalaninol (**66**) was subjected to Swern oxidation,²⁴⁰ and the intermediate aldehyde was transformed by Wittig reaction to the corresponding γ -amino α,β -unsaturated ester **68**. The configuration of the olefinic double bond of **68** is defined *trans* in the reference paper; in our work, the configuration was not determined. Upon treatment of the electron-deficient γ -amino olefin **68** with *m*-chloroperbenzoic acid (MCPBA), the relatively smooth oxidation to the glycidic ester **69** took place. In the reference work, examination of the crude reaction mixtures revealed the highly diastereoselective formation of the desired (*2S,3R,4S*) compound **69** in a 90% excess with respect to the undesired (*2S,3S,4S*) compound. The reaction was very straightforward and no undesired by-products were detected beside non reacted starting material **68**.

The diastereomeric mixture of epoxides **69** was reacted in the next ring opening step with a Grignard reagent (MeMgBr). For this crucial step, the choice of the correct conditions was essential: a number of catalysts (CuI, CuCN), solvents (THF, Et₂O) and temperatures (-78 °C, 0 °C, RT) were tried, and the final combination (CuCN, Et₂O, RT) resulted essential for the proceeding of the synthesis. The product (of unidentified stereochemistry) was identified with mass spectrometry (MW: 351.45; molecular ions identified: m/z 352.2 [M+1]⁺; 296.2 and 252.2, peaks derived from the fragmentation of the protecting group Boc) and was purified by semipreparative HPLC.

Despite the final success in synthesizing the di-substituted statine, this route was abandoned for a number of reasons. First of all, the final mixture presented, with the desired product, also numerous unidentified compounds, which explained the extremely low yields. Considering the stereochemistry requirements for the final desired product, this low yields would be further decreased in the amount of final material available. Furthermore, the synthesis was performed using a commercially available Grignard reagent. The difficulty in the preparation and reactivity of such reagents in the case in which a vast variety

of nucleophiles -carrying different aliphatic, aromatic or functional groups- makes this path not easily accessible and inadequately flexible.

3.2 MMP-9: a Target for Drug Development

In recent years, numerous studies have shown the importance of MMP-9 in cancer and atherosclerosis. For example, in colorectal, breast, prostate and bladder cancer, most patients with aggressive disease have increased plasma levels of MMP-9.²⁴¹ In advanced colorectal cancer, high levels of MMP-9 have been associated with shortened survival.²⁴² In cardiovascular diseases, MMP-9 has been identified in human atherosclerotic lesions and the enhanced expression of MMP-9 has been linked to plaque rupture.^{243,244}

Clinical trials of compounds with efficacy as cancer treatments have involved several synthetic low-molecular-weight inhibitors of MMP activity, including batimastat (BB-94) and marimastat (BB-2516) among others. Preclinical studies showed that treatment of heart failure in animal models with MMP inhibitors results in less tissue damage and improved cardiac function.²⁴⁵ Limited clinical trials have been undertaken for rheumatoid arthritis.²⁴⁶⁻²⁴⁸ The results are sometimes not fully clear, but inhibition of MMPs remains a primary therapeutic target and inhibitors that can selectively bind to MMP-9 are expected to be of value in treating a variety of pervasive diseases.

Resolution of the overall tertiary structure of full length MMP-9 has provided important information for the structure-directed design of new enzyme inhibitors directed toward the catalytic site. It has also given us hints for the development of potentially highly selective bifunctional inhibitors capable of differentiating between gelatinases (MMP-9 and -2) and the other enzymes of the MMP family.

Indeed the gelatinases 2 and 9 differ from other MMPs by the presence of the three fibronectin type-II (FnII) like domains which are thought to mediate

gelatin binding.^{111,249-252} In the crystal structure the three FnII domains aggregate at the tip of the elongated catalytic domain. The small propeptide is bound to one side of the catalytic domain while its extended N-terminus reaches out to one of the three FnII domains from the active-site cleft of the catalytic domain where the three helices of the prodomain are clustered. The gap between the third FnII domain and the compact globular propeptide domain is connected by a bridge of amino acids between the first part of the construct, Val²⁹, and the first residue of the first helix, Thr⁴⁰. The most relevant feature of this bridge is that on the N-terminal side of the gap, the side chain of Phe³¹ is constrained against the hydrophobic side chains of residues Trp³⁷², Phe³⁷⁹ and Trp³⁸⁵ of the third FnII domain, as shown in Fig. 3.26.

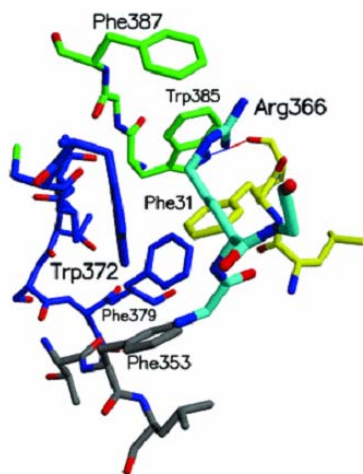


Figure 3.26. Stereoview of Phe³¹ of the propeptide (light green) that interacts with a cluster of aromatic side chains in the third FnII domain.

The design of potential bivalent inhibitors was conceived from this interaction between Phe³¹ and the aromatic cluster. Even though the role of the N-terminal tip of the propeptide domain is still under investigation, it appeared clear from modelling experiments that it might serve as an important anchoring motif, that could introduce a selectivity point for inhibitors specifically designed for

gelatinases and less potent toward other classes of MMPs. Indeed there is the established notion that the gaining in affinity and selectivity of a bivalent interaction of an inhibitor, compared to a monovalent one, is achieved by exploiting the entropy effect.²⁵³

The bivalent inhibitors should consist of a binding head for the catalytic domain, e.g. a hydroxamic acid derivative, which is connected via a flexible linker of appropriate length to a portion of the propeptide sequence centred on the Phe³¹ that exploits the hydrophobic pocket of the third FnII domain for exosite binding. A schematic representation of head and tail groups interacting simultaneously with the two distinct sites of the enzyme is depicted in Fig. 3.27.

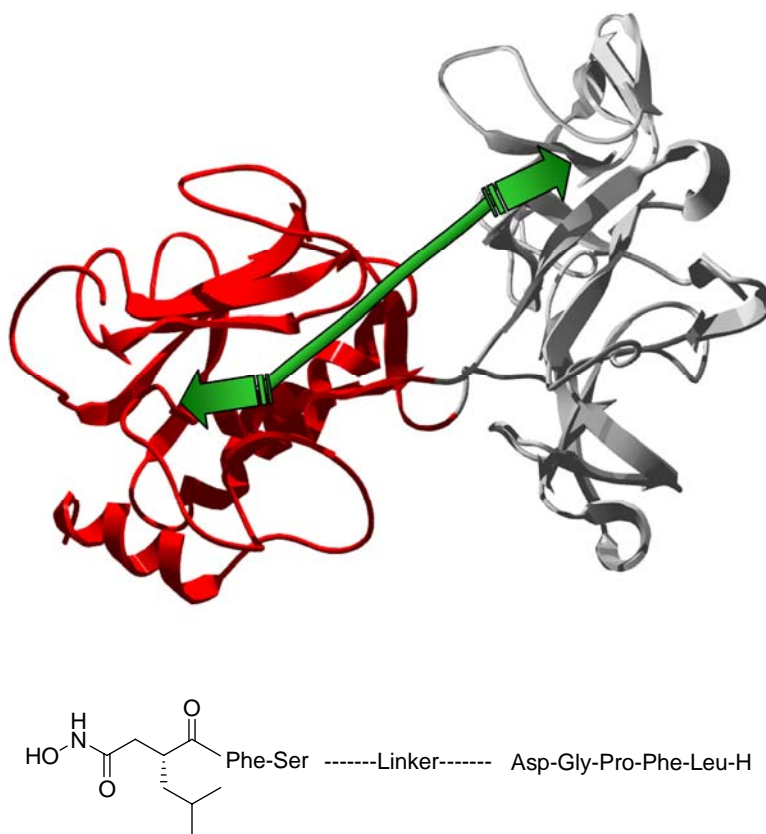
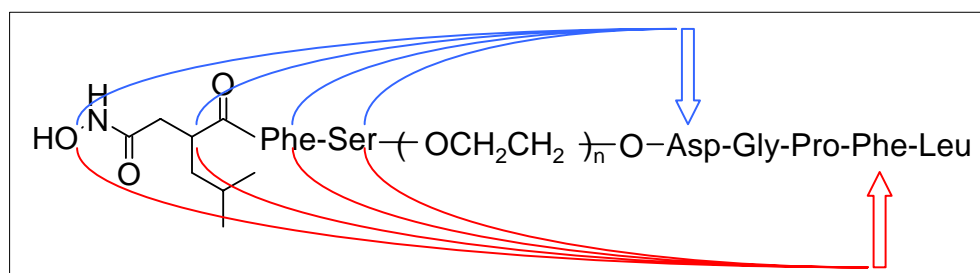


Figure 3.27. Schematic representation of the inhibitors designed and modelled on the crystal structure of proMMP-9. The catalytic domain is shown in red and the three FnII domains are in grey. The propeptide domain is erased and is replaced by the drawing of a bivalent inhibitor containing the binding head for the catalytic domain (e.g. a hydroxamate moiety) and the pentapeptide (corresponding to the sequence surrounding Phe³¹) connected by a flexible linker.

For the Zn^{2+} binding head group, a pseudotriptide was chosen with a hydroxamate as the metal chelating group. In analogy with batimastat, a Phe residue was introduced in position P_2' ; the essential S_1' pocket was occupied by the *i*But lateral chain present also in batimastat, while in order to diminish binding affinities, the C^α of the hydroxamic acid was left unsubstituted. A Ser was introduced as P_3' residue in analogy with the natural sequence of the propeptide, although it is not essential for recognition by the enzyme. As binding head group for the fibronectin exosite the pentapeptide portion present of the propeptide, i.e. Asp-Pro-Gly-Phe-Leu was selected. The orientation of the two peptide sequences is antiparallel, a fact which affects the choice of possible spacers. From flexibility and solubility considerations, and because of its modular character, a PEG spacer was selected to connect the two peptidic portions of the bivalent inhibitor. PEG is one of the best biocompatible polymers and possesses a multitude of useful properties.²⁵⁴ It is soluble in both organic and aqueous media, lacks toxicity and immunogenicity,²⁵⁵ it is easily excreted from living organisms²⁵⁶ and resistant to degradation and modification.^{257,258}

To identify the the optimal spacer length the two binding heads were docked on the MMP-9 structure in optimal interaction position; then the distances between selected atoms of the two portions were measured; finally, these distances were compared with the corresponding length of a modelled bifunctional inhibitor with the hydroxamic acid portion linked to the pentapeptide portion with PEGs of differing lengths; the results are reported in Table 3.10. As shown in the table, the linker PEG₃ is too small to allow interaction with both the catalytic cleft and the FnII domain; for PEG₄, the calculated distance was minimal, but more appropriate. Therefore, taking into account possible movements of the protein domain, it was decided to attempt a scan for the distances with PEG₄, PEG₆, and PEG₈.



Distance	crystal (Å)	n=3 (Å)	n=4 (Å)	n=5 (Å)	n=6 (Å)
C^αPhe -OH hydrox ac	35.0	31.62	35.74	38.66	42.60
C^αPhe -C^αhydr	31.3	30.04	33.92	36.85	40.26
C^αPhe -C^αPhe	28.0	26.71	30.30	33.67	37.04
C^αPhe -C^αSer	25.3	22.90	26.66	29.83	33.30
C^αAsp -OH hydrox ac	29.9	24.55	28.04	31.61	34.96
C^αAsp -C^αhydr	26.3	22.75	26.36	29.64	32.83
C^αAsp -C^αPhe	23.0	19.23	22.82	26.28	29.60
C^αAsp -C^αSer	21.0	15.52	19.08	22.51	25.81

Table 3.10. Measured distances between the α carbon of the Phe (in red) and Asp (in blue) residues of the exosite binding head and various atoms of the inhibitory portion; the proposed molecules contain PEGs of differing lengths (n) and are measured in their energy-minimized structures.

3.2.1 Synthesis of the Bivalent Inhibitors

Route A

For the synthesis of this series of inhibitors, a strategy based on fragment condensation was applied based on the use of suitable orthogonal protecting groups. The first route, outlined in Fig. 3.28, consisted in the preparation of the two binding heads for their subsequent assembly into the linear construct via the PEG spacers.

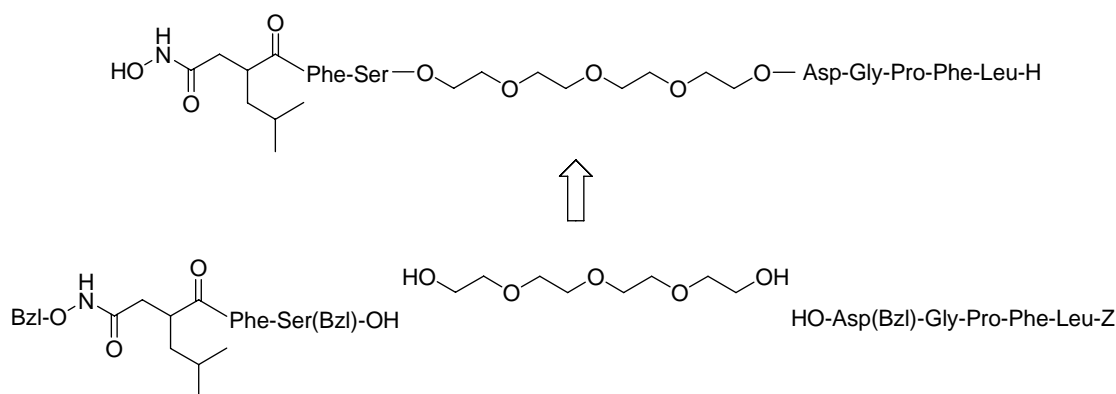
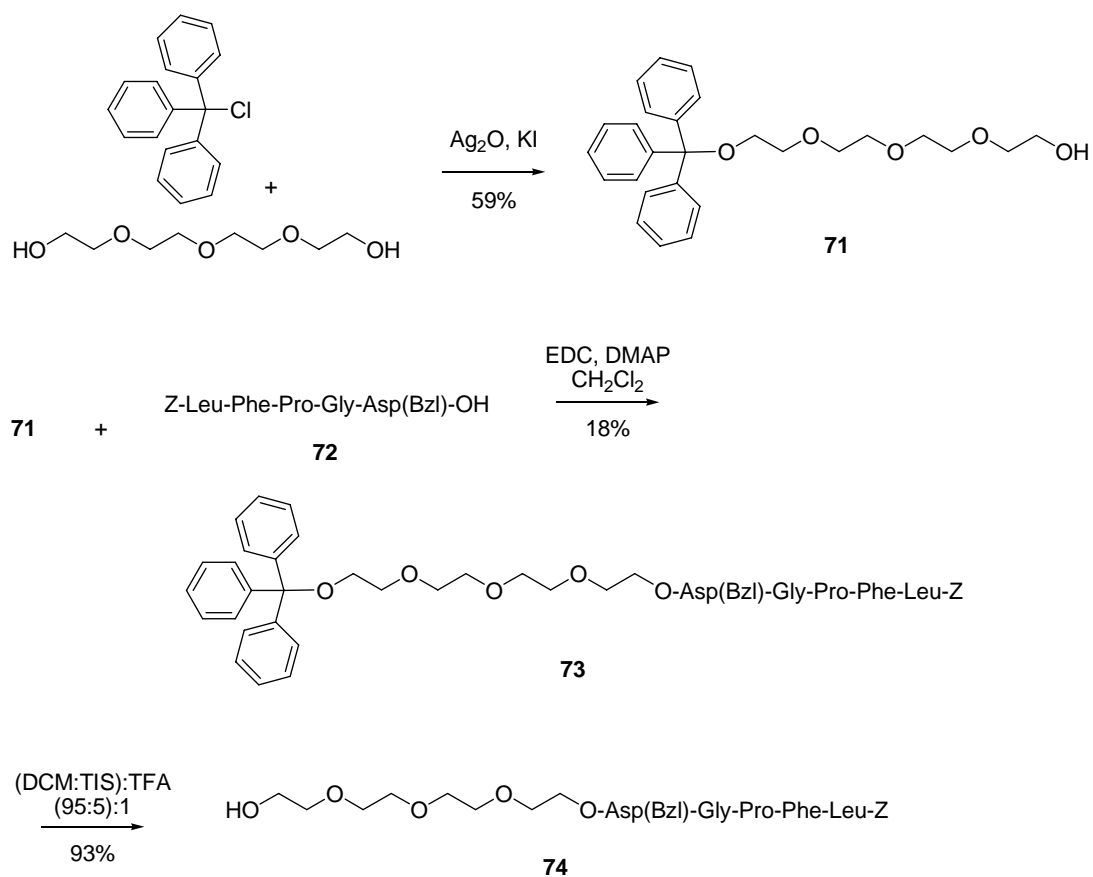


Figure 3.28. Route A for the synthesis of bivalent inhibitors of MMP-9.

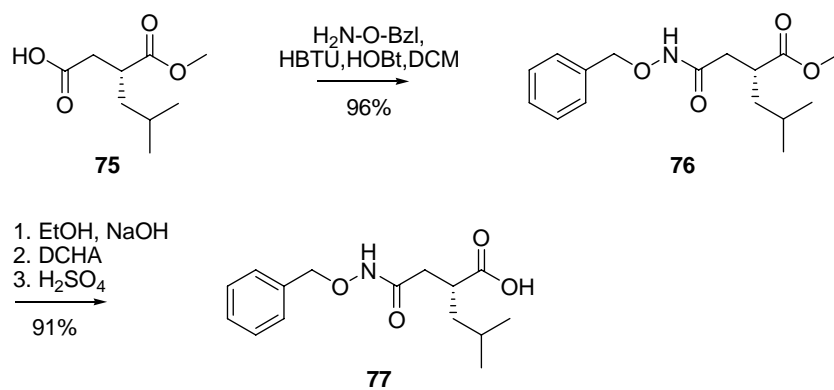
The pentapeptide Z-Leu-Phe-Pro-Gly-Asp(Bzl)-OH (**72**, Scheme 3.17) was synthesized on the 2-chlorotrityl chloride resin with Fmoc/HOBT chemistry. Since the protecting groups for the N-terminal amino group and Asp carboxylate lateral chain had to be orthogonal to the Fmoc group and resistant to the acid resin-cleavage, Z- and Bzl-protecting groups were selected which can be removed in the last step by hydrogenation. A similar protection scheme was applied for the hydroxamate head moiety. To assemble the linear construct the PEG spacers required monoprotection with a group that can be inserted easily on its hydroxy group and is removed selectively. For this purpose the trityl group was selected which is cleaved under weak acidic conditions (1% TFA). The monoprotected PEG (**71**) was obtained by known procedures²⁵⁹ in good yields.

The subsequent esterification of the carboxyl group of **72** with the PEG derivative **71** to afford compound **73** proved to be difficult particularly in terms of yields, even using 4-(dimethylamino)pyridine (DMAP) as a well established catalyst.²⁶⁰ Scandium(III) triflate was previously reported to be an efficient catalyst for reactions of acid anhydrides with primary, secondary and tertiary alcohols.²⁶¹⁻²⁶³ For our purpose the use of 5 % Sc(OTf)₃ (mol %) in the reaction mixture did not improve sensibly the yields. The trityl group was then cleaved under usual conditions to afford **74** in quantitative yields.



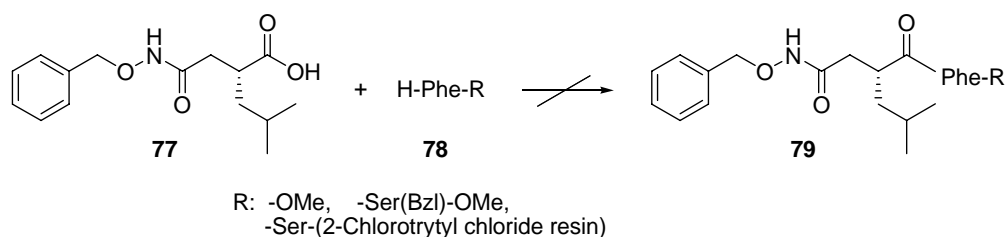
Scheme 3.17.

For the synthesis of the hydroxamate-containing pseudotriptide, a commercially available (*R*)-2-isobutylsuccinic acid-1-methyl ester (**75**, Scheme 3.18) was used as starting material. This compound was first reacted with (benzyloxy)amine following essentially known procedures,²⁶⁴⁻²⁶⁶ to produce compound **76**, which was then converted to the free carboxylate by saponification with 1 equiv of NaOH (**77**, Scheme 3.18). Since the oily free acid was not stable on storage even in the cold it was converted to the DCHA salt.



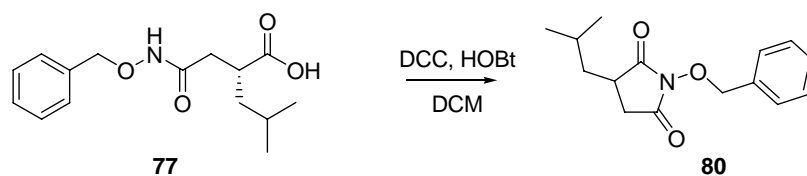
Scheme 3.18.

The subsequent reaction of **77** (Scheme 3.19) with the amino group of the phenylalanine derivatives **78**, both in solution or solid phase) failed using the DCC/HOBT ²⁶⁴ or other the more efficient acylation methods (HATU/HOAt , HBTU/HOBT , EDC/HOBT).



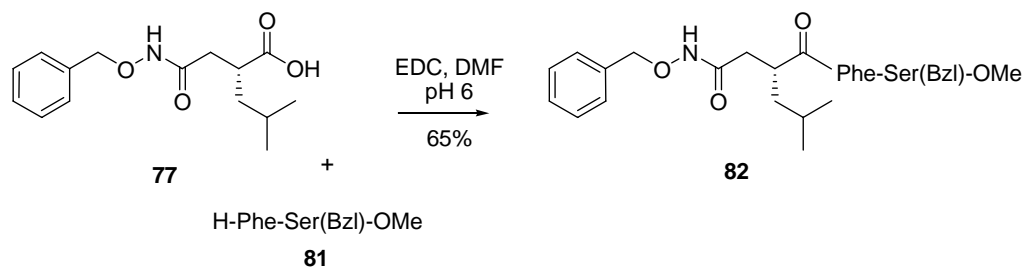
Scheme 3.19.

To explain these results, the acid was treated with coupling reagents (DCC , HOBT) in absence of the amino component, which resulted in quantitative ring closure to the succinimide derivative (**80**, Scheme 3.20), as well assessed by the single product peak in HPLC with a mass of m/z 262,2 amu (MW_{calc} : 261,32).



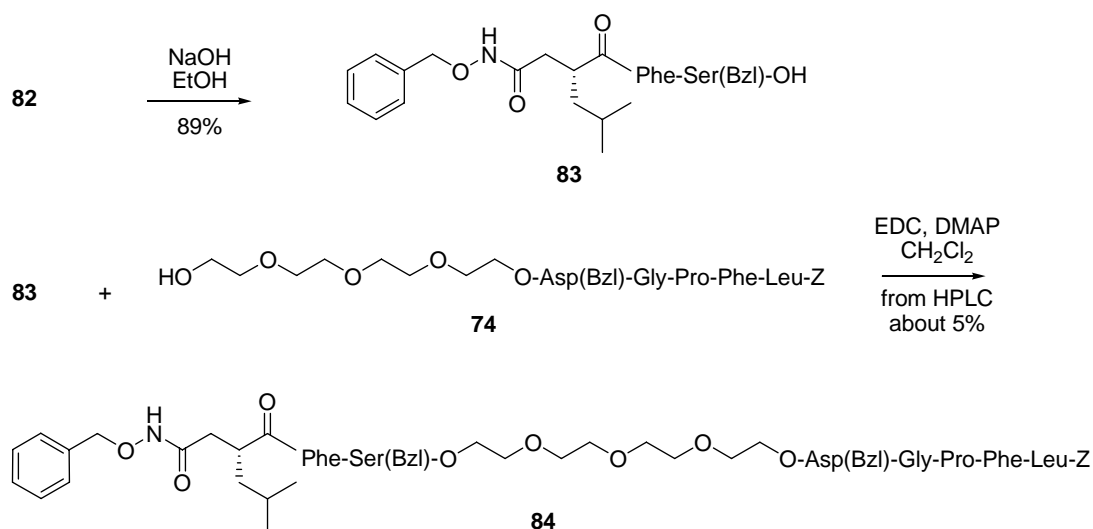
Scheme 3.20.

The side reaction could be bypassed by coupling with EDC (or DCC) in absence of HOBT and under pH control and the desired product (**82**) was obtained in satisfactory yields (Scheme 3.21).



Scheme 3.21.

After saponification of compound **82** with 1.1 eq of NaOH, the resulting **83** was reacted with the PEG-pentapeptide construct **74** to produce the difficult ester bond (Scheme 3.22). The yields were even lower than those obtained in the first esterification step. Therefore an alternative route was required.



Scheme 3.22.

Route B

A possible solution of the problems encountered in route A was the transformation of the alcoholic groups of PEG into amine groups which are more reactive. This would lead to amide bonds between PEG and the two peptidic binding heads and thus to an increased tendency for hydrogen bonding with the enzyme. At the point where the amide would be formed, the inhibitor molecules were supposed to protrude out of the protein surface. The possibility of hydrogen bond formation that would attract this part to the surface, was envisaged as a possibly negative interaction. Moreover, although yields in the esterification steps can be improved with large excesses of alcohols, this bypass can be used in the first esterification, but is rather uneconomical in the second step.

To improve the economy of these synthesis, we decided to esterify the PEG spacer with only the suitably protected amino acid that is supposed to be directly linked to the spacer (Fig. 3.29). Upon selective deprotection of one of the two amino acids, the more efficient acylation of the free amine group should be readily carried out with the remaining of the peptide. After an additional

deprotection and coupling step the final, fully protected endproduct should become accessible.

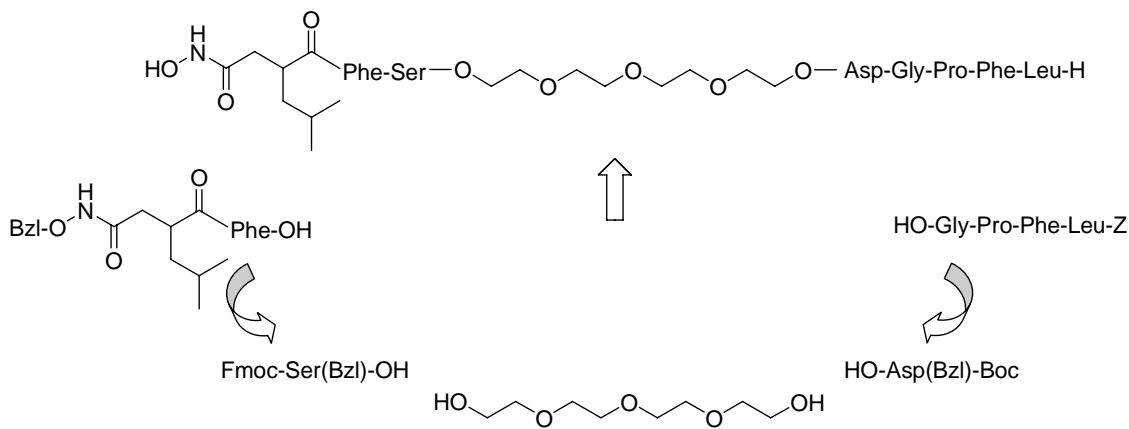
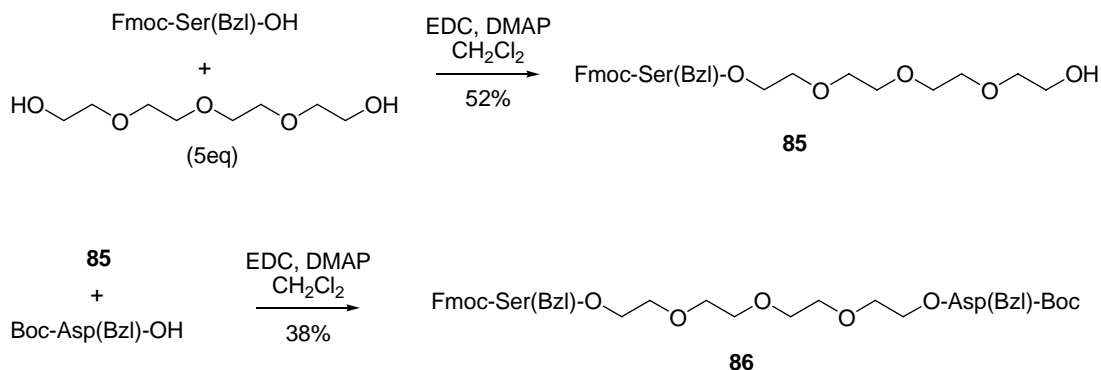


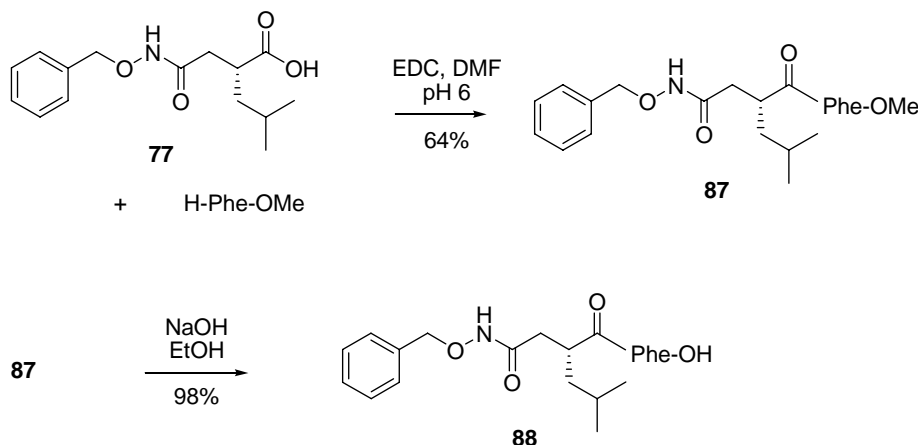
Figure 3.29. Route B for the synthesis of bivalent inhibitors of MMP-9.

The details of this route are reported in Scheme 3.23-25. Given the low yield and the large excess of PEG that was used (5 eq, corresponding for the first esterification reaction, to a 10 eq excess, considering the two equivalent alcoholic groups), PEG was not previously monoprotected as in route A. The difficulty encountered in this step was the separation of unreacted PEG from the product mixture, which could be resolved by extensive extractions with water (up to 15 times). The PEG derivative **86** was obtained and for the required orthogonality in the amino protection, Boc and Fmoc were applied.



Scheme 3.23.

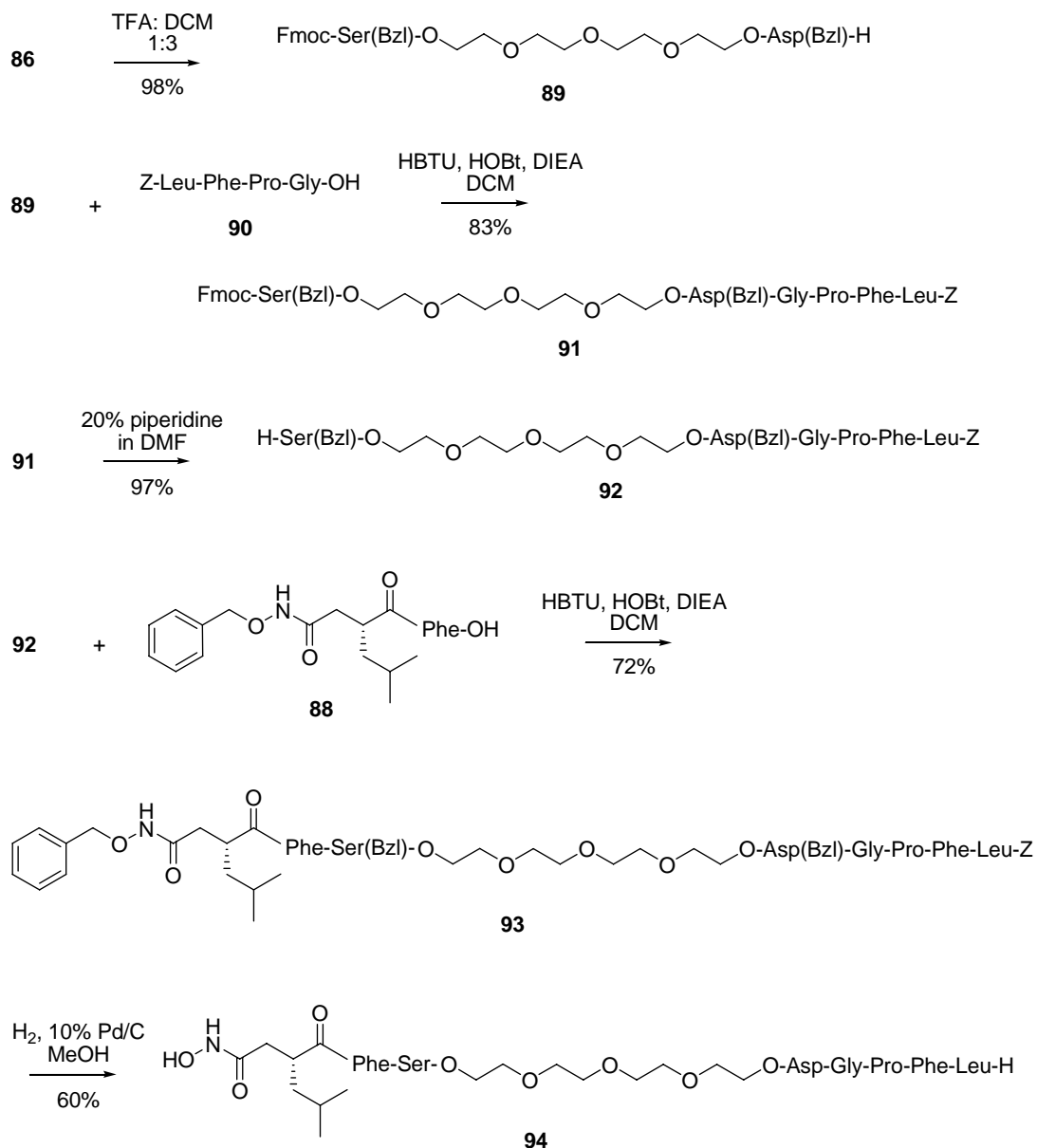
The hydroxamic acid moiety **77** was readily synthesized from compound **77**, with the sole attention paid to the coupling reagent as reported previously (Scheme 3.24). The methyl ester was then saponified to compound **88** under standard conditions.



Scheme 3.24.

To prevent low yields of Z-Leu-Phe-Pro-Gly-OH (**90**) as resulting from diketopiperazine formation at the Pro-Gly-resin step, the synthesis was carried out on a 2-chlorotrityl chloride resin since the bulk of the trityl handle is known to minimize this side reaction. However, even this procedure did not fully prevent the side reaction and therefore Fmoc-Phe-Pro-OH was directly coupled to the resin-linked Gly and the final product was readily purified to homogeneity as judged by HPLC.

Finally, stepwise deprotection of the Boc and Fmoc groups and condensation of the peptide **90** followed by the pseudopeptide **88** produced the final protected compound **93** in very good yields (Scheme 3.25).



Scheme 3.25.

Rather problematic proved to be the final cleavage of the protecting groups by hydrogenolysis. While in the case of the PEG₄ compound **93**, quantitative cleavage of the Z and Bzl groups was obtained after 4 h by standard catalytic hydrogenation (H₂ and 10% Pd/C in MeOH, Scheme 3.25), for the longer PEG molecules this procedure led only to removal of the Z and of two benzyl groups. Longer hydrogenation times resulted in reduction of the hydroxamic acid and

other methods such as catalytic transfer hydrogenolysis²⁶⁷⁻²⁶⁹ with ammonium formate, or changes in the experimental parameters (higher temperatures, increased H₂ pressure, other solvents and longer reaction times) did not improve the results. Among the protecting groups present in the final compounds the benzyl ether derivative of Ser is the most difficult to remove. However, from modelling experiments and the binding modes of hydroxamate-type inhibitors to the catalytic domain of MMPs as derived from X-ray analysis strongly suggest a minimal role of this residue in the binding process. Therefore the bivalent constructs with PEG₆ (**95**) and PEG₈ (**96**) were used as Ser(Bzl) derivatives in the enzyme assays.

3.2.2 Inhibitory Potencies

The three potential bivalent constructs were assayed for their inhibitory potencies on two MMP-9 constructs: i) an enzyme containing the prodomain, catalytic, fibronectin domain, which has to be preactivated and ii) the catalytic domain.

With the catalytic domain very similar inhibitory potencies were determined (Table 3.11) which clearly confirms a minimal interaction and thus interference of the spacer and FnII binding head with the catalytic site of the enzyme. Moreover, the almost identical K_i values support the hypothesis of a minimal effect of the Ser(Bzl) group on binding affinities. As expected from the structure of the hydroxamate head group of the bivalent constructs the affinities are lower than those of batimastat, taken as reference hydroxamate-type inhibitor.

Inhibitor	IC ₅₀
HA-PEG ₄ -PP (94)	~ 10-20 nM
HA-PEG ₆ -PP (95)	~ 10-20 nM
HA-PEG ₈ -PP (96)	~ 10-20 nM
Batimastat	~ 0.8 nM

Table 3.11. Preliminary inhibition potencies of the three bivalent inhibitors. HA indicates the hydroxamic acid unit; PP is the pentapeptide HA-Leu-Phe-Pro-Gly-Asp-; PEG_n is poly(oxyethylene), where n indicates the number of hydroxyethylene units.

Preliminary results with the larger MMP-9 construct containing the FnII domain are intriguing, since these would suggest in first instance a very strong bivalent binding that, rather unexpectedly converts to monovalent binding by the presence of excesses of the inhibitors. These observations require additional and confirming experiments.

4. Perspectives

The challenging task of converting the relatively large and linear peptidic inhibitors of BACE-1, reported so far in the literature, into proteolitically more stable peptidomimetic structures such as peptoids, hybrid peptide-peptoids and retroinverso analogs failed due to the loss of inhibitory potency. Conversely, molecular modeling experiments based on the known X-ray structures of BACE-1/peptidic inhibitors led to the design of novel cyclic peptidic structures of reduced size and containing statine as the transition-state analogue. These were found to retain efficient affinities for the aspartic protease and thus to present the statine moiety in correct orientation to the active site of the enzyme with the short peptide-backbone in the β -type extended conformation for additional interactions with the active-site cleft. First attempts to improve the structure of the transition-state analogue statine and to restrict the side-chain cyclized peptide backbone in the extended conformation by incorporation of aminobenzoic acid residues, led to important hints for further developments of peptidomimetic cyclic compounds as BACE-1 inhibitors with enhanced stability against protease degradation and thus more suitable for *in vivo* biological studies on the role of this enzyme in amyloidogenesis in Alzheimer's disease.

The difficult problem of developing MMP inhibitors capable of differentiating the gelatinases MMP-2 and -9 from the other members of the large MMPs family including the collagenases, was again tackled by a structure-based design relying on the peculiar interaction of a propeptide portion in MMP-9 with a well delineated hydrophobic pocket of the third fibronectin domain. By exploiting the binding affinities of metal chelating groups at the active site and the exosite binding of a polipeptide portion to the fibronectin domain, application

of the concept of bivalent inhibitors was attempted. For this purpose molecular modeling experiments were performed to assess the size of the PEG spacer chosen as linker of the two binding groups. Correspondingly PEG spacers of different lengths were used to crosslink a hydroxamate head group containing phenylalanine as P₁' residue for recognition and binding to the MMP-9 active site, and a pentapeptide head for exosite binding. First enzymatic assays seem to confirm the working hypothesis.

In summary, progresses were achieved in both projects that are most promising for further developments of low mass peptidomimetic inhibitors of BACE-1 and of highly selective inhibitors of the two gelatinases by applying the concept of bivalency.

5. Zusammenfassung

Die Aspartat-Protease BACE-1 ist eines der wichtigsten Enzyme, die entscheidend die Amyloidbildung beeinflussen und somit für die Auslösung der Alzheimer Erkrankung mitverantwortlich sind. Trotz der sehr intensiven Arbeit akademischer und industrieller Forschung sind bislang als Hemmstoffe dieser Aspartat-Protease weitgehend nur Statine-Peptide erheblicher Länge bekannt. Diese können zwar erfolgreich für biochemische Untersuchungen eingesetzt werden, was auch durch die Strukturauflösung der entsprechenden Komplexe mit BACE-1 voll bestätigt wurde, doch sind solche peptische Inhibitoren wegen des schnellen enzymatischen Verdaus und wegen der schlechten Bioverfügbarkeit als Werkzeuge für biologische Studien an Zellen and Versuchstieren ungeeignet. Zielsetzung des Forschungsprojektes war deshalb der Struktur-basierte Design von Proteolyse-resistenteren Hemmstoffen 1) durch Konvertierung der peptidischen Strukturen in peptidomimetische Verbindungen und 2) durch Cyclisierung der minimalen Bindungssequenz um dadurch den Konformations-Freiraum einzuschränken und die Ligandenaffinität thermodynamisch zu favorisieren.

Der Einsatz von peptidomimetischen Strategien zur Synthese von Peptoiden, hybriden Peptoid-Peptiden und Retroinverso-peptiden mit Statine als Übergangszustand-Analogon bewirkte einen starken und zum Teil auch vollen Verlust der Hemmwirkung. Die alternative Strategie eines Struktur-basierten Designs von cyclischen Statine-Peptiden führte hingegen zu vielversprechenden Leitstrukturen. Aufgrund von Modellingexperimenten mit den bekannten Kristallstrukturen der BACE-1/Inhibitor Komplexe wurde eine minimale Bindungssequenz durch unterschiedliche Seitenketten-Cyclisierungen in ihrer

ausgestreckten β -artigen Konformation stabilisiert um thermodynamisch das Andocken dieser neuartigen Liganden an die Aktivitätstasche des Enzyms zu favorisieren und gleichzeitig den Statinerest optimal für die Ausbildung der Wasserstoffbindungen mit den Aspartresten des Aktivzentrum zu präsentieren. Die diffizilen Synthesen konnten erfolgreich durchgeführt werden und die erhaltenen cyclischen Statinepeptide den Enzymtests zugeführt werden. Interessante neuartige cyclische Verbindungen konnten auf diesem Wege erhalten werden, in denen der Verlust an Bindungsaffinität durch Kürzung der Bindungssequenz vor allem entropisch genügend kompensiert wird. Für eine weitere Optimierung der Hemmeigenschaften durch Versteifung des Peptidrückgrats in ausgestreckter Konformation wurden unterschiedlich substituierte Aminobenzoesäure-Reste zunächst in das Statine-Peptid eingebaut. Auch hier konnten wertvolle Hinweise für neue cyclische Strukturen gewonnen werden. Ein zusätzlicher Gewinn an Affinität könnte laut Modelling eine Disubstitution des Statine-Restes bringen um gleichzeitig als Übergangszustand-Analogon und P_1' Rest zu fungieren. Erste Syntheseversuche in dieser Richtung waren aber wegen der benötigten raumfüllenden hydrophoben Reste aus sterischen Gründen nicht erfolgreich. Insgesamt ergaben die neu aufgefundenen verhältnismäßig kleinen Inhibitoren mit micromolarer Affinität für BACE-1 wichtige Hinweise für weitere zukünftige Arbeiten auf diesem Gebiet.

Zweite Zielsetzung war die Entwicklung neuartiger spezifischer Hemmstoffe der Gelatinasen MMP-2 und MMP-9 basierend auf dem Bivalenzprinzip, das die Natur so vielseitig und erfolgreich in Protein/Protein Wechselwirkungen zur Erhöhung von Spezifität und Affinität einsetzt. Ein Erfolg in dieser Synthese von bivalenten spezifischen Inhibitoren der Gelatinasen könnte in entscheidendem Maße die Entwicklung effizienter Pharmaka für die Krebs- und Arthritistherapie beeinflussen. Wichtige Hinweise für das Design solcher bivalenten Inhibitoren erbrachte eine detaillierte Inspektion der Kristallstruktur des „Full-Length“ MMP-9 inklusiv des Propeptids. Der Phe³¹ Rest des Propeptids

bindet in eine hydrophobe Tasche der dritten Fibronectin-Domäne dieser Gelatinase, die durch die Reste Trp³⁷², Phe³⁷⁹ and Trp³⁸⁵ ausgebildet wird. Modellierungsexperimente an dieser räumlichen Struktur führte zum Design bivalenter Konstrukte. In diesen sollte ein Peptidhydroxamat-Derivat an das Zn²⁺ Atom des katalytischen Aktivzentrums binden und somit die Metalloprotease desaktivieren und gleichzeitig eine Pentapeptidsequenz des Propeptids mit Phe³¹ über einen Spacer geeigneter Länge für optimale Erkennung und Bindung an die Fibronectin-Domäne angeboten werden. Da die Peptidrichtungen des Hydroxamat-Kopfes und des Exosite-bindenden Pentapeptids antiparallel sein sollten, wurden PEG-Spacer unterschiedlicher Länge eingesetzt um gleichzeitig auch die Flexibilität und hydrophilen Eigenschaften dieser Oligomere auf der Proteinoberfläche auszunutzen. Die Synthese dieser Konstrukte durch Veresterung der peptidischen Kopfgruppen mit den endständigen Hydroxylfunktionen der PEG-Oligomere war wegen sehr schlechter Veresterungsausbeuten unter Standardbedingungen herausfordernd, konnte aber nach vielen Optimierungsschritten zufriedenstellend gelöst werden. Erste Enzymhemmungen waren erfolgversprechend. Somit konnten auch in dieser herausfordernden Fragestellung wertvolle Hinweise für nachfolgende Arbeiten erzielt werden.

6. Experimental Part

6.1 Materials and Methods

Solvents and Reagents

Purchased solvents and reagents were of the highest quality commercially available and used without further purification; they were purchased from Sigma-Aldrich, Fluka and Merck. The HBTU and EDC·HCl were from Senn Chemicals while HATU from PE Biosystems. For analytic and preparative HPLC acetonitrile was purchased by Merck in LiChrosolv[®] gradient grade for liquid chromatography. Amino acids were all by the company Iris Biochem GmbH. Sta and (Phe)Sta were from Neosystem, as well as the amino-benzoic acid derivatives. The solid supports were purchased from Rapp Polymere GmbH and Novabiochem. The fluorogenic substrate for inhibition activity measures of BACE-1 was Mca-(Asn⁶⁷⁰,Leu⁶⁷¹)-amyloid β 1A4 protein precursor₇₇₀₍₆₆₇₋₆₇₅₎-Lys(Dnp) ammonium salt, purchased from Bachem.

TLC plates were precoated Silica gel F₂₅₄ plates by Merck, provided with fluorescent indicator. For preparative gel chromatography Silica gel 60 (40-60 μ M) from Merck was used.

Analytical and Preparative HPLC

Analytical RP-HPLC was carried out on an assembled system supplied by Waters, composed of two 515 HPLC pumps, a 600S pump control module, a 717 plus autosampler and a 996 photodiode array detector. The system was controlled

by a Millennium 2000 software version 3.00 supplied by Waters. The separations were monitored at 210 nm using 5 different systems:

- System I:* Chromolith Performance RP 18-e, 100 x 4,6 mm C18 by Merck; linear gradient from 100% solvent A [2% H₃PO₄/CH₃CN 95:5] to 100% solvent B [2% H₃PO₄/ CH₃CN 90:10] in 6 min, followed by 1 min isocratic elution; flow: 3ml/min.
- System II:* Xterra-TM-C8 MS 5 μ m, 150 x 3.9 mm by Waters; linear gradient from 100% solvent A [2% H₃PO₄/CH₃CN 95:5] to 100% solvent B [2% H₃PO₄/ CH₃CN 90:10] in 17 min, followed by 1 min isocratic elution; flow: 1.5ml/min.
- System III:* ET 125/4 Nucleosil 100-5 C₈, 125 x 4 mm by Macherey-Nagel; linear gradient from 100% solvent A [H₂O + 1%TFA] to 100% solvent B [CH₃CN + 0.8%TFA] in 13 min, followed by 1 min isocratic elution; flow: 1.5ml/min.
- System IV:* Chromolith Performance RP 18-e, 100 x 4,6 mm C18 by Merck; linear gradient from 100% solvent A [2% H₃PO₄/CH₃CN 95:5] to 50% solvent B [2% H₃PO₄/ CH₃CN 90:10] in 15 min, followed by 1 min isocratic elution; flow: 3ml/min.
- System V:* Chromolith Performance RP 18-e, 100 x 4,6 mm C18 by Merck; linear gradient from 100% solvent A [2% H₃PO₄/CH₃CN 95:5] to 50% solvent B [2% H₃PO₄/ CH₃CN 90:10] in 30 min, followed by 1 min isocratic elution; flow: 3ml/min.

Preparative RP-HPLC was carried out on an assembled system supplied by Abimed-Gilson, composed of two 321 HPLC pumps, a 202 fraction collector and a 152 UV/VIS detector. The system was controlled by a UniPoint system software version 2.10 equipped with a 506C system interface module. The purifications were performed using 2 different systems:

- System 1:* VP 250/21 Nucleosil 300-5 C₈ PPN by Macherey-Nagel; gradient as specified for each compound, using solvents A [H₂O + 1%TFA] and B [CH₃CN + 0.8%TFA]; flow: 10 ml/min.
- System 2:* VP 250/21 Nucleosil 100-5 C₁₈ PPN by Macherey-Nagel; gradient as specified for each compound, using solvents A [H₂O + 1%TFA] and B [CH₃CN + 0.8%TFA]; flow: 10 ml/min.

Loading of 2-Chlorotrityl Chloride Resin

The attachment of the first amino acid on a 2-chlorotrityl chloride resin is performed placing the desired amount of resin in an overnight dried, argon flushed flask. The N-protected amino acid (1 eq, relative to the resin), dissolved in dry DCM, and DIEA (4 eq) are added to the mixture. The mixture is let to stir for 30 minutes, then the resin is washed three times with a solution of DCM/MeOH/DIEA 17:2:1, three times with DCM, three times with DMF and three times with DCM. Before further functionalization, the effective loading of the resin is determined.

Determination of the First Amino Acid Attachment on 2-Chlorotrityl Chloride Resin

A small amount (1-5 mg) of the resin loaded with the first desired amino acid and overnight dried on NaOH is weight and placed into a 10 ml graduated flask. 1 ml of freshly prepared solution of piperidine in DMF (20% v/v) is added and let to react for 30 minutes. A reference solution is prepared in the same manner without adding the resin. After 30 minutes, the graduated flasks are filled with MeOH, and the absorption of the dibenzofulven-piperidin adduct ($\epsilon = 7800 \text{ M}^{-1}\text{cm}^{-1}$) solution is measured at 301 nm vs. the standard prepared in the same way. The estimate of the first residue attachment is obtained from the following Lambert-Beer's equation:²⁷⁰

Fmoc loading(mmol/g) =

$$[A_{301\text{nm}} \cdot V_{\text{graduate flask}}(\text{ml})] / [7800 \text{ M}^{-1}\text{cm}^{-1} \cdot D(\text{cm}) \cdot m_{\text{resin}}(\text{mg})]$$

where: $A_{301\text{nm}}$ is the absorption of the solution at 301 nm; $V_{\text{graduate flask}}(\text{ml})$ is the volume of the graduate flask expressed in ml; $7800 \text{ M}^{-1}\text{cm}^{-1}$ is the empirically

derived value of the extinction coefficient for the dibenzofulvene-piperidine adduct; D (cm) is the optical path length expressed in cm; m_{resin} (mg) is the mass of dry resin expressed in mg.

Mass Spectrometry

Routine ESI-MS analysis were run on a Perkin-Elmer SCIEX API 165 spectrometer equipped with a nebulizer-assisted electrospray source.

The ESI-MS and ESI-MS/MS spectra for the peptoids study were measured using an Applied Biosystems API300 triple quadrupole mass spectrometer by Applied Biosystems (Weiterstadt, Germany) equipped with an in-house-built nanospray source. Compounds were diluted with 80% MeOH in 0.5 mM ammonium acetate buffer and approximately 3 μl were transferred to an in-house-pulled nanospray capillary tube and mounted in the source. Usually, a small pressure of compressed air was applied to the capillary tube to initiate the spray. The high voltage applied to the capillary varied from 800 to 1,000 V. The orifice voltage was optimized for each experiment. Compressed nitrogen 5.0 (Linde, Pullach, Germany) was used as curtain and as collision gas in MS/MS experiments. The scan range was 500-1000 m/z (2 s/scan) for the ESI-MS spectra and 30 m/z units above the m/z value of the parent ion (2 s/scan) for the ESI-MS/MS spectra.

NMR Spectrometry

NMR experiments were carried out on Bruker DRX 500 and Bruker AMX 400 spectrometers. Deuterated solvents were purchased from Eurisotop (France). The 2D-total correlated spectroscopy (TOCSY) spectra were recorded with spin lock periods of 60 ms using the MLEV-17 sequence for isotropic mixing.²⁷¹ For ROESY experiments the standard pulse program from Bruker was used. Data processing and assignment was performed using XWINNMR-v3.

Modeling Studies

Distance geometry (DG) and molecular dynamics-simulated annealing (MD-SA) calculations were performed with the INSIGHT II (version 98.0) software package (Accelrys, San Diego, CA) on Silicon Graphics O2 R5000 computers (Silicon Graphics, Inc., Mountain View, CA). One hundred structures were generated from the distance-bound matrices. Triangle-bound smoothing was used. NOE intensities were extracted from 4°C spectra and were converted into interproton distance constraints using the following classification: very strong (vs) 1.7-2.3 Å, strong (s) 2.2-2.8 Å, medium (m) 2.6-3.4 Å, weak (w) 3.0-4.0 Å, very weak (vw) 3.2-4.8 Å, and the distances of pseudo atoms were corrected as described by Wüthrich.²⁷² The structures were generated in four dimensions and then reduced to three dimensions with the EMBED algorithm and optimized with a simulated annealing step according to the standard protocol of the DG II package of INSIGHT II. All one hundred structures were refined with a short MD-SA protocol: after an initial minimization, 5 ps at 300 K were simulated followed by exponential cooling to ~0 K during 10 ps. A time step of 1 fs was used with the CVFF force field while simulating the solvent H₂O with a dielectric constant of 80.0. The experimental dihedral and distance constraints were applied at every stage of the calculation with 30 kcal·mol⁻¹·rad⁻² and 50 kcal·mol⁻¹·Å⁻², respectively.

BACE-1 Assays

Reversible kinetic assays were performed on a 96 well Synergy HT Bio-Tek plate reader using a BACE stock solution in phosphate-buffered saline 0.1% Triton X-100 and stored at -80 °C in aliquots. The concentration of the enzyme in the stock solution was 1.25 nM, as estimated by Bradford assay (Bio-Rad). Active enzyme concentrations were obtained by active site titration using the statine-based inhibitor H-EVN-Statine-VAEFNH₂ and by fitting data from inhibition experiments approaching titration conditions to the general equation for

tight binding inhibitors.²⁷³ Enzyme inhibition was measured in 50 mM NaOAc (pH 4.5) at 37 °C, using Mca-(Asn⁶⁷⁰,Leu⁶⁷¹)-amyloid β 1A4 protein precursor₇₇₀₍₆₆₇₋₆₇₅₎-Lys(Dnp) ammonium salt purchased from Bachem as the fluorogenic substrate (68 μ M final concentration) and 0.14 nM enzyme concentration at 328 nm excitation and 420 nm emission. Enzyme and buffer were incubated for 10 min at 37 °C prior to addition of substrate and inhibitor. Substrate hydrolysis was monitored over 20 min with inhibitor concentrations ranging from 0 μ M to 77.8 μ M while gentle shaking the samples. Obtaining relative fluorescent units (RFU)/min permitted calculation of a K_i using non-linear regression analysis ($v_i/v_o = 1/(1+[I]/[K_i])$).

6.2 Synthesis

6.2.1 Peptoids, Hybrids Peptoid-peptides and Retroinverted Peptide Approach

6.2.1.1 Peptides Synthesis

Peptides **1**, **5**, **6** and **7** were synthesized by automated solid-phase methodology on an ABI-Pioneer Perceptive Biosystems peptide synthesizer using Fmoc/HBTU/DMF chemistry. The side chains of all the residues were protected in the standard manner compatible with TFA cleavage and deprotection protocols. The synthesis of peptide **1** was carried out on a 0.1-mmol scale of TentaGel S PHB resin (substitution: 0.25 mmol/g). The protocol included extended cycles and double coupling steps (4 mmol of activated amino acid derivative per cycle). The peptide was obtained as an acid peptide and the N-terminus was left free, the final Fmoc removal step been performed on the synthesizer. Peptides **5**, **6** and **7** were synthesized on a TentaGel S RAM support

(substitution: 0.24 mmol/g), which allows the synthesis of peptide amides, on a 0.1-mmol scale. The protocol included extended cycles (4 mmol of activated amino acid derivative per cycle). The final Fmoc removal step was performed on the synthesizer, followed by a final capping reaction with Ac₂O : 2,6-Lutidine : DMF = 5:6:89. All the products were then cleaved from the resin by TFA in the presence of 2.5% TIS and 2.5% water at room temperature in 2 h, the resin was filtered off and the crude peptides were precipitated with a cold solution of *tert*-butyl methyl ether/hexane 2:1 and lyophilised over night. The peptides were then purified by preparative RP-HPLC. The purity of the peptides exceeded 97% as determined by analytical RP-HPLC and their structural integrity was confirmed by electrospray ionization mass spectrometry.

Compound 1: Purification (System 1): gradient: from 20 to 70%B in 60 min. HPLC (System I): t_R 3.27 min; (System II): t_R 10.24 min; (System III): t_R 6.39 min; ESI-MS: m/z: 963.8 [M+H]⁺, calculated monoisotopic mass for C₄₄H₇₀N₁₀O₁₄: 963.

Compound 5: Purification (System 2): gradient: from 10 to 30%B in 7 min, then 30 to 60%B in 60 min. HPLC (System I): t_R 1.63 min; (System III): t_R 7.83 min; ESI-MS: m/z: 960.8 [M+H]⁺, calculated monoisotopic mass for C₄₄H₆₈N₁₀O₁₄: 960.

Compound 6: Purification (System 2): gradient: from 10 to 30%B in 7 min, then 30 to 60%B in 60 min. HPLC (System I): t_R 1.72 min; (System III): t_R 7.91 min; ESI-MS: m/z: 976.6 [M+H]⁺, calculated monoisotopic mass for C₄₅H₆₉N₉O₁₅: 976.

Compound 7: Purification (System 2): gradient: from 10 to 30%B in 7 min, then 30 to 60%B in 60 min. HPLC (System I): t_R 1.92 min; (System III): t_R 8.44 min; ESI-MS: m/z: 977.8 [M+H]⁺, calculated monoisotopic mass for C₄₃H₆₄N₁₀O₁₆: 977.

6.2.1.2 Peptoid and Peptide-Peptoid Hybrids Synthesis

Two methods for the synthesis of peptoids by organic solid-phase chemistry have been described in the literature. In the submonomer method, the oligomer is prepared on the resin by repeated coupling of bromoacetic acid followed by a substitution reaction with an appropriate amine that comprises the side chain functionality.¹⁹⁰ In the monomer approach, 9-fluorenylmethoxycarbonyl (Fmoc)-protected N-substituted glycines are coupled.

Peptoid **2** and peptide-peptoid hybrids **3** and **4** were synthesized manually on Rink amide MBHA resin (substitution: 0.64 mmol/g, scale: 0.08 mmol) and obtained as amides at the C-terminus. The synthesis of the peptoidic parts were performed using a combination of the two peptoid synthesis approaches. According to the two submonomers assembly method, acylation reactions were performed by addition of bromoacetic acid (0.8 mmol, 112 mg) in DMF (2 ml), followed by addition of *N,N'*-diisopropylcarbodiimide (0.8 mmol, 123.8 μ L) in DMF (1 ml). Reaction mixtures were agitated at room temperature for 30 minutes and then the couplings repeated under the same conditions. Each reaction was then monitored using the chloranil test²⁰¹ for acylations of secondary amines or TNBS¹⁹⁹ and/or Keiser tests²⁰⁰ for acylations of primary amines. Bromo displacement reactions were performed by addition of the primary amine (0.8 mmol) as 2M solutions in DMSO and in the case of isopropyl amine the reaction was repeated a second time. Reactions were agitated at room temperature for 1 h. Nglu side chain was introduced protected as H- β -Ala-O*t*Bu · HCl. The Nala was introduced using the presynthesized commercially available monomer Fmoc-Sar-OH. Sta was introduced after preactivation of Fmoc-Sta-OH (1.4 mmol, 55.7 mg) with HATU/HOAt/DIEA. The products were then cleaved from the resin by TFA in the presence of 2.5% TIS and 2.5% water at room temperature in 2 h, the resin was filtered off and the crude peptides were precipitated with a cold solution of *tert*-butyl methyl ether/hexane 2:1 and lyophilised over night. The peptides were then purified by preparative RP-HPLC.

Their structural integrity was confirmed by electrospray ionization mass spectrometry.

Compound 2: Purification (System 1): gradient: from 15 to 30%B in 45 min. HPLC (System I): t_R 2.77 min; (System II): t_R 9.72 min; ESI-MS: m/z : 963.6 $[M+H]^+$, calculated monoisotopic mass for $C_{44}H_{70}N_{10}O_{14}$: 963.

Compound 3: Purification (System 1): gradient: from 5 to 15%B in 5 min, then 15 to 45%B in 60 min. HPLC (System II): t_R 8.93 min; ESI-MS: m/z : 978.6 $[M+H]^+$, calculated monoisotopic mass for $C_{45}H_{71}N_9O_{15}$: 978.

Compound 4: Purification (System 1): gradient: from 5 to 30%B in 60 min. HPLC (System II): t_R 8.63 min; ESI-MS: m/z : 978.6 $[M+H]^+$, calculated monoisotopic mass for $C_{45}H_{71}N_9O_{15}$: 978.

6.2.2 Macrocycles Approach

6.2.1.2 Synthesis of Peptides 8-19

Peptides **8**, **9**, **10**, **11**, **12**, **13**, **14**, **15**, **16**, **17**, **18** and **19** were synthesized by manual solid-phase methodology using Fmoc/HBTU/DMF chemistry. The side chains of all the residues were protected in the standard manner compatible with TFA cleavage and deprotection protocols and obtained as *N*-acetyl-peptide amides. Peptides were synthesized on a Rink Amide MBHA Resin (loading: 0.64 mmol/g for peptide **8**, **9**, **10**, **11**, **12**; loading: 0.69 mmol/g for peptides **13**, **14**, **15**, **16**, **17**, **18** and **19**), which allows the synthesis of peptide amides, on a 0.1-mmol scale. Amino acids, HOBt and HBTU were used in a 2 eq excess respect to the scale of the resin in each cycle. After removal of the last Fmoc protecting group, the final acetylation reaction was performed with DMF: Ac_2O : pyridine = 8:1:1 during 10 minutes and then repeated a second time. The extent of coupling and acetylation at each step was verified with the qualitative TNBS¹⁹⁹ and/or Keiser

tests²⁰⁰ on a sample of a few resin beads. The products were then cleaved from the resin by TFA in the presence of 2.5% TIS and 2.5% water at room temperature in 2 h, the resin was filtered off and the crude peptides were precipitated with a cold solution of *ter*-butyl methyl ether/hexane 2:1 and lyophilised over night. The peptides were then purified by preparative RP-HPLC. Their structural integrity was confirmed by electrospray ionization mass spectrometry.

Compound 8: Purification (System 1): gradient: from 12 to 42%B in 60 min. HPLC (System I): t_R 2.05 min; ESI-MS: m/z : 578.4 $[M+H]^+$, calculated monoisotopic mass for $C_{28}H_{43}N_5O_8$: 577.

Compound 9: Purification (System 1): gradient: from 7 to 37%B in 60 min. HPLC (System I): t_R 1.49 min; ESI-MS: m/z : 479.2 $[M+H]^+$, 958.0 $[2M+H]^+$, calculated monoisotopic mass for $C_{23}H_{34}N_4O_7$: 478.

Compound 10: Purification (System 1): gradient: from 7 to 37%B in 60 min. HPLC (System I): t_R 1.43 min; ESI-MS: m/z : 465.2 $[M+H]^+$, 929.6 $[2M+H]^+$, calculated monoisotopic mass for $C_{22}H_{32}N_4O_7$: 464.

Compound 11: Purification (System 1): gradient: from 10 to 40%B in 60 min. HPLC (System I): t_R 1.95 min; ESI-MS: m/z : 693.4 $[M+H]^+$, calculated monoisotopic mass for $C_{32}H_{48}N_6O_{11}$: 692.

Compound 12: Purification (System 1): gradient: from 7 to 37%B in 60 min. HPLC (System I): t_R 1.33 min; ESI-MS: m/z : 580.4 $[M+H]^+$, 1159.6 $[2M+H]^+$, calculated monoisotopic mass for $C_{26}H_{37}N_5O_{10}$: 579.

Compound 13: Purification (System 1): gradient: from 10 to 40%B in 60 min. HPLC (System I): t_R 1.84 min; ESI-MS: m/z : 659.4 $[M+H]^+$, 1318.0 $[2M+H]^+$, calculated monoisotopic mass for $C_{29}H_{50}N_6O_{11}$: 658.

Compound 14: Purification (System 1): gradient: from 20 to 50%B in 60 min. HPLC (System I): t_R 2.46 min; ESI-MS: m/z : 521.4 $[M+H]^+$, 1041.8 $[2M+H]^+$, calculated monoisotopic mass for $C_{26}H_{40}N_4O_7$: 520.

Compound 15: Purification (System 1): gradient: from 20 to 50%B in 60 min. HPLC (System I): t_R 2.42 min; ESI-MS: m/z : 521.4 $[M+H]^+$, 1041.8 $[2M+H]^+$, calculated monoisotopic mass for $C_{26}H_{40}N_4O_7$: 520.

Compound 16: Purification (System 1): gradient: from 20 to 50%B in 60 min. HPLC (System I): t_R 2.36 min; ESI-MS: m/z : 541.2 $[M+H]^+$, 1081.8 $[2M+H]^+$, calculated monoisotopic mass for $C_{28}H_{36}N_4O_7$: 540.

Compound 17: Purification (System 1): gradient: from 20 to 50%B in 60 min. HPLC (System I): t_R 2.43 min; ESI-MS: m/z : 559.4 $[M+H]^+$, 1117.4 $[2M+H]^+$, calculated monoisotopic mass for $C_{28}H_{35}N_4O_7$: 558.

Compound 18: Purification (System 1): gradient: from 20 to 50%B in 60 min. HPLC (System I): t_R 2.52 min; ESI-MS: m/z : 672.6 $[M+H]^+$, 1343.8 $[2M+H]^+$, calculated monoisotopic mass for $C_{32}H_{41}N_5O_{11}$: 671.

Compound 19: Purification (System 1): gradient: from 20 to 50%B in 60 min. HPLC (System I): t_R 2.42 min; ESI-MS: m/z : 638.4 $[M+H]^+$, 1275.8 $[2M+H]^+$, calculated monoisotopic mass for $C_{29}H_{43}N_5O_{11}$: 637.

6.2.2.2 Macrocycles

Synthesis of Substituted Asp of General Formula Z/Fmoc-Asp(R)-OH

1-(N-Boc-aminomethyl)-3-aminomethylbenzene

A solution of di-*tert*-butyl dicarbonate (1.5 g, 6.9 mmol) in dioxane (40 ml) was added drop wise at room temperature over a period of 3 h to a solution of α,α' -diamino-*m*-xylol (7.5 g, 55.0 mmol) in dioxane (40 ml). The mixture was stirred for 22 h and the solvent was then removed using a rotary evaporator. Water (50 ml) was added to the residue and the insoluble bis-substituted product was collected by filtration (32 mg, 1.3% based on dicarbonate). The filtrate was then extracted with methylene chloride (3 \times 50 ml) and the methylene chloride extract was backwashed with water (5 \times 50 ml). The solvent was dried over

MgSO₄ and evaporated, the resulting crude was purified on a silica gel column with a gradient from DCM/MeOH 95:5 to DCM/MeOH 8:2, to yield the pure product as a yellow oil. Yield: 1.28 g (79%); TLC: DCM/MeOH 6:4, R_f 0.38; HPLC (System I): t_R 1.58 min; ESI-MS: m/z: 237.2 [M+H]⁺, 473.8 [2M+H]⁺, calculated monoisotopic mass for C₁₃H₂₀N₂O₂: 236.

Fmoc-Asp[3-(Boc-aminomethyl)-benzylamine]-OAll

Fmoc-Asp-OAll (600 mg, 1.52 mmol) in DMF (5 ml) was preactivated during 10 minutes with HOBt (205 mg, 1.52 mmol), HBTU (575 mg, 1.52 mmol) and DIEA (520 μl, 3.03 mmol). A solution of 3-(Boc-aminomethyl)-benzylamine (326 mg, 1.38 mmol) in DMF (2 ml) was added and the solution stirred for 12 h at room temperature. The DMF was then evaporated and the oily residue redissolved in EtOAc (50 ml). The organic layer was washed with H₂O (1 × 50 ml), NaHCO₃ 5% (3 × 50 ml), H₂O (1 × 50 ml), KHSO₄ 5% (3 × 50 ml) and saturated NaCl (1 × 50 ml), dried over MgSO₄ and concentrated. The pure product was obtained by precipitation from EtOAc/petroleum ether as a crystalline solid. Yield: 815.4 mg (97%); HPLC (System I): t_R 4.52 min; ESI-MS: m/z: 614.4 [M+H]⁺, 558.4 [(M-*t*Bu)+H]⁺, 514.4 [(M-Boc)+H]⁺, 1227.6 [2M+H]⁺, calculated monoisotopic mass for C₃₅H₃₉N₃O₇: 613.

Fmoc-Asp[3-(Boc-aminomethyl)-benzylamine]-OH

Fmoc-Asp[3-(Boc-aminomethyl)-benzylamine]-OAll (815 mg, 1.33 mmol), dried over-night under reduced pressure, was dissolved in DMF (10 ml) in an Argon atmosphere with PhSiH₃ (0.82 ml, 6.6 mmol). Pd(PPh₃)₄ (31 mg, 27 μmol) was flushed with Argon, suspended in DMF (10 ml) and added to the solution. The mixture was stirred at room temperature under an inert atmosphere for 30 minutes and the progress of the reaction checked via HPLC. Upon completion of the reaction, the DMF was evaporated, the residue redissolved in

EtOAc (30 ml) and the organic layer washed with H₂O (1 × 30 ml), citric acid 5% (5 × 30 ml) and saturated NaCl (1 × 30 ml), dried over MgSO₄ and concentrated. The pure product was obtained by precipitation from DCM/petroleum ether as a crystalline solid. Yield: 594 mg (78%); HPLC (System I): t_R 3.89 min; ESI-MS: m/z: 574.4 [M+H]⁺, 518.4 [(M-*t*Bu)+H]⁺, 474.4 [(M-Boc)+H]⁺, 1147.8 [2M+H]⁺, calculated monoisotopic mass for C₃₂H₃₅N₃O₇: 573.

Z-Asp[3-(Boc-aminomethyl)-benzylamine]-OBzl

3-(Boc-aminomethyl)-benzylamine (0.62 g, 2.64 mmol) was added to a solution of Z-Asp(OSu)-OBzl (1.00 g, 2.20 mmol) in DCM (20 ml) and the mixture stirred for 12 h at room temperature. The DCM was then evaporated and the residue redissolved in EtOAc (50 ml). The organic layer was washed with H₂O (1 × 50 ml), NaHCO₃ 5% (3 × 50 ml), H₂O (1 × 50 ml), KHSO₄ 5% (3 × 50 ml) and saturated NaCl (1 × 50 ml), dried over MgSO₄ and concentrated. The pure product was obtained by precipitation from EtOAc/petroleum ether as a crystalline solid. Yield: 1.03 g (93%); TLC: DCM/MeOH 9:1, R_f 0.34; HPLC (System I): t_R 4.04 min; ESI-MS: m/z: 576.4 [M+H]⁺, 520.4 [(M-*t*Bu)+H]⁺, 476.2 [(M-Boc)+H]⁺, calculated monoisotopic mass for C₃₂H₃₇N₃O₇: 575.

Z-Asp[3-(Boc-aminomethyl)-benzylamine]-OH

Z-Asp[3-(Boc-aminomethyl)-benzylamine]-OBzl (1.13 g, 1.96 mmol) was hydrolysed in EtOH using NaOH (1 M aqueous, 1.1 eq). The reaction was stirred for 30 minutes at room temperature and the progress of it checked via HPLC. Upon completion of the reaction, the EtOH was diluted with water, the pH of the solution decreased to 2 with HCl 1 N and the product extracted with EtOAc (3 × 50 ml). The organic layer was washed with H₂O (3 × 50 ml), citric acid 5% (5 × 30 ml) and saturated NaCl (1 × 30 ml), dried over MgSO₄ and concentrated. The

pure product was obtained by precipitation from EtOAc/petroleum ether as a crystalline solid. Yield: 681 mg (72%); HPLC (System I): t_R 3.44 min; ESI-MS: m/z : 486.4 $[M+H]^+$, 430.4 $[(M-tBu)+H]^+$, 386.2 $[(M-Boc)+H]^+$, 971.6 $[2M+H]^+$, calculated monoisotopic mass for $C_{25}H_{31}N_3O_7$: 485.

N-Boc-1,4-phenyldiamine

A solution of di-*tert*-butyl dicarbonate (2.0 g, 9.2 mmol) in dioxane (40 ml) was added drop wise at room temperature over a period of 3 h to a solution of 1,4-phenyldiamine (7.9 g, 73.3 mmol) in dioxane (80 ml). The mixture was stirred for 22 h and the solvent was then removed using a rotary evaporator. Water (50 ml) was added to the residue and the insoluble bis-substituted product was collected by filtration (0.9 mg, 3% based on dicarbonate). The filtrate was then extracted with methylene chloride (3 \times 50 ml) and the methylene chloride extract was backwashed with water (8 \times 50 ml). The solvent was dried over $MgSO_4$ and evaporated and the pure product was crystallized from petroleum ether. Yield: 1.50 g (78%); TLC: DCM/MeOH 95:5, R_f 0.56; HPLC (System I): t_R 1.44 min; ESI-MS: m/z : 209.0 $[M+H]^+$, 417.2 $[2M+H]^+$, calculated monoisotopic mass for $C_{11}H_{16}N_2O_2$: 208.

Fmoc-Asp[4-(Boc-amino)-1,4-phenyldiamine]-OAll

Fmoc-Asp-OAll (600 mg, 1.52 mmol) in DMF (5 ml) was preactivated during 10 minutes with HOAt (205 mg, 1.52 mmol), HATU (577 mg, 1.52 mmol) and DIEA (520 μ l, 3.03 mmol). A solution of Boc-1,4-phenyldiamine (287 mg, 1.38 mmol) in DMF (2 ml) was added and the solution stirred for 12 h at room temperature. The DMF was then evaporated and the oily residue redissolved in EtOAc (50 ml). The organic layer was washed with H_2O (1 \times 50 ml), $NaHCO_3$ 5% (3 \times 50 ml), H_2O (1 \times 50 ml), $KHSO_4$ 5% (3 \times 50 ml) and saturated $NaCl$ (1 \times 50 ml), dried over $MgSO_4$ and concentrated. The pure product was obtained by

precipitation from EtOAc/petroleum ether as a crystalline solid. Yield: 739 mg (91%); HPLC (System I): t_R 4.51 min; ESI-MS: m/z : 586.4 $[M+H]^+$, 530.4 $[(M-tBu)+H]^+$, 1171.6 $[2M+H]^+$, calculated monoisotopic mass for $C_{33}H_{35}N_3O_7$: 585.

Fmoc-Asp[4-(Boc-amino)-1,4-phenyldiamine]-OH

Fmoc-Asp[4-(Boc-amino)-1,4-phenyldiamine]-OAll (739 mg, 1.20 mmol), dried over-night under reduced pressure, was dissolved in DMF (10 ml) in an Argon atmosphere with $PhSiH_3$ (1.6 ml, 12.6 mmol). $Pd(PPh_3)_4$ (73 mg, 63 μ mol) was flushed with Argon, suspended in DMF (10 ml) and added to the solution. The mixture was stirred at room temperature under an inert atmosphere for 30 minutes and the progress of the reaction checked via HPLC. Upon completion of the reaction, the DMF was evaporated, the residue redissolved in EtOAc (30 ml) and the organic layer washed with H_2O (1 \times 30 ml), citric acid 5% (5 \times 30 ml) and saturated NaCl (1 \times 30 ml), dried over $MgSO_4$ and concentrated. The pure product was obtained by precipitation from DCM/petroleum ether as a crystalline solid. Yield: 505 mg (77%); HPLC (System I): t_R 3.96 min; ESI-MS: m/z : 546.4 $[M+H]^+$, 490.4 $[(M-tBu)+H]^+$, 1091.6 $[2M+H]^+$, calculated monoisotopic mass for $C_{30}H_{31}N_3O_7$: 545.

Z-Asp[4-(Boc-amino)-1,4-phenyldiamine]-OBzl

Boc-1,4-phenyldiamine (0.55 g, 2.64 mmol) was added to a solution of Z-Asp(OSu)-OBzl (1.00 g, 2.20 mmol) in DCM (20 ml) and the mixture stirred for 12 h at room temperature. The DCM was then evaporated and the residue redissolved in EtOAc (50 ml). The organic layer was washed with H_2O (1 \times 50 ml), $NaHCO_3$ 5% (3 \times 50 ml), H_2O (1 \times 50 ml), $KHSO_4$ 5% (3 \times 50 ml) and saturated NaCl (1 \times 50 ml), dried over $MgSO_4$ and concentrated. The pure product was obtained by precipitation from EtOAc/petroleum ether as a brown

crystalline solid. Yield: 1.02 g (85%); TLC: DCM/MeOH 95:5, R_f 0.54; HPLC (System I): t_R 4.11 min; ESI-MS: m/z : 548.6 $[M+H]^+$, 492.2 $[(M-tBu)+H]^+$, 448.2 $[(M-Boc)+H]^+$, 1095.9 $[2M+H]^+$, calculated monoisotopic mass for $C_{30}H_{33}N_3O_7$: 547.

Z-Asp[4-(Boc-amino)-phenylamine]-OH

Z-Asp[4-(Boc-amino)-phenylamine]-OBzl (1.09 g, 1.99 mmol) was hydrolysed in EtOH using NaOH (1 M aqueous, 1.1 eq). The reaction was stirred for 30 minutes at room temperature and the progress of it checked via HPLC. Upon completion of the reaction, the EtOH was diluted with water, the pH of the solution decreased to 2 with HCl 1 N and the product extracted with EtOAc (3 × 50 ml). The organic layer was washed with H₂O (3 × 50 ml), citric acid 5% (5 × 30 ml) and saturated NaCl (1 × 30 ml), dried over MgSO₄ and concentrated. The pure product was obtained by precipitation from EtOAc/petroleum ether as a crystalline solid. Yield: 728 mg (80%); HPLC (System I): t_R 3.21 min; ESI-MS: m/z : 458.4 $[M+H]^+$, 402.4 $[(M-tBu)+H]^+$, 358.2 $[(M-Boc)+H]^+$, 915.6 $[2M+H]^+$, calculated monoisotopic mass for $C_{23}H_{27}N_3O_7$: 457.

N-Boc-1,3-diaminopropane

A solution of di-*tert*-butyl dicarbonate (3.7 g, 16.86 mmol) in dioxane (40 ml) was added drop wise at room temperature over a period of 3 h to a solution of 1,3-diaminopropane (10.0 g, 134.9 mmol) in dioxane (80 ml). The mixture was stirred for 22 h and the solvent was then removed using a rotary evaporator. Water (50 ml) was added to the residue and the insoluble bis-substituted product was collected by filtration (18 mg, 4% based on dicarbonate). The filtrate was then extracted with methylene chloride (3 × 50 ml) and the methylene chloride extract was backwashed with water (8 × 50 ml). The solvent was dried over MgSO₄ and evaporated, the resulting crude was purified on a silica gel column

with a gradient from DCM/MeOH 95:5 to DCM/MeOH 8:2, to yield the pure product as an oil. Yield: 1.93 g (66%); TLC: DCM/MeOH 4:1, R_f 0.26; HPLC (System I): t_R 5.20 min; ESI-MS: m/z : 175.2 $[M+H]^+$, 348.6 $[2M+H]^+$, calculated monoisotopic mass for $C_8H_{18}N_2O_2$: 174.

Fmoc-Asp[3-(Boc-amino)-1,3-diaminopropane]-OAll

Fmoc-Asp-OAll (600 mg, 1.52 mmol) in DMF (5 ml) was preactivated during 10 minutes with HOBt (205 mg, 1.52 mmol), HBTU (577 mg, 1.52 mmol) and DIEA (520 μ l, 3.03 mmol). A solution of Boc-1,3-diaminopropane (240 mg, 1.38 mmol) in DMF (2 ml) was added and the solution stirred for 12 h at room temperature. The DMF was then evaporated and the oily residue redissolved in EtOAc (50 ml). The organic layer was washed with H_2O (1 \times 50 ml), $NaHCO_3$ 5% (3 \times 50 ml), H_2O (1 \times 50 ml), $KHSO_4$ 5% (3 \times 50 ml) and saturated NaCl (1 \times 50 ml), dried over $MgSO_4$ and concentrated. The pure product was obtained by precipitation from EtOAc/petroleum ether as a crystalline solid. Yield: 717 mg (94%); HPLC (System I): t_R 4.11 min; ESI-MS: m/z : 552.4 $[M+H]^+$, 496.6 $[(M-tBu)+H]^+$, 452.4 $[(M-Boc)+H]^+$, 1103.6 $[2M+H]^+$, calculated monoisotopic mass for $C_{30}H_{37}N_3O_7$: 551.

Fmoc-Asp[3-(Boc-amino)-1,3-diaminopropane]-OH

Fmoc-Asp[3-(Boc-amino)-1,3-diaminopropane]-OAll (717 mg, 1.30 mmol), dried over-night under reduced pressure, was dissolved in DMF (10 ml) in an Argon atmosphere with $PhSiH_3$ (0.8 ml, 6.5 mmol). $Pd(PPh_3)_4$ (30 mg, 26 μ mol) was flushed with Argon, suspended in DMF (10 ml) and added to the solution. The mixture was stirred at room temperature under an inert atmosphere for 30 minutes and the progress of the reaction checked via HPLC. Upon completion of the reaction, the DMF was evaporated, the residue redissolved in EtOAc (30 ml) and the organic layer washed with H_2O (1 \times 30 ml), citric acid 5%

(5 × 30 ml) and saturated NaCl (1 × 30 ml), dried over MgSO₄ and concentrated. The pure product was obtained by precipitation from DCM/petroleum ether as a crystalline solid. Yield: 652 mg (98%); HPLC (System I): t_R 3.56 min; ESI-MS: m/z: 512.4 [M+H]⁺, 456.4 [(M-*t*Bu)+H]⁺, 412.2 [(M-Boc)+H]⁺, 1023.6 [2M+H]⁺, calculated monoisotopic mass for C₂₇H₃₃N₃O₇: 511.

N-Boc-1,4-diaminobutane

A solution of di-*tert*-butyl dicarbonate (3.1 g, 14.2 mmol) in dioxane (40 ml) was added drop wise at room temperature over a period of 3 h to a solution of 1,4-diaminobutane (10.0 g, 113.4 mmol) in dioxane (80 ml). The mixture was stirred for 22 h and the solvent was then removed using a rotary evaporator. Water (50 ml) was added to the residue and the insoluble bis-substituted product was collected by filtration (13 mg, 3% based on dicarbonate). The filtrate was then extracted with methylene chloride (3 × 50 ml) and the methylene chloride extract was backwashed with water (8 × 50 ml). The solvent was dried over MgSO₄ and evaporated, the resulting crude was purified on a silica gel column with eluent DCM/MeOH 8:2, to yield the pure product as an oil. Yield: 2.00 g (75%); TLC: DCM/MeOH 4:1, R_f 0.24; ESI-MS: m/z: 189.0 [M+H]⁺, 377.6 [2M+H]⁺, calculated monoisotopic mass for C₉H₂₀N₂O₂: 188.

Fmoc-Asp[4-(Boc-amino)-1,4-diaminobutane]-OAll

Fmoc-Asp-OAll (600 mg, 1.52 mmol) in DMF (5 ml) was preactivated during 10 minutes with HOBt (205 mg, 1.52 mmol), HATU (577 mg, 1.52 mmol) and DIEA (520 μl, 3.03 mmol). A solution of Boc-1,4-diaminobutane (260 mg, 1.38 mmol) in DMF (2 ml) was added and the solution stirred for 12 h at room temperature. The DMF was then evaporated and the oily residue redissolved in EtOAc (50 ml). The organic layer was washed with H₂O (1 × 50 ml), NaHCO₃

5% (3 × 50 ml), H₂O (1 × 50 ml), KHSO₄ 5% (3 × 50 ml) and saturated NaCl (1 × 50 ml), dried over MgSO₄ and concentrated. The pure product was obtained by precipitation from EtOAc/petroleum ether as a crystalline solid. Yield: 780 mg (92%); HPLC (System I): t_R 4.14 min; ESI-MS: m/z: 566.4 [M+H]⁺, 510.6 [(M-*t*Bu)+H]⁺, 466.4 [(M-Boc)+H]⁺, 1131.8 [2M+H]⁺, calculated monoisotopic mass for C₃₁H₃₉N₃O₇: 565.

Fmoc-Asp[4-(Boc-amino)-1,4-diaminobutane]-OH

Fmoc-Asp[4-(Boc-amino)-1,4-diaminobutane]-OAll (713 mg, 1.26 mmol), dried over-night under reduced pressure, was dissolved in DMF (5 ml) in an Argon atmosphere with PhSiH₃ (1.6 ml, 12.6 mmol). Pd(PPh₃)₄ (146 mg, 0.13 mmol) was flushed with Argon, suspended in DMF (5 ml) and added to the solution. The mixture was stirred at room temperature under an inert atmosphere for 30 minutes and the progress of the reaction checked via HPLC. Upon completion of the reaction, the DMF was evaporated, the residue redissolved in EtOAc (30 ml) and the organic layer washed with H₂O (1 × 30 ml), citric acid 5% (5 × 30 ml) and saturated NaCl (1 × 30 ml), dried over MgSO₄ and concentrated. The pure product was obtained by precipitation from DCM/petroleum ether as a crystalline solid. Yield: 576 mg (87%); HPLC (System I): t_R 3.61 min; ESI-MS: m/z: 526.4 [M+H]⁺, 470.4 [(M-*t*Bu)+H]⁺, 426.2 [(M-Boc)+H]⁺, 1051.6 [2M+H]⁺, calculated monoisotopic mass for C₂₈H₃₅N₃O₇: 525.

N-Boc-1,5-diaminopentane

A solution of di-*tert*-butyl dicarbonate (2.3 g, 10.6 mmol) in dioxane (30 ml) was added drop wise at room temperature over a period of 3 h to a solution of 1,5-diaminopentane (8.7 g, 85.1 mmol) in dioxane (50 ml). The mixture was stirred for 22 h and the solvent was then removed using a rotary evaporator. Water (50 ml) was added to the residue and the insoluble bis-substituted product

was collected by filtration (9 mg, 3% based on dicarbonate). The filtrate was then extracted with methylene chloride (3 × 50 ml) and the methylene chloride extract was backwashed with water (8 × 50 ml). The solvent was dried over MgSO₄ and evaporated, the resulting crude was purified on a silica gel column with eluent DCM/MeOH 8:2, to yield the pure product as an oil. Yield: 2.15 g (61%); TLC: DCM/MeOH 4:1, R_f 0.24; ESI-MS: m/z: 202.8 [M+H]⁺, 404.6 [2M+H]⁺, calculated monoisotopic mass for C₁₀H₂₂N₂O₂: 202.

Fmoc-Asp[5-(Boc-amino)-1,5-diaminopentane]-OAll

Fmoc-Asp-OAll (600 mg, 1.52 mmol) in DMF (5 ml) was preactivated during 10 minutes with HOBt (205 mg, 1.52 mmol), HBTU (577 mg, 1.52 mmol) and DIEA (520 μl, 3.03 mmol). A solution of Boc-1,5-diaminopentane (279 mg, 1.38 mmol) in DMF (2 ml) was added and the solution stirred for 12 h at room temperature. The DMF was then evaporated and the oily residue redissolved in EtOAc (50 ml). The organic layer was washed with H₂O (1 × 50 ml), NaHCO₃ 5% (3 × 50 ml), H₂O (1 × 50 ml), KHSO₄ 5% (3 × 50 ml) and saturated NaCl (1 × 50 ml), dried over MgSO₄ and concentrated. The pure product was obtained by precipitation from EtOAc/petroleum ether as a crystalline solid. Yield: 682 mg (85%); HPLC (System I): t_R 4.36 min; ESI-MS: m/z: 580.4 [M+H]⁺, 524.6 [(M-*t*Bu)+H]⁺, 480.4 [(M-Boc)+H]⁺, 1159.8 [2M+H]⁺, calculated monoisotopic mass for C₃₂H₄₁N₃O₇: 579.

Fmoc-Asp[5-(Boc-amino)-1,5-diaminopentane]-OH

Fmoc-Asp[5-(Boc-amino)-1,5-diaminopentane]-OAll (682 mg, 1.18 mmol), dried over-night under reduced pressure, was dissolved in DMF (10 ml) in an Argon atmosphere with PhSiH₃ (0.7 ml, 5.9 mmol). Pd(PPh₃)₄ (27 mg, 23.5 μmol) was flushed with Argon, suspended in DMF (10 ml) and added to the

solution. The mixture was stirred at room temperature under an inert atmosphere for 45 minutes and the progress of the reaction checked via HPLC. Upon completion of the reaction, the DMF was evaporated, the residue redissolved in EtOAc (30 ml) and the organic layer washed with H₂O (1 × 30 ml), citric acid 5% (5 × 30 ml) and saturated NaCl (1 × 30 ml), dried over MgSO₄ and concentrated. The pure product was obtained by precipitation from DCM/petroleum ether as a crystalline solid. Yield: 470 mg (74%); HPLC (System I): t_R 3.73 min; ESI-MS: m/z: 540.6 [M+H]⁺, 484.6 [(M-*t*Bu)+H]⁺, 440.4 [(M-Boc)+H]⁺, 1079.8 [2M+H]⁺, calculated monoisotopic mass for C₂₉H₃₇N₃O₇: 539.

Synthesis of Peptides of General Formula Z-Asp(R)-Sta-Val-Asp-NH₂

Z-Asp(3-aminomethyl)-benzylamine)-Sta-Val-Asp-NH₂ (20)

Z-Asp(4-amino-phenylamine)-Sta-Val-Asp-NH₂ (22)

The synthesis was conducted by manual solid-phase methodology using Fmoc/HBTU/DMF chemistry. Asp¹ was introduced as Z-Asp[3-(Boc-aminomethyl)-benzylamine]-OH (AL121) for peptide **20** and as Z-Asp[4-(Boc-amino)-phenylamine]-OH for peptide **22**. The peptides were synthesized as peptide amides on a Rink amide MBHA Resin (loading: 0.66 mmol/g) on a 0.125-mmol scale. Amino acids, HOBt and HBTU were used in a 2 eq excess respect to the scale of the synthesis in each cycle. The extent of coupling at each step was verified with the qualitative TNBS and/or Kaiser tests on a sample of a few resin beads. The products were then cleaved from the resin by TFA in the presence of 2.5% TIS and 2.5% water at room temperature in 2 h, the resin was filtered off and the crude peptides were precipitated with a cold solution of *tert*-butyl methyl ether/hexane 2:1 and lyophilised over night. The purity of the peptides exceeded 90% as determined by analytical RP-HPLC and were used for the cyclization reaction without further purification. Their structural integrity was confirmed by electrospray ionization mass spectrometry.

Compound 20. Yield: 94.5 mg (85%); HPLC (System I): t_R 2.15 min; ESI-MS: m/z : 756.6 $[M+H]^+$, calculated monoisotopic mass for $C_{37}H_{53}N_7O_{10}$: 755.

Compound 22. Yield: 86 mg (94%); HPLC (System I): t_R 2.07 min; ESI-MS: m/z : 728.4 $[M+H]^+$, calculated monoisotopic mass for $C_{35}H_{49}N_5O_{10}$: 727.

Compound 21

Peptide **20** (18.6 mg, 24.6 μ mol) was dissolved in DMF (250 ml, to give a 10^{-4} M concentration). HOAt (16.8 mg, 0.12 mmol), HATU (46.8 mg, 0.12 mmol) and DIEA (42 μ l, 0.25 mmol) were added and the solution stirred for 12 h at room temperature. The DMF was then evaporated and the product was purified by preparative RP-HPLC (System 2, gradient: from 0 to 10%B in 5 min, then from 10 to 40%B in 60 min). Yield: 2.2 mg (12%); HPLC (System I): t_R 2.65 min; (System IV): t_R 8.26 min; ESI-MS: m/z : 738.4 $[M+H]^+$, calculated monoisotopic mass for $C_{37}H_{51}N_7O_9$: 737.

Compound 23

Peptide **22** (27.0 mg, 37.1 μ mol) was dissolved in DMF (370 ml, to give a 10^{-4} M concentration). HOAt (25.3 mg, 0.19 mmol), HATU (70.6 mg, 0.19 mmol) and DIEA (64 μ l, 0.37 mmol) were added and the solution stirred for 12 h at room temperature. The DMF was then evaporated and the product was purified by preparative RP-HPLC (System 2, gradient: from 10 to 20%B in 5 min, then from 20 to 50%B in 60 min). Yield: 2.6 mg (13%); HPLC (System I): t_R 3.02 min; (System V): t_R 7.61 min; ESI-MS: m/z : 710.6 $[M+H]^+$, calculated monoisotopic mass for $C_{35}H_{47}N_7O_9$: 709.

*Synthesis of Peptides of General Formula Z-Asp(R)-Sta-Val-OH*Z-Asp-Sta-Val-OH (24)Z-Asp(3-aminomethyl-benzylamine)-Sta-Val-OH (25)Z-Asp(4-amino-phenylamine)-Sta-Val-OH (27)

The synthesis was conducted by manual solid-phase methodology using Fmoc/HBTU/DMF chemistry. Asp was introduced as Z-Asp(*t*Bu)-OH for peptide **24**, Z-Asp[3-(Boc-aminomethyl)-benzylamine]-OH (AL121) for peptide **25** and as Z-Asp[4-(Boc-amino)-phenylamine]-OH (AL120) for peptide **27**. The peptides were synthesized as peptide acids on a 2-Chlorotrytyl chloride Resin (loading: 0.83 mmol/g, as estimated using the procedure reported in Chapter 6.1) on a 0.25-mmol scale. Amino acids, HOBt and HBTU were used in a 2 eq excess respect to the scale of the synthesis in each cycle. The extent of coupling at each step was verified with the qualitative TNBS and/or Kaiser tests on a sample of a few resin beads. The products were then cleaved from the resin by TFA in the presence of 2.5% TIS and 2.5% water at room temperature in 2 h, the resin was filtered off and the crude peptides were precipitated with a cold solution of *ter*-butyl methyl ether/hexane 2:1 and lyophilised over night. The purity of the peptides exceeded 90% as determined by analytical RP-HPLC and were used for the cyclization reaction without further purification. Their structural integrity was confirmed by electrospray ionization mass spectrometry.

Compound 24. Yield: 115 mg (88%); HPLC (System I): t_R 1.24 min; ESI-MS: m/z : 524.8 $[M+H]^+$, calculated monoisotopic mass for $C_{25}H_{37}N_3O_9$: 523.

Compound 25. Yield: 136 mg (85%); HPLC (System I): t_R 1.39 min; ESI-MS: m/z : 642.6 $[M+H]^+$, calculated monoisotopic mass for $C_{33}H_{47}N_5O_8$: 641.

Compound 27. Yield: 112 mg (73%); HPLC (System I): t_R 2.36 min; ESI-MS: m/z : 614.6 $[M+H]^+$, calculated monoisotopic mass for $C_{31}H_{43}N_5O_8$: 613.

Compound 26

Peptide **25** (20.52 mg, 32.0 μmol) was dissolved in DMF (320 ml, to give a 10^{-4} M concentration). HOAt (21.8 mg, 0.16 mmol), HATU (61 mg, 0.16 mmol) and DIEA (55 μl , 0.32 mmol) were added and the solution stirred for 12 h at room temperature. The DMF was then evaporated and the product was purified by preparative RP-HPLC (System 2, gradient: from 15 to 25%B in 5 min, then from 25 to 55%B in 60 min). Yield: 2.6 mg (13%); HPLC (System I): t_{R} 3.09 min; (System IV): t_{R} 10.19 min; ESI-MS: m/z : 624.6 $[\text{M}+\text{H}]^+$, calculated monoisotopic mass for $\text{C}_{33}\text{H}_{45}\text{N}_5\text{O}_7$: 623.

Compound 28

Peptide **27** (17.66 mg, 28.8 μmol) was dissolved in DMF (290 ml, to give a 10^{-4} M concentration). HOAt (19.6 mg, 0.14 mmol), HATU (54.7 mg, 0.14 mmol) and DIEA (49 μl , 0.29 mmol) were added and the solution stirred for 12 h at room temperature. The DMF was then evaporated and the product was purified by preparative RP-HPLC (System 2, gradient: from 10 to 20%B in 5 min, then from 20 to 50%B in 60 min). Yield: 1.1 mg (6%); HPLC (System I): t_{R} 2.79 min; (System IV): t_{R} 8.14 min; ESI-MS: m/z : 596.4 $[\text{M}+\text{H}]^+$, 1191.8 $[2\text{M}+\text{H}]^+$, calculated monoisotopic mass for $\text{C}_{31}\text{H}_{41}\text{N}_5\text{O}_7$: 595.

Z-Asp-Sta-Val-Asp-OH (29)

The synthesis was conducted by manual solid-phase methodology using Fmoc/HBTU/DMF chemistry. The peptide was synthesized as peptide acid on a 2-chlorotrytyl chloride resin (loading: 0.76 mmol/g, as estimated using the procedure reported in Chapter 6.1) on a 0.25-mmol scale. Amino acids, HOBt and HBTU were used in a 2 eq excess respect to the scale of the synthesis in each cycle. The extent of coupling at each step was verified with the qualitative TNBS

and/or Kaiser tests on a sample of a few resin beads. The product was then cleaved from the resin by TFA in the presence of 2.5% TIS and 2.5% water at room temperature in 2 h, the resin was filtered off and the crude peptide was precipitated with a cold solution of *ter*-butyl methyl ether/hexane 2:1 and lyophilised over night. The purity of the peptide exceeded 90% as determined by analytical RP-HPLC and were used for the cyclization reaction without further purification. Their structural integrity was confirmed by electrospray ionization mass spectrometry.

Compound 29. Yield: 120 mg (75%); HPLC (System I): t_R 1.22 min; ESI-MS: m/z : 639.2 $[M+H]^+$, calculated monoisotopic mass for $C_{25}H_{37}N_3O_9$: 638.

Z-Asp[(3-aminomethyl)-benzylamine]-Sta-Val-Asp(ODmab)-OH (30-protected)

The synthesis was conducted by manual solid-phase methodology using Fmoc/HBTU/DMF chemistry. Asp¹ was introduced as Z-Asp[3-(Boc-aminomethyl)-benzylamine]-OH and Asp⁴ as Fmoc-Asp(ODmab)-OH. The peptide was synthesized as peptide acid on a 2-Chlorotrytyl chloride resin (loading: 0.78 mmol/g, as estimated using the procedure reported in Chapter 6.1) on a 0.15-mmol scale. Amino acids, HOBt and HBTU were used in a 2 eq excess respect to the scale of the synthesis in each cycle. The extent of coupling at each step was verified with the qualitative TNBS and/or Kaiser tests on a sample of a few resin beads. The products were then cleaved from the resin by TFA in the presence of 2.5% TIS and 2.5% water at room temperature in 2 h, the resin was filtered off and the crude peptides were precipitated with a cold solution of *ter*-butyl methyl ether/hexane 2:1 and lyophilised over night. The purity of the peptide exceeded 90% as determined by analytical RP-HPLC and was used for the cyclization reaction without further purification. Its structural integrity was confirmed by electrospray ionization mass spectrometry.

Compound 30-protected. Yield: 117.0 mg (73%); HPLC (System I): t_R 3.46 min; ESI-MS: m/z : 1068.8 $[M+H]^+$, 535.0 $[(M+2H)/2]^+$, calculated monoisotopic mass for $C_{57}H_{77}N_7O_{13}$: 1067.

Compound 30

Peptide **30**-protected (4.2 mg, 3.9 μ mol) was dissolved in DMF (980 μ l). hydrazine (20 μ l) was added and the solution stirred for 10 min at room temperature. The product was then precipitated from the solution with diethyl ether and used without further purification. Yield: 2.8 mg (76%); HPLC (System I): t_R 4.52 min; ESI-MS: m/z : 757.4 $[M+H]^+$, calculated monoisotopic mass for $C_{37}H_{52}N_6O_{11}$: 736.

Compound 31-protected

Peptide **30**-protected (54.1 mg, 50.6 μ mol) was dissolved in DMF (500 ml, to give a 10^{-4} M concentration). HOAt (34.4 mg, 0.25 mmol), HATU (96.2 mg, 0.25 mmol) and DIEA (60 μ l, 0.51 mmol) were added and the solution stirred for 12 h at room temperature. The DMF was then evaporated and the product was dissolved in acetonitrile/ H_2O 1:1 and lyophilised. Yield: 7.9 mg (15%); HPLC (System I): t_R 1.34 min; ESI-MS: m/z : 1050.6 $[M+H]^+$, 526.0 $[(M+2H)/2]^+$, calculated monoisotopic mass for $C_{57}H_{75}N_7O_{12}$: 1049.

Compound 31

Peptide **31**-protected (7.9 mg, 7.5 μ mol) was dissolved in DMF (980 μ l). hydrazine (20 μ l) was added and the solution stirred for 10 min at room temperature. The product was then precipitated from the solution with diethyl ether and purified by preparative RP-HPLC (System 2, gradient: from 0 to 25%B in 10 min, then from 25 to 55%B in 60 min). Yield: 2.8 mg (51%); HPLC

(System I): t_R 2.92 min; ESI-MS: m/z : 739.4 $[M+H]^+$, calculated monoisotopic mass for $C_{37}H_{50}N_6O_{10}$: 738.

Synthesis of Peptides of General Formula Ac-Ile-Asp(R)-(Phe)Sta-Val-Asp-NH₂

Ac-Ile-Asp[3-(Boc-amino)-1,3-diaminopropane]-(Phe)Sta-Val-Asp-NH₂ (32)

Ac-Ile-Asp[4-(Boc-amino)-1,4-diaminobutane]-(Phe)Sta-Val-Asp-NH₂ (34)

Ac-Ile-Asp[5-(Boc-amino)-1,5-diaminopentane]-(Phe)Sta-Val-Asp-NH₂ (36)

Ac-Ile-Asp[3-(Boc-aminomethyl)-benzylamine]-(Phe)Sta-Val-Asp-NH₂ (38)

Ac-Ile-Asp[4-(Boc-amino)-1,4-phenyldiamine]-(Phe)Sta-Val-Asp-NH₂ (40)

The synthesis was conducted by manual solid-phase methodology using Fmoc/HBTU/DMF chemistry. The side chain of Asp⁵ was protected with *t*Bu, following the standard procedure compatible with TFA cleavage and deprotection protocols. Asp² was introduced as Fmoc-Asp(R)-OH. The peptide was synthesized as peptide amide on a Rink Amide MBHA Resin (loading: 0.69 mmol/g) on a 0.125-mmol scale. Amino acids, HOBt and HBTU were used in a 2 eq excess respect to the scale of the synthesis in each cycle. After removal of the last Fmoc protecting group, the final acetylation reaction was performed with DMF/Ac₂O/pyridine 8:1:1 during 10 minutes and then repeated a second time. The extent of coupling and acetylation at each step was verified with the qualitative TNBS and/or Kaiser tests on a sample of a few resin beads. The products were then cleaved from the resin by TFA in the presence of 2.5% TIS and 2.5% water at room temperature in 2 h, the resin was filtered off and the crude peptides were precipitated with a cold solution of *ter*-butyl methyl ether/hexane 2:1 and lyophilised over night. The purity of the peptides exceeded 90% as determined by analytical RP-HPLC and were used for the cyclization reaction without further purification. Their structural integrity was confirmed by electrospray ionization mass spectrometry.

6. Experimental Part

Compound 32. Yield: 93 mg (89%); HPLC (System I): t_R 1.75 min; ESI-MS: m/z : 749.6 $[M+H]^+$, calculated monoisotopic mass for $C_{35}H_{56}N_8O_{10}$: 748.

Compound 34. Yield: 95 mg (88%); HPLC (System I): t_R 1.71 min; ESI-MS: m/z : 763.6 $[M+H]^+$, calculated monoisotopic mass for $C_{36}H_{58}N_8O_{10}$: 762.

Compound 36. Yield: 65 mg (67%); HPLC (System I): t_R 1.74 min; ESI-MS: m/z : 777.6 $[M+H]^+$, calculated monoisotopic mass for $C_{37}H_{60}N_8O_{10}$: 776.

Compound 38. Yield: 84 mg (83%); HPLC (System I): t_R 1.85 min; ESI-MS: m/z : 811.4 $[M+H]^+$, calculated monoisotopic mass for $C_{40}H_{58}N_8O_{10}$: 810.

Compound 40. Yield: 98 mg (91%); HPLC (System I): t_R 1.75 min; ESI-MS: m/z : 783.4 $[M+H]^+$, calculated monoisotopic mass for $C_{38}H_{54}N_8O_{10}$: 782.

Compound 33

Peptide **32** (51.2 mg, 68.4 μ mol) was dissolved in DMF (690 ml, to give a 10^{-4} M concentration). HOAt (46.6 mg, 0.34 mmol), HATU (130.1 mg, 0.34 mmol) and DIEA (117 μ l, 0.68 mmol) were added and the solution stirred for 12 h at room temperature. The DMF was then evaporated and the residue redissolved in EtOAc (5 ml). The organic layer was washed with H_2O (1 \times 5 ml), $NaHCO_3$ 5% (3 \times 5 ml), H_2O (1 \times 5 ml), $KHSO_4$ 5% (3 \times 5 ml) and saturated $NaCl$ (1 \times 5 ml) and concentrated. The product was dissolved in acetonitrile, lyophilised and used without further purification. Yield: 20.0 mg (40%); HPLC (System I): t_R 2.04 min; ESI-MS: m/z : 731.6 $[M+H]^+$, calculated monoisotopic mass for $C_{35}H_{54}N_8O_9$: 730.

Compound 35

Peptide **34** (52.4 mg, 68.7 μ mol) was dissolved in DMF (690 ml, to give a 10^{-4} M concentration). HOAt (46.7 mg, 0.34 mmol), HATU (130.6 mg, 0.34 mmol) and DIEA (118 μ l, 0.68 mmol) were added and the solution stirred for 12

h at room temperature. The DMF was then evaporated and the residue redissolved in EtOAc (5 ml). The organic layer was washed with H₂O (1 × 5 ml), NaHCO₃ 5% (3 × 5 ml), H₂O (1 × 5 ml), KHSO₄ 5% (3 × 5 ml) and saturated NaCl (1 × 5 ml) and concentrated. The product was dissolved in acetonitrile, lyophilised and used without further purification. Yield: 19.0 mg (37%); HPLC (System I): t_R 2.13 min; ESI-MS: m/z: 745.4 [M+H]⁺, calculated monoisotopic mass for C₃₆H₅₆N₈O₉: 744.

Compound 37

Peptide **36** (32.4 mg, 41.7 μmol) was dissolved in DMF (420 ml, to give a 10⁻⁴ M concentration). HOAt (28.4 mg, 0.21 mmol), HATU (79 mg, 0.21 mmol) and DIEA (71 μl, 0.42 mmol) were added and the solution stirred for 12 h at room temperature. The DMF was then evaporated and the residue redissolved in EtOAc (5 ml). The organic layer was washed with H₂O (1 × 5 ml), NaHCO₃ 5% (3 × 5 ml), H₂O (1 × 5 ml), KHSO₄ 5% (3 × 5 ml) and saturated NaCl (1 × 5 ml) and concentrated. The product was dissolved in acetonitrile, lyophilised and used without further purification. Yield: 6.6 mg (21%); HPLC (System I): t_R 2.25 min; ESI-MS: m/z: 759.6 [M+H]⁺, calculated monoisotopic mass for C₃₇H₅₈N₈O₉: 758.

Compound 39

Peptide **38** (50.5 mg, 62.3 μmol) was dissolved in DMF (620 ml, to give a 10⁻⁴ M concentration). HOAt (42.4 mg, 0.31 mmol), HATU (118.4 mg, 0.31 mmol) and DIEA (107 μl, 0.62 mmol) were added and the solution stirred for 12 h at room temperature. The DMF was then evaporated and the residue redissolved in EtOAc (5 ml). The organic layer was washed with H₂O (1 × 5 ml), NaHCO₃ 5% (3 × 5 ml), H₂O (1 × 5 ml), KHSO₄ 5% (3 × 5 ml) and saturated NaCl (1 × 5 ml) and concentrated. The product was dissolved in acetonitrile, lyophilised and

used without further purification. Yield: 9.0 mg (18%); HPLC (System I): t_R 2.55 min; ESI-MS: m/z : 793.6 $[M+H]^+$, calculated monoisotopic mass for $C_{40}H_{56}N_8O_9$: 792.

Compound 41

Peptide **40** (33.8 mg, 43.2 μ mol) was dissolved in DMF (430 ml, to give a 10^{-4} M concentration). HOAt (29.4 mg, 0.21 mmol), HATU (82.1 mg, 0.21 mmol) and DIEA (89 μ l, 0.52 mmol) were added and the solution stirred for 12 h at room temperature. The DMF was then evaporated and the residue washed with H_2O (3×5 ml), $NaHCO_3$ 5% (3×5 ml), $KHSO_4$ 5% (3×5 ml), acetonitrile (3×5 ml) and saturated NaCl (1×5 ml). The product was then lyophilised and used without further purification. Yield: 3.4 mg (10%); HPLC (System I): t_R 2.50 min; ESI-MS: m/z : 765.4 $[M+H]^+$, calculated monoisotopic mass for $C_{38}H_{52}N_8O_9$: 764.

6.2.3 Amino-Benzoic Acid Containing Molecules

Peptide **42**, **43**, **44** and **45** were synthesized by manual solid-phase methodology using Fmoc/HBTU/DMF chemistry and obtained as *N*-acyl-peptide amides. Peptides were synthesized on a Rink Amide MBHA Resin (loading: 0.69 mmol/g), which allows the synthesis of peptide amides, on a 0.125-mmol scale. Amino acids, HOBt and HBTU were used in a 2 eq excess respect to the scale of the resin in each cycle. After removal of the last Fmoc protecting group, the final acetylation reaction was performed with DMF: Ac_2O : pyridine = 8:1:1 during 10 minutes and then repeated a second time. The extent of coupling at each step was verified with the qualitative TNBS and/or Kaiser tests on a sample of a few resin beads. The products were then cleaved from the resin by TFA in the presence of 2.5% TIS and 2.5% water at room temperature in 2 h, the resin was filtered off and the crude peptides were precipitated with a cold solution of *ter*-butyl methyl ether/hexane 2:1 and lyophilised over night. The peptides were then purified by

preparative RP-HPLC. The purity of the peptides exceeded 97% as determined by analytical RP-HPLC and their structural integrity was confirmed by electrospray ionization mass spectrometry.

Compound 42. Purification (System 1): gradient: from 20 to 50%B in 60 min. HPLC (System I): t_R 2.87 min; ESI-MS: m/z : 582.4 $[M+H]^+$, 1164.8 $[2M+H]^+$, calculated monoisotopic mass for $C_{31}H_{43}N_5O_6$: 581.

Compound 43. Purification (System 1): gradient: from 20 to 50%B in 60 min. HPLC (System I): t_R 2.57 min; ESI-MS: m/z : 582.4 $[M+H]^+$, 1164.8 $[2M+H]^+$, calculated monoisotopic mass for $C_{31}H_{43}N_5O_6$: 581.

Compound 44. Purification (System 1): gradient: from 20 to 50%B in 60 min. HPLC (System I): t_R 2.56 min; ESI-MS: m/z : 582.4 $[M+H]^+$, 1164.0 $[2M+H]^+$, calculated monoisotopic mass for $C_{31}H_{43}N_5O_6$: 581.

Compound 45. Purification (System 1): gradient: from 20 to 50%B in 60 min. HPLC (System I): t_R 2.69 min; ESI-MS: m/z : 612.6 $[M+H]^+$, 1224.8 $[2M+H]^+$, calculated monoisotopic mass for $C_{32}H_{45}N_5O_7$: 611.

6.2.4 Di-substituted Statine Synthesis

6.2.4.1 Lithium Enolates

2,4-Dimethylphenyl isocaproate (48)

4-methylvaleric acid (2.32 g, 20 mmol) was added dropwise to a stirred solution of carbonyldiimidazole (3.41 g, 21 mmol) in THF (20 ml) and stirred for 2 h. A solution of 2,4-dimethylphenol (3.67 g, 30 mmol) in THF (10 ml) was added to a suspension NaH (810 mg, 32 mmol) in THF (20 ml) at 0 °C and stirred for 60 min. During this time, the solution became homogeneous with a light purple colour. The acyl imidazole solution was added dropwise over 5 min to the sodium phenolate solution at 0 °C, and was stirred for 3 h. Ethyl acetate (100 ml)

was added and the solution was extracted with citric acid (3 x 30 ml), NaHCO₃ (3 x 30 ml), and brine (60 ml). Concentration of the solution followed by chromatography (10-30% DCM in PE) yielded 2.42 g (55%) the aryl ester. HPLC (System I): t_R 4.90 min; ESI-MS: m/z : 221.2 [M+H]⁺, calculated monoisotopic mass for C₁₄H₂₀O₂: 220.

Boc-Leu-*N*-methoxy-*N*-methylester (49)

2-(1H-Benzotriazole-1-yl)-1,1,3,3-tetramethyluronium tetrafluoroborate (TBTU) (5.12 g, 16 mmol), *N*-Hydroxybenzotriazole (HOBT) (2.12 g, 16 mmol) and diisopropylethylamine (DIEA) (2.73 ml, 16mmol) were added to a stirred solution of Boc-Leu-OH (3.70 g, 16 mmol) in dichloromethane (100 ml) at 0°C. After 5 minutes of stirring, *O,N*-dimethylhydroxyamine hydrochloride (1.71 g, 18 mmol) was added, followed by DIEA (3 ml, 18 mmol). All solid material dissolved within 10 minutes and the mixture was stirred overnight at RT. The solvent was evaporated, the reaction mixture redissolved in AcOEt and washed with H₂O (30 ml), citric acid 5% (5 x 30 ml), H₂O (1 x 30 ml), 5% aqueous NaHCO₃ solution (3 x 30 ml) and saturated NaCl (1 x 30 ml). The solution was dried over MgSO₄, the solvent removed *in vacuo* to give the product as a colourless oil (4.20 g, 95%). HPLC (System I): t_R 3.23 min; ESI-MS: m/z : 275.2 [M+H]⁺, 219.2 [(M-*t*Bu)+H]⁺, 175.2 [(M-Boc)+H]⁺, 571.4 [2M+H]⁺, calculated monoisotopic mass for C₁₃H₂₆N₂O₄: 274.

Boc-Leucinal (50)

Boc-Leu-*N*-methoxy-*N*-methylester (3.54 g, 12.8 mmol) was dissolved in dry Et₂O (90 ml) at 0°C. Argon was flushed and LiAlH₄ (0.63 g, 16.6 mmol) was added slowly. The mixture was stirred for 1h at RT. Then a 0.1 M HCl solution was added under vigorous stirring until pH 7 (76 ml, 7.6 mmol). The product was extracted twice with methylterbutyl ether (50ml) and washed with citric acid 5%

(5 × 50 ml), H₂O (1 × 50 ml), 5% aqueous NaHCO₃ solution (3 × 50 ml) and saturated NaCl (1 × 50 ml). The solution was dried over MgSO₄, the solvent removed *in vacuo* to give the product as a colourless oil (2.75 g, 98%). HPLC (System II): t_R 11.98 min (broad peak); ESI-MS: m/z: 216.4 [M+H]⁺, 160.2 [(M-*t*Bu)+H]⁺, 116.2 [(M-Boc)+H]⁺, 431.4 [2M+H]⁺, calculated monoisotopic mass for C₁₁H₂₁NO₃: 215.

2,6-dimethylphenyl 2-[hydroxyl (4-methoxyphenyl) methyl] -4-methylpentanoate (53)

A solution of 2,4-dimethylphenyl isocaproate (2) (1.10 g, 5.0 mmol) in THF (20 ml) was added dropwise over 10 min to a THF solution of LDA *circa* 2 M (3 ml, 6 mmol) in THF (40 ml) at -78 °C. After the solution was stirred for 1 h at -78 °C, a -78 °C solution of anisaldehyde (0.727 ml, 6 mmol) in THF (5 ml) was added dropwise over 2 min. The solution was stirred for 1 h during which the reaction warmed to -20 °C. The reaction was quenched with AcOH (up to pH 5), EtOAc was added (120 ml), and the solution was washed with 5% citric acid (3 × 30 ml), NaHCO₃ (3 × 30 ml), and brine (60 ml). The solution was dried over MgSO₄ and the solvent concentrated to yield the desired crude product. HPLC (System I): t_R 5.01 min; ESI-MS: m/z: 339.2 [M-H₂O+H]⁺, 217.2 [M-(2,6-dimethylphenol)+H]⁺; calculated monoisotopic mass for C₂₂H₂₈O₄: 356.

Boc-Statine-ethyl ester (55)

A solution of ethyl acetate (0.49 ml, 5.0 mmol) in THF (20 ml) was added dropwise over 10 min to a THF solution of LDA *circa* 2 M (3 ml, 6 mmol) in THF (40 ml) at -78 °C. After the solution was stirred for 1 h at -78 °C, a -78 °C solution of Boc-Leucinal (5) (1.29 mg, 6 mmol) in THF (5 ml) was added dropwise over 2 min. The solution was stirred for 1 h during which the reaction warmed to -20 °C. The reaction was quenched with AcOH (up to pH 5), EtOAc

was added (120 ml), and the solution was washed with 5% citric acid (3 x 30 ml), NaHCO₃ (3 x 30 ml), and brine (60 ml). The solution was dried over MgSO₄ and the solvent concentrated to yield the desired crude product. HPLC (System I): t_R 4.19 min; ESI-MS: m/z: 304.2 [M+H]⁺, 248.2 [(M-*t*Bu)+H]⁺, 204.2 [(M-Boc)+H]⁺, calculated monoisotopic mass for C₁₅H₂₉NO₅: 303.

6.2.4.2 Boron Enolates

2-(*N*-mesitylenesulfonyl)amino-1-phenyl-1-propanol (57)

To a stirred solution (-)-norefedrine (1.0 g, 6.6 mmol) and triethylamine (1.10 ml, 7.9 mmol) in dry DCM (10 ml) mesitylenesulfonyl chloride (1.44 g, 6.6 mmol) was added at 0°C. The reaction was stirred at 0°C for 2 h and then diluted with diethyl ether (200 ml). The mixture was washed successively with 100 ml each of water, 1M HCl, water, saturated NaHCO₃ and brine, dried over MgSO₄. The organic solution is filtered, the filtrate is concentrated to give an oily residue, which is redissolved in DCM and precipitated with hexane. Yield: 1.99 g (90%). TLC: Hexane/EtOAc 3:1, R_f 0.46; HPLC (System I): t_R 3.95 min; HPLC (System II): t_R 13.73 min; ESI-MS: m/z: 334.2 [M+H]⁺, 667.2 [2M+H]⁺, calculated monoisotopic mass for C₁₈H₂₃NO₃S: 333.

2-(*N*-benzyl-*N*-mesitylenesulfonyl)amino-1-phenyl-1-propanol (58)

A mixture of 2-(*N*-mesitylenesulfonyl)amino-1-phenyl-1-propanol (13) (1.9 g, 5.7 mmol), benzyl chloride (0.79 ml, 6.84 mmol), tetrabutyl ammonium iodide (22 mg, 0.06 mmol) and potassium carbonate (0.95 g, 6.84 mmol) in 100 ml acetonitrile is heated under reflux for 17 hr. The cooled mixture is filtered and the salt is washed with diethyl ether (100 ml). The combined organic layers are concentrated and the residue is crystallized from DCM and hexane to give the product. Yield: 1.88 g (78%). TLC: Hexane/EtOAc 3:1, R_f 0.59; HPLC (System

I): t_R 5.03 min; HPLC (System II): t_R 16.98 min; ESI-MS: m/z : 424.2 $[M+H]^+$, 847.4 $[2M+H]^+$, calculated monoisotopic mass for $C_{25}H_{29}NO_3S$: 423.

2-(*N*-benzyl-*N*-mesitylenesulfonyl) amino-1-phenyl-1-propyl 4-methylpentanoate (61)

To a solution of 4-methylpentanoic acid (160 μ l, 1.26 mmol) in DCM (10ml) at 0 °C $SOCl_2$ (110.4 μ l, 1.52 mmol) is added slowly and the mixture is left to react at RT for 3 h. After this time another 1 eq of $SOCl_2$ is added and the reaction let stirring for 1 more h. The solvent is then evaporated, the solution is diluted with DCM and the solvent re-evaporated: this procedure is repeated 4 times. The oil obtained (60) is used in the next reaction without further purification.

The 4-methylpentanoyl chloride obtained is added dropwise at 0°C to a solution of 2-(*N*-benzyl-*N*-mesitylenesulfonyl)amino-1-phenyl-1-propanol (300 mg, 0.71 mmol) and pyridine (74.1 μ l, 0.92 mmol) in DCM (20 ml). The reaction mixture is stirred at room temperature for 13 h and then diluted with diethyl ether (50 ml). The mixture is washed successively with 50 ml each of water, 1M HCl, water, saturated $NaHCO_3$ and brine, dried over $MgSO_4$. The organic solution is filtered, the filtrate is concentrated to give a crystalline residue, which was triturated with hexane to yield 315 mg (85%). HPLC (System II): t_R 14.05 min; ESI-MS: m/z : 522.4 $[M+H]^+$, calculated monoisotopic mass for $C_{31}H_{39}NO_4S$: 521.

Dicyclohexylboron trifluoromethanesulfonate (63)

An oven-dried, 250 ml, round bottom flask containing a stir bar and capped with a rubber septum is charged with cyclohexene (17.02 ml, 168 mmol) and dry diethyl ether (25 ml) and kept under argon at 0°C. The 2M solution of borane-dimethyl sulphide complex in diethyl ether (40 ml, 80 mmol) is added

dropwise during 30 min with stirring. The reaction mixture is stirred for 3 h at 0°C, the solid is allowed to settle without stirring. The supernatant organic solution is removed as much as possible with a syringe and the residue is dried flushing argon, to give dicyclohexylborane, which is used without purification for the preparation of the triflate.

The solid obtained is suspended in 100 ml of dry hexane and trifluoromethanesulfonic acid (17.13 ml, 80 mmol) is added dropwise via a glass syringe over 30 min with constant stirring, during which time vigorous gas evolution occurs; the solid gradually dissolves and the solution develops a yellow-orange colour. Stirring is continued at RT for 1 h, then the reaction mixture is left for 2 h without stirring. A semisolid phase separate and the top layer is transferred via syringe into a dry, 250 ml round-bottom flask. The flask is placed in a freezer at -20°C for 36 h. Large crystals form and the mother liquor is transferred via syringe to another dry round-bottom flask for further crystallization. The crystals are dried flushing Argon for 5 hr giving 9.1 g (35%) of dicyclohexylboron trifluoromethanesulfonate. ¹H NMR (400 MHz, CDCl₃): 0.79 (m, 10 H), 1.26 (m, 12 H).

6.2.4.3 Epoxide Opening with Grignard Reagent

Boc-Phenylalaninal (67)

Oxalyl chloride (1.69 ml, 20 mmol) is dissolved in 20 ml of dry DCM and cooled to -55°C. 1.28 ml (18 mmol) of dimethyl sulfoxide was added dropwise. Then, Boc-Phenylalaninol (2.54 g, 10 mmol), dissolved in 20 ml of DCM is added dropwise, and then more dimethyl sulfoxide (1.70 ml, 24 mmol) was added at -55°C. The reaction mixture was stirred at -55°C for 1 h, reacted with triethylamine (9.7 ml, 70 mmol), and stirred until room temperature was reached. After dilution with 100 ml of DCM, the mixture was washed with 1 N HCl and dried over MgSO₄, and the solvent evaporated to yield 2.04 g (82%) of product.

HPLC (System I): t_R 2.82 min (broad peak); ESI-MS: m/z : 250.2 $[M+H]^+$, calculated monoisotopic mass for $C_{14}H_{19}NO_3$: 249.

4(S)-[(1,1-dimethylethoxy)carbonyl amino]-5-phenyl-2-(E)-pentenoic acid ethyl ester (68)

To Boc-Phenylalaninal (2.04 g, 8.2 mmol) dissolved in toluene, (ethoxycarbonyl)-methylenetriphenylphosphorane (3.83 g, 11 mmol) was added, and the reaction mixture was heated to 80°C for 1 h. The solvent was then evaporated and the resulting crude was purified on a silica gel column with a gradient from DCM to DCM/MeOH 95:5, to yield the pure product as a yellow oil. Yield: 2.10 g (80%). TLC: to DCM/MeOH 95:5, R_f 0.74; HPLC (System I): t_R 3.89 min; ESI-MS: m/z : 320.4 $[M+H]^+$, 264.2 $[(M-tBu)+H]^+$, 220.2 $[(M-Boc)+H]^+$, calculated monoisotopic mass for $C_{18}H_{25}NO_4$: 319.

(2S/R, 3S/R, 4S) - 4 - [(1,1-dimethylethoxy) carbonyl amino] - 2,3 - epoxy - 5 - phenylpentanoic acid ethyl ester (69)

4(S)-[(1,1-dimethylethoxy)carbonyl amino]-5-phenyl-2-(E)-pentenoic acid ethyl ester (0.5 g, 1.57 mmol) is dissolved in 30 ml of dichloromethane and *m*-chloroperbenzoic acid (0.5 g, *circa* 2.66 mmol) was added. The reaction mixture was stirred for 5 d. The solvent was evaporated and the pure product obtained after purification on a silica gel column with a gradient from PE/EtOAc 4:1 to PE/EtOAc 8:1, to yield the pure product as a clear oil. Yield: 1.58 g (53%). TLC: toluene/EtOAc 4:1, R_f 0.56; TLC: PE/EtOAc 4:1, R_f 0.50; HPLC (System I): t_R 4.15 min; ESI-MS: m/z : 336.2 $[M+H]^+$, 280.2 $[(M-tBu)+H]^+$, 236.2 $[(M-Boc)+H]^+$, calculated monoisotopic mass for $C_{18}H_{25}NO_5$: 335.

(4S) - 2 - (methyl) - 4 [(1,1 - dimethylethoxy carbonyl) amino] - 3 - hydroxyl - 5 -phenylpentanoic acid ethyl ester (70)

CuCN (87 mg, 1 mmol) are suspended in anhydrous ethyl ether (5 ml) and cooled to -78°C . A solution of CH_3MgBr *circa* 3M in ethyl ether (0.5 ml, 1.50 mmol) is added and at this temperature (2S/R,3S/R,4S)-4-[(1,1-dimethylethoxy)carbonyl amino]-2,3-epoxy-5-phenylpentanoic acid ethyl ester (25) (330 mg, 0.98 mmol), dissolved in 20 ml of ethyl ether is added. The reaction mixture is brought to room temperature and stirred for 2 h. The solvent was then evaporated, and the residue was analyzed. HPLC (System I): t_{R} 3.45 min; ESI-MS: m/z : 352.6 $[\text{M}+\text{H}]^+$, 296.2 $[(\text{M}-t\text{Bu})+\text{H}]^+$, 252.2 $[(\text{M}-\text{Boc})+\text{H}]^+$, calculated monoisotopic mass for $\text{C}_{19}\text{H}_{29}\text{NO}_5$: 351.

6.2.5 Synthesis of Bivalent Inhibitors for MMP-9

6.2.5.1 Route A

Trt-(O-CH₂-CH₂)₄-OH (71)

To a solution of H-(O-CH₂-CH₂)₄-OH (2.0 g, 10.30 mmol) in DCM (40 ml), Ag₂O (3.58 g, 15.45 mmol), KI (0.68 g, 4.12 mmol) and Trt-Cl (3.16 g, 11.33 mmol) were added. The resulting mixture was heated to reflux for 22 h. After this time, the silver salts were removed by filtration through a pad of celite, which was thoroughly washed with EtOAc. The filtrates were combined, evaporated under reduced pressure and the residue was purified by silica gel column chromatography with a gradient from EtOAc/petroleum ether 1:1 to EtOAc/petroleum ether 3:1, to yield the pure product as an oil. Yield: 2.7 g (59%); TLC: DCM/MeOH 95:5, R_{f} 0.79; EtOAc/petroleum ether 3:1, R_{f} 0.40; HPLC (System I): t_{R} 4.11 min; ESI-MS: m/z : 454.4 $[(\text{M}+\text{H}_2\text{O})+\text{H}]^+$, calculated monoisotopic mass for $\text{C}_{27}\text{H}_{32}\text{O}_5$: 436; ¹H NMR (CDCl_3) δ 3.27 (t, 2H), 3.60 (t, 2H), 3.69-3.80 (m, 12H), 7.20-7.57 (m, 15H).

Z-Leu-Phe-Pro-Gly-Asp(OBzl)-OH (72):

The synthesis was conducted by manual solid-phase methodology using Fmoc/HBTU/DMF chemistry. The peptide was synthesized as peptide acid on a 2-chlorotrytyl chloride resin (loading: 1.1 mmol/g, as estimated using the procedure reported in Chapter 6.1) on a 1.0-mmol scale. Amino acids, HOBt and HBTU were used in a 2 eq excess respect to the scale of the synthesis in each cycle. The extent of coupling at each step was verified with the qualitative TNBS and/or Kaiser tests on a sample of a few resin beads. The products were then cleaved from the resin by TFA in the presence of 2.5% TIS and 2.5% water at room temperature in 2 h, the resin was filtered off and the crude peptides were precipitated with a cold solution of *ter*-butyl methyl ether/hexane 2:1 and lyophilised over night. The purity of the peptide exceeded 97% as determined by analytical RP-HPLC and used without further purification. Its structural integrity was confirmed by electrospray ionization mass spectrometry. Yield: 866 mg (90%); HPLC (System I): t_R 3.80 min; ESI-MS: m/z : 772.6 $[M+H]^+$, calculated calculated monoisotopic mass for $C_{41}H_{49}N_5O_{10}$: 771.

Trt-(O-CH₂-CH₂)₄-Asp(OBzl)-Gly-Pro-Phe-Leu-Z (73)

To a solution of Z-Leu-Phe-Pro-Gly-Asp(OBzl)-OH (150 mg, 0.19 mmol) in DCM (2 ml), DMAP (23.7 mg, 0.19 mmol), EDC (36.2 mg, 0.23 mmol) and Trt-(O-CH₂-CH₂)₄-OH (102 mg, 0.23 mmol) were added. The solution was stirred for 12 h at room temperature. The DCM was then evaporated and the oily residue redissolved in EtOAc (20 ml). The organic layer was washed with H₂O (1 × 20 ml), NaHCO₃ 5% (3 × 20 ml), H₂O (1 × 20 ml), KHSO₄ 5% (3 × 20 ml) and saturated NaCl (1 × 20 ml), dried over MgSO₄ and concentrated under reduced pressure. The residue was purified by silica gel column chromatography with a gradient DCM/MeOH 98:2 to DCM/MeOH 95:5, to yield the pure product as an oil. Yield: 41.6 mg (18%); TLC: DCM/MeOH 95:5, R_f 0.29; EtOAc/petroleum

ether 4:1, R_f 0.23; HPLC (System I): t_R 5.56 min; ESI-MS: m/z : 1190.8 $[M+H]^+$, 1207.8 $[(M+H_2O)+H]^+$, calculated monoisotopic mass for $C_{68}H_{79}N_5O_{14}$: 1189.

H-(O-CH₂-CH₂)₄-Asp(OBzl)-Gly-Pro-Phe-Leu-Z (74)

Trt-(O-CH₂-CH₂)₄-Asp(OBzl)-Gly-Pro-Phe-Leu-Z (34.8 mg, 29.4 μ mol) was dissolved in DCM/MeOH 95:5 (990 μ l), then TFA (10 μ l) were added and the reaction stirred for 45 minutes at room temperature. The product is obtained as an oil after precipitation with a cold solution of *ter*-butyl methyl ether/hexane 2:1, lyophilised and purified by preparative RP-HPLC (System 1, gradient: from 45 to 55%B in 5 min, then from 55 to 80%B in 60 min). Yield: 25.9 mg (93%); HPLC (System I): t_R 3.77 min; (System III): t_R 10.43 min; (System VI): t_R 8.89 min; ESI-MS: m/z : 948.8 $[M+H]^+$, 965.8 $[(M+H_2O)+H]^+$, calculated monoisotopic mass for $C_{49}H_{65}N_5O_{14}$: 947.

[4-(*N*-benzyloxyamino)-2(*R*)-isobutylsuccinyl]-methyl ester (76)

To (*R*)-2-isobutyl succinic acid-1-methyl ester (75) (1.00 g, 5.31 mmol) in DCM (30 ml) were added HOBt (0.98 g, 6.38 mmol) and HBTU (2.42 g, 6.38 mmol). A solution of benzyloxyamin-hydrochloride (1.02 g, 6.38 mmol) and DIEA (2.18 μ l, 12.75 mmol) in DCM (20 ml) was added and the solution stirred for 12 h at room temperature. The DCM was then evaporated and the oily residue redissolved in EtOAc (50 ml). The organic layer was washed with H₂O (1 \times 50 ml), NaHCO₃ 5% (3 \times 50 ml), H₂O (1 \times 50 ml), KHSO₄ 5% (3 \times 50 ml) and saturated NaCl (1 \times 50 ml), dried over MgSO₄ and concentrated. The pure product was obtained as an oil. Yield: 1.50 g (96%); HPLC (System I): t_R 3.19 min; (System III): t_R 9.27 min; ESI-MS: m/z : 294.2 $[M+H]^+$, 587.6 $[2M+H]^+$, calculated monoisotopic mass for $C_{16}H_{23}NO_4$: 293.

4-(*N*-benzyloxyamino)-2(*R*)-isobutylsuccinic acid · Na

[4-(*N*-benzyloxyamino)-2(*R*)-isobutylsuccinyl]-methyl ester (500 mg, 1.7 mmol) was hydrolysed in MeOH (5 ml) using NaOH (1 M aqueous, 1.1 eq). The reaction was stirred for 30 minutes at room temperature and the progress of it checked via HPLC. Upon completion of the reaction, the MeOH was diluted with water, the pH of the solution decreased to 2 with HCl 0.5 N and the product extracted with EtOAc (3 × 10 ml). The organic layer was washed with H₂O (1 × 50 ml), citric acid 5% (3 × 50 ml) and saturated NaCl (1 × 50 ml), dried over MgSO₄ and concentrated. The resulting oil was then redissolved in dioxane (30 ml) and an aqueous solution of concentrated NaCl is added dropwise (1.1 eq) under vigorous stirring. Precipitation occurred within 5 min to give a light mixture. The mixture is diluted with Et₂O, stirred vigorously for 30 min and left for 8 h at 4 °C. The product, white solid, is then filtered, washed with Et₂O and dried in vacuum. Yield: 408 mg (79%); HPLC (System I): t_R 2.55 min; ESI-MS: m/z: 302.2 [M+H]⁺, 603.4 [2M+H]⁺, calculated monoisotopic mass for C₁₆H₂₃NO₄Na: 301; ¹H NMR (CDCl₃) δ 0.81 (d, 6H), 1.05-1.17 (m, 1H), 1.35-1.51 (m, 2H), 2.00-2.11 (m, 1H), 2.51 (d, 2H), 4.73 (s, 1H), 7.27-7.38 (m, 6H).

4-(*N*-benzyloxyamino)-2(*R*)-isobutylsuccinic acid · DCHA

[4-(*N*-benzyloxyamino)-2(*R*)-isobutylsuccinyl]-methyl ester (1.6 g, 5.5 mmol) was hydrolysed in MeOH (10 ml) using NaOH (1 M aqueous, 1.1 eq). The reaction was stirred for 30 minutes at room temperature and the progress of it checked via HPLC. Upon completion of the reaction, the MeOH was diluted with water, the pH of the solution decreased to 2 with HCl 0.5 N and the product extracted with EtOAc (3 × 50 ml). The organic layer was washed with H₂O (1 × 50 ml), citric acid 5% (3 × 50 ml) and saturated NaCl (1 × 50 ml), dried over MgSO₄ and then treated with dicyclohexylamine (1.2 ml, 6.1 mmol) under vigorous stirring. Precipitation occurred within 5 min to give a thick mixture. The mixture

is diluted with Et₂O, stirred vigorously for 30 min and left for 8 h at 4 °C. The product, white solid, is then filtered, washed with Et₂O and dried in vacuum. Yield: 2.17 g (86%); HPLC (System I): t_R 2.53 min; ESI-MS: m/z: 302.2 [M+H]⁺, 603.4 [2M+H]⁺, calculated monoisotopic mass for C₁₆H₂₃NO₄Na: 301.

Boc-Phe-Ser(Bzl)-OMe

Boc-Phe-OSu (3.6 g, 10.00 mmol) and H₂N-Ser(Bzl)-OMe (2.3 g, 10.99 mmol) were dissolved in DCM (50 ml) and the solution stirred for 12 h at room temperature. The DCM was then evaporated and the residue redissolved in EtOAc (100 ml). The organic layer was washed with H₂O (1 × 50 ml), NaHCO₃ 5% (3 × 50 ml), H₂O (1 × 50 ml), citric acid 5% (3 × 50 ml) and saturated NaCl (1 × 50 ml), dried over MgSO₄ and concentrated. The pure product was obtained by precipitation from EtOAc/petroleum ether as a crystalline solid. Yield: 4.57 g (91%); HPLC (System I): t_R 3.94 min; ESI-MS: m/z: 457.4 [M+H]⁺, 401.4 [(M-*t*Bu)+H]⁺, 357.2 [(M-Boc)+H]⁺, 913.8 [2M+H]⁺, calculated monoisotopic mass for C₂₅H₃₂N₂O₆: 456.

H-Phe-Ser(Bzl)-OMe (81)

Boc-Phe-Ser(Bzl)-OMe (644 mg, 1.41 mmol) was dissolved in DCM/TFA 4:1 (10 ml) and stirred for 1 h. After addition of toluene (10 ml), the solvent was evaporated to dryness under reduced pressure and further evaporated two times with toluene (2 × 10 ml). The crude product was triturated using a diethyl ether, filtered and washed with diethyl ether to give H-Phe-Ser(Bzl)-OMe as a white precipitate. Yield: 493 mg (98%); HPLC (System I): t_R 2.24 min; ESI-MS: m/z: 357.2 [M+H]⁺, 713.6 [2M+H]⁺, calculated monoisotopic mass for C₂₀H₂₄N₂O₄: 356.

[4-(*N*-benzyloxyamino)-2(*R*)-isobutylsuccinyl]-Phe-Ser(Bzl)-OMe (**82**)

4-(*N*-benzyloxyamino)-2(*R*)-isobutylsuccinic acid DCHA salt (500 mg, 1.01 mmol) was suspended in EtOAc (10 ml) in a separating funnel, an ice-cold solution of H₂SO₄ (2 M, 1.1 eq) was added and the mixture shaken until it became clear. The organic layer was separated, cold water (10 ml) was added to the aqueous layer and it was further extracted with EtOAc (2 × 10 ml). The combined organic layers were washed with H₂O (1 × 30 ml) and saturated NaCl (1 × 30 ml) and concentrated under reduced pressure to obtain compound **77** as an oil. It was then redissolved in DMF (5 ml), EDC (270 mg, 1.41 mmol) and H-Phe-Ser(Bzl)-OMe (644 mg, 1.41 mmol) was added, the pH increased to 6 and the solution stirred for 12 h at room temperature. The DMF was then evaporated and the residue redissolved in CHCl₃ (20 ml). The organic layer was washed with H₂O (1 × 20 ml), NaHCO₃ 5% (3 × 20 ml), H₂O (1 × 20 ml), HCl 0.1 N (3 × 20 ml) and saturated NaCl (1 × 20 ml), dried over MgSO₄ and concentrated. The pure product was obtained by precipitation from CHCl₃/petroleum ether as a crystalline solid. Yield: 435 mg (65%); HPLC (System I): t_R 3.950 min; ESI-MS: m/z: 618.6 [M+H]⁺, calculated monoisotopic mass for C₃₅H₄₃N₃O₇: 617.

[4-(*N*-benzyloxyamino)-2(*R*)-isobutylsuccinyl]-Phe-Ser(Bzl)-OH (**83**)

[4-(*N*-benzyloxyamino)-2(*R*)-isobutylsuccinyl]-Phe-Ser(Bzl)-OMe (400 mg, 0.65 mmol) was hydrolysed in MeOH (20 ml) using NaOH (1 M aqueous, 1.1 eq). The reaction was stirred for 30 minutes at room temperature and the progress of it checked via HPLC. Upon completion of the reaction, the MeOH was diluted with water, the pH of the solution decreased to 2 with HCl 0.5 N and the product extracted with EtOAc (3 × 20 ml). The organic layer was washed with H₂O (1 × 20 ml), citric acid 5% (3 × 20 ml) and saturated NaCl (1 × 20 ml), dried over MgSO₄. The pure product was obtained by precipitation from EtOAc/petroleum ether as a crystalline solid. Yield: 349 mg (89%); HPLC

(System I): t_R 3.57 min; ESI-MS: m/z : 604.4 $[M+H]^+$, calculated monoisotopic mass for $C_{34}H_{41}N_3O_7$: 603.

[4-(*N*-benzyloxyamino)-2(*R*)-isobutylsuccinyl]-Phe-Ser(Bzl)-(O-CH₂-CH₂)₄-Asp(OBzl)-Gly-Pro-Phe-Leu-Z (84)

To a solution of [4-(*N*-Benzyloxyamino)-2(*R*)-isobutylsuccinyl]-Phe-Ser(Bzl)-OH (12.7 mg, 21.1 μ mol) in DCM (10 ml) were added DMAP (0.6 mg, 21.1 μ mol), EDC (4.3 mg, 27.6 μ mol) and H-(O-CH₂-CH₂)₄-Asp(OBzl)-Gly-Pro-Phe-Leu-Z (20.0 mg, 21.1 μ mol). The solution was stirred for 12 h at room temperature. The DCM was then evaporated and the oily residue redissolved in EtOAc (20 ml). The organic layer was washed with H₂O (1 \times 10 ml), NaHCO₃ 5% (3 \times 10 ml), H₂O (1 \times 10 ml), KHSO₄ 5% (3 \times 10 ml). Yield from HPLC (crude): 5%; HPLC (System I): t_R 4.820 min; ESI-MS: m/z : 1534.1 $[M+H]^+$, 1552.2 $[(M+H_2O)+H]^+$, 768.0 $[(M+2H)/2]^+$, calculated monoisotopic mass for $C_{83}H_{104}N_8O_{20}$: 1532.

6.2.5.2 Route B: PEG₄

Fmoc-Ser(Bzl)-(O-CH₂-CH₂)₄-OH (85)

To a solution of Fmoc-Ser(Bzl)-OH (1.0 g, 2.4 mmol) in DCM (50 ml) were added DMAP (146.3 mg, 0.1 mmol), EDC (483.3 mg, 3.11 mmol) and H-(O-CH₂-CH₂)₄-OH (4.7 g, 23.9 mmol). The solution was stirred for 12 h at room temperature. The DCM was then evaporated and the oily residue redissolved in EtOAc (50 ml). The organic layer was washed with H₂O (5 \times 50 ml), NaHCO₃ 5% (3 \times 50 ml), H₂O (5 \times 50 ml), KHSO₄ 5% (3 \times 50 ml) and saturated NaCl (2 \times 50 ml), dried over MgSO₄ and concentrated under reduced pressure. The residue was purified by silica gel column chromatography with EtOAc as eluent, to yield the pure product as an oil. Yield: 877 mg (62%); TLC: EtOAc, R_f 0.24; HPLC

(System I): t_R 3.87 min; ESI-MS: m/z : 594.4 $[M+H]^+$, 611.8 $[(M+H_2O)+H]^+$, calculated monoisotopic mass for $C_{33}H_{39}NO_9$: 593.

Fmoc-Ser(Bzl)-(O-CH₂-CH₂)₄-O-Asp(OBzl)-Boc (86)

To a solution of Boc-Asp(OBzl)-OH (478 mg, 1.5 mmol) in DCM (30 ml) were added DMAP (90.2 mg, 0.7 mmol), EDC (298.0 mg, 1.92 mmol) and Fmoc-Ser(Bzl)-(O-CH₂-CH₂)₄-OH (877 mg, 1.5 mmol). The solution was stirred for 12 h at room temperature. The DCM was then evaporated and the oily residue redissolved in EtOAc (30 ml). The organic layer was washed with H₂O (1 × 20 ml), NaHCO₃ 5% (3 × 20 ml), H₂O (1 × 20 ml), KHSO₄ 5% (3 × 20 ml) and saturated NaCl (1 × 20 ml), dried over MgSO₄ and concentrated under reduced pressure. The pure product was obtained as a clear oil. Yield: 504 mg (38%); HPLC (System I): t_R 5.08 min; ESI-MS: m/z : 899.6 $[M+H]^+$, 916.6 $[(M+H_2O)+H]^+$, 843.6 $[(M-tBu)+H]^+$, 799.4 $[(M-Boc)+H]^+$, calculated monoisotopic mass for $C_{34}H_{41}N_3O_7$: 603.

[4-(*N*-benzyloxyamino)-2(*R*)-isobutylsuccinyl]-Phe-OMe (87)

4-(*N*-benzyloxyamino)-2(*R*)-isobutylsuccinic acid DCHA salt (680 mg, 1.48 mmol) was suspended in EtOAc (20 ml) in a separating funnel, an ice-cold solution of H₂SO₄ (2 M, 1.1 eq) was added and the mixture shaken until it became clear. The organic layer was separated, cold water (20 ml) was added to the aqueous layer and it was further extracted with EtOAc (2 × 20 ml). The combined organic layers were washed with H₂O (1 × 50 ml) and saturated NaCl (1 × 50 ml) and concentrated under reduced pressure. It was then redissolved in DMF (15 ml), EDC (298 mg, 1.92 mmol) and H-Phe-OMe·HCl (414 g, 1.92 mmol) were added, pH increased to 6 and the solution stirred for 12 h at room temperature. The DMF was then evaporated and the residue redissolved in CHCl₃

(50 ml). The organic layer was washed with H₂O (1 × 50 ml), NaHCO₃ 5% (3 × 50 ml), H₂O (1 × 50 ml), HCl 0.1 N (3 × 50 ml) and saturated NaCl (1 × 50 ml), dried over MgSO₄ and concentrated. The pure product was obtained by precipitation from CHCl₃/petroleum ether as a crystalline solid. Yield: 436 mg (64%); HPLC (System I): t_R 3.33 min; ESI-MS: m/z: 441.4 [M+H]⁺, 881.6 [2M+H]⁺, calculated monoisotopic mass for C₂₅H₃₂N₂O₇: 440.

[4-(*N*-benzyloxyamino)-2(*R*)-isobutylsuccinyl]-Phe-OH (**88**)

[4-(*N*-benzyloxyamino)-2(*R*)-isobutylsuccinyl]-Phe-OMe (350 mg, 0.77 mmol) was hydrolysed in MeOH (20 ml) using NaOH (1 M aqueous, 1.1 eq). The reaction was stirred for 1 h at room temperature and the progress of it checked via HPLC. Upon completion of the reaction, the MeOH was diluted with water, the pH of the solution decreased to 2 with HCl 0.5 N and the product extracted with EtOAc (3 × 20 ml). The organic layer was washed with H₂O (1 × 20 ml), citric acid 5% (3 × 20 ml) and saturated NaCl (1 × 20 ml), dried over MgSO₄. The pure product was obtained by precipitation from EtOAc/petroleum ether as a crystalline solid. Yield: 324 mg (98%); HPLC (System I): t_R 2.93 min; ESI-MS: m/z: 427.4 [M+H]⁺, 853.6 [2M+H]⁺, calculated monoisotopic mass for C₂₄H₃₀N₂O₅: 426.

Fmoc-Ser(Bzl)-(O-CH₂-CH₂)₄-O-Asp(OBzl)-H (**89**)

Fmoc-Ser(Bzl)-(O-CH₂-CH₂)₄-O-Asp(OBzl)-Boc (400 mg, 0.44 mmol) was dissolved in DCM/TFA 4:1 (20 ml), the reaction stirred for 30 minutes at room temperature and the progress of it checked via HPLC. After addition of toluene (10 ml), the solvent was evaporated to dryness under reduced pressure and further evaporated two times with toluene (2 × 10 ml). The crude product was triturated using a diethyl ether, filtered and washed with diethyl ether to give Fmoc-Ser(Bzl)-(O-CH₂-CH₂)₄-O-Asp(OBzl)-H as a clear oil. Yield: 348 mg

(98%); HPLC (System I): t_R 3.95 min; ESI-MS: m/z : 799.4 $[M+H]^+$, calculated monoisotopic mass for $C_{44}H_{50}N_2O_{12}$: 798.

Z-Leu-Phe-Pro-Gly-OH (90) (first method)

The synthesis was conducted by manual solid-phase methodology using Fmoc/HBTU/DMF chemistry. The peptide was synthesized as peptide acid on a TCP-Harz-Gly-Fmoc Resin (loading: 0.53 mmol/g) on a 1.3-mmol scale. Amino acids, HOBt and HBTU were used in a 2 eq excess respect to the scale of the synthesis in each cycle. The extent of coupling at each step was verified with the qualitative TNBS and/or Kaiser tests on a sample of a few resin beads. The products were then cleaved from the resin by TFA in the presence of 2.5% TIS and 2.5% water at room temperature in 2 h, the resin was filtered off and the crude peptides were precipitated with a cold solution of *ter*-butyl methyl ether/hexane 2:1 and lyophilised over night. The purity of the peptide exceeded 97% as determined by analytical RP-HPLC and used without further purification. Its structural integrity was confirmed by electrospray ionization mass spectrometry. Yield: 529 mg (55%); HPLC (System I): t_R 3.15 min; ESI-MS: m/z : 567.4 $[M+H]^+$, 1133.8 $[2M+H]^+$, calculated monoisotopic mass for $C_{30}H_{38}N_4O_7$: 566.

Fmoc-Phe-Pro-O t Bu

Fmoc-Phe-OH (4.6 g, 12.0 mmol), HOBt (1.9g, 14.4 mmol) and HBTU (5.5 g, 14.4 mmol) were dissolved in DCM (100 ml). H_2N -Pro-O t Bu HCl (3.0 g, 14.4 mmol) and DIEA (4.9 ml, 28.8 mmol) were then added and the solution stirred for 12 h at room temperature. The DCM was then evaporated and the residue redissolved in EtOAc (100 ml). The organic layer was washed with H_2O (1 \times 50 ml), $NaHCO_3$ 5% (3 \times 50 ml), H_2O (1 \times 50 ml), citric acid 5% (3 \times 50 ml) and saturated NaCl (1 \times 50 ml), dried over $MgSO_4$ and concentrated. The pure

product was obtained by precipitation from EtOAc/petroleum ether as a crystalline solid. Yield: 6.0 g (92%); HPLC (System I): t_R 4.82 min; ESI-MS: m/z : 541.2 $[M+H]^+$, calculated monoisotopic mass for $C_{33}H_{36}N_2O_5$: 540.

Fmoc-Phe-Pro-OH

Fmoc-Phe-Pro-O t Bu (6.0 g, 11.0 mmol) was dissolved in DCM/TFA 4:1 (50 ml), the reaction stirred for 30 minutes at room temperature and the progress of it checked via HPLC. After addition of toluene (10 ml), the solvent was evaporated to dryness under reduced pressure and further evaporated two times with toluene (2×10 ml). The crude product was triturated using a diethyl ether, filtered and washed with diethyl ether to give Fmoc-Phe-Pro-OH as a crystalline solid. Yield: 5.2 g (97%); HPLC (System I): t_R 3.76 min; ESI-MS: m/z : 485.4 $[M+H]^+$, 969.6 $[2M+H]^+$, calculated monoisotopic mass for $C_{29}H_{28}N_2O_5$: 484.

Z-Leu-Phe-Pro-Gly-OH (90) (second method)

The synthesis was conducted by manual solid-phase methodology using Fmoc/HBTU/DMF chemistry as reported in the previous synthesis of compound **90**, but using the building block Fmoc-Phe-Pro-OH. Yield: 894 mg (93%); HPLC (System I): t_R 3.18 min; ESI-MS: m/z : 567.6 $[M+H]^+$, 1133.8 $[2M+H]^+$, calculated monoisotopic mass for $C_{30}H_{38}N_4O_7$: 566.

Fmoc-Ser(Bzl)-(O-CH₂-CH₂)₄-O-Asp(OBzl)-Gly-Pro-Phe-Leu-Z (91)

Z-Leu-Phe-Pro-Gly-OH (**90**) (277 mg, 0.49 mmol) in DMF (10 ml) was preactivated during 10 minutes with HOAt (66.6 mg, 0.49 mmol), HATU (186.1 mg, 0.49 mmol) and DIEA (190 μ l, 1.11 mmol). Fmoc-Ser(Bzl)-(O-CH₂-CH₂)₄-O-Asp(OBzl)-H (**89**) (348 mg, 0.44 mmol) was added and the solution stirred for 12 h at room temperature. The DMF was then evaporated and the oily residue

redissolved in EtOAc (50 ml). The organic layer was washed with H₂O (1 × 50 ml), NaHCO₃ 5% (3 × 50 ml), H₂O (1 × 50 ml), KHSO₄ 5% (3 × 50 ml) and saturated NaCl (1 × 50 ml), dried over MgSO₄ and concentrated. The pure product was obtained as a clear oil. Yield: 498 mg (83%); HPLC (System I): t_R 5.15 min; ESI-MS: m/z: 1349.0 [M+H]⁺, 1366.0 [(M+H₂O)+H]⁺, calculated monoisotopic mass for C₇₄H₈₆N₆O₁₈: 1346.

H-Ser(Bzl)-(O-CH₂-CH₂)₄-O-Asp(OBzl)-Gly-Pro-Phe-Leu-Z (92)

Fmoc-Ser(Bzl)-(O-CH₂-CH₂)₄-O-Asp(OBzl)-Gly-Pro-Phe-Leu-Z (91) (498 mg, 0.37 mmol) was dissolved in DMF/DEA 9:1 (5 ml), the reaction stirred for 2 hours at room temperature and the progress of it checked via HPLC. The solvent was evaporated to dryness under reduced pressure and further evaporated two times with DMF (2 × 5 ml). The crude product was triturated using diethyl ether and washed with diethyl ether to give H-Ser(Bzl)-(O-CH₂-CH₂)₄-O-Asp(OBzl)-Gly-Pro-Phe-Leu-Z as a precipitate. Yield: 403 mg (97%); HPLC (System I): t_R 3.77 min; ESI-MS: m/z: 1125.8 [M+H]⁺, calculated monoisotopic mass for C₅₉H₇₆N₆O₁₆: 1124.

[4-(N-benzyloxyamino)-2(R)-isobutylsuccinyl]-Phe-Ser(Bzl)-(O-CH₂-CH₂)₄-O-Asp(OBzl)-Gly-Pro-Phe-Leu-Z (93)

[4-(N-benzyloxyamino)-2(R)-isobutylsuccinyl]-Phe-OH (88) (132 mg, 0.31 mmol) in DMF (10 ml) was preactivated during 10 minutes with HOAt (46.3 mg, 0.34 mmol), HATU (129.3 mg, 0.34 mmol) and DIEA (116 µl, 0.68 mmol). H-Ser(Bzl)-(O-CH₂-CH₂)₄-O-Asp(OBzl)-Gly-Pro-Phe-Leu-Z (92) (403 mg, 0.36 mmol) was added and the solution stirred for 12 h at room temperature. The DMF was then evaporated and the oily residue redissolved in EtOAc (50 ml). The organic layer was washed with H₂O (1 × 50 ml), NaHCO₃ 5% (3 × 50 ml), H₂O

(1 × 50 ml), KHSO₄ 5% (3 × 50 ml) and saturated NaCl (1 × 50 ml), dried over MgSO₄ and concentrated. The pure product was obtained as a yellow oil. Yield: 342 mg (72%); HPLC (System I): t_R 4.64 min; ESI-MS: m/z: 1535.0 [M+H]⁺, 1552.0 [(M+H₂O)+H]⁺, 767.4 [(M+2H)/2]⁺, calculated monoisotopic mass for C₈₃H₁₀₄N₈O₂₀: 1532.

[4-(N-hydroxyamino)-2(R)-isobutylsuccinyl]-Phe-Ser-(O-CH₂-CH₂)₄-O-Asp-Gly-Pro-Phe-Leu-H (94)

[4-(N-benzyloxyamino)-2(R)-isobutylsuccinyl]-Phe-Ser(Bzl)-(O-CH₂-CH₂)₄-O-Asp(OBzl)-Gly-Pro-Phe-Leu-Z (93) (130 mg, 84.8 μm) was hydrogenated in methanol (100 ml) with 10% Pd/C under hydrogen atmosphere at room temperature. The catalyst was removed by filtration and the filtrate was evaporated. The pure product was obtained from EtOAc/(*ter*-butyl methyl ether/hexane 2:1) as an orange crystal. Yield: 57.3 mg (60%); HPLC (System I): t_R 2.28 min; ESI-MS: m/z: 1129.8 [M+H]⁺, 565.4 [(M+2H)/2]⁺, calculated monoisotopic mass for C₅₄H₈₀N₈O₁₈: 1128.

6.2.5.3 Route B: PEG₆

Fmoc-Ser(Bzl)-(O-CH₂-CH₂)₆-OH

To a solution of Fmoc-Ser(Bzl)-OH (2.95 g, 7.08 mmol) in DCM (50 ml) were added DMAP (0.43 g, 3.54 mmol), EDC (1.43 g, 9.21 mmol) and H-(O-CH₂-CH₂)₆-OH (10.0 g, 35.43 mmol). The solution was stirred for 12 h at room temperature. The DCM was then evaporated and the oily residue redissolved in EtOAc (50 ml). The organic layer was washed with H₂O (5 × 50 ml), NaHCO₃ 5% (3 × 50 ml), H₂O (5 × 50 ml), KHSO₄ 5% (3 × 50 ml) and saturated NaCl (1 × 50 ml), dried over MgSO₄ and concentrated under reduced pressure. The product was obtained as an oil and used without further purification. Yield: 2.73 g (56%);

HPLC (System I): t_R 4.12 min; ESI-MS: m/z : 682.8 $[M+H]^+$, 699.8 $[(M+H_2O)+H]^+$, calculated monoisotopic mass for $C_{37}H_{47}NO_{11}$: 681.

Fmoc-Ser(Bzl)-(O-CH₂-CH₂)₆-O-Asp(OBzl)-Boc

To a solution of Boc-Asp(OBzl)-OH (1.7 g, 5.21 mmol) in DMF (50 ml) were added DMAP (0.24 g, 2.00 mmol), EDC (1.00 g, 6.41 mmol) and Fmoc-Ser(Bzl)-(O-CH₂-CH₂)₆-OH (2.73 g, 4.01 mmol). The solution was stirred for 12 h at room temperature. The DMF was then evaporated and the oily residue redissolved in EtOAc (100 ml). The organic layer was washed with H₂O (1 × 50 ml), NaHCO₃ 5% (3 × 50 ml), H₂O (1 × 50 ml), KHSO₄ 5% (3 × 50 ml) and saturated NaCl (1 × 50 ml), dried over MgSO₄ and concentrated under reduced pressure. The pure product was obtained as an oil. Yield: 1.7 mg (42%); HPLC (System I): t_R 5.34 min; ESI-MS: m/z : 988.0 $[M+H]^+$, 1005.0 $[(M+H_2O)+H]^+$, 932.0 $[(M-tBu)+H]^+$, 887.8 $[(M-Boc)+H]^+$, calculated monoisotopic mass for $C_{53}H_{66}N_2O_{16}$: 986.

Fmoc-Ser(Bzl)-(O-CH₂-CH₂)₆-O-Asp(OBzl)-H

Fmoc-Ser(Bzl)-(O-CH₂-CH₂)₆-O-Asp(OBzl)-Boc (600 mg, 0.61 mmol) was dissolved in DCM/TFA 4:1 (50 ml), the reaction stirred for 30 minutes at room temperature and the progress of it checked via HPLC. After addition of toluene (10 ml), the solvent was evaporated to dryness under reduced pressure and further evaporated two times with toluene (2 × 10 ml). The crude product was triturated using a diethyl ether, filtered and washed with diethyl ether to give Fmoc-Ser(Bzl)-(O-CH₂-CH₂)₆-O-Asp(OBzl)-H as a clear oil. Yield: 512 mg (95%); HPLC (System I): t_R 4.01 min; ESI-MS: m/z : 887.6 $[M+H]^+$, calculated monoisotopic mass for $C_{48}H_{58}N_2O_{14}$: 887.

Fmoc-Ser(Bzl)-(O-CH₂-CH₂)₆-O-Asp(OBzl)-Gly-Pro-Phe-Leu-Z

Z-Leu-Phe-Pro-Gly-OH (260 mg, 0.46 mmol) in DMF (10 ml) was preactivated during 10 minutes with HOAt (68.8 mg, 0.51 mmol), HATU (192.2 mg, 0.51 mmol) and DIEA (173 μ l, 1.01 mmol). Fmoc-Ser(Bzl)-(O-CH₂-CH₂)₆-O-Asp(OBzl)-H (530 mg, 0.60 mmol) was added and the solution stirred for 12 h at room temperature. The DMF was then evaporated and the oily residue redissolved in EtOAc (50 ml). The organic layer was washed with H₂O (1 \times 50 ml), NaHCO₃ 5% (3 \times 50 ml), H₂O (1 \times 50 ml), KHSO₄ 5% (3 \times 50 ml) and saturated NaCl (1 \times 50 ml), dried over MgSO₄ and concentrated. The pure product was obtained as a clear oil. Yield: 568 mg (86%); HPLC (System I): t_R 5.20 min; ESI-MS: m/z: 1436.4 [M+H]⁺, 1453.8 [(M+H₂O)+H]⁺, calculated monoisotopic mass for C₇₈H₉₄N₆O₂₀: 1435.

H-Ser(Bzl)-(O-CH₂-CH₂)₆-O-Asp(OBzl)-Gly-Pro-Phe-Leu-Z

Fmoc-Ser(Bzl)-(O-CH₂-CH₂)₆-O-Asp(OBzl)-Gly-Pro-Phe-Leu-Z (550 mg, 0.38 mmol) was dissolved in DMF/DEA 9:1 (10 ml), the reaction stirred for 2 hours at room temperature and the progress of it checked via HPLC. The solvent was evaporated to dryness under reduced pressure and further evaporated two times with DMF (2 \times 5 ml). The crude product was triturated using diethyl ether and washed with diethyl ether to give H-Ser(Bzl)-(O-CH₂-CH₂)₆-O-Asp(OBzl)-Gly-Pro-Phe-Leu-Z as a precipitate. Yield: 460 mg (99%); HPLC (System I): t_R 3.82 min; ESI-MS: m/z: 1214.0 [M+H]⁺, 607.8 [(M+2H)/2]⁺, calculated monoisotopic mass for C₆₃H₈₄N₆O₁₈: 1213.

[4-(*N*-benzyloxyamino)-2(*R*)-isobutylsuccinyl]-Phe-Ser(Bzl)-(O-CH₂-CH₂)₆-O-Asp(OBzl)-Gly-Pro-Phe-Leu-Z

[4-(*N*-benzyloxyamino)-2(*R*)-isobutylsuccinyl]-Phe-OH (196 mg, 0.46 mmol) in DMF (10 ml) was preactivated during 10 minutes with HOAt (62.6 mg, 0.46 mmol), HATU (174.9 mg, 0.46 mmol) and DIEA (157 μ l, 0.92 mmol). H-Ser(Bzl)-(O-CH₂-CH₂)₆-O-Asp(OBzl)-Gly-Pro-Phe-Leu-Z (460 mg, 0.38 mmol) was added and the solution stirred for 12 h at room temperature. The DMF was then evaporated and the oily residue redissolved in EtOAc (50 ml). The organic layer was washed with H₂O (1 \times 50 ml), NaHCO₃ 5% (3 \times 50 ml), H₂O (1 \times 50 ml), KHSO₄ 5% (3 \times 50 ml) and saturated NaCl (1 \times 50 ml), dried over MgSO₄ and concentrated. The pure product was obtained as a yellow oil. Yield: 509 mg (65%); HPLC (System I): t_R 4.89 min; ESI-MS: m/z : 1623.0 [M+H]⁺, 812.0 [(M+2H)/2]⁺, calculated monoisotopic mass for C₈₇H₁₁₂N₈O₂₂: 1622.

[4-(*N*-hydroxyamino)-2(*R*)-isobutylsuccinyl]-Phe-Ser(Bzl)-(O-CH₂-CH₂)₆-O-Asp-Gly-Pro-Phe-Leu-H (95)

[4-(*N*-benzyloxyamino)-2(*R*)-isobutylsuccinyl]-Phe-Ser(Bzl)-(O-CH₂-CH₂)₆-O-Asp(OBzl)-Gly-Pro-Phe-Leu-Z (100 mg, 61.7 μ m) was hydrogenated in methanol (100 ml) with 10% Pd/C under hydrogen atmosphere at room temperature. The catalyst was removed by filtration and the filtrate was evaporated. The pure product was obtained from EtOAc/(*ter*-butyl methyl ether/hexane 2:1) as a pale yellow crystal. Yield: 57.3 mg (71%); HPLC (System I): t_R 2.83 min; ESI-MS: m/z : 1308.2 [M+H]⁺, 654.8 [(M+2H)/2]⁺, calculated monoisotopic mass for C₆₅H₉₄N₈O₂₀: 1307.

6.2.5.4 Route B: PEG₈

Fmoc-Ser(Bzl)-(O-CH₂-CH₂)₈-OH

To a solution of Fmoc-Ser(Bzl)-OH (2.25 g, 5.4 mmol) in DCM (50 ml) were added DMAP (0.33 g, 2.7 mmol), EDC (1.09 g, 7.02 mmol) and H-(O-CH₂-CH₂)₈-OH (10.0 g, 27.0 mmol). The solution was stirred for 12 h at room temperature. The DCM was then evaporated and the oily residue redissolved in EtOAc (50 ml). The organic layer was washed with H₂O (1 × 50 ml), NaHCO₃ 5% (3 × 50 ml), H₂O (1 × 50 ml), KHSO₄ 5% (3 × 50 ml) and saturated NaCl (1 × 50 ml), dried over MgSO₄ and concentrated under reduced pressure. The product was obtained as an oil and used without further purification. Yield: 2.06 g (49%); HPLC (System I): t_R 4.14 min; ESI-MS: m/z: 770.8 [M+H]⁺, 788.0 [(M+H₂O)+H]⁺, calculated monoisotopic mass for C₄₁H₅₅NO₁₃: 769.

Fmoc-Ser(Bzl)-(O-CH₂-CH₂)₈-O-Asp(OBzl)-Boc

To a solution of Boc-Asp(OBzl)-OH (1.12 g, 3.47 mmol) in DMF (50 ml) were added DMAP (0.16 g, 1.33 mmol), EDC (0.66 g, 4.27 mmol) and Fmoc-Ser(Bzl)-(O-CH₂-CH₂)₈-OH (2.06 g, 2.67 mmol). The solution was stirred for 12 h at room temperature. The DMF was then evaporated and the oily residue redissolved in EtOAc (100 ml). The organic layer was washed with H₂O (1 × 50 ml), NaHCO₃ 5% (3 × 50 ml), H₂O (1 × 50 ml), KHSO₄ 5% (3 × 50 ml) and saturated NaCl (1 × 50 ml), dried over MgSO₄ and concentrated under reduced pressure. The pure product was obtained as an oil. Yield: 1.23 mg (43%); HPLC (System I): t_R 5.236 min; ESI-MS: m/z: 1075.8 [M+H]⁺, 1093.0 [(M+H₂O)+H]⁺, 1019.8 [(M-*t*Bu)+H]⁺, 976.0 [(M-Boc)+H]⁺, calculated monoisotopic mass for C₅₇H₇₄N₂O₁₆: 1074.

Fmoc-Ser(Bzl)-(O-CH₂-CH₂)₈-O-Asp(OBzl)-H

Fmoc-Ser(Bzl)-(O-CH₂-CH₂)₈-O-Asp(OBzl)-Boc (600 mg, 0.56 mmol) was dissolved in DCM/TFA 4:1 (20 ml), the reaction stirred for 30 minutes at room temperature and the progress of it checked via HPLC. After addition of toluene (10 ml), the solvent was evaporated to dryness under reduced pressure and further evaporated two times with toluene (2 × 10 ml). The crude product was triturated using diethyl ether, filtered and washed with diethyl ether to give Fmoc-Ser(Bzl)-(O-CH₂-CH₂)₈-O-Asp(OBzl)-H as a clear oil. Yield: 533 mg (98%); HPLC (System I): t_R 4.13 min; ESI-MS: m/z: 976.2 [M+H]⁺, calculated monoisotopic mass for C₅₂H₆₆N₂O₁₆: 975.

Fmoc-Ser(Bzl)-(O-CH₂-CH₂)₈-O-Asp(OBzl)-Gly-Pro-Phe-Leu-Z

Z-Leu-Phe-Pro-Gly-OH (241 mg, 0.43 mmol) in DMF (10 ml) was preactivated during 10 minutes with HOAt (63.8 mg, 0.47 mmol), HATU (178.2 mg, 0.47 mmol) and DIEA (160 μl, 0.94 mmol). Fmoc-Ser(Bzl)-(O-CH₂-CH₂)₈-O-Asp(OBzl)-H (533 mg, 0.54 mmol) was added and the solution stirred for 12 h at room temperature. The DMF was then evaporated and the oily residue redissolved in EtOAc (50 ml). The organic layer was washed with H₂O (1 × 50 ml), NaHCO₃ 5% (3 × 50 ml), H₂O (1 × 50 ml), KHSO₄ 5% (3 × 50 ml) and saturated NaCl (1 × 50 ml), dried over MgSO₄ and concentrated. The pure product was obtained as a clear oil. Yield: 583 mg (89%); HPLC (System I): t_R 5.22 min; ESI-MS: m/z: 1523.8 [M+H]⁺, 1541.0 [(M+H₂O)+H]⁺, calculated monoisotopic mass for C₈₂H₁₀₂N₆O₂₂: 1523.

H-Ser(Bzl)-(O-CH₂-CH₂)₈-O-Asp(OBzl)-Gly-Pro-Phe-Leu-Z

Fmoc-Ser(Bzl)-(O-CH₂-CH₂)₈-O-Asp(OBzl)-Gly-Pro-Phe-Leu-Z (583 mg, 0.38 mmol) was dissolved in DMF/DEA 9:1 (20 ml), the reaction stirred for 2

hours at room temperature and the progress of it checked via HPLC. The solvent was evaporated to dryness under reduced pressure and further evaporated two times with DMF (2×5 ml). The crude product was triturated using diethyl ether and washed with diethyl ether to give H-Ser(Bzl)-(O-CH₂-CH₂)₈-O-Asp(OBzl)-Gly-Pro-Phe-Leu-Z as a precipitate. Yield: 483 mg (97%); HPLC (System I): t_R 3.85 min; ESI-MS: m/z : 1302.2 [M+H]⁺, 651.8 [(M+2H)/2]⁺, calculated monoisotopic mass for C₆₇H₉₂N₆O₂₀: 1301.

[4-(N-benzyloxyamino)-2(R)-isobutylsuccinyl]-Phe-Ser(Bzl)-(O-CH₂-CH₂)₈-O-Asp(OBzl)-Gly-Pro-Phe-Leu-Z

[4-(N-benzyloxyamino)-2(R)-isobutylsuccinyl]-Phe-OH (187 mg, 0.44 mmol) in DMF (10 ml) was preactivated during 10 minutes with HOAt (59.9 mg, 0.44 mmol), HATU (167.3 mg, 0.44 mmol) and DIEA (151 μ l, 0.88 mmol). H-Ser(Bzl)-(O-CH₂-CH₂)₈-O-Asp(OBzl)-Gly-Pro-Phe-Leu-Z (483 mg, 0.37 mmol) was added and the solution stirred for 12 h at room temperature. The DMF was then evaporated and the oily residue redissolved in EtOAc (50 ml). The organic layer was washed with H₂O (1 \times 50 ml), NaHCO₃ 5% (3 \times 50 ml), H₂O (1 \times 50 ml), KHSO₄ 5% (3 \times 50 ml) and saturated NaCl (1 \times 50 ml), dried over MgSO₄ and concentrated. The pure product was obtained as a yellow oil. Yield: 424 mg (67%); HPLC (System I): t_R 4.82 min; ESI-MS: m/z : 1710.8 [M+H]⁺, 1727.0 [(M+H₂O)+H]⁺, 856.0 [(M+2H)/2]⁺, calculated monoisotopic mass for C₉₁H₁₂₀N₈O₂₄: 1710.

[4-(N-hydroxyamino)-2(R)-isobutylsuccinyl]-Phe-Ser(Bzl)-(O-CH₂-CH₂)₈-O-Asp-Gly-Pro-Phe-Leu-H (96)

[4-(N-benzyloxyamino)-2(R)-isobutylsuccinyl]-Phe-Ser(Bzl)-(O-CH₂-CH₂)₈-O-Asp(OBzl)-Gly-Pro-Phe-Leu-Z (100 mg, 58.5 μ m) was hydrogenated in methanol (100 ml) with 10% Pd/C under hydrogen atmosphere at room

temperature. The catalyst was removed by filtration and the filtrate was evaporated. The product was obtained from EtOAc/(*ter*-butyl methyl ether/hexane 2:1) as an orange crystal. Yield: 55.5 mg (68%); HPLC (System I): t_R 2.90 min; ESI-MS: m/z : 1396.2 $[M+H]^+$, 698.8 $[(M+2H)/2]^+$, calculated monoisotopic mass for $C_{69}H_{102}N_8O_{22}$: 1128.

7. References

- (1) Seife, C. *Science* 1997, 277, 1602-1603.
- (2) Menon, A. S.; Goldberg, A. L. *J. Biol. Chem.* 1987, 262, 14929-14934.
- (3) Barrett, A. J.; Rawlings, N. D. *Biological Chemistry* 2001, 382, 727-733.
- (4) Barrett, A. J.; Rawlings, N. D.; O'Brien, E. A. *Journal of Structural Biology* 2001, 134, 95-102.
- (5) Rawlings, N. D.; Morton, F. R.; Barrett, A. J. *Nucl. Acids Res.* 2006, 34, D270-272.
- (6) Rawlings, N. D.; Barrett, A. J. *Biochemical Journal* 1993, 290, 205-218.
- (7) Schechter, I.; Berger, A. *Biochemical and Biophysical Research Communications* 1967, 27, 157-162.
- (8) Hill, J.; Phylip, L. H. *FEBS Letters* 1997, 409, 357-360.
- (9) Saftig, P.; Hetman, M.; Schmahl, W.; Weber, K.; Heine, L.; Mossmann, H.; Koster, A.; Hess, B.; Evers, M.; Vonfigura, K.; Peters, C. *Embo Journal* 1995, 14, 3599-3608.
- (10) Kageyama, T. *European Journal of Biochemistry* 1998, 253, 804-809.
- (11) Chetana Rao-Naik, K. G. B. B. S. R. J. H. T. B. J. K. B. M. D. *Proteins: Structure, Function, and Genetics* 1995, 22, 168-181.
- (12) Sielecki, A. R.; Fujinaga, M.; Read, R. J.; James, M. N. G. *Journal of Molecular Biology* 1991, 219, 671-692.
- (13) Tang, J. *Molecular and Cellular Biochemistry* 1979, 26, 93-109.
- (14) Miller, M.; Jaskolski, M.; Rao, J. K. M.; Leis, J.; Wlodawer, A. *Nature* 1989, 337, 576-579.
- (15) Holm, I.; Ollo, R.; Panthier, J. J.; Rougeon, F. *Embo Journal* 1984, 3, 557-562.
- (16) Veerapandian, B.; Cooper, J. B.; Sali, A.; Blundell, T. L.; Rosati, R. L.; Dominy, B. W.; Damon Db Hoover, D. J. *Protein Sci* 1992, 1, 322-328.
- (17) Northrop, D. B. *Acc. Chem. Res.* 2001, 34, 790-797.
- (18) Dunn, B. M. *Chem. Rev.* 2002, 102, 4431-4458.
- (19) Fitzgerald, P. M.; McKeever, B. M.; VanMiddlesworth, J. F.; Springer, J. P.; Heimbach, J. C.; Leu, C. T.; Herber, W. K.; Dixon, R. A.; Darke, P. L. *J. Biol. Chem.* 1990, 265, 14209-14219.
- (20) James, M. N. G.; Siliecki, A. *Biological Macromolecules and Assemblies: Active Sites of Enzymes*; John Wiley and Sons: New York, 1987.
- (21) Umezawa, H.; Aoyagi, T.; Morishim.H; Matsuzak.M; Hamada, M.; Takeuchi, T. *Journal of Antibiotics* 1970, 23, 259.
- (22) Aoyagi, T.; Kunimoto, S.; Morishim.H; Takeuchi, T.; Umezawa, H. *Journal of Antibiotics* 1971, 24, 687.
- (23) Kunimoto, S.; Aoyagi, T.; Takeuchi, T.; Umezawa, H.; Morishim.H *Journal of Antibiotics* 1972, 25, 251.

7. References

- (24) Kunimoto, S.; Aoyagi, T.; Nishizawa, R.; Komai, T.; Takeuchi, T.; Umezawa, H. *Journal of Antibiotics* 1974, 27, 413-424.
- (25) Workman, R. J.; Burkitt, D. W. *Archives of Biochemistry and Biophysics* 1979, 194, 157-164.
- (26) Knight, C. G.; Barrett, A. J. *Biochemical Journal* 1976, 155, 117-125.
- (27) Barrett, A. J.; Dingle, J. T. *Biochemical Journal* 1972, 127, 439.
- (28) Aoyagi, T.; Morishima, H.; Nishizawa, R.; Kunimoto, S.; Takeuchi, T.; Umezawa, H.; Ikezawa, H. *Journal of Antibiotics* 1972, 25, 689-694.
- (29) Rich, D. H.; Sun, E. T. O. *Biochemical Pharmacology* 1980, 29, 2205-2212.
- (30) Rich, D. H.; Sun, E. T. O.; Ulm, E. *Journal of Medicinal Chemistry* 1980, 23, 27-33.
- (31) Rich, D. H.; Salituro, F. G. *Journal of Medicinal Chemistry* 1983, 26, 904-910.
- (32) Boger, J.; Lohr, N. S.; Ulm, E. H.; Poe, M.; Blaine, E. H.; Fanelli, G. M.; Lin, T.-Y.; Payne, L. S.; Schorn, T. W.; LaMont, B. I.; Vassil, T. C.; Stabilito, I. I.; Veber, D. F.; Rich, D. H.; Bopari, A. S. *Nature* 1983, 303, 81-84.
- (33) Marshall, G. R. *Federation Proceedings* 1976, 35, 2494-2501.
- (34) Marciniszyn, J.; Hartsuck, J. A.; Tang, J. *Journal of Biological Chemistry* 1976, 251, 7088-7094.
- (35) Rich, D. H. *Journal of Medicinal Chemistry* 1985, 28, 263-273.
- (36) Pauling, L. *Chemical and engineering News* 1946, 24, 1375-1377.
- (37) Lienhard, G. E. *Science* 1973, 180, 149-154.
- (38) Wolfenden, R. *Annual Review of Biophysics and Bioengineering* 1976, 5, 271-306.
- (39) Powers, J. C.; Harley, A. D.; Myers, D. V. *Subsite specificity of porcine pepsin*; Tang J. ed.; Plenum: New York, 1977.
- (40) Bott, R.; Subramanian, E.; Davies, D. R. *Biochemistry* 1982, 21, 6956-6962.
- (41) Boger, J. *Renin inhibitors. Design of angiotensinogen transition-state analogs containing statine.*; Hruby, V.J. and Rich D.H. ed. Rockford, IL, 1983.
- (42) Leung, D.; Abbenante, G.; Fairlie, D. P. *Journal of Medicinal Chemistry* 2000, 43, 305-341.
- (43) Holladay, M. W.; Rich, D. H. *Tetrahedron Letters* 1983, 24, 4401-4404.
- (44) Greenlee, W. J. *Medicinal Research Reviews* 1990, 10, 173-236.
- (45) Gordon, E. M.; Godfrey, J. D.; Pluscec, J.; Vonlangen, D.; Natarajan, S. *Biochemical and Biophysical Research Communications* 1985, 126, 419-426.
- (46) Rich, D. H.; Green, J.; Toth, M. V.; Marshall, G. R.; Kent, S. B. H. *Journal of Medicinal Chemistry* 1990, 33, 1285-1288.
- (47) Lebon, F.; Ledecq, M. *Current Medicinal Chemistry* 2000, 7, 455-477.
- (48) Lien, E. J.; Gao, H.; Lien, L. L. *Prog. Drug Research* 1994, 43, 43-86.
- (49) Geldmacher, D. S.; Whitehouse, P. J. *N Engl J Med* 1996, 335, 330-336.
- (50) Kokmen, E.; Beard, C. M.; Offord, K. P.; Kurland, L. T. *Neurology* 1989, 39, 773-776.
- (51) Gautrin, D.; Froda, S.; Tetreault, H.; Gauvreau, D. *CAN. J. PSYCHIATRY* 1990, 35, 162-165.
- (52) Bachman, D. L.; Wolf, P. A.; Linn, R.; Knoefel, J. E.; Cobb, J.; Belanger, A.; D'Agostino, R. B.; White, L. R. *Neurology* 1992, 42, 115-119.
- (53) Alloul, K.; Sauriol, L.; Kennedy, W.; Laurier, C.; Tessier, G.; Novosel, S.; Contandriopoulos, A. *Archives of Gerontology and Geriatrics* 1998, 27, 189-221.

-
- (54) Selkoe, D. J. *Physiol. Rev.* 2001, 81, 741-766.
- (55) Hardy, J.; Selkoe, D. J. *Science* 2002, 297, 353-356.
- (56) Hock, C.; Konietzko, U.; Streffer, J. R.; Tracy, J.; Signorell, A.; Muller-Tillmanns, B.; Lemke, U.; Henke, K.; Moritz, E.; Garcia, E. *Neuron* 2003, 38, 547-554.
- (57) Vassar, R. *Journal of Molecular Neuroscience* 2001, 17, 157-170.
- (58) Seubert, P.; Oltersdorf, T.; Lee, M. G.; Barbour, R.; Blomquist, C.; Davis, D. L.; Bryant, K.; Fritz, L. C.; Galasko, D.; Thal, L. J.; Lieberburg, I.; Schenk, D. B. *Nature* 1993, 361, 260-263.
- (59) Haass, C. *Embo Journal* 2004, 23, 483-488.
- (60) Esch, F. S.; Keim, P. S.; Beattie, E. C.; Blacher, R. W.; Culwell, A. R.; Oltersdorf, T.; McClure, D.; Ward, P. J. *Science* 1990, 248, 1122-1124.
- (61) Sisodia, S. S.; Koo, E. H.; Beyreuther, K.; Unterbeck, A.; Price, D. L. *Science* 1990, 248, 492-495.
- (62) Haass, C.; Schlossmacher, M. G.; Hung, A. Y.; Vigo-Pelfrey, C.; Mellon, A.; Ostaszewski, B. L.; Lieberburg, I.; Koo, E. H.; Schenk, D.; Teplow, D. B.; Selkoe, D. J. *Nature* 1992, 359, 322-325.
- (63) Haass, C.; Hung, A. Y.; Schlossmacher, M. G.; Teplow, D. B.; Selkoe, D. J. *J. Biol. Chem.* 1993, 268, 3021-3024.
- (64) Citron, M.; Oltersdorf, T.; Haass, C.; McConlogue, L.; Hung, A. Y.; Seubert, P.; Vigo-Pelfrey, C.; Lieberburg, I.; Selkoe, D. J. *Nature* 1992, 360, 672-674.
- (65) Hussain, I.; Powell, D.; Howlett, D. R.; Tew, D. G.; Meek, T. D.; Chapman, C.; Gloger, I. S.; Murphy, K. E.; Southan, C. D.; Ryan, D. M. *Molecular and Cellular Neuroscience* 1999, 14, 419-427.
- (66) Sinha, S.; Anderson, J. P.; Barbour, R.; Basi, G. S.; Caccavello, R.; Davis, D.; Doan, M.; Dovey, H. F.; Frigon, N.; Hong, J.; Jacobson-Croak, K.; Jewett, N.; Keim, P.; Knops, J.; Lieberburg, I.; Power, M.; Tan, H.; Tatsuno, G.; Tung, J.; Schenk, D.; Seubert, P.; Suomensaaari, S. M.; Wang, S.; Walker, D.; Zhao, J.; McConlogue, L.; John, V. *Nature* 1999, 402, 537-540.
- (67) Vassar, R.; Bennett, B. D.; Babu-Khan, S.; Kahn, S.; Mendiaz, E. A.; Denis, P.; Teplow, D. B.; Ross, S.; Amarante, P.; Loeloff, R.; Luo, Y.; Fisher, S.; Fuller, J.; Edenson, S.; Lile, J.; Jarosinski, M. A.; Biere, A. L.; Curran, E.; Burgess, T.; Louis, J.-C.; Collins, F.; Treanor, J.; Rogers, G.; Citron, M. *Science* 1999, 286, 735-741.
- (68) Yan, R.; Bienkowski, M. J.; Shuck, M. E.; Miao, H.; Tory, M. C.; Pauley, A. M.; Brashler, J. R.; Stratman, N. C.; Mathews, W. R.; Buhl, A. E.; Carter, D. B.; Tomasselli, A. G.; Parodi, L. A.; Heinrikson, R. L.; Gurney, M. E. *Nature* 1999, 402, 533-537.
- (69) Hong, L.; Koelsch, G.; Lin, X.; Wu, S.; Terzyan, S.; Ghosh, A. K.; Zhang, X. C.; Tang, J. *Science* 2000, 290, 150-153.
- (70) Haniu, M.; Denis, P.; Young, Y.; Mendiaz, E. A.; Fuller, J.; Hui, J. O.; Bennett, B. D.; Kahn, S.; Ross, S.; Burgess, T.; Katta, V.; Rogers, G.; Vassar, R.; Citron, M. *J. Biol. Chem.* 2000, 275, 21099-21106.
- (71) Bodendorf, U.; Fischer, F.; Bodian, D.; Multhaup, G.; Paganetti, P. *J. Biol. Chem.* 2001, 276, 12019-12023.
- (72) Tanahashi, H.; Tabira, T. *Neuroscience Letters* 2001, 307, 9-12.
- (73) Cai, H.; Wang, Y.; McCarthy, D.; Wen, H.; Borchelt, D. R.; Price, D. L.; Wong, P. C. *Nat Neurosci* 2001, 4, 233-234.

7. References

- (74) Roberds, S. L.; Anderson, J.; Basi, G.; Bienkowski, M. J.; Branstetter, D. G.; Chen, K. S.; Freedman, S.; Frigon, N. L.; Games, D.; Hu, K.; Johnson-Wood, K.; Kappenman, K. E.; Kawabe, T. T.; Kola, I.; Kuehn, R.; Lee, M.; Liu, W.; Motter, R.; Nichols, N. F.; Power, M.; Robertson, D. W.; Schenk, D.; Schoor, M.; Shopp, G. M.; Shuck, M. E.; Sinha, S.; Svensson, K. A.; Tatsuno, G.; Tintrup, H.; Wijsman, J.; Wright, S.; McConlogue, L. *Hum. Mol. Genet.* 2001, *10*, 1317-1324.
- (75) Strooper, B. D.; Annaert, W. *Nat Cell Biol* 2001, *3*, E221-E225.
- (76) Petit, A.; Bihel, F.; da Costa, C. A.; Pourquie, O.; Checler, F.; Kraus, J.-L. *Nat Cell Biol* 2001, *3*, 507-511.
- (77) Farzan, M.; Schnitzler, C. E.; Vasilieva, N.; Leung, D.; Choe, H. *PNAS* 2000, *97*, 9712-9717.
- (78) Hong, L.; Turner, R. T.; Koelsch, G.; Shin, D.; Ghosh, A. K.; Tang, J. *Biochemistry* 2002, *41*, 10963-10967.
- (79) Davies, D. R. *Annual Review of Biophysics and Biophysical Chemistry* 1990, *19*, 189-215.
- (80) Hong, L.; Tang, J. *Biochemistry* 2004, *43*, 4689-4695.
- (81) Yan, R.; Han, P.; Miao, H.; Greengard, P.; Xu, H. *J. Biol. Chem.* 2001, *276*, 36788-36796.
- (82) Ghosh, A. K.; Shin, D.; Downs, B.; Koelsch, G.; Lin, X.; Ermolieff, J.; Tang, J. *J. Am. Chem. Soc.* 2000, *122*, 3522-3523.
- (83) Gruninger-Leitch, F.; Schlatter, D.; Kung, E.; Nelbock, P.; Dobeli, H. *J. Biol. Chem.* 2002, *277*, 4687-4693.
- (84) Marcinkeviciene, J.; Luo, Y.; Graciani, N. R.; Combs, A. P.; Copeland, R. A. *J. Biol. Chem.* 2001, *276*, 23790-23794.
- (85) Rich, D. H. *Journal of Medicinal Chemistry* 1985, *28*, 263-273.
- (86) Turner, R. T.; Koelsch, G.; Hong, L.; Castenheira, P.; Ghosh, A.; Tang, J. *Biochemistry* 2001, *40*, 10001-10006.
- (87) Christie, G.; Hussain, I.; Powell, D. J. In *PCT Int. Appl.* 2001, p 34 pp.
- (88) Tung, J. S.; Davis, D. L.; Anderson, J. P.; Walker, D. E.; Mamo, S.; Jewett, N.; Hom, R. K.; Sinha, S.; Thorsett, E. D.; John, V. *J. Med. Chem.* 2002, *45*, 259-262.
- (89) Maillaird, M.; Hom, C.; Gailunas, A.; Jagodzinska, B.; Fang, L. Y.; John, V.; Freskos, J. N.; Pulley, S. R.; Beck, J. P.; Tenbrink, R. E. E. P., Inc., USA; Pharmacia & Upjohn Company) 2002.
- (90) Beck, J. P.; Gailunas, A.; Hom, R.; Jagodzinska, B.; John, V.; Maillaird, M. In *PCT Int. Appl.* 2002, p 286 pp.
- (91) Miyamoto, M.; Matsui, J.; Fukumoto, H.; Tarui, N. T. C. I., Ltd., Japan) In *PCT Int. Appl.* 2001, p 86 pp.
- (92) Ramakrishna, N. V. S.; Kumar, E. K. S. V.; Kulkarni, A. S.; Jain, A. K.; Bhat, R. G.; Parikh, S.; Quadros, A.; Deuskar, N.; Kalakoti, B. S. *Indian Journal of Chemistry, Section B* 2001, *40*, 539-540.
- (93) Gross, J.; Lapiere, C. M. *Proceedings of the National Academy of Sciences of the United States of America* 1962, *48*, 1014.
- (94) Stocker, W.; Grams, F.; Baumann, U.; Reinemer, P.; Gomis-Ruth, F. X.; McKay, D. B.; Bode, W. *Protein Sci* 1995, *4*, 823-840.
- (95) Sternlicht, M. D.; Bissell, M. J.; Werb, Z. *Oncogene* 2000, *19*, 1102-1113.
- (96) StetlerStevenson, W. G. *American Journal of Pathology* 1996, *148*, 1345-1350.

-
- (97) Cawston, T. E. *Pharmacology & Therapeutics* 1996, 70, 163-182.
- (98) Chandler, S.; Miller, K. M.; Clements, J. M.; Lury, J.; Corkill, D.; Anthony, D. C. C.; Adams, S. E.; Gearing, A. J. H. *Journal of Neuroimmunology* 1997, 72, 155-161.
- (99) Dollery, C. M.; McEwan, J. R.; Henney, A. M. *Circ Res* 1995, 77, 863-868.
- (100) Sternlicht, M. D.; Werb, Z. *Annual Review of Cell and Developmental Biology* 2001, 17, 463-516.
- (101) Nelson, A. R.; Fingleton, B.; Rothenberg, M. L.; Matrisian, L. M. *J Clin Oncol* 2000, 18, 1135-.
- (102) Coussens, L. M.; Tinkle, C. L.; Hanahan, D.; Werb, Z. *Cell* 2000, 103, 481-490.
- (103) Pozzi, A.; Moberg, P. E.; Miles, L. A.; Wagner, S.; Soloway, P.; Gardner, H. A. *PNAS* 2000, 97, 2202-2207.
- (104) Mudgett, J. S.; Hutchinson, N. I.; Chartrain, N. A.; Forsyth, A. J.; McDonnell, J.; Singer, II; Bayne, E. K.; Flanagan, J.; Kawka, D.; Shen, C. F.; Stevens, K.; Chen, H.; Trumbauer, M.; Visco, D. M. *Arthritis and Rheumatism* 1998, 41, 110-121.
- (105) Harper, E.; Bloch, K. J.; Gross, J. *Biochemistry* 1971, 10, 3035.
- (106) Bauer, E. A.; Stricklin, G. P.; Jeffrey, J. J.; Eisen, A. Z. *Biochemical and Biophysical Research Communications* 1975, 64, 232-240.
- (107) Nagase, H.; Woessner, J. F., Jr. *J. Biol. Chem.* 1999, 274, 21491-21494.
- (108) Lohi, J.; Wilson, C. L.; Roby, J. D.; Parks, W. C. *J. Biol. Chem.* 2001, 276, 10134-10144.
- (109) Bode, W.; Reinemer, P.; Huber, R.; Kleine, T.; Schnierer, S.; Tschesche, H. *Embo Journal* 1994, 13, 1263-1269.
- (110) Salowe, S. P.; Marcy, A. I.; Cuca, G. C.; Smith, C. K.; Kopka, I. E.; Hagmann, W. K.; Hermes, J. D. *Biochemistry* 1992, 31, 4535-4540.
- (111) Murphy, G.; Nguyen, Q.; Cockett, M. I.; Atkinson, S. J.; Allan, J. A.; Knight, C. G.; Willenbrock, F.; Docherty, A. J. *J. Biol. Chem.* 1994, 269, 6632-6636.
- (112) Shipley, J. M.; Doyle, G. A. R.; Fliszar, C. J.; Ye, Q.-Z.; Johnson, L. L.; Shapiro, S. D.; Welgus, H. G.; Senior, R. M. *J. Biol. Chem.* 1996, 271, 4335-4341.
- (113) Gururajan, R.; Grenet, J.; Lahti, J. M.; Kidd, V. J. *Genomics* 1998, 52, 101-106.
- (114) Park, H. I.; Ni, J.; Gerkema, F. E.; Liu, D.; Belozarov, V. E.; Sang, Q.-X. *J. Biol. Chem.* 2000, 275, 20540-20544.
- (115) Murphy, G.; Allan, J. A.; Willenbrock, F.; Cockett, M. I.; O'Connell, J. P.; Docherty, A. J. *J. Biol. Chem.* 1992, 267, 9612-9618.
- (116) Sanchez-Lopez, R.; Alexander, C. M.; Behrendtsen, O.; Breathnach, R.; Werb, Z. *J. Biol. Chem.* 1993, 268, 7238-7247.
- (117) Murphy, G.; Knauper, V. *Matrix Biology* 1997, 15, 511-518.
- (118) Knauper, V.; Docherty, A. J. P.; Smith, B.; Tschesche, H.; Murphy, G. *FEBS Letters* 1997, 405, 60-64.
- (119) Sato, H.; Kinoshita, T.; Takino, T.; Nakayama, K.; Seiki, M. *FEBS Letters* 1996, 393, 101-104.
- (120) Itoh, T.; Tanioka, M.; Yoshida, H.; Yoshioka, T.; Nishimoto, H.; Itohara, S. *Cancer Res* 1998, 58, 1048-1051.

7. References

- (121) Kojima, S.-i.; Itoh, Y.; Matsumoto, S.-i.; Masuho, Y.; Seiki, M. *FEBS Letters* 2000, *480*, 142-146.
- (122) Gomis-Ruth, F.-X.; Maskos, K.; Betz, M.; Bergner, A.; Huber, R.; Suzuki, K.; Yoshida, N.; Nagase, H.; Brew, K.; Bourenkov, G. P.; Bartunik, H.; Bode, W. *Nature* 1997, *389*, 77-81.
- (123) Docherty, A. J. P.; Lyons, A.; Smith, B. J.; Wright, E. M.; Stephens, P. E.; Harris, T. J. R.; Murphy, G.; Reynolds, J. J. *Nature* 1985, *318*, 66-69.
- (124) Stetler-Stevenson, W. G.; Kruttsch, H. C.; Liotta, L. A. *J. Biol. Chem.* 1989, *264*, 17374-17378.
- (125) Apte, S. S.; Mattei, M.-G.; Olsen, B. R. *Genomics* 1994, *19*, 86-90.
- (126) Greene, J.; Wang, M.; Liu, Y. E.; Raymond, L. A.; Rosen, C.; Shi, Y. E. *J. Biol. Chem.* 1996, *271*, 30375-30380.
- (127) Butler, T. A.; Zhu, C.; Mueller, R. A.; Fuller, G. C.; Lemaire, W. J.; Woessner, J. F., Jr. *Biol Reprod* 1991, *44*, 1183-1188.
- (128) Graham, C. H.; Lala, P. K. *Journal of Cellular Physiology* 1991, *148*, 228-234.
- (129) Gack, S.; Vallon, R.; Schmidt, J.; Grigoriadis, A.; Tuckermann, J.; Schenkel, J.; Weiher, H.; Wagner, E. F.; Angel, P. *Cell Growth Differ* 1995, *6*, 759-767.
- (130) Karelina, T. V.; Goldberg, G. I.; Eisen, A. Z. *Journal of Investigative Dermatology* 1994, *103*, 482-487.
- (131) Grass, S.; Arnold, H. H.; Braun, T. *Development* 1996, *122*, 141-150.
- (132) O'Byrne, E. M.; Parker, D. T.; Roberts, E. D.; Goldberg, R. L.; MacPherson, L. J.; Blancuzzi, V.; Wilson, D.; Singh, H. N.; Ludewig, R.; Ganu, V. S. *Inflammation Research* 1995, *44*, S117-S118.
- (133) Chambers, A. F.; Matrisian, L. M. *J Natl Cancer Inst* 1997, *89*, 1260-1270.
- (134) Gijbels, K.; Masure, S.; Carton, H.; Opendenakker, G. *Journal of Neuroimmunology* 1992, *41*, 29-34.
- (135) Chandler, S.; Coates, R.; Gearing, A.; Lury, J.; Wells, G.; Bone, E. *Neuroscience Letters* 1995, *201*, 223-226.
- (136) Rosenberg, G. A. *Journal of Neurotrauma* 1995, *12*, 833-842.
- (137) Strauss, B. H.; Robinson, R.; Batchelor, W. B.; Chisholm, R. J.; Ravi, G.; Natarajan, M. K.; Logan, R. A.; Mehta, S. R.; Levy, D. E.; Ezrin, A. M.; Keeley, F. W. *Circ Res* 1996, *79*, 541-550.
- (138) Thompson, R. W.; Parks, W. C. *Ann NY Acad Sci* 1996, *800*, 157-174.
- (139) Saarialho-Kere, U. K.; Vaalamo, M.; Puolakkainen, P.; Airola, K.; Parks, W. C.; Karjalainen-Lindsberg, M. L. *Am J Pathol* 1996, *148*, 519-526.
- (140) Golub, L. M.; Wolff, M.; Roberts, S.; Lee, H. M.; Leung, M.; Payonk, G. S. *J Am Dent Assoc* 1994, *125*, 163-169.
- (141) Vanwart, H. E.; Birkedalhansen, H. *Proceedings of the National Academy of Sciences of the United States of America* 1990, *87*, 5578-5582.
- (142) Pei, D.; Weiss, S. J. *Nature* 1995, *375*, 244-247.
- (143) Wang, X.; Pei, D. *J. Biol. Chem.* 2001, *276*, 35953-35960.
- (144) Kang, T.; Nagase, H.; Pei, D. *Cancer Res* 2002, *62*, 675-681.
- (145) Baker, A. H.; Edwards, D. R.; Murphy, G. *J Cell Sci* 2002, *115*, 3719-3727.
- (146) Mott, J. D.; Thomas, C. L.; Rosenbach, M. T.; Takahara, K.; Greenspan, D. S.; Banda, M. J. *J. Biol. Chem.* 2000, *275*, 1384-1390.
- (147) Oh, J.; Takahashi, R.; Kondo, S.; Mizoguchi, A.; Adachi, E.; Sasahara, R. M.; Nishimura, S.; Imamura, Y.; Kitayama, H.; Alexander, D. B. *Cell* 2001, *107*, 789-800.

- (148) Takahashi, C.; Sheng, Z. Q.; Horan, T. P.; Kitayama, H.; Maki, M.; Hitomi, K.; Kitaura, Y.; Takai, S.; Sasahara, R. M.; Horimoto, A.; Ikawa, Y.; Ratzkin, B. J.; Arakawa, T.; Noda, M. *Proceedings of the National Academy of Sciences of the United States of America* 1998, 95, 13221-13226.
- (149) Lovejoy, B.; Cleasby, A.; Hassell, A. M.; Longley, K.; Luther, M. A.; Weigl, D.; McGeehan, G.; McElroy, A. B.; Drewry, D.; Lambert, M. H.; Jordan, S. R. *Science* 1994, 263, 375-377.
- (150) Borkakoti, N.; Winkler, F. K.; Williams, D. H.; Darcy, A.; Broadhurst, M. J.; Brown, P. A.; Johnson, W. H.; Murray, E. J. *Nature Structural Biology* 1994, 1, 106-110.
- (151) Stams, T.; Spurlino, J. C.; Smith, D. L.; Wahl, R. C.; Ho, T. F.; Qoronfle, M. W.; Banks, T. M.; Rubin, B. *Nature Structural Biology* 1994, 1, 119-123.
- (152) Reinemer, P.; Grams, F.; Huber, R.; Kleine, T.; Schnierer, S.; Piper, M.; Tschesche, H.; Bode, W. *FEBS Letters* 1994, 338, 227-233.
- (153) Gooley, P. R.; Oconnell, J. F.; Marcy, A. I.; Cuca, G. C.; Salowe, S. P.; Bush, B. L.; Hermes, J. D.; Esser, C. K.; Hagmann, W. K.; Springer, J. P.; Johnson, B. A. *Nature Structural Biology* 1994, 1, 111-118.
- (154) Lovejoy, B.; Hassell, A. M.; Luther, M. A.; Weigl, D.; Jordan, S. R. *Biochemistry* 1994, 33, 8207-8217.
- (155) Spurlino, J. C.; Smallwood, A. M.; Carlton, D. D.; Banks, T. M.; Vavra, K. J.; Johnson, J. S.; Cook, E. R.; Falvo, J.; Wahl, R. C.; Pulvino, T. A.; Wendoloski, J. J.; Smith, D. L. *Proteins-Structure Function and Genetics* 1994, 19, 98-109.
- (156) Browner, M. F.; Smith, W. W.; Castelhana, A. L. *Biochemistry* 1995, 34, 6602-6610.
- (157) Becker, J. W.; Marcy, A. I.; Rokosz, L. L.; Axel, M. G.; Burbaum, J. J.; Fitzgerald, P. M. D.; Cameron, P. M.; Esser, C. K.; Hagmann, W. K.; Hermes, J. D.; Springer, J. P. *Protein Sci* 1995, 4, 1966-1976.
- (158) Dhanaraj, V.; Ye, Q. Z.; Johnson, L. L.; Hupe, D. J.; Ortwine, D. F.; Dunbar, J. J. B.; Rubin, J. R.; Pavlovsky, A.; Humblet, C.; Blundell, T. L. *Structure* 1996, 4, 375-386.
- (159) Van-Doren, S. R.; Kurochkin, A. V.; Hu, W.; Ye, Q.; Johnson, L. L.; Hupe, D. J.; Zuiderweg, E. R. P. *Protein Sci* 1995, 4, 2487-2498.
- (160) Wetmore, D. R.; Hardman, K. D. *Biochemistry* 1996, 35, 6549-6558.
- (161) Grams, F.; Reinemer, P.; Powers, J. C.; Kleine, T.; Pieper, M.; Tschesche, H.; Huber, R.; Bode, W. *European Journal of Biochemistry* 1995, 228, 830-841.
- (162) Grams, F.; Crimmin, M.; Hinnes, L.; Huxley, P.; Pieper, M.; Tschesche, H.; Bode, W. *Biochemistry* 1995, 34, 14012-14020.
- (163) Fernandez-Catalan, C.; Bode, W.; Huber, R.; Turk, D.; Calvete, J. J.; Lichte, A.; Tschesche, H.; Maskos, K. *Embo Journal* 1998, 17, 5238-5248.
- (164) Li, J.; Brick, P.; O'Hare, M. C.; Skarzynski, T.; Lloyd, L. F.; Curry, V. A.; Clark, I. M.; Bigg, H. F.; Hazleman, B. L.; Cawston, T. E.; Blow, D. M. *Structure* 1995, 3, 541-549.
- (165) Libson, A. M.; Gittis, A. G.; Collier, I. E.; Marmer, B. L.; Goldberg, G. I.; Lattman, E. E. *Nat Struct Mol Biol* 1995, 2, 938-942.
- (166) Gohlke, U.; Gomis-Ruth, F.-X.; Crabbe, T.; Murphy, G.; Docherty, A. J. P.; Bode, W. *FEBS Letters* 1996, 378, 126-130.
- (167) Gomis-Ruth, F. X.; Gohlke, U.; Betz, M.; Knauper, V.; Murphy, G.; Lopez-Otin, C.; Bode, W. *Journal of Molecular Biology* 1996, 264, 556-566.

7. References

- (168) Bode, W. *Structure* 1995, 3, 527-530.
- (169) Bode, W.; Gomis-Ruth, F.-X.; Stockler, W. *FEBS Letters* 1993, 331, 134-140.
- (170) Stocker, W.; Bode, W. *Current Opinion in Structural Biology* 1995, 5, 383-390.
- (171) Harrison, R. K.; Chang, B.; Niedzwiecki, L.; Stein, R. L. *Biochemistry* 1992, 31, 10757-10762.
- (172) Babine, R. E.; Bender, S. L. *Chem. Rev.* 1997, 97, 1359-1472.
- (173) Finzel, B. C.; Baldwin, E. T.; Bryant-Jr, G. L.; Hess, G. F.; Wilks, J. W.; Trepod, C. M.; Mott, J. E.; Marshall, V. P.; Petzold, G. L.; Poorman, R. A.; O'Sullivan, T. J.; Schostarez, H. J.; Mitchell, M. A. *Protein Sci* 1998, 7, 2118-2126.
- (174) Stockman, B. J.; Waldon, D. J.; Gates, J. A.; Scahill, T. A.; Kloosterman, D. A.; Mizensak, S. A.; Jacobsen, E. J.; Belonga, K. L.; Mitchell, M. A.; Mao, B.; Petke, J. D.; Goodman, L.; Powers, E. A.; Ledbetter, S. R.; Kaytes, P. S.; Vogeli, G.; Marshall, V. P.; Petzold, G. L.; Poorman, R. A. *Protein Sci* 1998, 7, 2281-2286.
- (175) Whittaker, M.; Floyd, C. D.; Brown, P.; Gearing, A. J. H. *Chem. Rev.* 1999, 99, 2735-2776.
- (176) Whittaker, M. *Current Opinion in Chemical Biology* 1998, 2, 386-396.
- (177) Johnson, W. H.; Roberts, N. A.; Borkakoti, N. *J. Enz. Inhib.* 1987, 2, 1.
- (178) Gante, J. *Angewandte Chemie-International Edition* 1994, 33, 1699-1720.
- (179) Simon, R. J.; Kania, R. S.; Zuckermann, R. N.; Huebner, V. D.; Jewell, D. A.; Banville, S.; Ng, S.; Wang, L.; Rosenberg, S.; Marlowe, C. K.; Spellmeyer, D. C.; Tan, R.; Frankel, A. D.; Santi, D. V.; Cohen, F. E.; Bartlett, P. A. *PNAS* 1992, 89, 9367-9371.
- (180) Kerr, J. M.; Banville, S. C.; Zuckermann, R. N. *Journal of the American Chemical Society* 1993, 115, 2529-2531.
- (181) Zuckermann, R. N.; Martin, E. J.; Spellmeyer, D. C.; Stauber, G. B.; Shoemaker, K. R.; Kerr, J. M.; Figliozzi, G. M.; Goff, D. A.; Siani, M. A.; Simon, R. J.; Banville, S. C.; Brown, E. G.; Wang, L.; Richter, L. S.; Moos, W. H. *Journal of Medicinal Chemistry* 1994, 37, 2678-2685.
- (182) Miller, S. M.; Simon, R. J.; Ng, S.; Zuckermann, R. N.; Kerr, J. M.; Moos, W. H. *Bioorganic & Medicinal Chemistry Letters* 1994, 4, 2657-2662.
- (183) Wang, Y.; Lin, H.; Tullman, R.; Jr, C. F. J.; Weetall, M. L.; Tse, F. L. S. *Biopharmaceutics & Drug Disposition* 1999, 20, 69-75.
- (184) Martin, E. J.; Blaney, J. M.; Siani, M. A.; Spellmeyer, D. C.; Wong, A. K.; Moos, W. H. *Journal of Medicinal Chemistry* 1995, 38, 1431-1436.
- (185) Lipinski, C. A.; Lombardo, F.; Dominy, B. W.; Feeney, P. J. *Advanced Drug Delivery Reviews* 1997, 23, 3-25.
- (186) Veber, D. F.; Johnson, S. R.; Cheng, H. Y.; Smith, B. R.; Ward, K. W.; Kopple, K. D. *J. Med. Chem.* 2002, 45, 2615-2623.
- (187) Chorev, M.; Shavitz, R.; Goodman, M.; Minick, S.; Guillemin, R. *Science* 1979, 204, 1210-1212.
- (188) Pallai, P. V.; Struthers, R. S.; Goodman, M.; Moroder, L.; Wunsch, E.; Vale, W. *Biochemistry* 1985, 24, 1933-1941.
- (189) Rodriguez, M.; Lignon, M. F.; Galas, M. C.; Fulcrand, P.; Mendre, C.; Aumelas, A.; Laur, J.; Martinez, J. *Journal of Medicinal Chemistry* 1987, 30, 1366-1373.

- (190) Zuckermann, R. N.; Kerr, J. M.; Kent, S. B. H.; Moos, W. H. *Journal of the American Chemical Society* 1992, *114*, 10646-10647.
- (191) Sheehan, J. C.; Hess, G. P. *Journal of the American Chemical Society* 1955, *77*, 1067-1068.
- (192) Carpino, L. A. *Journal of the American Chemical Society* 1993, *115*, 4397-4398.
- (193) Carpino, L. A.; Elfaham, A.; Albericio, F. *Tetrahedron Letters* 1994, *35*, 2279-2282.
- (194) Carpino, L. A.; Elfaham, A.; Minor, C. A.; Albericio, F. *Journal of the Chemical Society-Chemical Communications* 1994, 201-203.
- (195) Castro, B.; Dormoy, J. R.; Evin, G.; Selve, C. *Tetrahedron Letters* 1975, 1219-1222.
- (196) Coste, J.; Lenguyen, D.; Castro, B. *Tetrahedron Letters* 1990, *31*, 205-208.
- (197) Konig, W.; Geiger, R. *Chemische Berichte-Recueil* 1970, *103*, 788.
- (198) Dourtoglou, V.; Ziegler, J. C.; Gross, B. *Tetrahedron Letters* 1978, 1269-1272.
- (199) Hancock, W. S.; Battersby, J. E. *Analytical Biochemistry* 1976, *71*, 260-264.
- (200) Kaiser, E.; Colescot, R.; Bossinger, C.; Cook, P. I. *Analytical Biochemistry* 1970, *34*, 595.
- (201) Vojtkovsky, T. *Peptide Research* 1995, *8*, 236-237.
- (202) Oneal, K. D.; Chari, M. V.; McDonald, C. H.; Cook, R. G.; YuLee, L. Y.; Morrisett, J. D.; Shearer, W. T. *Biochemical Journal* 1996, *315*, 833-844.
- (203) Armand, P.; Kirshenbaum, K.; Goldsmith, R. A.; Farr-Jones, S.; Barron, A. E.; Truong, K. T. V.; Dill, K. A.; Mierke, D. F.; Cohen, F. E.; Zuckermann, R. N.; Bradley, E. K. *PNAS* 1998, *95*, 4309-4314.
- (204) Heerma, W.; Versluis, C.; Koster, C. G. d.; Kruijtzter, J. A. W.; Zigrovic, I.; Liskamp, R. M. J. *Rapid Communications in Mass Spectrometry* 1996, *10*, 459-464.
- (205) Wigger Heerma, J. *Journal of Mass Spectrometry* 1997, *32*, 697-704.
- (206) Roepstorff, P.; J. Fohlman *Biomedical Mass Spectrometry* 1984, *11*, 601.
- (207) Johnson, R. S.; Martin, S. A.; Biemann, K.; Stults, J. T.; Watson, J. T. *Analytical Chemistry* 1987, *59*, 2621-2625.
- (208) Carpino, L. A.; Han, G. Y. *Journal of the American Chemical Society* 1970, *92*, 5748.
- (209) Chan, W. C.; Bycroft, B. W.; Evans, D. J.; White, P. D. *Journal of the Chemical Society-Chemical Communications* 1995, 2209-2210.
- (210) Waldmann, H.; Kunz, H. *Liebigs Annalen Der Chemie* 1983, 1712-1725.
- (211) Teixido, M.; Altamura, M.; Quartara, L.; Giolitti, A.; Maggi, C. A.; Giralt, E.; Albericio, F. *J. Comb. Chem* 2003, *5*, 760-768.
- (212) Dale, J. *Angewandte Chemie-International Edition* 1966, *5*, 1000.
- (213) Kessler, H.; Kutscher, B. *Liebigs Annalen Der Chemie* 1986, 869-892.
- (214) Kessler, H.; Kutscher, B. *Liebigs Annalen Der Chemie* 1986, 914-931.
- (215) Chen, F. M. F.; Benoiton, N. L. *International Journal of Peptide and Protein Research* 1991, *38*, 285-286.
- (216) Izumiya, N.; Kato, T.; Waki, M. *Biopolymers* 1981, *20*, 1785-1791.
- (217) Schmidt, R.; Neubert, K. *International Journal of Peptide and Protein Research* 1991, *37*, 502-507.
- (218) Knorr, R.; Trzeciak, A.; Bannwarth, W.; Gillessen, D. *Tetrahedron Letters* 1989, *30*, 1927-1930.

7. References

- (219) Felix, A. M.; Wang, C. T.; Heimer, E. P.; Fournier, A. *International Journal of Peptide and Protein Research* 1988, *31*, 231-238.
- (220) Benoiton, N. L.; Lee, Y. C.; Steinaur, R.; Chen, F. M. F. *International Journal of Peptide and Protein Research* 1992, *40*, 559-566.
- (221) Kaldor, S. W.; Dressman, B. A.; Hammond, M.; Appelt, K.; Burgess, J. A.; Lubbehusen, P. P.; Muesing, M. A.; Hatch, S. D.; Wiskerchen, M. A.; Baxter, A. J. *Bioorganic & Medicinal Chemistry Letters* 1995, *5*, 721-726.
- (222) Hom, R. K.; Gailunas, A. F.; Mamo, S.; Fang, L. Y.; Tung, J. S.; Walker, D. E.; Davis, D.; Thorsett, E. D.; Jewett, N. E.; Moon, J. B.; John, V. J. *Med. Chem.* 2004, *47*, 158-164.
- (223) Narita, M.; Otsuka, M.; Kobayashi, S.; Ohno, M.; Umezawa, Y.; Morishima, H.; Saito, S.-i.; Takita, T.; Umezawa, H. *Tetrahedron Letters* 1982, *23*, 525-528.
- (224) DiPardo, R. M.; Bock, M. G. *Tetrahedron Letters* 1983, *24*, 4805-4808.
- (225) Tomioka, K.; Kanai, M.; Koga, K. *Tetrahedron Letters* 1991, *32*, 2395-2398.
- (226) Shioiri, T.; Hayashi, K.; Hamada, Y. *Tetrahedron* 1993, *49*, 1913-1924.
- (227) Bock, M. G.; Dipardo, R. M.; Evans, B. E.; Rittle, K. E.; Boger, J. S.; Freidinger, R. M.; Veber, D. F. *Journal of the Chemical Society-Chemical Communications* 1985, 109-110.
- (228) Rivero, R. A.; Greenlee, W. J. *Tetrahedron Letters* 1991, *32*, 2453-2456.
- (229) Hayashi, K.; Hamada, Y.; Shioiri, T. *Tetrahedron Letters* 1991, *32*, 7287-7290.
- (230) Travins, J. M.; Bursavich, M. G.; Veber, D. F.; Rich, D. H. *Org. Lett.* 2001, *3*, 2725-2728.
- (231) Nahm, S.; Weinreb, S. M. *Tetrahedron Letters* 1981, *22*, 3815-3818.
- (232) Zimmerman, H. E.; Traxler, M. D. *Journal of the American Chemical Society* 1957, *79*, 1920-1923.
- (233) Abiko, A.; Liu, J. F.; Masamune, S. *J. Am. Chem. Soc.* 1997, *119*, 2586-2587.
- (234) Abiko, A. *Anti-selective boron-mediated asymmetric aldol reaction of carboxylic esters: synthesis of (2S,3R)-2,4-dimethyl-1,3-pentanediol*; John Wiley & Sons, Inc., 2002; Vol. 79.
- (235) Abiko, A. *2-(N-benzyl-N-mesitylenesulfonyl)amino-1-phenyl-1-propyl propionate*; John Wiley & Sons, Inc., 2002; Vol. 79.
- (236) Reetz, M. T.; Kukenhohner, T.; Weinig, P. *Tetrahedron Letters* 1986, *27*, 5711-5714.
- (237) Abiko, A. *Dicyclohexylboron trifluoromethanesulfonate*; John Wiley & Sons, Inc.: New York, 2002; Vol. 79.
- (238) Inoue, T.; Liu, J. F.; Buske, D. C.; Abiko, A. *J. Org. Chem.* 2002, *67*, 5250-5256.
- (239) Scholz, D.; Billich, A.; Charpiot, B.; Etmayer, P.; Lehr, P.; Rosenwirth, B.; Schreiner, E.; Gstach, H. *Journal of Medicinal Chemistry* 1994, *37*, 3079-3089.
- (240) Mancuso, A. J.; Swern, D. *Synthesis-Stuttgart* 1981, 165-185.
- (241) Zucker, S.; Hymowitz, M.; Conner, C.; Zarrabi, H. M.; Hurewitz, A. N.; Matrisian, L.; Boyd, D.; Nicolson, G.; Montana, S. *Ann NY Acad Sci* 1999, *878*, 212-227.
- (242) Yao, J.; Xiong, S. B.; Klos, K.; Nguyen, N.; Grijalva, R.; Li, P.; Yu, D. *Oncogene* 2001, *20*, 8066-8074.
- (243) Galis, Z. S.; Sukhova, G. K.; Libby, P. *FASEB J.* 1995, *9*, 974-980.

- (244) Spinale, F. G.; Coker, M. L.; Bond, B. R.; Zellner, J. L. *Cardiovascular Research* 2000, *46*, 225-238.
- (245) Li, Y. Y.; Feldman, A. M. *Drugs* 2001, *61*, 1239-1252.
- (246) Jackson, C.; Nguyen, M.; Arkell, J.; Sambrook, P. *Inflammation Research* 2001, *50*, 183-186.
- (247) Shaw, T.; Nixon, J. S.; Bottomley, K. M. *Expert Opinion on Investigational Drugs* 2000, *9*, 1469-1478.
- (248) Elliott, S.; Cawston, T. *Drugs & Aging* 2001, *18*, 87-99.
- (249) Collier, I. E.; Krasnov, P. A.; Strongin, A. Y.; Birkedal-Hansen, H.; Goldberg, G. I. *J. Biol. Chem.* 1992, *267*, 6776-6781.
- (250) Banyai, L.; Patthy, L. *FEBS Letters* 1991, *282*, 23-25.
- (251) Banyai, L.; Tordai, H.; Patthy, L. *Biochemical Journal* 1994, *298*, 403-407.
- (252) Allan, J. A.; Docherty, A. J. P.; Barker, P. J.; Huskisson, N. S.; Reynolds, J. J.; Murphy, G. *Biochemical Journal* 1995, *309*, 299-306.
- (253) Mathai Mammen, S.-K. C. G. M. W. *Angewandte Chemie International Edition* 1998, *37*, 2754-2794.
- (254) Zalipsky, S. *Bioconjugate Chemistry* 1995, *6*, 150-165.
- (255) Dreborg, S.; Akerblom, E. B. *Critical Reviews in Therapeutic Drug Carrier Systems* 1990, *6*, 315-365.
- (256) Yamaoka, T.; Tabata, Y.; Ikada, Y. *Journal of Pharmaceutical Sciences* 1994, *83*, 601-606.
- (257) Mutter, M.; Hagenmaier, H.; Bayer, E. *Angewandte Chemie-International Edition* 1971, *10*, 811.
- (258) Lu, Y. A.; Felix, A. M. *Peptide Research* 1993, *6*, 140-146.
- (259) Loiseau, F. A.; Hii, K. K. M.; Hill, A. M. *J. Org. Chem.* 2004, *69*, 639-647.
- (260) Scriven, E. F. V. *Chemical Society Reviews* 1983, *12*, 129-161.
- (261) Ishihara, K.; Kubota, M.; Kurihara, H.; Yamamoto, H. *Journal of the American Chemical Society* 1995, *117*, 4413-4414.
- (262) Ishihara, K.; Kubota, M.; Kurihara, H.; Yamamoto, H. *Journal of Organic Chemistry* 1996, *61*, 4560-4567.
- (263) Barrett, A. G. M.; Braddock, D. C. *Chemical Communications* 1997, 351-352.
- (264) Bihovsky, R.; Levinson, B. L.; Loewi, R. C.; Erhardt, P. W.; Polokoff, M. A. *Journal of Medicinal Chemistry* 1995, *38*, 2119-2129.
- (265) Fourniezalwski, M. C.; Coulaud, A.; Bouboutou, R.; Chaillet, P.; Devin, J.; Waksman, G.; Costentin, J.; Roques, B. P. *Journal of Medicinal Chemistry* 1985, *28*, 1158-1169.
- (266) Nishino, N.; Powers, J. C. *Biochemistry* 1979, *18*, 4340-4347.
- (267) Anantharamaiah, G. M.; Sivanandaiah, K. M. *Journal of the Chemical Society-Perkin Transactions I* 1977, 490-491.
- (268) Anwer, M. K.; Spatola, A. F. *An advantageous method for the rapid removal of hydrogenolysable protecting groups under ambient conditions; Synthesis of leucine-enkephalin*, 1980.
- (269) Ram, S.; Spicer, L. D. *Synthetic Communications* 1987, *17*, 415-418.
- (270) Gude, M.; Ryf, J.; White, P. D. *Letters in Peptide Science* 2002, *9*, 203-206.
- (271) Bax, A.; Davis, D. G. *Journal of Magnetic Resonance* 1985, *65*, 355-360.
- (272) Wüthrich, K. *NMR of Proteins and Nucleic Acids*; John Wiley: New York, USA, 1986.

7. References

- (273) Westmeyer, G. G.; Willem, M.; Lichtenthaler, S. F.; Lurman, G.; Multhaup, G.; Assafalg-Machleidt, I.; Reiss, K.; Saftig, P.; Haass, C. *Journal of Biological Chemistry* 2004, 279, 53205-53212.